UNIVERSITA' DEGLI STUDI DI NAPOLI FEDERICO II

Dottorato di Ricerca in Ingegneria Chimica, dei Materiali e della Produzione
(XVIII Ciclo)

CuO/CeO_2 CATALYSTS FOR THE PREFERENTIAL OXIDATION OF CO IN H_2 RICH MIXTURE FOR FUEL CELL APPLICATIONS

Scientific Commitee:

Prof. Gennaro Russo
Prof. Guido Saracco
Prof. Alessandro Trovarelli
Dott. Raffaele Pirone

Candidate:

Tiziana Caputo

INDEX

Study and Research Abroad

During the doctorate, from November 2004 to May 2005, Au/TiO_2 catalytic systems have been investigated for the reaction of CO oxidation at low temperature at the Department of Chemical and Biological Engineering of the Northwestern University (Evanston, IL, USA) under the supervision of Professor Harold H. Kung.

The interest in Gold/titania catalysts lays in their similarity to the CuO/CeO_2 catalysts: both catalytic systems exhibit a significant activity towards CO oxidation at low temperature, and to a high degree of interaction with the support.

The Gold/titania systems investigated were prepared via deposition-precipitation method at a constant pH, with the purpose of achieving a mean particle size of the gold particles in the range 1-3nm, as was confirmed by the TEM and XANES analysis.

Moreover, also more complex preparation techniques were employed in the preparation of bimetallic copper-gold catalysts supported on titania, such as the reverse micelles method and the via dendrimer method.

The catalytic systems have been characterized by in situ IR spectroscopy and in situ XANES at the temperature of -60°C.

The use of isotopes in the IR experiments led to the identification of the hydroxyl-carbonyl as intermediate in the CO oxidation reaction.

The in situ XANES analysis, which, due to the expensive and dangerous facilities required, were performed in the National Laboratories of Argonne, where I was hosted 10 days, financed by the Northwestern University, led to the identification of state and coordination number of the gold oxidation under reaction conditions.

The intense and fatigued characterization work conducted at the Northwestern University was rewarded by two publications on international journals with high impact factors:

1. the first published on Journal of Physical Chemistry B (J.H. Yang, J.D. Henao, M. C. Raphlulu, Y. Wing, T. Caputo, M.C. Kung, H.H. Kung (2005) Activation of Au/TiO_2 catalyst for CO oxidation, Journal of Physical Chemistry B, 109 (20), 10319-10326 (2005)
2. the second one recently submitted to Journal of Catalysis (Juan D. Henao[1], Jeff Yang[1], Tiziana Caputo[2], Mayfair C. Kung[1] and Harold H. Kung[1], In-situ FTIR and XANES study of the evolution of surface species during transient CO oxidation on supported Au/TiO_2)

The financial support for the period abroad was provided by the University of Naples with a short mobility scholarship in the period between 1/11/2004 until the 15/12/2004, and by a second short mobility scholarship financed by the CNR in the period from the 1/5/2005 until 22/5/2005.

Aknowledgments

I wish to thank Prof. G. Russo for his advice and guidance over the past years, and its ability to understand the situations also without too many comments either in the scientific field or in the laboratory life.

I would like to thank Prof. Harold H. Kung, and Prof. Mayfair Kung for the fruitful work, the patience showed in introducing me to completely new aspects of catalysis, and the kind hospitality during the months spent at the Northwestern University. With their support the very cold Chicago appeared to me cozy and familiar. Moreover I thank all the Kung group especially Juan Henao and Jeff Yang for the great time we had together and to introduce me to Chicago nightlife, to the Chinese food, to the NBA, and to the South American friends. Well, moreover I want to thank Taki for my bike!

I should also thank Lello Pirone for useful suggestions and for its presence in the laboratory during last summer.

I would especially like to thank Luciana Lisi for the scientific and moral support extremely necessary in the last months.

Moreover I want to thank Almerinda Di Benedetto for her kindness.

I have to give props to Russo group for moral support, and to my PhD fellows: Giuseppe Russo and Achille Ascione.

I want to thank also all those, who contributed scientifically and in less scientific way to this research.

ABSTRACT

This thesis is focused on CuO/CeO_2 catalysts for the preferential oxidation of CO in H_2 rich mixtures (CO PROX). After a brief introduction of the general problem (energy production with novel processes or raw materials, fuel cells) and a more detailed description of the CO PROX unit in a fuel processor in order to deliver to fuel cells a CO-free H_2-containing stream. An overview of most representative and interesting catalytic systems proposed or utilised for the process has been also presented, before introducing the properties and the motivation of the choice of investigating catalysts based on copper oxide supported on ceria (or mixed ceria-zirconia).

Results of catalytic tests carried out under experimental conditions in the range of interest for applications show that an increase of redox properties of catalyst obtained by supporting CuO on Ce-Zr mixed oxide is not directly linked to higher activity, the optimal catalyst formulation found corresponds to 4wt% CuO/CeO_2, whose performances appear higher than commercially available Pt based catalysts. The catalyst is very selective (100% up to about 100°C, about 60-80% at higher temperatures), the selectivity is a unique function of temperature, slightly depending on the CO/H_2 ratio, on O_2 partial pressure and on the presence of CO_2 and H_2O in the gas. The kinetics has been modelled by considering reactions of both CO and H_2 oxidation. The experimental data have been fitted by rate expressions based on LH (or Eley-Rideal) reaction mechanism describing the interaction between surface oxygen species and adsorbed CO or gas phase CO. For both reactions of CO and H_2 oxidation a weak dependence on O_2 partial pressure has been found, while the competitive adsorption with reactants of CO_2 and H_2O on the active sites limits the CO conversion in the range of lower temperatures.

The analysis of the redox properties evidenced that CO is a stronger reductant than H_2 for catalyst sites. Indeed CO strongly interacts with completely oxidized sites already at room temperature, while hydrogen adsorbs exclusively on a pre-reduced sample. The re-oxidation rate of the active sites is faster than the hydrogen oxidation up to a temperature of 100°C, thus in this region the hydrogen oxidation does not take place and 100% selectivity is found for CO PROX process. The catalytic sites active in this temperature range (from room temperature up to 100°C) have been identified with TPR/TPD/TPO experiments with highly dispersed copper particles strongly interacting with ceria. Indeed it is strongly suggested that ceria also participates to redox processes already at very low temperatures and the sites at the borderline between ceria and copper have been identified as the main responsible for the activity and high selectivity in the process. At a temperature higher than 150°C CuO clusters are more active in the hydrogen oxidation, thus decreasing the overall efficiency of the CO PROX process.

CHAPTER 1

INTRODUCTION

1.1 Preface

The great demand of energy required by the industrial development brings about serious problems of economical and environmental issues. On one hand, these are strong driving forces to find novel processes of energy production able to exploit raw materials alternative to the conventional ones. On the other side, use of traditionally employed fossil fuels in energy production processes should be rationalised in order to achieve a higher efficiency for such processes.

For this purpose, hydrogen-fuelled cells are becoming a reliable option to the internal combustion engines in vehicle applications for their higher potential efficiency of energy production and practically no environmental impact.

Indeed fuel cells directly converts chemical energy into electricity avoiding the thermodynamic mechanical cycle losses associated with combustion in conventional power generation systems. For vehicle applications, the H_2 stream fed to the fuel cell should be produced in situ by a fuel processor using light hydrocarbons as a feed, rather than stored on board, in order to limits safety problems.

To date the main concern about the low scale hydrogen generation with the fuel cell technology is the poisoning of electrodes catalyst by CO contained in the reformate gases. For non-stationary applications the simplest method to decrease the CO concentration appears the preferential oxidation of carbon monoxide (CO-PROX). The process would be effective provided a proper catalyst is designed. Ideal features of the catalytic system for the CO-PROX process can be summarized as follows: high activity towards CO oxidation in the range fixed by the fuel processor (80-200°C), high selectivity towards the oxidation of CO rather than H_2 to limit the fuel consumption, high resistance towards CO_2 and H_2O present in the gas mixture and inactivity towards the reverse water gas-shift reaction that could limit the maximum CO abatement.

1.2 Fuel cells and fuel processor

A Fuel cell is a galvanic cell which works in continuum; it is a device in which the chemical energy bound in relatively high-enthalpy compounds can be converted directly into electricity while these reactants are converted to products of lower enthalpy (Perry, 1997).

Hydrogen is the preferred feed for fuel cells because of the easy integration system, high efficiency and practically zero emissions (Dudfield, 2000a). The fuel cell technology is able to produce electricity with very high efficiency and in a clean way because the only product of the H_2 oxidation reaction is H_2O.

In figure 1.1 a schematic representation of the reactions in a fuel cell operating on hydrogen and air with a hydrogen-ion conducting electrolyte is reported. The hydrogen flows over the anode, where the molecules are separated into ions and electrons. The ions migrate through the ionically conducting but electronically insulating electrolyte to the cathode, and the electrons flow through the outer circuit energizing an electric load. The electrons combine eventually with oxygen molecules flowing over the surface of the cathode and hydrogen ions migrating across the electrolyte, forming water, which leaves the fuel cell in the depleted air stream.

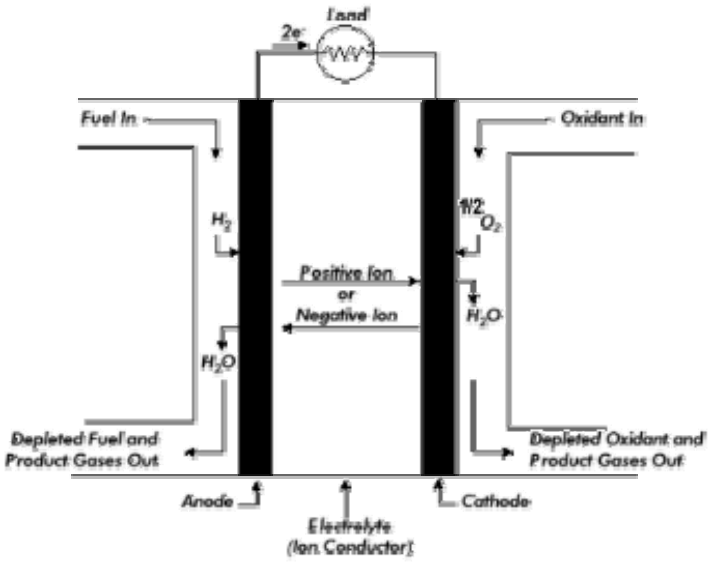

Figure 1.1: Scheme of a Fuel cell (Fuel cell handbook, 2000).

The anode and cathode must be good electronic conductors, porous, in order to allow diffusion to the reactive sites to the fuel and to the oxidants gases, and finally they must have catalytic properties in order to facilitate the anodic and cathodic reactions.

The electrolyte must be chemically stable in hydrogen and oxygen, and must have ionic conductivity to let and efficient ionic transportation (Fuel cell Handbook, 2000). Five classes of electrolyte have been found to meet these requirements: potassium hydroxide, perfuorinated sulfonic acids resins (polymeric membrane), phosphoric acid, oxide-ion-conducting ceramics and molten carbonates.

Fuel cells are generally classified according to the type of electrolyte used in the cells which includes: AFC (Alkaline fuel cell), PEMFC (Polymer electrolite membrane fuel cell), PAFC (Phosphoric acid fuel cell), MCFC (Molten carbonate fuel cell), SOFC (Solid oxide fuel cell).

MCFC and SOFC operate at elevated temperatures (600°C) and use systems based on nickel oxides or perovskite as catalysts for the electrodes. The other types of fuel cells work at low temperature, between 65°C and 200°C for AFC, at 80°C for the PEMFC, and at 200°C for PAFC respectively. The low temperature fuel cells use platinum supported on powders or carbon fibres as electrode catalysts. Pt based catalysts are sensitive to the presence of CO in the feed because it strongly adsorbs on the catalytic surface blocking the reaction sites. Lower the anode catalyst operating temperature, higher the CO poisoning effect, because the CO desorption rate decreases with increasing the temperature. As a consequence the fuel cells which shows the lowest tolerance limit to CO are the PEMFC because works at the lowest temperature (80°C).

Actually PEMFC are the preferred fuel cells used in a fuel processor for vehicular applications, that through an autothermal reforming or a partial oxidation, produces the H_2 to be fed to the fuel cell (Trimm, 2001).

A schematic diagram of a fuel processor with an autothermal reforming is showed in figure 1.2.

.

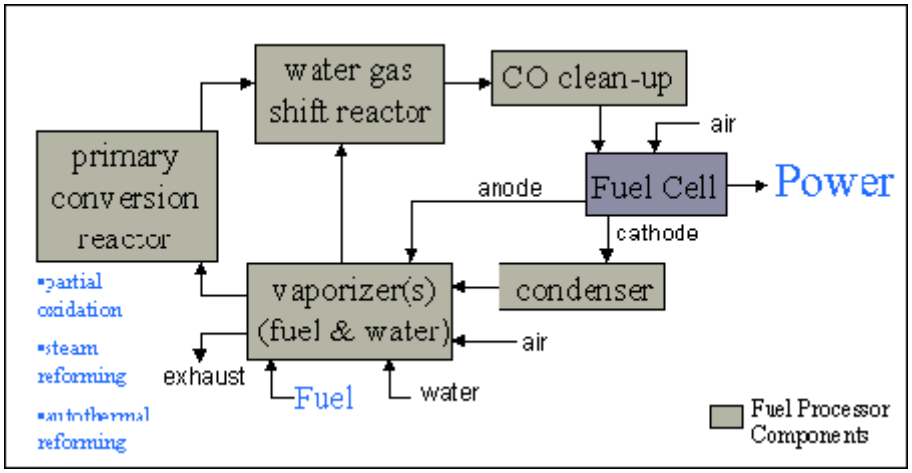

Figura 1.2: Fuel processor

In a fuel processor, the fuel, generally light hydrocarbons, is converted mainly to H_2 and CO in an *auto-thermal reformer,* while two stadio, respectively of high temperature and low temperature *water-gas-shift* (HWGS 350-400°C; LWGS 200-260°C) provide to convert the great part of CO in CO_2, and to produce additional H_2. Thus the gases are fed to a CO preferential oxidation stadio (CO-PROX) that should provide to decrease the CO concentration up to the fuel cell catalyst tolerance limit.

PEMFC are the preferred fuel cells because of the low operation temperature (80°C) associated to a high tolerance to the CO_2 present in the reformate gases. Indeed among the low temperature fuel cells, the PEMFC are the only which exhibits a complete tolerance to CO_2.

The PEMFC working temperature (80°C) represents a compromise between the necessity to have efficient ion exchange properties of the electrolyte, which decreases with the temperature, and the necessity to increase the CO tolerance limit of the anode catalyst with increasing the temperature. At this working temperature, the conventional Pt catalysts used for the fuel cell electrodes fixed the CO tolerance limit at about 10ppm (Qi, 2002; Akiyama, 1997). Recently less sensitive Pt-Ru catalysts have been studied for this application increasing the CO limit up to 1000ppm, greatly decreasing the fuel cell efficiency (Rohland, 1999).

1.3 Preferential Oxidation of CO (CO-PROX)

The composition of the gaseous stream at the inlet of the CO preferential oxidation reactor is typically constituted by: 45-75 vol% H_2, 15-25 vol% CO_2, 0.5-2 vol% CO, and small amounts of H_2O (up to 10%) in N_2 (0-25%). Even fractions of CO, as small as 1000 ppm, are poisonous to the Pt-based *fuel cell* catalyst, with the consequence that the CO content in the mixture fed to the *fuel cell* has to be markedly reduced.

In stationary plants for H_2 production on large scale, such as those for the production of chemical commodities (ammonia, methanol), CO is reduced by means of either *pressure swing adsorption* or *methanation* (Armor, 1998).

The *pressure swing adsorption* is not suitable for non-stationary applications, due to the large dimensions and high costs of the compressor.

On the other side, *methanation* reaction (5) occurs competitively with CO_2 methanation (6) dramatically increasing the fraction of H_2 consumed (Korotkikh, 2000).

The most desirable pathway is hence the catalytic preferential oxidation of CO with oxygen (1), which is in competition with H_2 oxidation (2), and hence should be carried out under conditions of higher selectivity to CO rather than to H_2. In the following, the chemical reactions, which are thermodynamically favoured for a typical gas composition at the inlet of the CO-PROX reactor, are reported (1-6). In addition, in Table 1 the corresponding values of the equilibrium constant are reported in the temperature range of interest for the CO-PROX reaction (80-200°C).

(1) $CO + \frac{1}{2}O_2 \rightarrow CO_2$ $\Delta H° = -284$ KJ/mole

(2) $H_2 + \frac{1}{2}O_2 \rightarrow H_2O$ $\Delta H° = -243$ KJ/mole

(3) $CO + H_2O \leftrightarrow CO_2 + H_2$ $\Delta H° = -41.35$ KJ/mole

(4) $2CO \leftrightarrow C + CO_2$ $\Delta H° = -173.12$ KJ/mole

(5) $CO + 3H_2 \leftrightarrow CH_4 + H_2O$ $\Delta H° = -207$ KJ/mole

(6) $CO_2 + 4H_2 \leftrightarrow CH_4 + 2H_2O$ $\Delta H° = -165.5$ KJ/mole

Table 1.1: Equilibrium constants for the reactions (1-6).

T(°C)	(1)	(2)	(3)	(4)	(5)	(6)
50	2×10^{41}	2×10^{41}	3×10^{4}	5×10^{18}	3×10^{22}	9×10^{17}
100	2×10^{35}	1×10^{36}	4×10^{3}	9×10^{14}	9×10^{17}	2×10^{14}
150	4×10^{30}	10^{32}	8×10^{2}	1×10^{12}	3×10^{14}	4×10^{11}
200	8×10^{26}	8×10^{28}	2×10^{2}	7×10^{9}	7×10^{11}	3×10^{9}
250	8×10^{23}	2×10^{26}	8×10	1×10^{8}	5×10^{9}	5×10^{7}
300	3×10^{21}	2×10^{24}	4×10	3×10^{6}	7×10^{7}	2×10^{6}

Reaction (1) is the target reaction (CO oxidation), while reaction (2), H_2 oxidation, is in competition with (1) and is also undesired because leads to the consumption of the product of the *fuel processor*, which must be fed to the *fuel cell*.

Both reactions (1) and (2) exhibit high equilibrium constants and thus in the range of the operation temperature they can be considered irreversible. Reaction (3) represents the inverse CO-shift, reaction (4) represents the Boudouart equilibrium and reactions (5) and (6) the methanation reactions. Coke formation (4) is by far unwanted, because coke deposition on the solid surface leads

to catalyst deactivation. Also reactions (2), (5) and (6) are undesired because reduce the selectivity of the process.

Due to the very low values of the equilibrium constant exhibited between 50 and 300°C, the reaction of inverse CO-shift (3) deserves careful consideration. In fact, the CO-shift reaction might represent a thermodynamic limit to CO conversion in the operational temperature range.

In the operating temperature range, the characteristic times of the inverse shift reaction in the homogeneous phase are extremely long, and hence it can be concluded that this reaction does not represent a limiting stage to CO preferential oxidation, unless the CO-PROX catalyst is also active towards the shift reaction. In this case the residence time in the CO-PROX reactor must be set to such a value that the inverse shift reaction can not proceed.

One of the requirements for CO-PROX catalysts is the high activity and hence very short characteristic reaction times for CO oxidation, due to the short residence time in the CO-PROX reactor. Since high H_2 flow rates are required by the fuel cell to supply the power for automotive applications (~20kW), very high flow rates must be fed to the fuel processor (i.e. 400 slpm for 20 kW). Moreover, due to the limited space available on-board, the volume usable for a CO-PROX reactor is relatively small (~1-2liters). Large flow rates and reduced volume imply residence times in the CO-PROX reactor of the order of 10^{-1}s (0.15-0.3s), which are short in comparison to the low operation temperature.

In conclusion, a good CO-PROX catalyst is required to be:

- very active towards the oxidation of CO (reaction 1);
- very selective towards the oxidation of CO (1). High selectivity means not only a reduced consumption of the fuel (H_2), but also to operate the process with lower O_2 concentration, and hence with less explosive mixtures;
- active at low temperature. The operational CO-PROX temperature is defined by the fuel processor (80-200°C);
- resistant to the deactivation caused by the presence of CO_2 and H_2O in the stream;
- not active towards the reaction of inverse CO-shift (3);
- deposited on a structured support, with low pressure drops at the process flow rates.

1.4 Catalytic systems for the CO-PROX reaction: state of the art

The catalysts which were first investigated for the preferential oxidation of CO at low temperature were chosen among the catalysts for the CO oxidation at low temperature.

Noble-metal based catalysts (Pt, Ru, Rh) exhibited interesting performances related to the possibility to operate under a variety of operating conditions, especially in the presence of CO_2 and H_2O, although not particularly selective (Oh and Sinkevitch, 1996; Kalich, 1997; Liu, 2002). Moreover, their use is penalized by the fact that above a critical temperature (~200°C) noble-metal based catalysts may catalyse the water gas shift (WGS) reaction, thus limiting the CO conversion; in addition they are expensive and their performances has been outscored by non-noble-metal based catalytic systems, recently investigated.

Pt-based catalysts are usually classified as high temperature catalysts on the basis of the temperature range of interest for CO-PROX; in fact their optimal operating temperature is about 200°C (Kahlich, 1997; Iragashi 1997; Dudfield, 2000b; Korotkikh, 2000; Manasilp, 2002;).

The main advantage of Pt-based catalysts is that they exhibit a good resistance to the presence of reformate species (CO_2 e H_2O) and on the contrary it has been found that on these catalytic systems H_2 and H_2O have a promoting effect on the CO oxidation reaction (Avgouropoulos, 2002).

Nevertheless Pt catalysts exhibit low intrinsic activity in promoting CO rather than H_2 oxidation. The constant value of the CO selectivity (~40%) measured in a wide range of temperatures (170-300°C) suggests that the activation energies of the two oxidation reactions in competition (CO and H_2) are comparable. Remarkably, the relative value of CO selectivity is quite high when compared to the extremely low CO/H_2 feed ratio, and can be attributed to the strong adsorption of CO on Pt surface, thus reducing the access of H_2 to the reaction sites.

Among the noble metal catalysts, Rh-based catalysts exhibit the lowest CO selectivity (~25%; Tanaka, 2003;), while on the Ru-based ones, CO conversion occurs via the metanation reaction, hence wasting large amounts of H_2 (Worner, 2003; Snytnikov, 2003; Marino, 2004).

More recently, gold based catalysts were investigated for the CO-PROX reaction. They exhibited very good performances in terms of both activity and selectivity in the presence of CO_2 or H_2O in the feed (Schubert, 2001 a-b; Bethke, 2000; Grisel, 2001).

Au catalysts may be operated in the low temperature range (80°C) and show an intrinsic capability to oxidise preferentially CO rather than H_2, hence with an activation energy for CO conversion remarkably lower than for H_2 conversion (Haruta, 1993; Torres and Sanchez, 1997; Kahlich, 1999; Schubert, 1999).

The high selectivity of these catalysts was attributed by many authors to the nano-dispersion of gold as microclusters, while the activity was associated to the interaction with the support, whose role is to increase the oxygen availability for the active phase, thus enhancing the reaction rate (Schubert 2001 a-b)

The limit to the application of gold based catalysts is due firstly to the scarce resistance to CO_2 and H_2O in the gas stream (Avgouropoulos, 2002), which depresses to a great extent the catalytic performance, and secondly to the difficulties of the preparation of the catalyst, which exhibits a significant activity only when dispersed on the support in the form of microclusters with an average size lower than ~10 nm.

An alternative to noble metals are represented by some transition metals oxides, whose activity may be in some cases comparable to that of noble metals, but with lower cost. In particular, cobalt (Simont, 1997; Janson, 2002; Lin, 2003;) and copper oxides (Fuller, 1974; Liu, 1995a-b, Xia, 1999; Radwan, 2003) show good catalytic properties for the low temperature reaction of CO oxidation.

Cobalt based catalysts were screened (Teng et al. 1999; Omata, 1996) for the CO preferential oxidation showing good performances, probably related to the low tendency of these systems to adsorb H_2 (Nicholls, 1990). Nevertheless the limit of these systems is bonded to the high tendency to form carbonate in the presence of CO_2 which poison the catalyst.

At this stadio the only viable alternative to the noble metals are copper-based catalysts supported on cerium oxide (CeO_2, ceria). These systems exhibit activity and selectivity comparable to golden based catalysts, but an increased resistance to CO_2 e H_2O (Avgouropoulos, 2000). These catalysts may be operated at temperature around 150°C, and probably show an intrinsic activity to oxidise CO rather than H_2.

The high performance of copper-ceria catalysts should be ascribed to the strong interaction between the active phase (CuO) and the support (CeO_2), generated by the elevated concentration of structural defects of the cerium oxide (Trovarelli, 2002).

CeO_2 is known as the main constituent of Three Way Catalysts, which are employed in the automotive mufflers for the concurrent abatement of CO, NO_x and HC in the exhaust gases (Trovarelli, 1996). It is particularly suitable for this applications due to the remarkable characteristics of *oxygen storage* (OS) and redox activity. These features are related to its microscopic structure: ceria has a crystalline structure of fluorite type, and is hence rich in defects, which determine high ionic conductivity and high electric conductibility. Defect concentration of ceria can be further increased by doping with ions having similar charge and ionic radius. In particular, doping ceria with zirconia leads to the increase of the high temperature stability and of the redox and OS properties.

The good catalytic performances of copper oxides supported on cerium oxides and ceria-zirconia are hence due not only to the active phase highly dispersed due to the large surface area of the support, but above all to the active role of ceria and/or ceria/zirconia in the reaction as *oxygen supplier*.

Actually CuO/CeO_2 systems have been widely studied for the CO oxidation reaction at low temperature, while up to now no mechanicistic study have been performed for the CO-PROX reaction.

Indeed, in the scientific literature the CO-PROX reaction mechanism occurring on copper ceria systems has not been clarified and is still debated, neither the kinetics of oxidation of CO with large excess of H_2 has been characterized. Moreover, the CO_2 and H_2O addition effect on the kinetics of the process has not been clarified nor described.

1.5 Aim of the work

Use of noble metals based catalysts in the preferential oxidation of CO appears disadvantageous for both the elevated costs and the lower intrinsic selectivity (Pt) or high sensitivity to the presence of CO_2 and H_2O (Au). On the other hand, transition metal oxides represents a cheap and viable alternative for those processes traditionally based on noble metals catalysts, even though, in order to be active at the very low temperatures required in the CO PROX (80-250°C), transition metal oxides must be dispersed on supports with high surface area.

The recent discover of the properties of high activity and selectivity in the CO PROX process of copper oxide catalysts supported on ceria renewed the interest towards materials other than noble metals. However, despite the potentiality as CO-PROX catalyst of CuO/CeO_2 and the relevant number of recent publications devoted to this subject, no significant mechanicistic studies have been reported yet, and important aspects such as the reaction kinetics, the identification of active phases and the properties of catalyst that makes it selective in the oxidation of CO rather than of H_2 appear to be not satisfactorily investigated. Actually, there are a lot of investigations on the catalytic properties of the catalyst, especially in relation with the preparation procedure, while the activity in the reaction is not widely investigated. The oxidation of CO at low temperature over such a catalyst has been very studied too, but the presence of high H_2 concentrations as well as large amounts of CO_2 and H_2O, as in the CO PROX process, is expected to strongly modify the proceeding of CO oxidation, as well as the capability of catalyst to convert CO to CO_2, without promoting the oxidation of the much larger amounts of H_2 present in the reacting mixture is not a trivial matter.

For all these reasons, this work is an investigation which mostly focuses the attention on the reaction mechanism and kinetics rather than to the study of the properties of catalyst. The catalytic system under investigation is constituted by the active phase (CuO) and the support, which is ceria, eventually doped with zirconia. The choice of CeO_2 is related to its peculiar characteristics of "active" support, capable of activating the metal-oxygen bond of the active phase and/or of releasing oxygen atoms with high reactivity. Among such active supports, cerium oxide is well known for its oxygen storage capacity, strictly related to its structural properties. Moreover, supporting a metal oxide on ceria, strong-metal-support interactions between the active phase and the support are generated and consequently a strong enhancement of redox properties and thermal stability of catalyst may be expected.

Aim of this work will be hence the study of CuO/CeO_2 system for the CO PROX reaction with a special attention to all those aspects, such as the reaction mechanism, the identification of active species and the nature of process selectivity, that seem less investigated up to now.

First of all, the influence of catalyst composition on the properties of the system will be assessed. The use of mixed ceria-zirconia oxides instead of pure ceria, as well as the use of catalyst at different CuO content will be evaluated, discussed and tested.

Catalyst will be prepared basically by impregnation technique. The materials will be characterised by means of XRD, BET, and TEM analyses. The activity of catalysts and the reaction kinetics will be measured under experimental conditions very representative of the application of interest: large H_2 concentration (50%), very low CO impurity (1000-5000 ppm), eventual presence of carbon dioxide and water vapour, contact times and temperature of realistic interest.

The work will be focused mainly on the origin of the high selectivity showed by this system in CO-PROX reaction which is still unclear. Strictly linked to this aspect is the interest towards the identification of the chemical species responsible for the high activity and selectivity of the catalyst. Such an investigation will be made by deeply studying the redox properties of catalyst sites, by means of TPR/TPD/TPO techniques (Temperature Programmed Reduction/Desorption/Oxidation), using H_2, CO and CO_2 as probe molecules. As a consequence, the reaction path activated by the catalyst during the reaction of CO oxidation in H_2 rich stream which is still little debated, could be discussed in more details.

CHAPTER 2

CuO/CeO_2 CATALYSTS: STATE OF THE ART

2.1 CuO/CeO_2 catalysts activity

$CuO\text{-}CeO_2$ catalytic systems has been examined for several processes including selective CO oxidation (Avgouropoulos, 2001-2002, Hocevar, 2001), but also catalytic wet oxidation of phenol (Hocevar, 2000), SO_2 reduction (Liu, 1996), NO reduction (Bera, 1999), and methane oxidation (Liu, 1995a-b). All these processes involves oxidation-reduction steps which are promoted by the presence of ceria in comparison to traditional copper based systems.

In 2001 Avgouropoulos tested CuO/CeO_2 systems for the reaction of CO oxidation in H_2 rich streams. A sample containing low copper concentration (6wt%) and relatively low surface area ($16m^2/g$), prepared via coprecipitation method, showed catalytic performances higher than noble metals based catalysts traditionally used for this application with 95% conversion at 200°C and 60% selectivity. Moreover these systems showed a very high selectivity (namely 80%) in a wide range of temperature (up to 150°C corresponding to 80% selectivity).

Since this work, different preparation methods were proposed for the copper-ceria catalysts, due to the large interest, not only in CO-PROX but in all the low temperature oxidation reactions.

Sedmak (2003) tested CuO/CeO_2 systems prepared via sol-gel method for the CO-PROX reaction obtaining a significant increase of the catalyst activity with 100% conversion at 100°C and 40% selectivity. A higher activity of catalysts prepared via sol-gel is also observed for the catalytic wet oxidation of the phenol, application in which the system is four time more active and 25% more selective than those prepared via co-precipitation methods.

Also CuO/CeO_2 catalysts, prepared by urea-nitrate combustion method, have been tested in CO-PROX without showing remarkable improvements (Avgouropoulos, 2003), but on the contrary a high dependence of the catalyst performances on the urea/nitrate ratio.

Wang (2002) proposed for CO-PROX systems based on copper and supported on ceria doped with samaria. The presence of a cation Sm^{+3} in the support generate in the ceria structure a charge defect which must be compensated with the vacancy formation. An increase of the vacancy concentration, increases the oxygen ion mobility in the structure, thus increasing the redox properties of the system. In relation to the CO-PROX reaction, the catalyst activity increases compared to CuO/CeO_2 catalysts prepared via coprecipitation methods but the selectivity decreases.

Actually catalytic systems based on copper oxide supported on ceria were firstly introduced by Liu et al. (1995a-b) for the low temperature CO oxidation in oxygen rich conditions, application in which those systems showed a high activity revealed by a significant decrease of the isoconversion temperature with respect to more conventional alumina-supported copper, or unsupported copper oxide, thus suggesting a promoting effect of ceria on the catalyst performances. The authors explained the increased activity of these catalysts by the stabilization of Cu^{+1} in catalysts prepared via coprecipitation methods, originated from the interaction between copper clusters and cerium oxide, and addresses to ceria the role of oxygen source. These conclusions were also supported by the study of Jernigan and Somorjai (1994) which demonstrated that the apparent activation energy for CO oxidation increases with increasing the oxidation state of copper by studying the reaction on Cu, Cu_2O, CuO foils and in oxygen lean conditions. Anyway it must be highlighted that catalysts supported on ceria, because of the high degree of interaction between active phase and support, are chemically completely different from copper foils. Moreover the different reaction conditions may influence the kinetics of the process.

The presence of Cu^{1+} in CuO/CeO_2 was also detected in samples prepared by co-precipitation method tested by Hocevar et al. (2000) for the catalytic wet oxidation of phenol and by Avgouropoulos (2001) for the CO preferential oxidation.

Nevertheless, Sedmak et al. (2003) demonstrated that it is possible to increase the CuO/CeO_2 catalytic performances by using a sol-gel preparation method. On these systems, characterization analysis evidenced the absence of interstitial copper ions, present in the samples prepared by coprecipitation, but CuO phase was finely dispersed on the surface of large CeO_2 crystallites (Hocevar, 2000). These high dispersed copper clusters are believed to play a key role in the enhancement of activity of these catalysts.

Thus, in contrast with Liu et al. (1996) who supposed that the stabilizing effect of ceria on certain redox states of copper is the main reason for better catalytic performances, Martinez- Arias et al. (1999-2004) supposed that the facile redox interplay between the two components is the key factor of high catalyst performances.

2.2 CuO/CeO_2 catalysts redox properties

2.2.1 Structural characteristic and properties of the cerium oxides

Nowadays the main use of ceria (CeO_2) is in the Three-Way-Catalysts, which are employed in the automotive mufflers for the concurrent abatement of CO, NOx and HC in the exhaust gases (Trovarelli, 1996). Under real operating conditions, where the engine regime depends on the traffic conditions, the exhaust gases can be either in oxidant or reducing conditions. Hence the use of ceria is specifically advantageous, due to its capability to store oxygen under oxidant conditions and to give it back under reducing conditions. The *oxygen storage capacity* (OSC) is strictly linked to the structural characteristics of the oxide, which are dependent on the preparation procedure, on the presence of dopants and on possible treatments after preparation.

The cerium atom is present in two oxidation states, +3 and +4, and hence can form oxides ranging from Ce_2O_3 to CeO_2. Metallic Ce is unstable in the presence of oxygen, which leads very easily to the formation of oxides, whose stoichiometry strongly depends on temperature and on the partial pressure of oxygen. In particular, at 300°C and for extremely low O_2 partial pressures (10^{-93}atm), metallic cerium is oxidised, forming Ce_2O_3, but for O_2 partial pressures above 10^{-40}atm, it is further oxidised to CeO_2 (Trovarelli, 2002).

CeO_2 has a fluorite type structure (figure 1.3). The elementary cell has a face centred cubic structure for the cerium ions, with all tetrahedral positions occupied by oxygen ions ($N.C._{Ce} = 8$; $N.C._{O} = 4$). From another point of view, the structure can also be considered as a row of cubic cells of oxygen ions, whose centre is alternatively occupied by cerium ions (figure 1.3b). In the CeO_2 structure a large number of octahedral vacancies are present, as shown in figure 1.3, strongly enhancing the ions mobility through the structural defects.

In the catalyst field, fluorite oxides have been occasionally explored as catalysts for the oxidation of carbon monoxide and methane (Claudel, 1969). A redox mechanism involving lattice oxygen/oxygen vacancy participation was proposed for the oxidation of carbon monoxide on cerium oxide (Breysse, 1972)

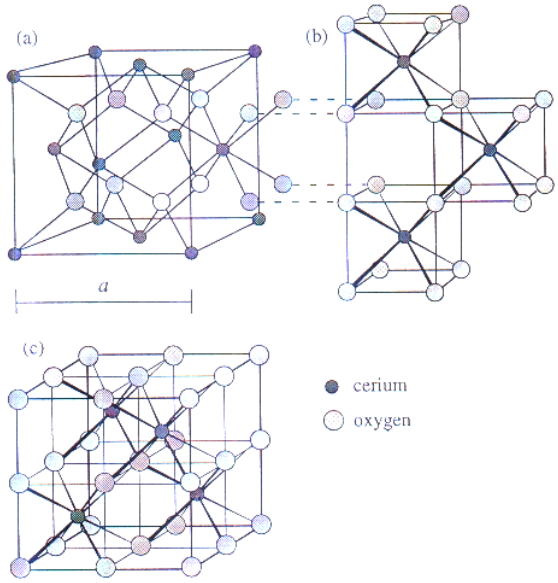

Figure 2.1: Structure of CeO_2: (a) unit cell depicted as a cfc array of cerium atoms; (b) and (c) same crystal depicted as a row of cubic cells of oxygen (Trovarelli, 2002)

In this mechanism the controlling step is the diffusion of the oxygen ions which depends on the level of stoichiometry of ceria. In particular, by reducing the level of stoichiometry of ceria, the diffusion of oxygen in the solid increases. This can be explained in terms of a reduction of the activation energy for creating defects and moving them at decreasing the level of stoichiometry. The diffusion of oxygen ions in ceria lattice can hence be increased by increasing the defect concentration.

Ceria can present intrinsic or extrinsic defects. Intrinsic defects are due either to thermal disorder of the structure or to the reaction between the solid and the surrounding atmosphere (redox processes), while the extrinsic defects are due either to the presence of impurities or to the introduction of dopants.

In general, intrinsic defects are present in low concentration and do not cause any deviation from the stoichiometric composition. Nevertheless, in CeO_2 it is possible to attain high concentration of intrinsic defects through exposition to a reducing environment.

An increase of the thermal stability, of the *OSC* and the redox properties of the ceria can be obtained by generation of extrinsic defects through introduction of dopants.

Indeed, the use of ceria as catalyst support was limited by its strong tendency to sintering under high temperature conditions (900°C). It was shown that by doping ceria with zirconium oxide, the thermal stability of the material is significantly increased because of the formation of a solid-solution which inhibits the sintering at high temperature.

The zirconium oxide has a cation (Zr^{4+}) iso-valent to Ce^{4+} with slightly lower dimension (0.84 vs 0.97 Å). The effect of the substitution of the Ce^{4+} cations with Zr^{4+} consists in the reduction of the unit cell volume, with consequent reduction of the activation energy of the diffusion of oxygen ions and, hence, with the consequent increase of the redox properties. The introduction of zirconium ions also increases the formation of structural defects, which play an important role in the determination of the oxidation-reduction conditions (Trovarelli, 1997; Hori, 1998; Boaro 2000-2002). Among the possible doping elements, zirconium is preferred because as already mentioned its ion has the same valence and very similar ionic radius with respect to Ce^{4+}, and can hence form solid solutions CeO_2-ZrO_2 in a wide range of zirconium concentrations. In fact, only when the dopant and the ceria form a solid solution of the two oxides, so that the fluorite-type structure is preserved and the formation of a separated phase or the lack of homogeneity due to scarce solubility are avoided, the ionic conductivity and the redox properties of the catalysts are maintained.

The main characteristic of ceria-zirconia mixed oxides is an increased oxygen storage capacity. Indeed, for pure ceria the oxygen exchange between the gas phase and the support is limited only to surface oxygen (homogeneous exchange), while the increased oxygen mobility obtained by doping ceria with zirconium extends the participation also to the bulk oxygen (heterogeneous exchange).

2.2.2 Strong metal support interactions

It is well known that, when metals are supported on ceria, their chemical properties are strongly modified (Trovarelli, 2002). The promoting effect of the cerium oxide was in a first attempt attributed to the enhancement of the metal dispersion and the stabilization of the support towards thermal sintering (Dictor, 1989) but this theory has been overcome by the observation of the enhancement of the reducibility and/or of chemisorption capability of both the active phase and support (Bernal, 1996). In particular, ceria is reduced in the presence of H_2 at a temperature higher than 500°C while in the H_2 TPR tests over Pt/CeO_2 catalysts it was evidenced a hydrogen uptake higher than that corresponding to the complete reduction of Pt at a temperature lower than 300°C (Yao, 1984; Trovarelli, 1996), suggesting the participation of ceria to the overall reduction of catalyst at relatively low temperature.

The enhancement of the redox properties has been recently explained by the occurrence of strong-metal-support-interactions between active phase and support, that is defined as a direct influence of the support on the chemisorption and catalytic properties of the metal phase across a stabilization of unusual metal particle structure obtained, by changing the electronic properties via electron transfer

processes between the metal particles and the support, or by chemical bonding -compound formation- between metal and support (Bernal,, 1999).

The supports which can generate these interactions should present a high oxygen vacancies concentration and can be divided in two classes as a function of their structure: the supports with cassierite structure like TiO_2, and those with fluorite structure like CeO_2. The difference between those two structures is that in the cassierite structure the O_2 is not caged by cations as in the fluorite one, thus the oxygen diffusion in the presence of O^{2-} vacancies is not blocked by the cation sublattice, at least in one direction (<001>).

Sanchez and Gazquez (1987) developed a model explaining in a general sense the strong-metal-support-interaction as an interaction between metal atoms with the oxygen ion lattice vacancies in the oxide supports. Accordingly, they suggest the occurrence of a "nesting" effect, consisting of the anchoring of the metal atoms/crystallites in the oxygen vacancies created at the surface of the support. In this way, they justify the good resistance against sintering of the metal phase, as well as the high chemisorption capability and catalytic activity of these systems.

The occupancy of vacancies by metal atoms is equally applicable to different oxide systems, but the resulting effects may vary strongly depending on the nature of the support.

For supports with cassierite structure (TiO_2, SnO_2) Sanchez and Gazquez (1987) suggested that, because of the open nature of the support cationic sublattice, a "high-temperature" reduction would induce the creation of vacancies at the support surface followed by diffusion of the metal atoms into the bulk of the reduced oxide. As a consequence of this effect, the chemisorptive and catalytic properties of the metal would become strongly disturbed. Subsequent "high temperature" (T>700K) reoxidation would drive the metal atoms back to the surface, so that a further mild reduction treatment would recover the chemisorptive and catalytic properties of the catalyst.

For oxide supports with fluorite-type structure, like ceria, Sanchez and Gazquez (1987) suggested that the structure of the cationic sublattice would present a high barrier to penetration of the bulk by the metal atoms. For this reason the interaction is limited at the surface.

2.2.3 Copper ceria catalysts redox properties

The strong-metal support effect on ceria has been mostly reported for noble metals supported materials. However, the system CuO/CeO_2 appears to have similar features as well.

Similarly to what observed for noble metals based catalysts (Luo, 1997; Zimmer, 2002) an enhanced reducibility of copper supported on ceria was found by TPR analysis. Indeed, reduction of copper occurring at about 300°C for alumina supported oxides (Kozlov, 2002), starts at 150°C for

CuO/CeO_2 samples. Moreover, a hydrogen consumption greater than that corresponding to the complete reduction of the all copper from the oxidation state +2 to zero has been evaluated, thus confirming the partecipation of ceria to the reduction at low temperature.

Moreover, Tang et al. (2004) in the H_2 TPR of CuO/CeO_2 catalysts observed an almost desappearance of the ceria reduction peak at 500°C attributed to the reduction of surface oxygen of CeO_2, while the peak near 900°C corresponding to the reduction of bulk oxygen of CeO_2 remaining unchanged.

These results was explained by assuming the occurance of strong-metal support interactions limited to copper and the ceria at the surface. As a consequence only a limited number of copper atoms are necessary to generate strong-metal-support-interactions (Shan, 2003). Indeed, in the Foger model, there are a limited number of anchoring sites which may generate this interaction. Increasing the copper load up to the concentration of these sites, initially independent CuO clusters easily reducible are formed, while a further increase of the copper load generates bulk CuO, which may cover the active centers thus decreasing the overall reducibility.

The degree of interaction between copper and ceria may be promoted with different preparation methods as demonstrated by Tang at al. (2004). The authors studied the redox properties of CuO/CeO_2 catalysts prepared by three different preparation methods, wet impregnation, coprecipitation, deposition-precipitation. The H_2 TPR, in dependence of the preparation method, evidenced three of four reduction peaks respectively at 130°C, 170-200°C and 210-260°C , in addition to a small hydrogen consumption at 430°C, associated to the reduction of residual surface ceria not involved in strong-metal support interactions. Samples prepared by coprecipitation exhibit a more uniform dispersion of the copper particles and a higher reducibility as suggested respectively by the TPR profiles and consumptions. The authors found a correlation between catalytic activity and redox properties or preparation method. In particular catalysts prepared by co-precipitation methods showed the best catalytic activity, that was ascribed to a more uniform dispersion and a stronger interaction between copper species and ceria.

These observations suggest that the enhanced activity showed by catalysts prepared by coprecipitation rather than by sol-gel methods (Sedmak, 2003; Avgouropoulos, 2003) is related to the increased degree of interaction between CuO and CeO_2, which increases the mutual interplay, positively affecting the redox properties and the catalytic activity.

The attribution of the reduction peaks obtained with H_2 TPR analysis could help to clarify the reduction mechanism on CuO/CeO_2 system.

When a quantitative analysis was not considered (Zheng, 1997; Kundakovic, 1998), the reduction peaks have been considered corresponding to the reduction of better and worse dispersed copper

species, not taking into account the partecipation the ceria to reduction. However, as pointed out above, such an interpretation seems not completely convincing, since from a quantitative analysis it seems sure that also a fraction of the ceria is reduced in the TPR experiment.

Nevertheless also in more recent works the reduction peak relative to the reduction of the ceria is not considered, such as for example Tang et al. (2004) which attribute the first reduction peak (~130°C) to the reduction of CuO on the ceria surface, the second peak (170-200°C) to the reduction of larger CuO species on the surface, and the third and fourth peak (210-260°C) to the reduction of bulk CuO and surface ceria.

More complex study is reported by Pintar et al. (2005), which by using the results of TPR, TPO and TPD performed on CuO/CeO_2 samples, recognize at least three reduction peaks associated to the reduction of the copper and to some hydrogen "incorporated in the catalyst structure". The latter contribution represents adsorbed hydrogen which desorbs at a temperature lower than that of at which the TPR analysis is closed. Thus, the identification of a desorption peak cannot explain the calculated value of H_2 consumption higher than that corresponding to the complete reduction of all copper in the catalyst.

Martinez-Arias et al. (1997) performed a detailed study on the redox properties of CuO/CeO_2 when using as reducing agent CO. The authors demonstrated a facile redox interplay with both reducing and oxidizing reactants. In particular, it was observed on catalysts prepared via impregnation that CO can reduce both copper and ceria already at room temperature. A simple reoxidation treatment at room temperature was able to reoxidize all the ceria and a great part of copper species. The authors postulated a redox model of CuO/CeO_2 systems in the presence of CO schematically reported in figure 4.3. First stage in the reduction process involves copper oxide and support reduction at interface positions, the latter being promoted by the copper oxide. Further progress of the reduction process appears to preferentially involve the reduction of the copper oxide microclusters extending later to support positions far from the interface. Reoxidation of the system from this latter stage involves preferentially the ceria component starting from positions far from the interface and progressing towards the interface positions.

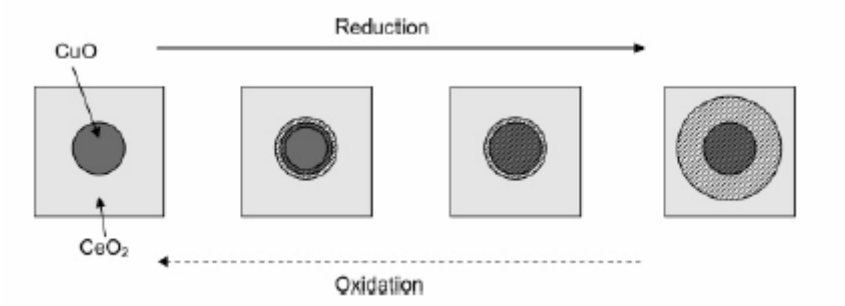

Figure 2.2: Model of redox processes in $CuCeO_2$ (Martinez-Arias et al. ,1997). Reduced regions are represented by dashed zones.

Moreover the authors leave open the debate about the identification of the species from which the reduction in the presence of CO start. Indeed, it is uncertain the possibility that the reduction takes place at interface positions thus accounting for promotion of the copper reduction by ceria, or if copper reduction activate the subsequent reduction of the borderline regions.

A slightly different system is obtained when doping ceria with zirconium. Indeed, the structural modification induced by the presence of Zr in the ceria fluorite structure strongly modify the redox properties as previously commented. As a consequence CuO/CeO_2-ZrO_2 catalysts presents an increased reducibility in comparison to ceria supported sytems, due to the promotion also of the bulk ceria to the reduction at low temperature (Ma, 2003; Kundakovic, 1998; Kozlov, 2002).

2.3 CuO/CeO_2 reaction mechanism for the CO oxidation reaction

On the basis of the structural and redox characterization studies, at low temperature a reaction path following a redox mechanism on CuO/CeO_2 catalysts, involving concomitant redox changes in the oxidation state of both active phase ($Cu^{2+} \leftrightarrow Cu^{1+}$) and support ($Ce^{4+} \leftrightarrow Ce^{3+}$) has been assumed (Martinez-Arias, 2000-2003; Shan, 2003) for the CO oxidation reaction. Thus the active sites for the CO oxidation reaction were identified in the interface sites between copper oxide and the support

The involvement of Cu^{2+}-Cu^{+} redox pair instead of other alternatives ($Cu^{2+} \rightarrow Cu^{0}$ or $Cu^{+} \rightarrow Cu^{0}$) was mainly based on the absence of spectroscopic evidence of the formation of the Cu^0 under reaction conditions, along with the quite easy restoring of the initial Cu^{2+} state upon interaction of the reduces catalyst with O_2.

More in detail the reaction path could be considered composed by four step. It is assumed that CO reacts on the active site generating CO_2 leading to generation of mainly Cu^{1+} and Ce^{3+} entities with doubly ionizated oxygen vacancies (V_O) being created at the interface between copper oxide clusters and support:

(1) $$Ce^{4+}\text{-}O^{2-}\text{-}Cu^{2+} + CO \rightarrow Ce^{3+}\text{-}V_O\text{-}Cu^{+} + CO_2$$

where Ce^{4+}-O^{2-}-Cu^{2+} is the active identified as a border line region between Cu and Ce, while Ce^{3+}-V_O-Cu^{+} represent a site with an oxygen vacancy.

Thus CO may adsorb on Cu^{1+}

(2) $$Ce^{3+}\text{-}V_O\text{-}Cu^{+} + CO \rightarrow Ce^{3+}\text{-}V_O\text{-}Cu^{+}\text{-}CO$$

The subsequent two steps are reoxidation steps. The oxygen involved in the oxidation reaction over oxide catalysts is present in two forms: surface-adsorbed oxygen and lattice oxygen ($O^{2-}_{lattice}$,) which is part of the oxide structure. Oxygen adsorbed on oxide surfaces can be present in different forms. The superoxide ion form (O_2^{2-}) and an ion radical form, O^-. There always exists a balance between these forms, which moves to the right at higher temperature (Liu, 1995a-b).

$$O_2 \leftrightarrow O_2^- \leftrightarrow O_2^{2-} \leftrightarrow O^- \leftrightarrow O^{2-}_{lattice}$$

Martinez Arias et al. (2000) proposed a reoxidation model which passes through the formation of an intermediate $O_2^- - Ce^{4+}$ showed at the interface by EPR analyses. The oxidation process progresses towards the formation of peroxide (step 3) or, going further, oxide species (step 4) with concomitant copper reoxidation thus closing the redox cycle:

(3) $Ce^{3+}\text{-}V^{O}\text{-}Cu^{+}\text{-}CO + O_2 \rightarrow Ce^{4+}\text{-}O_2^{-}\text{-}Cu^{+} + CO \rightarrow Ce^{4+}\text{-}O_2^{2-}\text{-}Cu^{2+} + CO$

(4) $Ce^{4+}\text{-}O_2^{2-}\text{-}Cu^{2+} + Ce^{3+}\text{-}V_O\text{-}Cu^{+}\text{-}CO \rightarrow 2Ce^{4+}\text{-}O^{2-}\text{-}Cu^{2+} + CO$

In stoichiometric conditions between CO and O_2, the rate determining step was attributed, mainly on the basis of in situ DRIFTS study, to the oxidation process and, in particular, to the steps involving oxygen dissociation or oxygen migration towards the oxygen vacancies.

On the basis of this reaction mechanism it was possible to explain also the observed lower activity of CuO/CZ catalysts for the CO oxidation reaction (Martinez- Arias, 2000).The lower activity of the samples supported on ceria-zirconia supports was explained with the lower redox activity of the interface sites. Indeed, despite of the increased overall reducibility of the sample, isothermal experiments performed at low temperature (100°C) showed not only a lower reducibility of copper oxide cluster on CZ supports but also a slower rate of oxidative steps (Martinez- Arias, 2000).

Also more recent proposals (Hocevar, 2004), based on kinetic modelling of redox changes of Cu-Ce catalysts under CO and O_2, suggest redox exchanges between Cu^{2+} and Cu^{1+} (and concomitantly Ce^{4+} and Ce^{3+}) as the main steps involved in the CO oxidation reaction mechanism.

A somewhat different mechanistic proposal has been recently put forward by Wang et al.. In their approach, the reaction is proposed to take place in two general sets of processes involving, respectively an induction and a light-off period. Although a role of interface vacancies at the support is recognized, this role appears to be mainly limited to facilitating oxygen activation during the induction steps prior to light-off while sites active during the light-off period are proposed to be related to oxygen vacancies on the top of the copper oxide component. However, a recent work on a $CuO_x/CeZrO_2$ system (Martinez-Arias, 2004) suggests that the CO oxidation reaction takes place exclusively at interface sites with a certain reductive preactivation of the copper oxide component apparently occurring just prior to reaction onset. The existence of induction periods within processes related to copper oxide reduction has been also observed during reduction under CO of bulk CuO and Cu_2O; the same study proposed that the magnitude of the induction time decreases with the introduction of defects and imperfections in the copper oxides.

Actually, recent studies of Martinez-Arias et al (2003) performed on Cu/CZ catalysts in the contemporary presence of CO and NO suggest that the copper oxide component is reductively pre-activated prior to the onset of CO oxidation.

2.4 Kinetic investigations on CuO/CeO_2 catalysts

Most of the recent works on the preferential oxidation of CO are focused on catalyst formulation, characterization, and basic performance such as activity and selectivity of CO. Few papers have investigated the kinetics and rate expressions of the reaction involved. Actually such features are strongly correlated to the reaction mechanism and could contribute to elucidate it.

For precious metal catalysts, several different kinetic studies and consequent rate expressions have been reported for the CO oxidation at low temperature. Amphlett et al. (1996) developed a simple first order rate expression for CO oxidation on a platinum/alumina catalysts. Kahlich et al (1997) and Kim et al.(2002) modelled the kinetic of CO oxidation in hydrogen rich mixture by a power law kinetics obtaining a negative apparent reaction order for CO and an apparent reaction order for oxygen of 0.82 and 0.76, respectively. Very recently, Choi et al. (2004) proposed a reaction model in which three reactions (CO oxidation, H_2 oxidation, and the water-gas-shift reaction) occur simultaneously to predict the PROX reactor performances. Using non-linear least squares, empirical power-law type rate expressions were found to fit the experimental data. It was critical to include all three reactions to obtain good fitting results. In particular, the reverse water gas shift reaction had an important role for a good fitting the experimental data and if explained the selectivity decrease at higher reaction temperatures and the typical appearance of a maximum in CO conversion as a function of the temperature.

For what concerns CuO/CeO_2 catalysts it is now widely accepted that both CO and H_2 oxidation reactions involve molecular oxygen over metal oxide catalysts and proceed by a redox mechanism (Bielanski, 1991; Golodets, 1983). In particular, CO oxidation over the nanostructured $Cu_xCe_{1-x}O_{2-y}$ catalysts was confirmed to obey this type of reaction scheme (Martinez-Arias, 2002). According to Lamonier et al. (1999) the oxidation of H_2 over the $CeCu_xO_y$ mixed oxide occurs through the same redox mechanism.

Such a redox mechanism can be generally described by the following two-step scheme:

$Cat\text{-}O + Red \rightarrow Cat + Red\text{-}O$

$Cat + Ox\text{-}O \rightarrow Cat\text{-}O + Ox$

The first step is the catalyst reduction: Cat-O represents oxidized catalyst site reduced by a reductant (Red). The second step represents reoxidation of the catalyst by the oxidant (Ox-O), which donates an oxygen atom to the catalyst while it is reduced.

On the basis of those considerations, Liu (1995b) found that the experimental data collected in CO oxidation conditions in large oxygen excess on $CuO\text{-}CeO_2$ catalysts, were fitted with a good approximation by the expression :

(1) $$r_{CO2} = \frac{k_{CO} \cdot K_{CO} \cdot P_{CO} \cdot P_{O2}^{n}}{1 + K_{CO} \cdot P_{CO}}$$

The authors estimate experimentally the kinetic constant and the CO adsorption constant. When using the rate expression (1) with the estimated constant values a good data fitting was obtained.

Experimentally the authors observed the P_{CO} reaction order to decrease from one to zero as P_{CO} increases, while a very weak dependence on the P_{O2} is observed at constant P_{CO}, indeed the estimated value for n is 0.08.

Actually, a first order dependence on P_{CO} is expected for equation (1) if the partial pressure of CO (P_{CO}) is low enough for $K_{CO}P_{CO}<1$. For higher P_{CO} the apparent CO reaction order decreases. The same happens by decreasing the temperature because the CO adsorption constant (K_{CO}) increases.

On the basis of the redox model, the equation (1) has been interpreted by the authors in term of a LH mechanism. They postulated a kinetic model in which some copper species, identified for a catalyst prepared by co-precipitation, as Cu^{+1} ions, provide sites for CO adsorption, while cerium oxide provides the oxygen source. The reaction proceeds at the boundary of the two kinds of materials.

The rate equation proposed by Liu (1995b) has been recently compared by Sedmak et al. (2004) with a Mars and van Krevelen type kinetics (2) and used to fit data set collected at temperature below 90°C. At those temperatures the authors verified the absence of the hydrogen oxidation reaction, thus taking into account only of kinetics of CO oxidation in the regression:

(2) $$r_{CO2} = \frac{k_{CO} \cdot k_{O2} \cdot P_{CO} \cdot P_{O2}^{n}}{0.5 \cdot k_{CO} \cdot P_{CO} + k_{O2} P_{O2}^{n}}$$

The parameters k_{CO} and k_{O2} in the equation (2) are the reaction rate constants for the reduction of surface by CO and reoxidation of it by O_2. The parameters k_{CO} and k_{O2}, and n were obtained at a given temperature by fitting experimental values of P_{CO}, P_{O2}, and reaction rate with equation (2). The parameter n has been estimated n= 0.2±0.05.

In the temperature range investigated (RT- 90°C), both the LH and Mars and van Krevelen kinetics fit the experimental data very well. Neverthless transient experiments performed by Hocevar et al. (2003) suggested the involvement of lattice oxygen even at low temperature, thus recommending the use of a steady state Mars and van Krevelen kinetic model.

CHAPTER 3

EXPERIMENTAL

3.1 Preparation of catalysts

Copper/ceria and copper/ceria-zirconia catalysts, have been prepared via wet impregnation method by using copper acetate (Aldrich) as copper precursor and commercial oxides ceria and ceria-zirconia (GRACE) as supports.

The ceria and ceria-zirconia mixed oxides were provided by GRACE company which prepared the support on the basis of a procedure patented by prof. Trovarelli able to obtain solid solution formation between CeO_2 and ZrO_2 for each zirconium percentage in ceria. After the synthesis the supports have been calcined up to 800°C.

Characterization analysis have been provided by the University of Udine. In table 3.1 the results of BET and TPR analysis performed up to 800°C are reported. In particular the reduction temperature for each sample and the formula corresponding to the catalyst reduction degree measured at the end of the TPR analysis are reported.

Table 3.1: ZrO_2 weight percentage, surface areas and supports reduction degree up to 800°C, for ceria and ceria-zirconia supports.

Sample	**wt% ZrO_2**	**BET (m^2/g)**	T^1_{max} ; T^2_{max}	**Final support formulation**
CeO_2	0	56	550;840	$CeO_{1.8}$
$Ce_{0.75}Zr_{0.25}O_2$	20	71	550	$CeO_{1.75}$
$Ce_{0.44}Zr_{0.56}O_2$	48	93	560	$CeO_{1.59}$
$Ce_{0.28}Zr_{0.72}O_2$	65	101	580	$CeO_{1.51}$

The supports show an enhanced reducibility with increasing the zirconium content due to the larger defect concentration related to the formation of a solid-solution between CeO_2 and ZrO_2.

Deposition of copper oxide was performed in an rotating evaporator at 50°C, 80mbar and with a velocity of 120rpm.

The samples were subsequently calcined in air at 450°C for 2h. The calcination temperature have been chosen by considering that the decomposition of copper acetate occurs within 300°C, as determined by thermogravimetric analysis.

In the following, the notation "x CuO/CeO_2" will be used to indicate catalysts supported on ceria with "x" the CuO weight percentage while the notation "x CuO/CZ (n/m)" represents catalysts supported on ceria-zirconia where "n" and "m" are the weight percentage of the two oxides in the support respectively.

A list of the all catalysts and supports used in this work is reported in the following table were the theoretical copper content is calculated on the basis of ceria and copper acetate used in the preparation method.

Table 3.2: List of catalysts prepared and supports. Theoretical zirconium and copper percentage and catalyst code.

Sample Molar composition	wt% ZrO_2	wt% CuO	Catalyst code
CeO_2	0	0	CeO_2
$Ce_{0.75}Zr_{0.25}O_2$	20	0	CZ (80/20)
$Ce_{0.44}Zr_{0.56}O_2$	48	0	CZ (52/48)
$Ce_{0.28}Zr_{0.72}O_2$	65	0	CZ (35/65)
CuO/CeO_2	0	2	2 CuO/CeO_2
CuO/CeO_2	0	3.5	3.5 CuO/CeO_2
CuO/CeO_2	0	4	4 CuO/CeO_2
CuO/CeO_2	0	4.5	4.5 CuO/CeO_2
CuO/CeO_2	0	5	5 CuO/CeO_2
CuO/CeO_2	0	8	8 CuO/CeO_2
CuO/CeO_2	0	9	9 CuO/CeO_2
$CuO/Ce_{0.44}Zr_{0.56}O_2$	20	5	5 CuO/CZ (80/20)
$CuO/Ce_{0.44}Zr_{0.56}O_2$	48	5	5 CuO/CZ (52/48)
$CuO/Ce_{0.44}Zr_{0.56}O_2$	48	7	7 CuO/CZ (52/48)

3.2 CHARACTERIZATION OF CATALYSTS

The catalysts have been characterized by means XRD, TEM, BET, temperature programmed analysis, adsorption measurements, while the effective copper percentage on the copper based catalysts has been obtained by spectrophotometric analysis.

3.2.1 Spectrophotometric analysis

The copper content in the catalysts has been evaluated by spectrophotometric analysis by dissolving 0.1g sample in a 4ml water solution containing 50% HF at 150°C for 5min. After diluting to 1 liter, pH was adjusted to 4-5 (for pH>5 ceria precipitation was observed) with NH_4OH. In the resulting solution CuVer2 (Hach) reactant, containing bicinconinic acid which forms violet complexes with copper, has been added. Copper concentration in the solution has then been evaluated with an UV Hach-Drel/2000 spectrophotometer at 560 nm.

3.2.2 XRD

XRD analysis were used for crystal phase identification. XRD were performed on a Philips PW 1710 Diffractometer with Rotating Anode Generators and monochromatic detector using Cu K_α radiation.

The data were elaborated by applying the Scherrer equation for an estimation of the mean particle size. Estimation of FWMH was made by using the program Peakfit.

The Sherrer equation may be written as:

$$D = \frac{\lambda}{B \cdot \cos(\theta)}$$

Where D is the mean particle size, B is the Half Width at the Maximum High (FWMH) of Miller index (111) ceria plane, θ is the diffraction angle in correspondence of the main diffraction peak, and λ is the wavelength.

3.2.3 TEM analysis

The ceria mean crystallite size evaluated by XRD analysis have been confirmed also by TEM analysis performed in the Philips EM2085 microscope.

3.2.4 BET

Specific surface area of the fresh, heat-treated catalyst samples was determined by the multi-points BET methods by means of a Carlo Erba Sorptomatic 1900.

3.2.5 Reduction-oxidation measurements

The reduction and oxidation measurements were performed in the same experimental apparatus used for the reaction tests.

Samples (0.3g) with a mesh size 200-300μm were placed in the quartz tube. A reaction gas flow of 14Nl/h downward the reactor was stabilized by mass flow controllers.

The TPR and TPO measurements were performed with a heating rate of 10°C/min.

Nitrogen with 99.9999% purity level has been used as a diluent for reduction-oxidation analysis.

In all these studies, in order to remove carbonate and hydrate adsorbates from the surface, the samples were pretreated by heating in O_2 at 400°C, cooled down in O_2, and successively purged in N_2 for 1/2h before staring the analysis. In addition a preliminary TPR measurement and reoxidation was performed and the data discarded, because the TPR profiles were found to become reproducible only after a first such cycle.

A standard reoxidation treatment of a reduced sample is performed at 430°C and consist in a purging treatment in N_2 for 10min and subsequently in a reoxidation in 1vol% oxygen stream (Q=14Nl/h) for 1h.

The reduction peaks in the concentration profiles were integrated after baseline subtraction. The absolute amount of reacted gases was then quantified from the total gas flow.

The quantitative results have been reported as micromoles of reductant consumed per gram of catalyst, and by rationing the micromoles of reductant consumed with the amount of copper in the sample (H_2/Cu or CO/Cu). This ratio is equal to one if the H_2 consumed corresponds to the complete reduction of the all copper from the oxidation state 2+ to zero.

The reduction peak have been deconvoluted by the use of the software PeakFit.

The operating conditions for the temperature programmed analysis were chosen by evaluating the Monti and Baiker (1983) factor K defined as

$$K = \frac{n_0}{(F \cdot C_0)}$$

where:

n_0 = numer of reducible species in the sample (μmoli)

F = flow rate (cm^3/s)

C_0 = concentration of the reducing specie in the gas phase ($\mu moli/cm^3$).

This factor is useful for evaluating experimental conditions in which the reducing peak are well discernable. Assuming 300mg of catalysts loaded, a flow rate of 14Nl/h; 1-2vol% as reductant concentration in the stream, and a number of oxidant species in the catalyst 1-1.5 times the number of copper atoms the factor K is in the range 55-110 as recommended by the authors.

3.2.5.1 H_2 TPR

H_2 TPR analysis have been performed by using a mixture of 2 vol% H_2/N_2 with an overall flow rate of 14Nl/h. The sample was stabilized 10 min in H_2 stream at room temperature, subsequently the temperature was raised up to 430°C. At this temperature 1/2h was waited for recovering the baseline. At 400°C, a slight catalyst reduction attributed to the surface ceria occurs (see paragraph 6.1). This contribution has not been evaluated in our calculation because it represent ceria not involved in strong-metal-support interactions.

H_2 TPR on pure CeO_2 and CZ (52/48) have been performed up to 800°C.

3.2.5.2 CO TPR

CO TPR analysis have been performed by using a mixture of 1 vol% CO/N_2 with an overall flow rate of 14Nl/h. The sample was stabilized 1/2h in CO stream at room temperature, subsequently the temperature was raised up to 430°C. At this temperature 1h was waited for recovering the base line. At 430°C, carbonate formation which decomposes between 500-700°C does allow the carbon balance to be closed. For this reason, when it possible CO TPR was performed up to 1100°C, a temperature at which the reducing phenomena may be considered finished.

3.2.5.3 CO and H_2 TPR

When CO and H_2 are are fed as reducing agent a mixture containing a 0.8vol% CO and 1.5vol% H_2 in N_2 has been used (Q=14Nl/h).

After stabilizing the sample for 1/2h at room temperature in the mixture the temperature is raised up to 430°C (10°C/min).

3.2.5.4 CO_2 and CO TPD

CO_2 TPD has been performed by saturating the catalyst with 1vol% CO_2/N_2 mixture (Q=14Nl/h) for 1h, then washed in N_2 (Q= 14Nl/h) for 1/2h before starting the temperature ramp (10°C/min).

A similar procedure has been also followed for CO TPD analysis. In this case the sample was saturated in 1vol% CO/N_2 mixture (14Nl/h) for 1/2h, then washed in N_2 (Q= 14Nl/h) for half an hour before starting the temperature ramp (10°C/min).
CO TPD on pre-reduced samples have been also performed. The sample has been reduced in H_2 at a fixed temperature, then washed in nitrogen for 1/2h at the reduction temperature, and cooled down in N_2 up to room temperature before CO saturation.

3.2.5.5 TPO

The TPO analysis have been performed on samples prereduced at 430°C, washed in N_2 at 430°C for 1/2h and cooled down in N_2. A mixture of 1 vol% O_2/N_2 with an overall flow rate of 14Nl/h has been used. The sample was stabilized 1/2h in O_2 stream at room temperature, subsequently the temperature was raised up to 430°C.
It has been verified that a complete reoxidation of the catalyst occurs after a thermal treatment in O_2 up to 430°C for 15 min.

3.2.5.6 Adsorption measuraments

Adsorption measurements were collected on samples oxidized and washed in nitrogen for 1/2h at the adsorption temperature.
Thus a mixture containing 1vol% CO or 2vol% H_2vol% has been fluxed at a fixed temperature (Q=14Nl/h).
A mixture containing a 0.8vol% CO and 1.5vol% H_2 in N_2 (Q=14Nl/h) has been used for the contemporary addition of CO and H_2.

3.2.5.7 Transient analysis

Transient analysis where performed to the purpose of observing the transient behaviours of the chemical species due to chemical transformations occurring on the catalyst surface when the reaction mixture is injected on the catalyst and not related to thermal effect. The reaction which takes place are highly exothermic, and in particular the CO oxidation reaction generate 0.7°C/% of CO converted, while the H_2 oxidation reaction generates 0.6°C/% of H_2 reacting. Thus the control of the temperature is critical in this experiment.
For a better heat dispersion, the catalyst bed has been diluted with quartz particles in a ratio 1/3 catalyst/diluent. In particular 200mg of catalyst and 600mg of quartz have been loaded. The particles size is the same for both catalyst and diluent for avoiding by-pass phenomena.

A reacting mixture similar to the reaction one has been used: 2vol% H_2; 1000ppm CO; 2000ppm O_2 in N_2 and a total flow rate of 36Nl/h. The inlet concentrations have been measured by-passing the reactor, while for measuring the concentration under reaction conditions the reactor is included in the line. The transient behaviour of the concentrations of the chemical species has been recordered by the acquisition program and analyzed.

3.2.6 Measuraments of catalytic activity

Reaction tests have been performed on CuO/CeO_2 and CuO/CZ samples with different copper and zirconium loads, by varing the parameters of interest for the kinetics in the following range:

- T = 25-400°C
- τ = 0.009-0.08 g·s/cm^3
- [CO]°= 200-10000ppm
- [O_2]°= 0.04- 1vol%
- [H_2]°= 50 vol%
- [CO_2]°= 0-20 vol%
- [H_2O]°= 0-10 vol%

The contact time has been varied by changing the gram of catalyst loaded between 300mg and 160mg and the overall flow rate between 14Nl/h and 48Nl/h.
The screening study (chapter 4) has been performed by using particles with a mesh size in between 200-300μm. Nevertheless the kinetic study performed exclusively on the sample 4 CuO/CeO_2 has been carried out by using particles with a mesh size in between 120-200μm to limit the occurrence of diffusion limitations (see chapter 5).
The experimental apparatus has been though to the purpose of guarantee the contemporary feed and analysis of the all the species which may be present in the reaction environment in the range previously specified. The description of the plant is reported in paragraph 3.3
The inlet concentrations have been measured by-passing the reactor, while for measuring the concentration under reaction conditions the reactor is inclused in the line. A change in the overall number of moles is expected when the reaction takes place:

(1) $$CO + \frac{1}{2}O_2 \rightarrow CO_2 \qquad \Delta H^{\circ}_{298} = -283\frac{kJ}{mol}$$

(2) $$H_2 + \frac{1}{2}O_2 \rightarrow H_2O \qquad \Delta H^{\circ}_{298} = -242\frac{kJ}{mol}$$

The variation of the number of moles before and after the reaction corresponds to about 0.5 % if only the CO oxidation reaction proceeds with complete conversion, and to 1.5% if only the

hydrogen oxidation reaction occurs. The latter number has been obtained considering that the concentrations measured by the analyzer are on dry base.

It is possible to take into account of the change in the overall moles number by the atomic balance on N_2, whose number of moles is unchanged before and after the reaction.

Ones calculated the moles of the species involved in the reaction it is possible to calculate the CO conversion and the selectivity of oxygen to oxidize CO, which are defined as:

$$S_{CO} = \frac{\Delta O_2^{(CO)}}{\Delta O_2^{(CO)} + \Delta O_2^{(H_2)}} \left(= \frac{0.5 \cdot n_{CO_2}^{OUT}}{n_{O_2}^{IN} - n_{O_2}^{OUT}} \right) \qquad X_{CO} = \frac{n_{CO}^{IN} - n_{CO}^{OUT}}{n_{CO}^{IN}}$$

where S_{CO}, X_{CO} are respectively the O_2 selectivity to CO_2 and the CO conversion, and $\Delta O_2^{(CO)}$ and $\Delta O_2^{(H_2)}$ are the oxygen mols consumed respectively in the CO oxidation reaction and in the H_2 oxidation reaction.

A characteristic parameter for the reaction tests performed is the feed ratio λ defined as:

$$\lambda = \frac{2 \cdot P_{O_2}^{\circ}}{P_{CO}^{\circ}}$$

that is the excess of oxygen with respect to the complete oxidation of CO to CO_2.

3.3 Experimental apparatus

The experimental apparatus has been projected to the purpose of carrying out both a kinetic and a characterization study on the samples investigated. Indeed, the same experimental apparatus has been used for reaction tests and reduction-oxidation analysis.

The main issues of the system are:

- The contemporary presence in reaction conditions of six different chemical species (CO, CO_2, H_2, H_2O, CO_2, N_2, O_2) complicated by the fact that H_2 is present in high concentrations and H_2O must be added to the reaction mixture up to concentration of 10vol%.
- The necessity of having a versatile system of analysis able to adapt to the different conditions in which activity tests and reduction oxidation studies must be carried out. In particular different contact time and concentrations must be used.

3.3.1 The reactor

The measurements were carried out in continuum by using a laboratory reactor having a cylindrical geometry and a annular gas flow section. A schematic representation of the reactor is reported in figure 3.1.

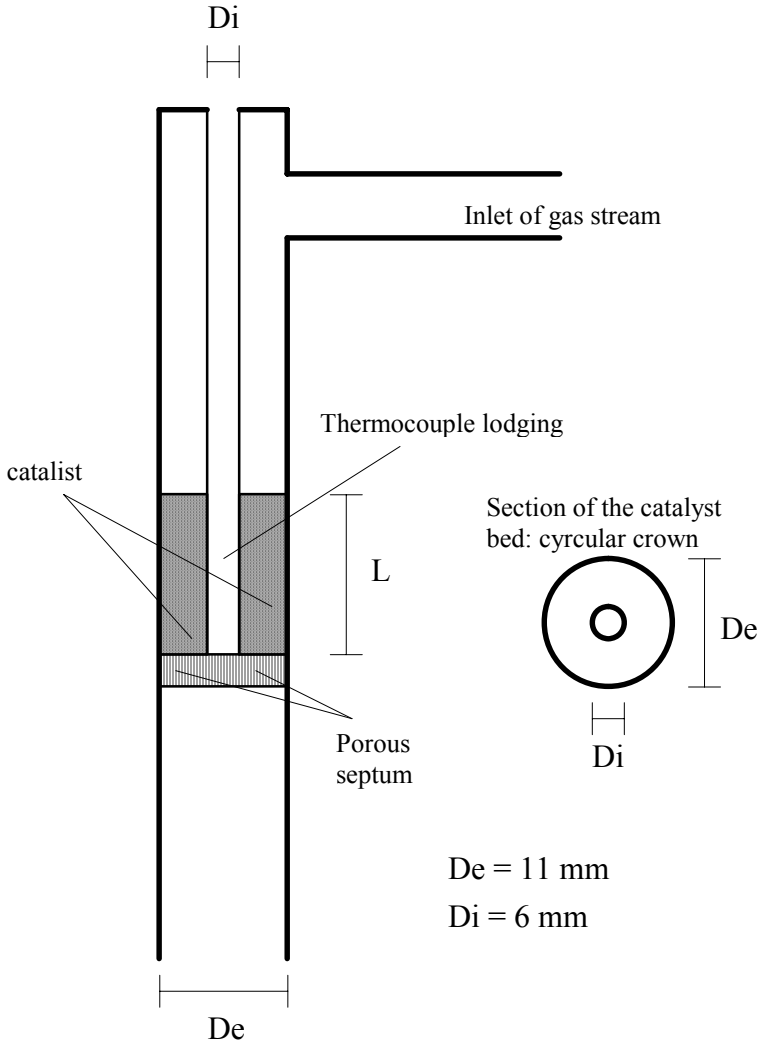

Figure 3.1: Reactor scheme

The microreactor used is composed by a quarz tube which internal diameter is 11mm (De in figure 3.1), with a porous septum sustaining the catalytic bed.
The thermocouple is placed in another quartz tube with an external diameter (Di) of 6mm, placed into the reactor and supported on the septum.
A cromel-alumel (K) thermocouple has been used, which measure the temperature with an error which can be estimated in ±0.2°C. By gradually extracting the thermocouple a continuum measure of the temperature along the reactor may be obtained.

The powder catalyst with a mesh size between 120-300μm is located on the porous septum with a porosity between 70 and 100 μm. In the reaction tests and characterization analysis the length of the catalyst bed has been varied between 1 and 3 cm, depending on the amount of catalyst loaded (between 160mg and 1g).

Many advantages derive from the use of a reactor with cylindrical geometry and anular section in comparison to a traditional reactor with a circular section:

1. the possibility to control the temperature along all the catalyst bed
2. The absence of perturbation on the fluidodynamic of the reacting stream, bonded to the presence of a thermocouple, as in a circular reactor
3. More efficient heat exchange with the exsternal environment because of the higher catalyst lenght bed at a fixed catalyst load in comparison to a circular reactor

The reactor is placed in an oven (LENTON LTD mod. PTF 12/38/500) whose lenght is 60 cm while its isothermal zone has been estimated 45 cm. Three different temperature controllers EUROTHERM 808 regulate the temperature by controlling three different resistances; in this manner a uniform profile along the catalyst bed, never higher than 3cm, is guaranteed.

The catalytic reactor in this thesis has been assumed to be an isothermal, fixed bed reactor with a plug flow. Moreover a constant pressure and equal to the inlet value, has been assumed along the catalyst bed.

The PFR assumption is a consequence of the estimation of the Peclet number which measure the degree of assail dispersion along the reactor.

For evaluating the Peclet number, the Reynolds and Schimdt number must be calculated:

$$\mathrm{Re} = \frac{\rho u d_p}{\mu} \qquad\qquad Sc = \frac{\mu}{\rho \cdot D_{CO-N2}}$$

The following experimental conditions have been used:

- Flow rate — Q — 36Nl/h
- Temperature — T — 150°C
- Pressure — P — 1
- Particle size — d_p — 150μm
- Degree of vacuum — ε — 0.37
- Anular section of the reactor — S — $6 \cdot 10^{-5} m^2$
- High of the catalyst bed — L — 0.01-0.03 m

- Density of the reacting mixture ρ 0.43 kg/ m^3
- Viscosity μ $0.02 \cdot 10^{-3} kg \cdot m^{-1} \cdot s^{-1}$

Where ε, the reactor vacuum degree and it is assumed equal to 0.37 corresponding to the maximum package degree for spherical particles. Moreover, taking into account the composition of the reacting mixture (50vol% H_2, 0.5 vol% CO, 0.5vol% O_2, in N_2) the density and the viscosity of a mixture composed by 50vol% of H_2 and 50vol% of N_2 at 150°C has been used.

The diffusivity of the carbon monoxide in N_2, D, expressed in $cm^2 \cdot s^{-1}$, has been estimated by using the formula: (Satterfield, Sherwood, 1989):

$$D_{CO-N_2} = 1.858 \cdot 10^{-3} \cdot T^{1.5} \cdot \frac{\left[\left(M_{CO} + M_{N_2}\right)/\left(M_{CO} \cdot M_{N_2}\right)\right]^{1/2}}{P \cdot \sigma^2_{CO-N_2} \cdot \Omega_D} \qquad \text{(A.8)}$$

where T is the temperature (K), P the pressure (atm), M_{CO} and M_{N2} are respectively the molecular weight of CO ed nitrogen, Ω_D, the collision integral, that is an adimensional function of the temperature and of the intermolecular potential, which has been evaluated by the Leonard – Jones expression.

Thus from the (A.8) equation the diffusivity of CO in N_2 has been estimated $0.38 \cdot 10^{-4} m^2 \cdot s^{-1}$.

In these conditions the Reynolds and Schmidt number may be calculated:

Re = 1.5 Sc =1.34

In these fluidodynamic conditions the adimensional number Pe_p is about 2 (Levenspiel, 1999)

$$Pe_p = \frac{u d_p}{D\varepsilon} \approx 2$$

where D is the dispersion coefficient.

In these conditions the peclet number may be calculated

$$Pe = Pe_p \cdot \frac{L \cdot \varepsilon}{d_p} = 50$$

The magnitude order of the Peclet number confirm the assumption of plug flow reactor (O. Levenspiel, 1966)

In the all reaction tests performed the ratio between the length of the catalyst bed and the characteristic particle size is always enough high to neglect the inlet effects (Westerterp, 1987). Indeed, for this value of the Reynolds number, it is enough that $L/d_p > 10$ where L is the length of the catalyst bed.

The assumption of a constant pressure profile along the catalyst bed is justified by the limited high of the bed (1-3cm) and not relevant changes in the pressure drops when the reactor is included in the gas route (max 40 mbar).

$$P = P_{atm} + \Delta P$$

Where ΔP are the pressure drops experimentally measured by an electronic pressure transducer placed along the gas stream line.

3.3.2 Experimental apparatus and analysis system

A high purity 5vol% CO/N_2 mixture (and pure gases CO_2 and O_2 were used in the feed. The possible formation of Fe-carbonyl in the CO cylinder by using an aluminium cylinder. Moreover a Fe-carbonyl trap was placed on the CO stream line.

Nitrogen may be fed by two cylinders with different purity level: 99.998% pure N_2 has been used for reaction tests while 99.9999% pure N_2 has been used for the reduction-oxidation studies.

In order to avoid safety risks related to H_2 storage, an Hydrogen generator (CLAIND) provide the H_2 to feed during the reaction tests up to 400cc/min. The H_2 generator is an electrolytic cell which produces H_2 by the H_2O dissociation. Nevertheless H_2 TPR were performed by using a mixture of 2vol% H_2 in N_2 with a certified purity of 99.9999%.

The apparatus was equipped with five Brooks 5850 mass flow controllers for all components except water, which is instead fed by saturating the reactive mixture in a thermostatic bath. It has been assumed that the water content at the outlet of the saturator is equal to the water vapour pressure at the temperature of the thermostatic bath. This assumption was verified by a control experiment by observing H_2O condensation at 0°C after saturation of the gas stream at 20°C.

It was possible to regulate the H_2O content in the mixture by changing the temperature of the thermostatic bath.

The reacting mixture passes through heated lines which connect to the microreactor placed in the oven (LENTON LTD mod. PTF 12/38/500).

The water possibly present at the outlet of the reactor is trapped in a condenser and successively in $CaCl_2$ chemical trap.

The dry mixture is thus fed to the analysis system consisting in a Fisher-Rosemount NGA2000 analyser equipped with four channels for the contemporary analysis of CO and CO_2 with an IR detector, H_2 with a thermoconducibility detector, and finally O_2 with a paramagnetic detector. Each analysis channel has four different range of measurement, whose sensitivity is estimated to be lower than 1% of the span gas concentration.

In the following table 3.3 the range of measurement for each specie is reported.

Table 3.3: Range of measurement for each chemical specie in the analyzer Fisher-Rosemount NGA 2000.

Chemical specie	*1° range*	*2° range*	*3° range*	*4° range*
CO (ppm)	0-500	0-3000	0-5000	0-10000
O_2 (%)	0-1	0-5	0-10	0-20
CO_2 (%)	0-1	0-3	0-5	0-10
H_2 (%)	0-5	0-10	0-30	0-50

Due to the high dependence of the paramagnetic detector on the flow rate the optimal flow rate range is fixed between 12 and 90Nl/h.

The possibility of changing range of measurement give an extreme flexibility to the system which is appropriate also for reduction-oxidation measurements.

The analyzer was calibrated with gas mixture of known composition so that a quantitative analysis of the reduction and oxidation was possible.

The overall plant is equipped with a safety electrovalve, which send to vent the gases in case of accidental overpressure.

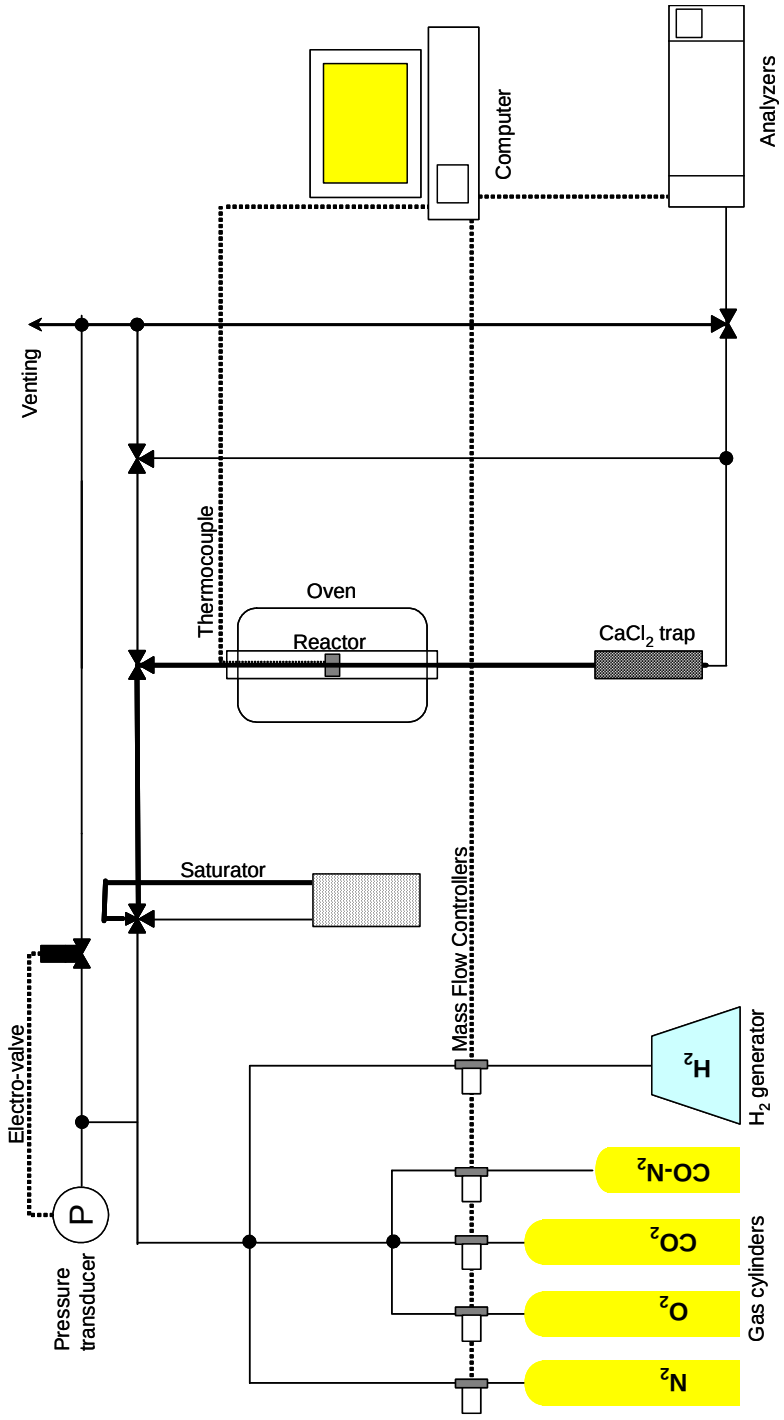

Figure 3.2: Scheme of the experimental plant for CO-PROX reaction.

CHAPTER 4

SCREENING OF COPPER BASED CATALYSTS FOR THE CO PREFERENTIAL OXIDATION REACTION

4.1 Characterization of CuO/CeO_2 and CuO/CeO_2-ZrO_2 catalysts

4.1.1 XRD, BET, TEM analysis

Copper/ceria-zirconia catalysts with different copper and zirconium content have been prepared via wet impregnation method. Commercial mixed oxides provided by GRACE containing respectively 0-20-48-65 wt% zirconium in ceria have been used as supports. In table 4.1 CuO content, estimated by spectrophotometric analysis, the mean crystallite size, evaluated by the XRD analysis, and the BET surface area have been reported.

Tabella 4.1: Spettrophotometric, XRD e BET analysis results.

Catalizzatore	CuO (wt%)	Mean size (nm)	BET (m^2/g)
CeO_2	_	11.2	56
CZ (80/20)	_	6.43	70
CZ (52/48)	_	5.4	85
CZ (35/65)	_		100
2 CuO/CeO_2	2	12.09	55
3.5 CuO/CeO_2	3.6		
4 CuO/CeO_2 (R)*	4.2	11.6	50
4 CuO/CeO_2	4.2	11.6	50
4.5 CuO/CeO_2	4.4		
5 CuO/CeO_2	5.4	11.6	50
8 CuO/CeO_2	7.8	12.5	48
9 CuO/CeO2	9.2		47
5 CuO/CZ (80/20)	4.8	6.8	
5 CuO/CZ (52/48)	4.7	5.6	79
7 CuO/CZ (52/48)	7.2		70

* Sample reduced at 430°C and subsequently reoxidated

Zirconia containing supports have higher surface area increasing the zirconia fraction in the materials.

In figure 4.1 XRD analysis of the all supports investigated and of some catalysts prepared is showed.

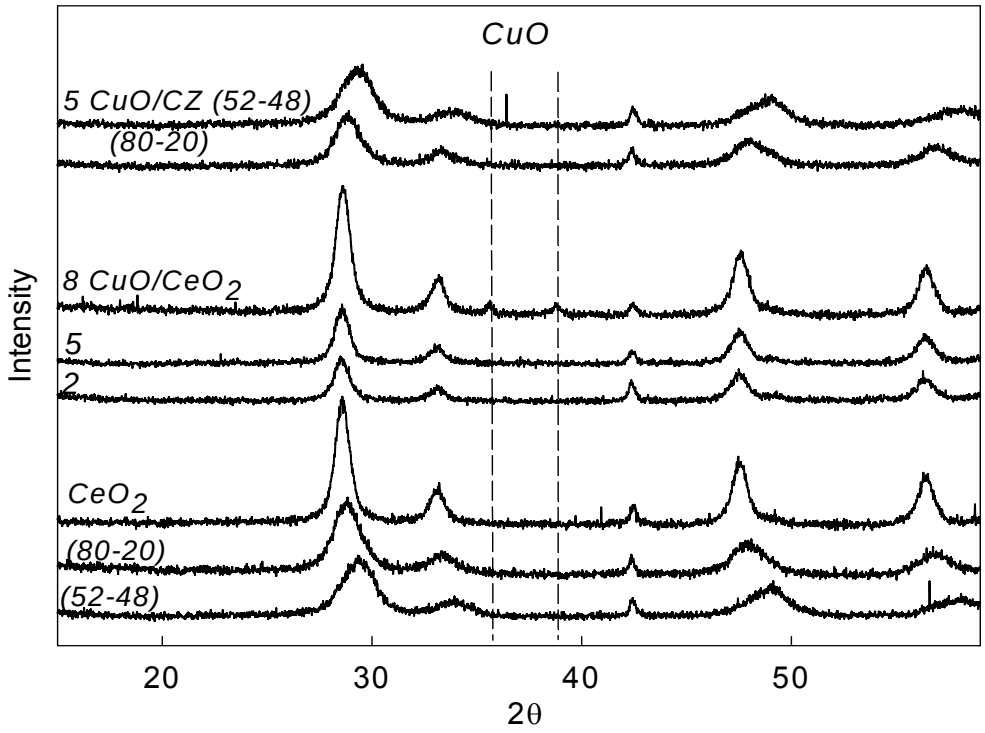

Figura 4.1: XRD patterns of ceria-zirconia supports and of catalysts with formulation 2-5-8 CuO/CeO_2, e 5 CuO/CZ (85/15) e (60/40).

X-ray powder diffraction patterns of all samples revealed the characteristic diffraction peaks of CeO_2 phase (cerianite, cubic: 2θ=28.6°,33.1°,47.5°,56.3°,59.1°).

In agreement with the observations of Trovarelli et al. (1997), Hocevar et al. (1999) e Ratnaznamy et al. (2004), the mean particle size, evaluated by the Sherrer equation (chapter 2),decreases when a solid-solution formation is induced between ceria and zirconia (table 4.1), and the position of the main ceria signals shift to higher diffraction angles (figure 4.1).

For example CeO_2 and $5CuO/CeO_2$ have a mean particle size of about 11nm while CZ (60/40) and 5CuO/CZ (60/40) of about 5nm respectively. The distortion of the ceria fluorite structure generated by the introduction of the Zr^{+4} ionic specie, induces a contraction of the elementar cell, due to the lower ionic radius of Zr^{+4} (0.84 Å) with respect to that of Ce^{+4} (0.97 Å).

The presence of CuO on the support does not change significantly the mean crystallite size (table 4.1), assuming that the small changes reported in the table 4.1 are due to experimental error.

For the 8wt% CuO/CeO_2 sample the XRD analysis shows the CuO bulk signal (tenorite, syn, monoclin: 2θ=35.5°,38.7°,48.7°,61.5°) in addition to the main sygnal corresponding to (111) ceria plane peaks has an intensity higher than that showed by the samples containing 5wt% and 2wt% CuO, but similar to pure ceria. This suggests that the sample with 8wt% CeO_2 has has a support with a more crystalline structure than those with a lower copper load.

XRD analysis have been performed also on a sample treated in H_2 at 400°C for 2h and subsequently reoxidated. This sample shows less intense CeO_2 signals than that corresponding to the fresh sample (figure 4.2b). This result could be explained by considering that the reducing/oxidizing treatment could induce a better copper dispersion and the consequent better interaction between copper and ceria, could result in lowering the ceria crystallinity.

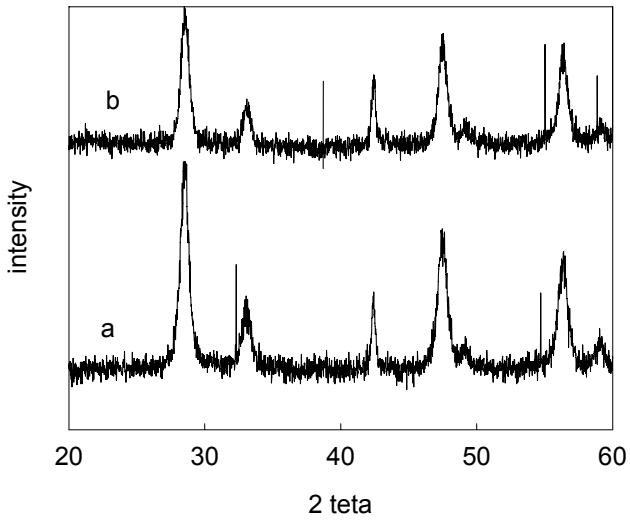

Figure 4.2: XRD patterns of (a) fresh 4.2wt% CuO/CeO_2; (b) 4.2wt% CuO/CeO_2 reduced in H_2 and reoxidated in air at 400°C.

In samples prepared via coprecipitation method a decrease of the unit cell parameter with increasing the copper content of copper/ ceria catalysts was observed and explained with the formation of a solid solution between copper and ceria or with the formation of copper-ceria mixed phase with perovskite like structure (Hocevar, 1999).

Nevertheless, for samples prepared via wet impregnation Martinez-Arias et al. (1997) did not evidence any mixed phase formation. The authors assert that all the copper should be in the oxidation state Cu^{+2}, about 20-25% of copper being more or less well dispersed on ceria, the main part of this fraction being present as isolated entities, while a smaller part forming Cu^{+2}-Cu^{+2} ionic pairs, and the remaining 80% being present as Cu^{+2} ions located in somewhat more aggregated CuO clusters.

The absence of significant changes in the ceria unit cell parameter evidenced by our analysis can be related to the fact that with the impregnation method, no mixed phases are generated according to the results of Martinez-Arias et al. (1999).

Figure 4.3 shows the HRTEM micrograph of the 5 CuO/CeO_2 samples. It is evident the regular morphology of the ceria used as support. The adjacent ceria nanocrystals intruded on each other and the different grain boundaries indicate that ceria is polycrystalline. Furthermore, the ceria particles have a regular spherical morphology with 10 nm average particle size. Copper particles are indiscernible even if atomic analysis revealed the presence of copper in the catalyst fraction showed in figure 4.3.

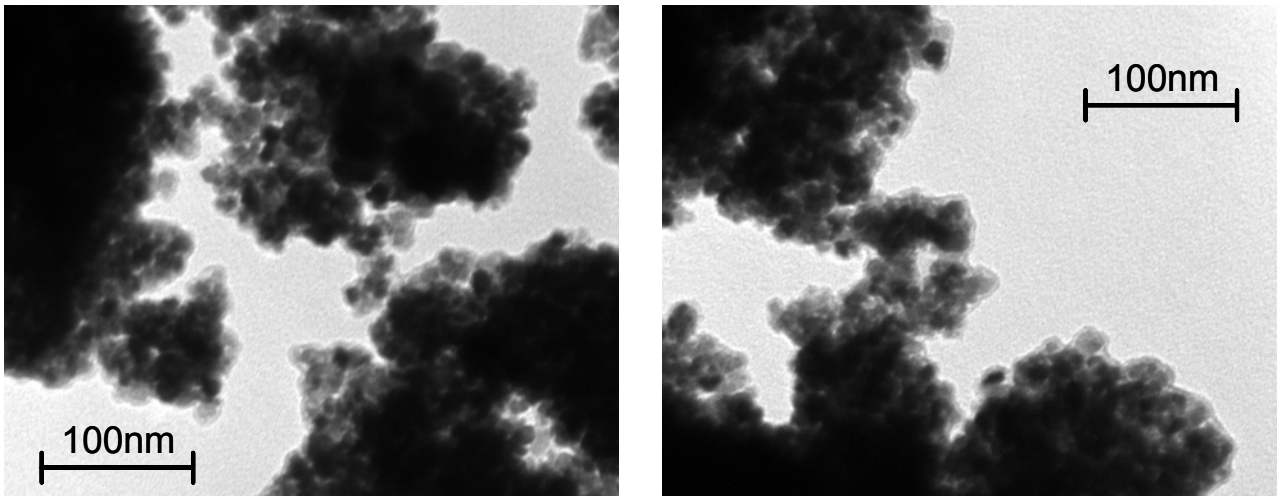

Figure 4.3 HRTEM analysis performed on sample 4 CuO/CeO_2

Stephanopoulos et al. (1996) reported SEM analysis performed on nano-CuO synthesized in an ultrahigh vacuum (UHV) apparatus by magneton sputtering in which it looks like amorphous powder and no CuO crystals were observed, neither with XRD analysis.

This can suggest that on our sample copper is highly dispersed and is probably present as an amorphous phase.

4.1.2 Temperature programmed reduction analysis

In figure 4.4 the hydrogen TPR analysis performed up to 800°C on CeO_2 and CZ (52/48) have been reported.

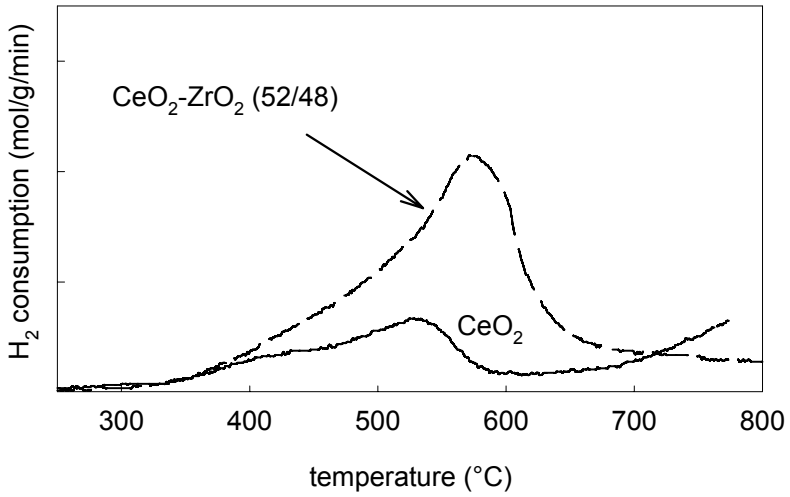

Figure 4.4: H_2 TPR on CeO_2 and CeO_2-ZrO_2 (52/48)

Ceria starts to be reduced at temperatures higher than 300°C and shows two reduction peaks, the first at 540°C and the second, according to the characterization analysis performed by the Univerisity of Udine (chapter 2), at about 840°C who estimated an overall ceria reduction corresponding to 48mol%.

The literature is in accordance to attribute the low temperature peak to the reduction of surface ceria, while the high temperature peak to the reduction of bulk ceria (Yao, 1996; Trovarelli, 2002, Boaro, 2003).

The hydrogen uptake of the first reduction peak corresponds to 355 μmoles/gram of catalyst, which corresponds to the reduction of the 12% of the all ceria from oxidation state +4 to oxidation state +3.

Table 4.2: Quantitative analysis of H_2 TPR on supports. Hydrogen consumption relative to the peak at 550°C.

Catalyst code	H_2 uptake (μmol/g)	Fraction of reduced ceria (%)	CeO_x
CeO_2	355	12	$CeO_{1.94}$
CeO_2-ZrO_2 (60/40)	1180	77	$CeO_{1.65}$

Considering that ceria has a face-centred cubic crystal structure, it can be calculated that the surface density of cerium cations in the most likely exposed faces of ceria, the (111) and (110) planes, is 7.9 and 4.85 Ce/nm^2 respectively. Considering a surface area of 56 m^2/g the calculated number of micromols of cerium ions at the surface is between 400 μmol/g and 700μmol/g, therefore of the order of magnitude of the first reduction peak which can reasonably associated to surface cerium.

The H_2 TPR of CeO_2-ZrO_2 52/48, reported in figure 4.4b, shows a unique reduction peak at a temperature of about 590°C and an overall H_2 uptake of 1180 μmol/g which, considering that Zr is irreducible, corresponds to the reduction of the 77% of the ceria which is present in the support thus obtaining a minimum formulation for the support of $CeO_{1.65}$-ZrO_2.

In conclusion by doping the ceria with zirconia the overall reducibility increases and only one reduction peak is present at 600°C.

This phenomenon is explainable considering the distortion of the O^{2-} sublattice in the mixed oxides due to the insertion of Zr^{4+} in the ceria structure, which permits a higher mobility of the lattice oxygen (Trovarelli 2002) so that the reduction is no longer confined to the surface but extends deep into the bulk. Thus no more distinction occurs in the reduction of bulk and surface ceria and all the sample is reduced in the same range of temperature.

In figure 4.5 the H_2 TPR performed up to 430°C on samples containing 5wt% CuO and supported on CeO_2, CZ (80/20) e CZ (52/48) are showed. The reduction profiles of the three catalysts are similar showing mainly two reduction peaks in correspondence of 130°C and 200°C.

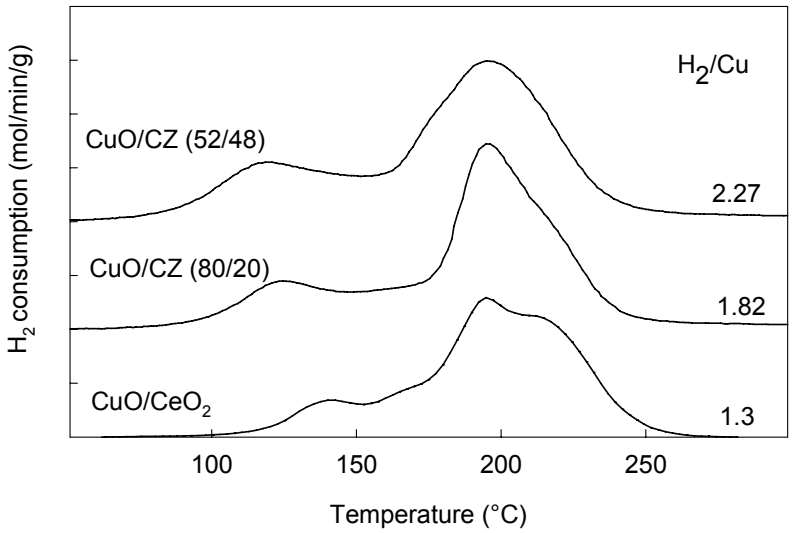

Figure 4.5: H_2 TPR performed on samples 5wt% CuO/CeO_2; 5wt% CuO/CZ (80/20); 5wt% CuO/CZ (52/48).

In table 4.3 the quantitative results are reported in term of hydrogen uptake per gram of catalyst, and ratio between the hydrogen consumed during the analysis and the number of copper atoms. This ratio should be equal to one if all the hydrogen consumed reduces all the copper in the sample from the oxidation state +2 to zero and no other cations are reduced. In the sample investigated H_2/Cu ratios higher than one have been obtained, thus suggesting that the H_2 consumption involves the reduction of species other than copper. Indeed, even if nude ceria is reduced at temperatures higher than 300°C, in the presence of a metal phase it can be reduced at lower temperatures if strong-metal-support interactions occur between the active phase and the support. In table 4.3 the percentage of ceria which supposed to participate to the reduction up to 300°C has been calculated, assuming that all the copper participate to the reduction changing oxidation state from +2 to zero. As a consequence, a minimal formula for the support has been reported.

Table 4.3: Quantitative analysis of H_2 TPR on 5 CuO/CeO_2, 5 CuO/CZ (80/20), 5 CuO/CZ (52/48). H_2 consumption, H_2/Cu ratio, percentage of ceria reduced up to 400°C, minimal formula for the support.

Catalyst code	Cu (μmol/g)	H_2 uptake (μmol/g)	H_2/Cu	Fraction of reduced ceria (%)	CeO_x-ZrO_2
5 CuO/CeO_2	687	889	1.3	7	1.96
5CuO/CZ (80/20)	607	1106	1.82	21	1.89
5CuO/CZ (52/48)	594	1351	2.27	50	1.75

For an assigned copper load, increasing the zirconium content in the support the overall reducibility of the sample increases that means that the percentage of ceria involved in the reduction at low temperature increases, in accordance with the TPR analysis performed on the nude supports. It is worth to underline that for each sample, the fraction of ceria which participate to the reduction is always lower than the overall amount of reducible ceria as calculated by the H_2 TPR performed on the nude supports.

On the same samples, 5% CuO/CZ, CO TPR analysis have been performed too and in figure 4.6 and table 4.4 the results are showed. The CO TPR analysis has been performed up to 430°C a temperature at which a CO consumption is still detected, thus 1h has been waited for closing the baseline.

Table 4.4: Quantitative analysis of CO TPR on 5 CuO/CeO_2, 5 CuO/CZ (80/20), 5 CuO/CZ (52/48). CO consumption, CO/Cu ratio, percentage of ceria reduced up to 400°C, minimal formula for the support.

Catalyst code	Cu (μmol/g)	CO uptake (μmol/g)	CO/Cu	Fraction of reduced ceria (%)	CeO_x-ZrO_2
5 CuO/CeO_2	687	1164	1.7	16	1.91
5CuO/CZ (80/20)	607	1515	2.5	41	1.8
5CuO/CZ (52/48)	594	1677	2.8	75	1.37

Similarly to what observed in the case of H_2, also in the presence of CO, increasing the zirconium content in the support, the CO/Cu ratio increases.

Performing the TPR up to 400°C, for each sample the CO uptake is higher than the H_2 one. Thus, in the temperature range of interest, for all the samples investigated CO is reducing agent stronger than H_2. Nevertheless, the reduction profiles in figure 4.6 suggests that increasing the zirconium content in the support the reducibility of the samples shifts to higher temperatures, indeed the intensity of the low temperature peaks decreases and that of the high temperature peaks increases.

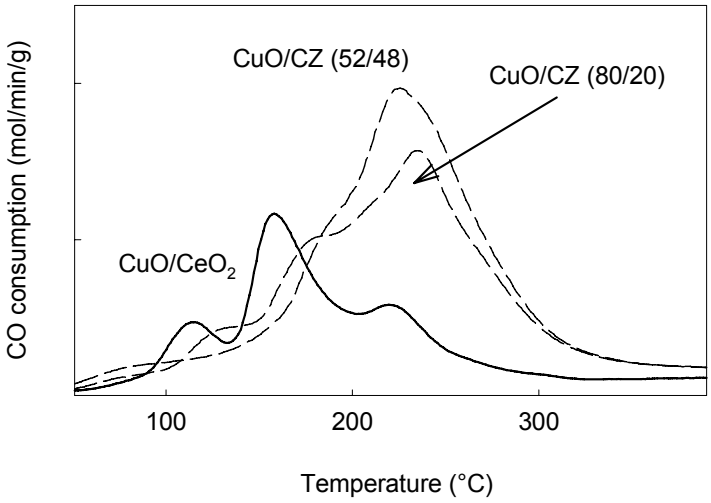

Figure 4.6: CO TPR on samples 5wt% CuO/CeO_2; 5wt% CuO/CZ (80/20); 5wt% CuO/CZ (52/48)

In conclusion the TPR analysis performed on CuO/CZ samples with different zirconium content showed that increasing the zirconium content in the support it increases the overall reducibility of the sample. Moreover the presence of zirconium in the support increases the reducibility of the samples at low temperature if H_2 is used as reducing agent, while shifting the reducibility to higher temperature in the presence of CO.

3.2 Activity tests on supports

Four different $Zr_xCe_{(1-x)}O_2$ supports containing respectively 0-20-48-65 wt% ZrO_2 have been tested under the real conditions of a CO-PROX process: 1vol% CO; 1vol% O_2; 50vol% H_2 in N_2.

Actually, it is already known in the literature that because of the high mobility of the surface oxygen/oxygen vacancy ceria related supports exhibit an intrinsic activity in the oxidation reactions even if at high temperature (Claudel, 1969).

In figure 4.7, the CO and O_2 conversion as a function of the temperature (fig. 4.7A/B) and the selectivity to CO_2 as a function of the CO conversion have been showed (fig. 4.7C).

The nude supports have their own activity for the CO oxidation reaction even if in a temperature range (250-450°C) strictly higher than that required for the CO-PROX process (80-200°C). The CO oxidation occurs in the presence of a H_2 concentration which is one order of magnitude higher than CO. This suggest that these supports have an intrinsic selectivity to oxidize CO more than H_2.

In figure 4.7A for temperature lower than 320°C, higher the zirconium content in the support, higher the catalyst activity. Nevertheless for temperature higher than 320°C this behaviour is inverted, meaning that in this temperature range the most active support for the CO oxidation is CeO_2.

By comparing the oxygen conversions in figure 4.7B results that CZ supports have the higher oxygen conversion for each temperature, suggesting that those supports are the most active for oxidation reactions. This is in accordance with the increased reducibility of the supports increasing the zirconium content.

Nevertheless by comparing the curve of the CO selectivity as a function of the CO conversion in figure 4.7C, can be observed that, in comparison to the other supports, ceria shows the higher selectivity to CO_2 in the all CO conversion range.

The higher selectivity to oxidize CO more than H_2 combined with the lower activity for oxidation reactions explain the trend of the CO conversion versus temperature previously commented.

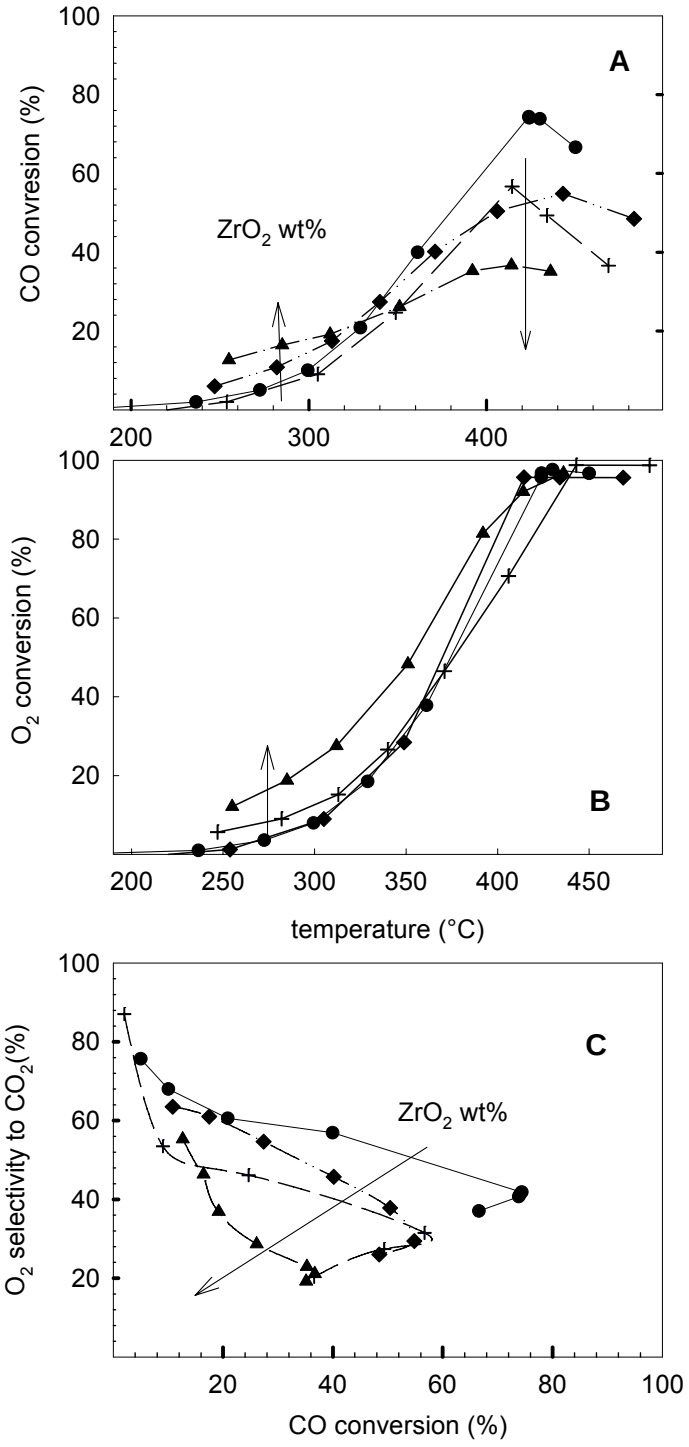

Figure 4.7: CO conversion versus temperature and selectivity to CO_2 versus CO conversion on ceria-zirconia supports with Zr wt%: 0 (•)-20 (♦)-48 (+)-65 (▲). Reaction conditions: [CO]°=1%; λ=2; [H_2]°=50% in N_2. W/F = 0.03 g s/cm^3

4.1 Activity of copper/ceria catalysts

4.3.1 Effect of the temperature and comparison with literature results

Figure 4.8 shows the results of the activity tests carried out over 5 CuO/CeO_2 sample for the preferential oxidation of CO in a mixture containing 0.5vol% CO, 0.5vol% O_2, 50 vol% H_2 in N_2.

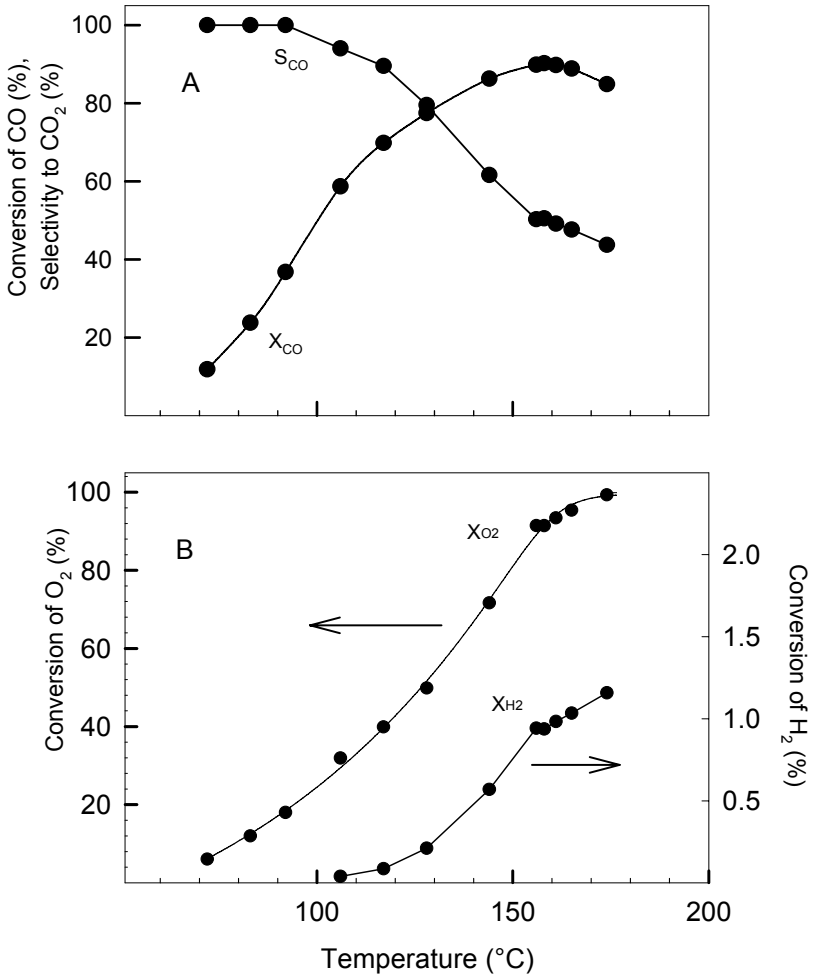

Figure 4.8: CO conversion and selectivity to CO_2 (A), oxygen and hydrogen conversion as a function of the temperature (B) on 5wt% CuO/CeO_2. reaction conditions: $[CO]°=0.5\%$; $\lambda=2$; $[H_2]°=50\%$ in N_2. W/F= 0.03g·s/cm^3

The catalyst exhibits high oxidation capacity at a temperature as low as 70°C and high selectivity towards CO oxidation (fig. 4.8A). 100% CO selectivity is shown up to 100°C, in correspondence of a conversion of CO equal to 40%; the highest value of selectivity was verified by a stoichiometric

O_2 consumption for the CO oxidation. At higher temperatures (T>100°C), the oxidation of hydrogen starts to take place in addition to that of CO, giving a higher O_2 conversion; the CO conversion increases with increasing the temperature up to 150°C, where a maximum is observed. Indeed, at higher temperatures carbon monoxide conversion starts to decrease (while the consumption of O_2 is quite complete).

The presence of a maximum of CO conversion with the temperature is frequently observed in CO PROX (Oh and Sinkevitch, 1992); its origin could be due either to the thermodynamic limit imposed on CO conversion by the occurrence of reverse water gas shift reaction or to a different dependence on temperature of the kinetics of the two reactions of hydrogen and CO oxidation (different activation energy).

CuO/CeO_2 catalyst is a promising catalyst for CO-PROX reaction, not only for the high activity in the CO oxidation, which is also higher than that of gold based catalysts (Kahlich, 1999; Rosso, 2004), but mainly for the high selectivity showed in the whole temperature range investigated.

A comparison between the catalytic performances of the catalytic system studied in this thesis, with those of noble metals based catalysts traditionally used for CO-PROX, Pt/zeolite and Au/Fe_2O_3, is reported in figure 4.9. Catalyst performances for the CO-PROX process must be compared not only in term of activity for the CO oxidation reaction as a function of the temperature (fig.4.9A), but also as selectivity to CO_2 as a function of the CO conversion (fig.4.9B). Indeed the latter plot gives an immediate idea of the width of the high selectivity zone for a catalyst.

Copper based catalysts, despite of their lower cost, show the higher selectivity, which remains constant at 100% up to 40% CO conversions, that is higher than that showed by the other catalytic systems.

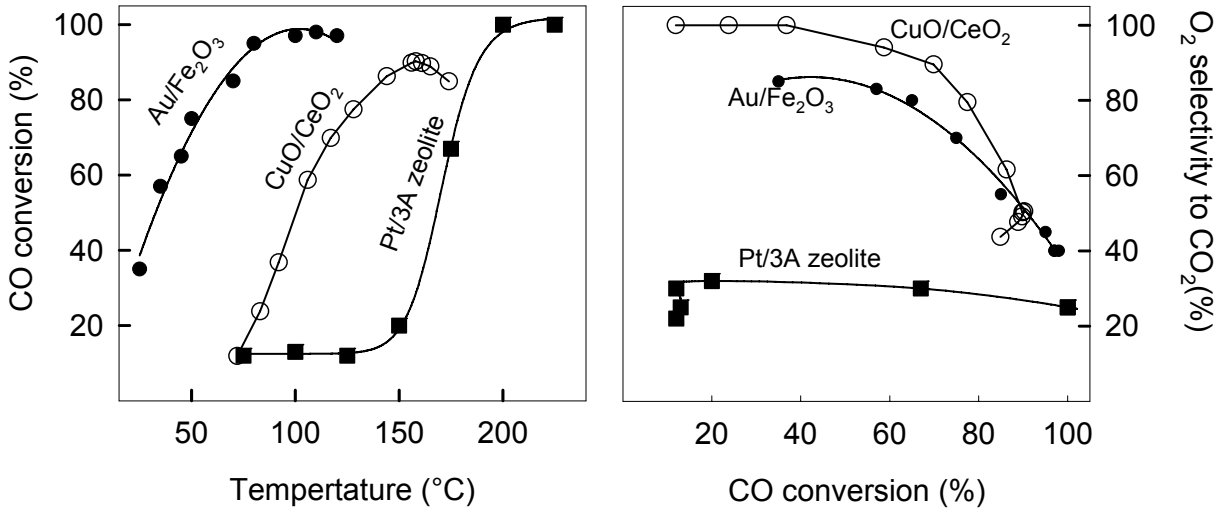

Figure 4.9: Comparison between the activity of 5 CuO/CeO_2, Au/Fe_2O_3 and Pt/3A-zeolite.
Reaction conditions:

(•) 3wt%Au/α-Fe_2O_3 (Kahlich, 1999) 1vol% CO, 50vol% H_2, λ=2.5, in N_2;W/F = 0.03 g·s/cm^3

(o) 5wt% CuO/CeO_2 (this thesis) 0.5 vol% CO, 50 vol% H_2, λ=2, in N_2, W/F = 0.03 g·s/cm^3

(■) 1wt% Pt/3A-zeolite (Rosso, 2004) 0.5 vol% CO, 50 vol% H_2, λ=4, in N_2, W/F = 0.09 g·s/cm^3

4.3.2 Activity tests on copper/ceria-zirconia samples

Samples containing 5wt% CuO and supported on ceria and ceria-zirconia containing respectively 0-20-48 wt% zirconium have been investigated for the CO-PROX process.

In figure 4.10 the CO and oxygen conversion and selectivity to CO_2 as a function of the temperature have been compared for the samples 5wt% CuO/CeO_2 and 5wt% CuO/CZ (52/48) tested in the following reaction conditions: 0.5vol% CO, 0.5vol% O_2, 50vol% H_2 in N_2.

The zirconium containing catalyst presents a higher light-off temperature (90°C) for the CO oxidation reaction in comparison to the catalyst supported on CeO_2. Moreover, for a fixed temperature, the CO conversion is always lower on the catalyst supported on ceria-zirconia.

Also in figure 4.10B it is evident that the light-off temperature for the CO oxidation reaction on CuO/CZ catalysts is higher. Nevertheless for temperature higher than 125°C, the oxygen conversion is greater on catalysts supported on CZ, suggesting that the oxygen reacts faster on catalyst supported on ceria-zirconia.

In figure 4.10C the selectivity remains 100% up to 100°C for both the catalysts. For higher temperatures the selectivity is always higher on ceria supported catalysts. Thus, on both the catalytic systems the H_2 oxidation reaction takes place for temperature higher than 100°C and it proceeds faster on CZ supported catalysts.

The different trend of CO and oxygen conversion is explained considering that at a fixed temperature the selectivity to oxidize CO is lower on catalysts supported on ceria-zirconia (fig.4.10C).

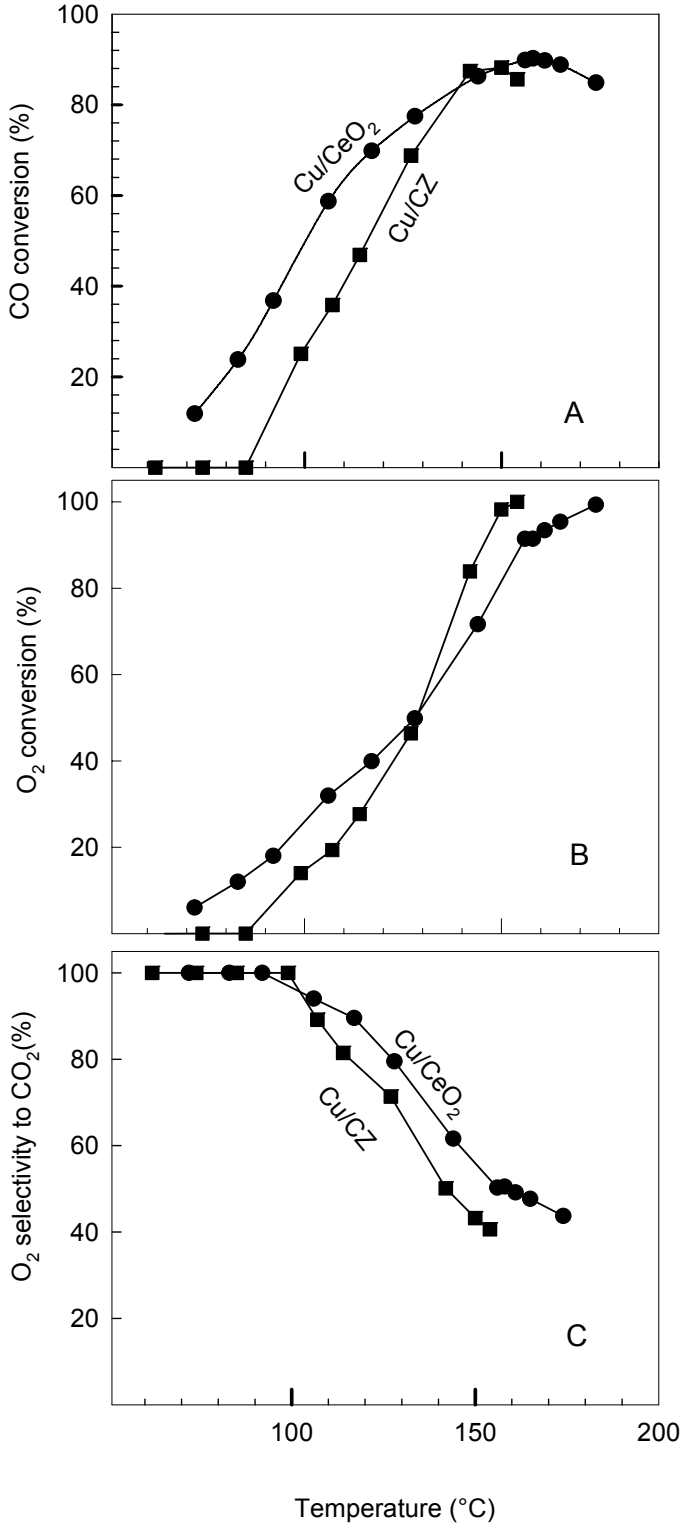

Figure 4.10: CO and O_2 conversion, selectivity to CO_2 as a function of the temperature for catalysts containing 5 wt% CuO supported on: (•) CeO_2; (■) CZ(52/48). Reaction conditions: $[CO]°=0.5$ vol%; $\lambda=2$; $[H_2]°=50$ vol% in N_2. W/F= 0.03g·s/cm^3

Those observations are confirmed also by the data of table 4.5 which reports the results of reaction tests performed on samples 5CuO/CeO_2, 5 CuO/CZ (80-20), 5 CuO/CZ (52-48), 7 CuO/CZ (52-48), in the presence of 1vol% CO, λ=2, and 50 vol%H_2 in N_2.

The results of the reaction tests have been reported as light-off temperature and temperature corresponding to 50% CO conversion with the relevant selectivity.

The exothermic nature of the process and adiabatic of the system, makes difficult to compare results especially when a mixture containing so high CO concentration is used, and the catalyst is very active as those supported on ceria-zirconia mixed oxides, which give rise to thermal overshoot and run-away phenomena.

Comparing the data of the samples with similar copper load (5wt%), increasing the zirconium content the light-off temperature and the temperature for 50 % CO conversion increases. At the same time the corresponding selectivity to oxidize CO decreases.

Table 4.5: Light-off temperature, temperature for 50% CO conversion and corresponding selectivity for samples containing 5wt% CuO and supported on CeO_2, CZ 80/20 and CZ 52/48 and on 7wt% CuO/CZ (52/48). Reaction conditions: 1vol%CO; 1vol% O_2; 50 vol% H_2 in N_2; W/F=0.03g·s/cm^3.

CATALYST	$T_{light-off}$	T_{50} (°C)	S^{CO}_{50} (%)
5 CuO/CeO_2	~50	<100	100
5 CuO/CZ (80-20)	50	116	100
5 CuO/CZ (52-48)	~60	<150	70
7 CuO/CZ (52-48)	~50	115	80

Nevertheless, it should be reminded that, the oxides used as supports have different surface areas. In particular, ceria-zirconia mixed oxides have a higher surface area (~80 m^2/g) than ceria (56 m^2/g).

In table 4.5 the activity of two catalysts with a copper content equal to the theoretical monolayer for the corresponding support are compared: 5 CuO/CeO_2 and 7 CuO/CZ (52/48).

Despite of the lower copper content, also in this case the catalyst supported on ceria exhibits catalytic performances higher than that supported on mixed oxides, and in particular lower light-off temperature, lower temperature for having 50% CO conversion and higher selectivity.

Among the catalysts investigated 5CuO/CeO_2 sample exhibits the best catalytic performances both as activity and selectivity to CO_2.

4.3.3 CO or H_2 oxidation tests

CO and H_2 oxidation been carried out on catalysts containing 5 wt% CuO supported on CeO_2 or CZ (52/48) under the same experimental conditions of CO PROX tests, but by feeding one reactant a time. Two different gas mixtures were used as reactor feed: one containing 0.5vol% CO and 0.5vol% O_2 in N_2 and the other containing 50vol% H_2, 0.5vol% O_2 in N_2.

In figure 4.11 are showed: the CO conversion as a function of the temperature for the CO oxidation test (fig.4.11a), the hydrogen conversion as a function of the temperature for the H_2 oxidation test (fig. 4.11b), and the oxygen conversion for both the activity tests as a function of the temperature (fig. 4.11c).

Figure 4.11 shows that the light-off temperature for the oxidation of CO is significantly lower than for the oxidation of H_2: the difference can be quantified in about 40°C, so showing that the CuO/CeO_2 catalyst exhibits an intrinsically higher capability in converting CO (light-off temperature at <70°C, Fig. 3a) rather than H_2 (light-off at about 100°C, Fig. 3b), even if the concentration of CO is significantly lower than that of H_2. Moreover, it seems that the activation energy for the oxidation of CO is lowered by the catalyst to values much lower than for the oxidation of hydrogen and consequently, with increasing temperature, the difference between the two reaction rates tends to diminish, since the derivative of H_2 oxidation rate is higher (being proportional to the activation energy) up to make the two reactants competing each other for the reaction with oxygen. In this way, the conversion of CO reaches a maximum, because limited by the consumption of O_2 due to the occurrence of H_2 oxidation.

Moreover, by comparing the conversion plots of both CO and H_2 oxidation with that of CO-PROX (namely when both reactant are fed to the reactor- fig.4.12), it seems evident that the oxidation of the two compounds are very weakly influenced by the contemporary presence of both. In particular, the conversion of hydrogen appears quite unaffected by the presence of CO, even though carbon monoxide reacts faster with oxygen thus reducing the O_2 concentration in the reactor. On the contrary, the conversion of CO, is weakly lowered by the presence of H_2, resulting in a difference of about 30°C in the light-off temperatures.

Finally, when CO and H_2 are both present in the reaction mixture, it is possible to affirm that the oxidation of CO starts at lower temperatures and exhibits a 100% selectivity till the hydrogen oxidation reaction starts (in the range from 70 to 100°C). On the other hand, when the hydrogen oxidation starts, it embezzles the oxygen from reaction environment thus limiting the CO conversion, that can decrease even increasing the temperature.

Therefore, the different values of the activation energies for the CO and H_2 oxidation may explain the presence of a maximum of the CO conversion curve towards the temperature under CO-PROX reaction conditions.

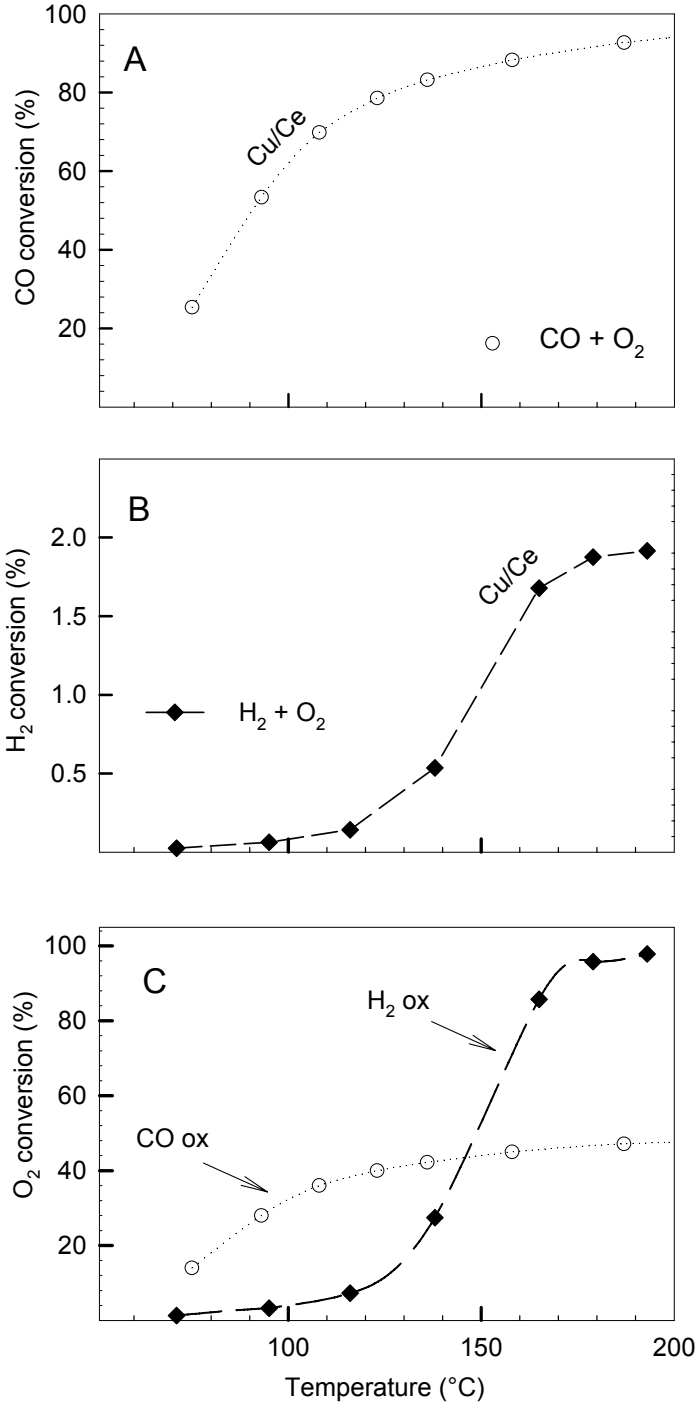

Figure 4.11: CO conversion as a function of the temperature (A), H_2 conversion as a function of the temperature (B), O_2 conversion as a function of the temperature (C). Reaction conditions: (o) 0.5vol% CO, 0.5vol% O_2.; (♦) 50vol% H_2, 0.5vol% O_2 in N_2. W/F = 0.03 g·s/cm^3

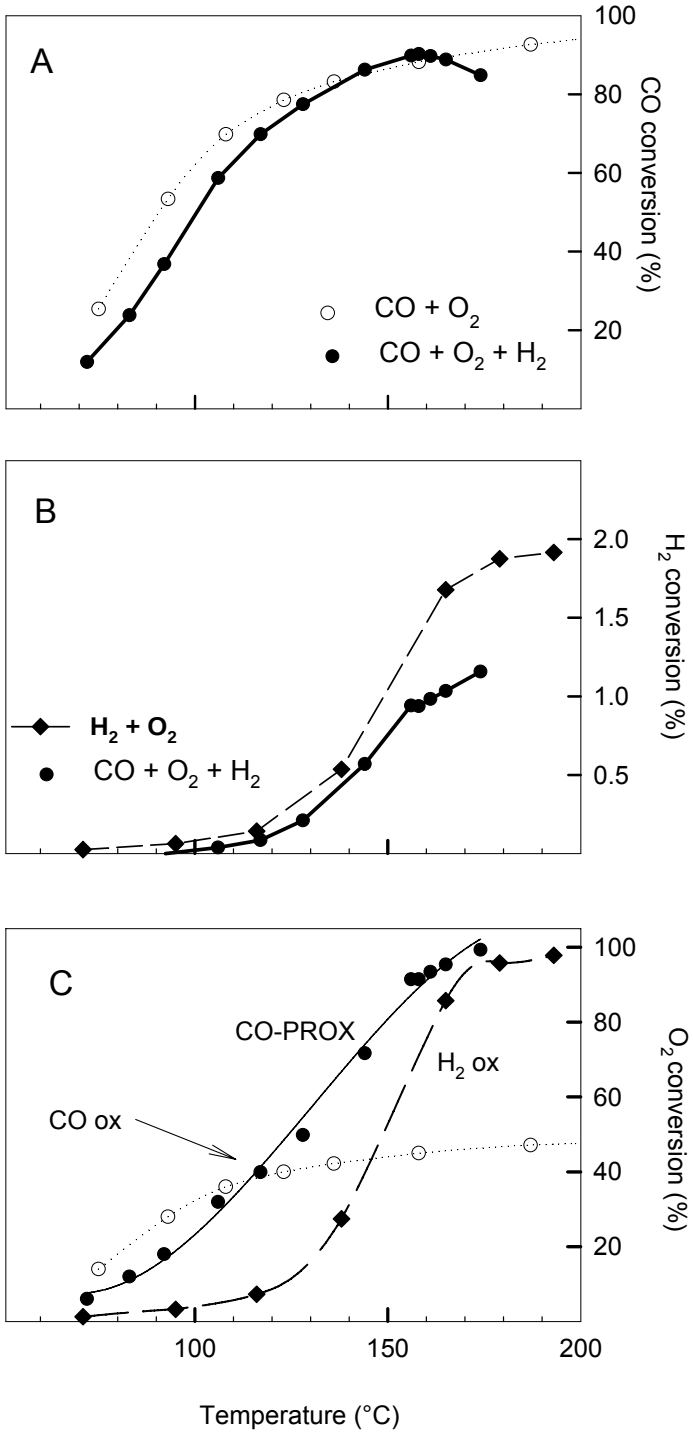

Figure 4.11: CO conversion as a function of the temperature (A), H_2 conversion as a function of the temperature (B), O_2 conversion as a function of the temperature (C). Reaction conditions: (o) 0.5vol% CO, 0.5vol% O_2.; (♦) 50vol% H_2, 0.5vol% O_2, (•) 0.5vol%, 0.5vol% O_2, 50vol% in N_2. W/F = 0.03 g·s/cm^3

The activity tests separately for CO and H_2 oxidation reactions, have been performed also on 5wt% CuO/CZ (52/48) sample. In figure 4.13 the results are compared with those obtained on CuO/CeO_2 catalysts. It is worth to underline that the light-off temperature for the CO reaction on 5wt% CuO/CZ is higher than on the catalyst supported on ceria while the light-off temperature of the hydrogen oxidation reaction remains unchanged but the hydrogen oxidation proceeds faster on CuO/CZ samples.

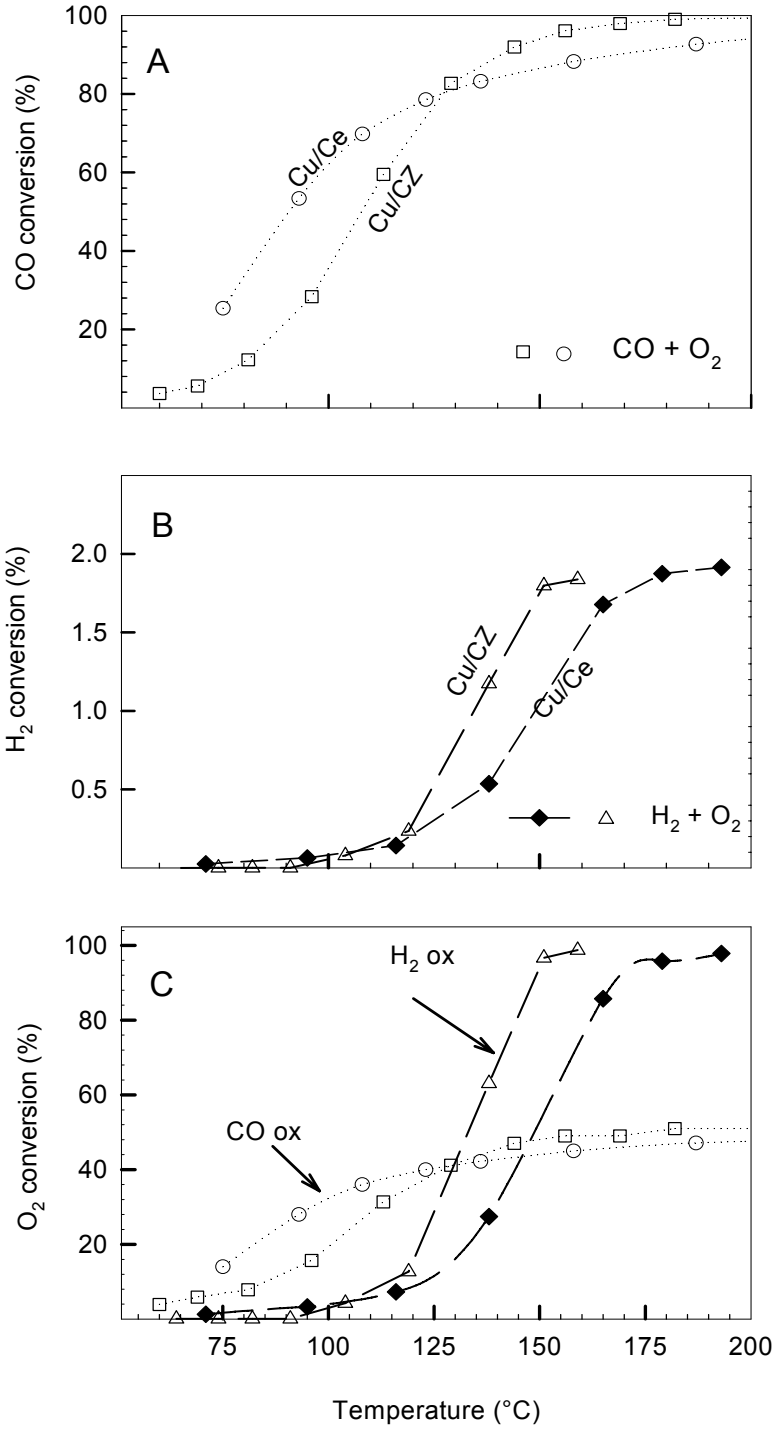

Figure 4.11: CO conversion as a function of the temperature (A), H_2 conversion as a function of the temperature (B), O_2 conversion as a function of the temperature (C). (o) CO oxidation on CuO/CeO2; (□) CO oxidation on Cu/CZ; (♦) H_2 oxidation on CuO/CeO_2 (Δ)H_2 oxidation on CuO/CZ. Reaction conditions: CO oxidation: 0.5vol% CO, 0.5vol% O_2.; H_2 oxidation: 50vol% H_2, 0.5vol% O_2 in N_2. W/F = 0.03 g·s/cm^3.

The study of CO and H_2 oxidation reactions separately performed on CuO/CeO_2 and CuO/CZ samples evidenced that:

- The kinetics of the two reaction in competition seems unaffected by the presence of the other reactant in CO-PROX conditions, except for the obvious limitation in the oxygen availability.
- CZ supported catalysts shows an apparent activation energy for the CO oxidation higher than that showed by ceria supported catalysts while lower apparent activation energy for the H_2 oxidation reaction.

As a consequence of the observations about the CO and H_2 oxidation kinetics, also in CO-PROX conditions the CO oxidation kinetics is more favoured on a catalyst supported on ceria than on a catalyst supported on ceria-zirconia. Indeed, the CO oxidation reaction has a lower light-off temperature on a catalyst supported on ceria than on that supported on ceria-zirconia CZ (52/42) (80°C). Moreover, on both catalysts at 100°C the H_2 oxidation reaction takes place, but the 100% selectivity region corresponds to a higher CO conversion for a catalyst supported on ceria.

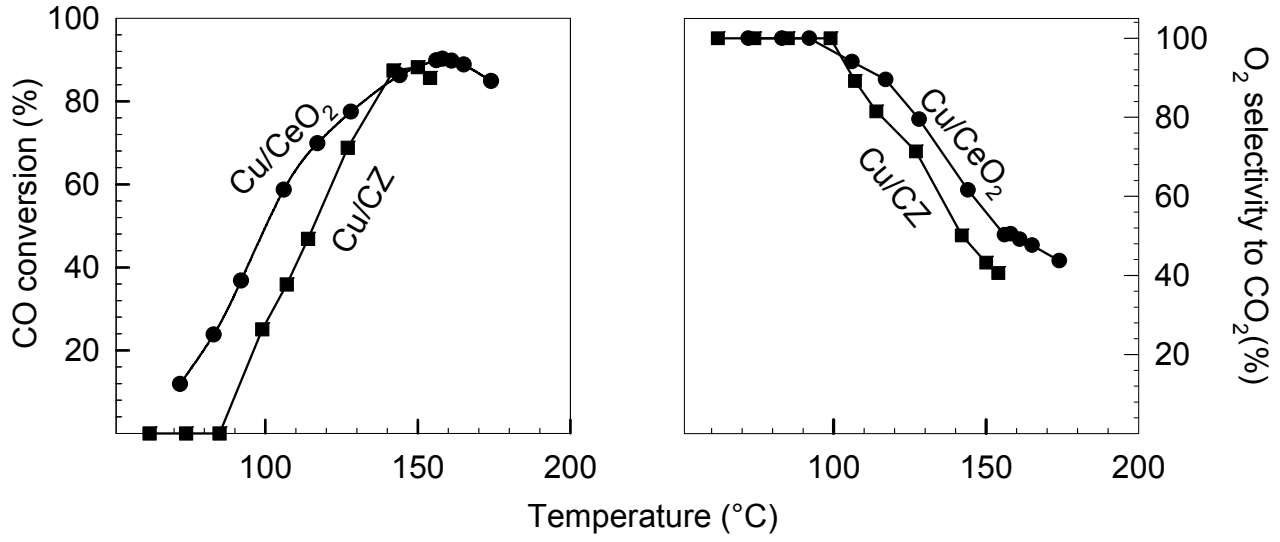

Figure 4.15: CO conversion and selectivity to CO_2 as a function of the temperature for: (•) 5 CuO/CeO_2; (■) 5 CuO/CZ(52/48). Reaction conditions: $[CO]°$=0.5 vol%; λ=2; $[H_2]°$=50 vol% in N_2. W/F= 0.03 g·s/cm^3

The study of the effect of the zirconium content in the support for copper based catalysts demonstrated that higher the zirconium content, lower the catalytic performances in the CO-PROX reaction. Therefore, only catalysts supported on ceria will be studied in the following.

4.3.4 Effect of the copper concentration

The effect of copper concentration on the CO-PROX activity has been investigated on ceria supported samples by comparing the activity of three different catalysts characterised by a different CuO amount (2-5-8wt%). Results of the activity tests are reported in figure 4.16, as CO and oxygen conversion and selectivity to CO_2 as a function of the temperature, and selectivity to CO_2 as a function of the CO conversion.

Increasing the copper concentration from 2 to 5 wt% the catalyst activity towards CO oxidation increases, while it decreases further increasing the copper concentration from 5 to 8 wt%, on the other hand, 2 wt % CuO/CeO_2 catalyst is the most selective in the high temperature range investigated. Nevertheless, it must be underlined that 5 wt % CuO/CeO_2 catalyst is the most selective for any given CO conversion providing a selectivity to CO_2 higher than 90% in a wide range of CO conversion (up to 90 %). This apparent reversal of trend can be explained by taking into account that selectivity is a unique function of the temperature. Due to the lower activity of 2 wt % CuO/CeO_2 catalyst, higher temperatures are necessary to obtain the same CO conversion of 5 wt % CuO/CeO_2 sample, as a consequnce, for the catalyst with the lowest copper load significant CO conversion values are obtained only at temperature promoting the oxidation of H_2 as well.

In conclusion, among the catalysts tested, $5CuO/CeO_2$ exhibits the best performances for the CO-PROX reaction in terms of both activity (fig.4.16A) and selectivity towards the oxidation of CO (fig. 4.16D).

It is known that only the copper species well-dispersed on the support are active towards CO oxidation in CuO/CeO_2 catalysts, while bulk CuO cannot adsorb CO and contributes only a little to the activity (Luo, 1997).

The lower activity for the oxidation reactions of the sample containing 2wt% can be explained by a copper content lower than the theoretical monolayer (about 4.7wt%). Therefore, the number of copper species, although well dispersed, is quite small. Otherwise, the presence of CuO particles (as detected by XRD analysis) for 8 wt.% CuO/CeO_2 catalyst can be related to the loss of both activity and selctivity observed for this catalyst.

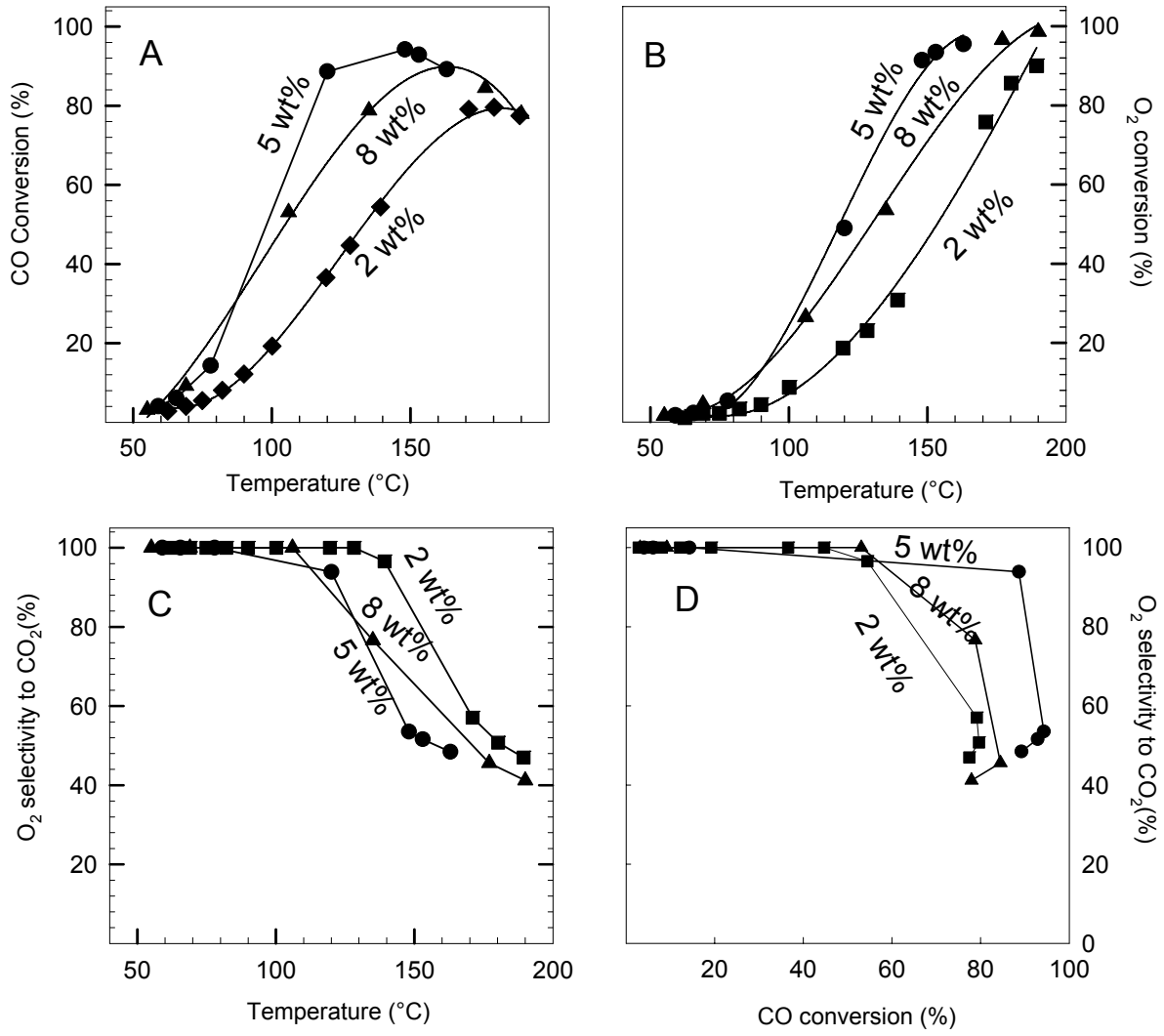

Figure 4.16: CO (A) and O_2 (B) conversion as a function of the temperature, selectivity to CO_2 as a function of the temperature (C) and selectivity to CO2 as a function of the CO conversion (D) on: (■)2 CuO/CeO_2; (•)5 CuO/CeO_2; (▲) 8wt% CuO/CeO_2. Reaction conditions: $[CO]°$=1%; λ=2; $[H_2]°$=50% in N_2. W/F= 0.03g·s/cm^3

In conclusion, the enhanced activity for the CO-PROX reaction when copper concentration increases from 2 to 5wt% can be correlated to the increased number of CuO active particle dispersed on the support, while the further increase in copper content (from 5 to 8wt%) could induce the formation of inactive copper species which, on the contrary, could decrease activity and the selectivity of CO oxidation hindering the access to the active sites for the CO oxidation or slowing down the reoxidation, thus favouring H_2 conversion.

A further investigation of the copper concentration in the region around the 5wt% CuO has been carried out in order to find the best catalyst formulation.

In figure 4.17 the results of the activity tests on sample with copper concentration in the range between 3.5 e 5 wt% are showed.

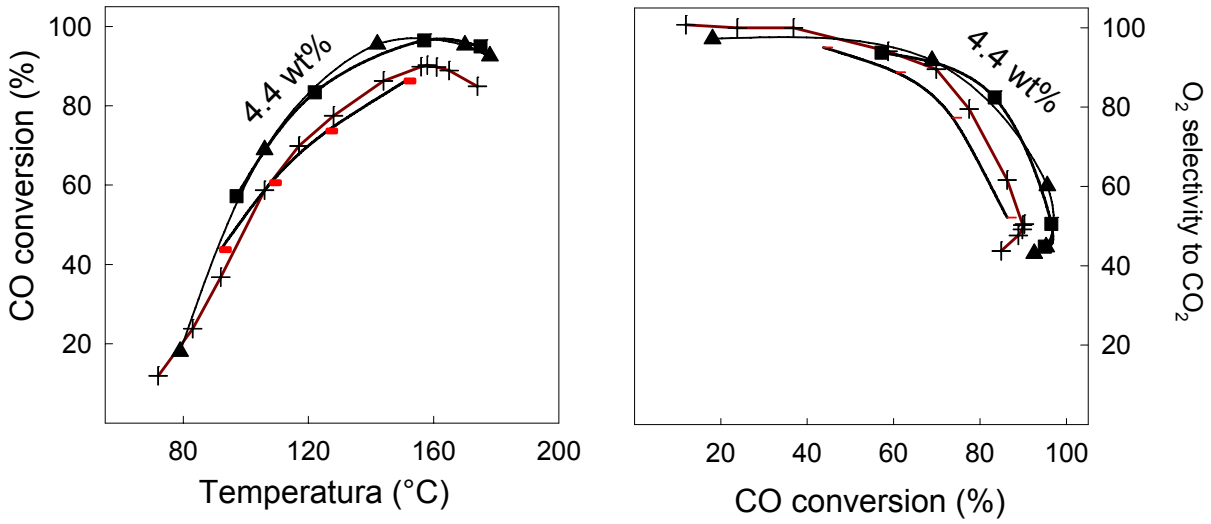

Figure 4.17: :CO conversion as a function of the temperature; selectivity to CO_2 as a function of the CO conversion on: (▲)3.5 CuO/CeO_2; (■) 4.5 CuO/CeO2; (+) 5 CuO/CeO_2. Reaction conditions: $[CO]°=1\%$; $\lambda=2$; $[H_2]°=50\%$ in N_2. W/F= 0.03g·s/cm^3

Decreasing the copper concentration from 5 (namely 5.4) to 4.5 wt% the catalytic activity increases but a further decrease of the copper concentration to 3.5wt% does not change significantly the activity.

The optimal catalyst composition is thus in the range between 4.5 and 3.5 wt% CuO, that is assumed to be the real monolayer concentration.

For CuO content higher than 4.5wt%, the copper concentration exceeds the monolayer coverage and the copper is not well dispersed, thus negatively affecting the catalyst performances.

On the other hand for copper concentrations lower than 3.5 wt% CuO, the copper content is lower than the monolayer and therefore, activity is limited by the low number of active sites.

In samples with copper content close to the monolayer, it has been verified that the catalytic performances does not depend on small changes in the parameters involved in the preparation method (pressure, temperature, rotational speed and dilution). On the contrary in samples with a copper content slightly higher than the monolayer (>4.5wt% CuO), a higher dilution and/or a longer time of preparation favours a better copper dispersion, and thus an increase of catalytic performances.

4.3.7 Effect of the calcination temperature

The study of the effect of the calcination temperature on the catalytic performances in the CO-PROX reaction has been carried out on a sample containing 5wt% CuO and calcined respectively at: 450-600-750°C.

In figure 4.18A-B the activity tests on the three samples studied have been reported. Increasing the calcination temperature up to 600°C, the catalytic performances decreases (fig.4.18A) and in particular at a fixed temperature the CO conversion is lower on the sample calcined at 750°C. Nevertheless the trend of the selectivity to CO_2 versus the CO conversion remains unchanged.

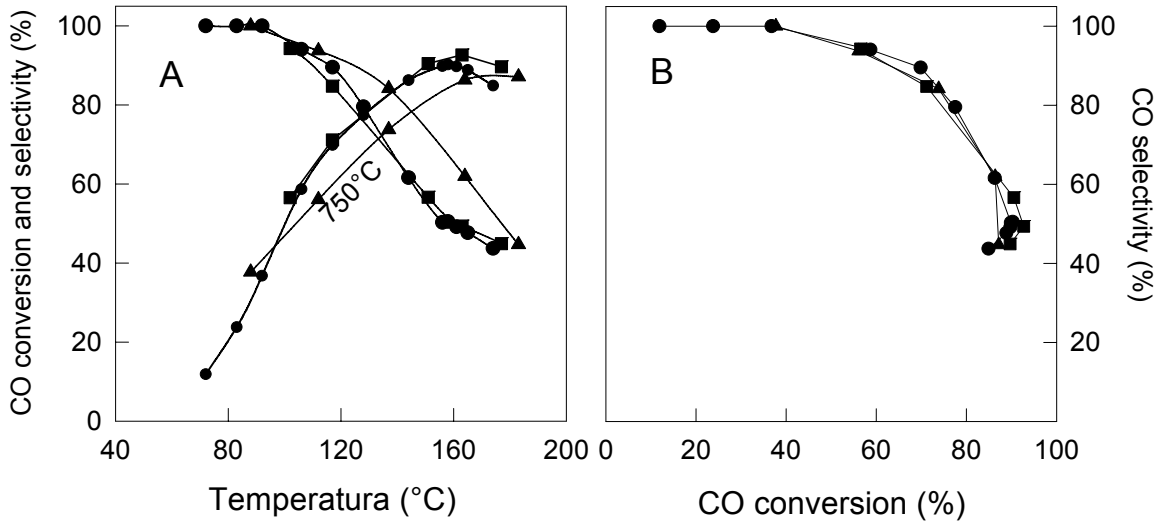

Figure 4.18: CO conversion and selectivity to CO_2 as a function of the temperature (A), and selectivity to CO_2 as a function of the CO conversion (B) on 5 CuO/CeO_2 catalyst calcined at 450°C(•); 600°C (■); 750°C(▲); Reaction conditions: $[CO]°=0.5\%$; $\lambda=2$; $[H_2]°=50\%$ in N_2. W/F=0.03 g·s/cm^3.

In figure 4.19 the H_2 TPR performed on $5CuO/CeO_2$ samples calcined at different temperatures are showed while the hydrogen consumption calculated in term of H_2/Cu ratio is reported in table 4.5 with the correspondent values of surface area and mean particle size.

The lower activity of the sample calcined at 750°C, is associated to a decrease of the sample redox properties (fig.4.19). Indeed, by the H_2 TPR analysis it appears evident a shift of the reduction peaks to higher temperatures and a decrease of the H_2/Cu ratio with increasing the calcination temperature.

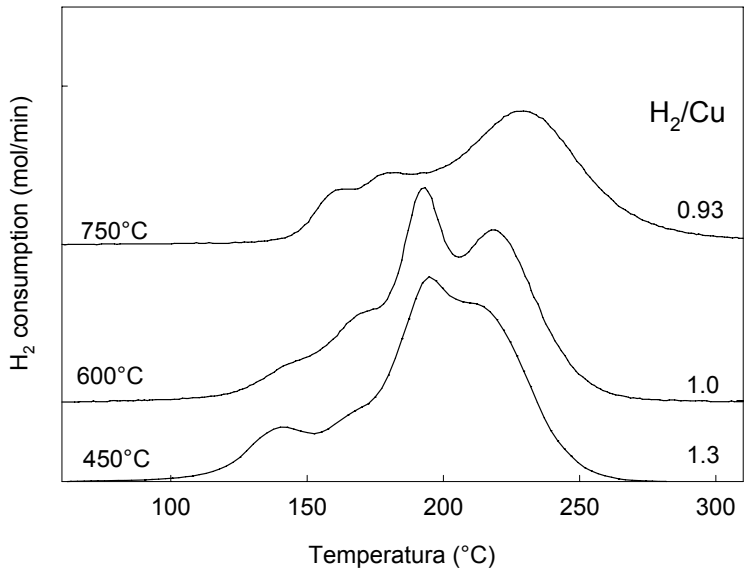

Figure 4.19: H_2 TPR analysis, Hydrogen uptake as a function of the temperature on $5CuO/CeO_2$ sample calcined at 450-600-750°C.

Those effects are probably related to a decrease of the surface area (table 4.6) due to the ceria aggregation in crystallites of dimensions much higher than those in the sample calcined at lower temperature (<600°C), as suggested by XRD analysis. Nevertheless from those analysis no informations about the copper cluster dimensions may be obtained. Those observations are in accordance with the literature results which, for the ceria supports, shows a *sintering* for calcinations temperature higher than 800°C (Trovarelli, 2002).
In conclusion 600°C in order to obtain the best catalytic performances a calcinations temperature of 600°C should not have exceeded.

Table 4.6: BET surface area, mean size of the ceria crystallites calculated by XRD analysis, and H_2/Cu ratio calculated by H_2 TPR analysis for 5 CuO/CeO_2 samples calcined at 450-600-750°C.

T calcination (°C)	BET (m^2/g)	D (nm)	H_2/Cu
450	50	11.6.	1.3
600	49	10.56	1.0
750	13	24.32	0.93

4.3.8 Effect of a redox cycle

Activity tests have been performed on a sample treated in CO or in H_2 at 400°C for 40min and subsequently re-oxidized in air for 2h at 400°C.

In figure 4.20 the comparison of activity tests performed on a sample, before and after the redox cycle previously described is reported.

The CO conversion curve shifts to lower temperature after the redox cycle in CO or in H_2, thus suggesting that the catalyst is more active. Moreover the redox treatment does not change significantly the trend of the oxygen selectivity to CO_2 as a function of the temperature.

These aspects will be examined more into details in chapter 6, where the redox properties of this sample will be investigated.

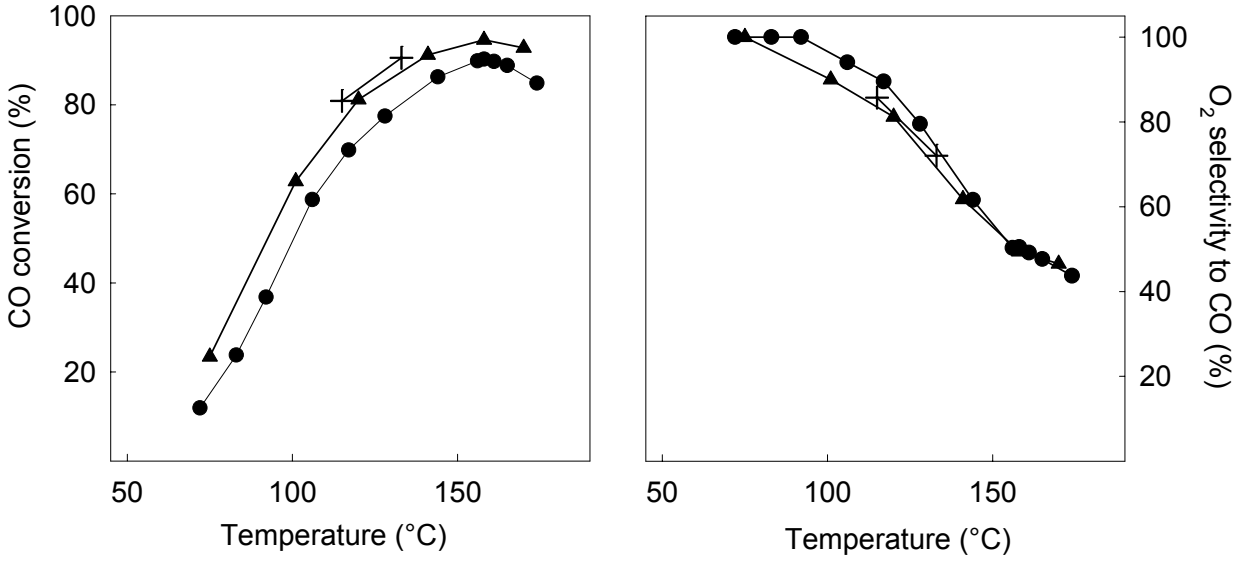

Figure 4.20: CO conversion as a function of the temperature (A), and selectivity to CO_2 as a function of the CO conversion (B) on 5 CuO/CeO_2 catalyst: fresh sample (•); treated in CO at 400°C (▲); treated in H_2 at 400°C (+). Reaction conditions: $[CO]°=0.5\%$; $\lambda=2$; $[H_2]°=50\%$ in N_2. W/F=0.03 g·s/cm^3.

Chapter 5

Kinetic study and mathematical model

Due to the high activity and selectivity towards CO oxidation exhibited by CuO/CeO_2 systems, a specific kinetic study is required, since in literature there are few investigations aiming to describe the reaction kinetics and can not be extended to the present case. Most of all, such studies are referred to catalytic systems intrinsically different from Cu/CeO_2 (for Pt-based systems; Choi et al, 2004), or if deals with copper oxide supported on ceria, are limited to the investigation of the oxidation of CO in the absence of large amounts of H_2 (Liu, 1995a-b; Hocevar, 2003; Sedmak, 2004).

In particular, the present investigation is focused on the dependence of the performance of the system on the CO/H_2 ratio, on the addition to the feed of reformate species such as CO_2 and H_2O, and on the characterisation of the reaction rate (apparent reaction orders, dependence on temperature and contact time).

Such a kinetic study may represent a useful tool in describing the reaction mechanism (that must be studied with other methods too) and summarise all the effects of major parameters on the performances of the process.

Finally, a more theoretical study will be carried out in a parallel way to the experimental investigation on the kinetics: a preliminary kinetic model will be developed with the final scope of achieving a deeper understanding on the mechanisms underlying the CO-PROX reaction, with specific interest on the effects on CO conversion and O_2 selectivity to CO_2 of the main parameters ruling the process.

The kinetic modeling was undertaken by means of a isothermal plug-flow model of the reactor, solved with MatLab interpreter. In a first approximation, the kinetics were represented by a power law for both the reactions of H_2 and CO oxidation; subsequently, rate expressions derived from mechanistic considerations were tested to describe the system.

In fact, the determination of the different kinetics leading to CO and H_2 oxidation represents the key factor for determining the consequences of changing the inlet temperatures or the feed composition.

5.1 Relevance of mass transfer resistance in the kinetic tests

The presence of limitations due to intra and extra-particle diffusional resistances has been both theoretically and experimentally verified.

Under the "first-approximation" of first order kinetics, at steady state the mass balance equation at the interface between solid and gas may be written as:

$$K_m \cdot a_v \cdot (C_0 - C_s) = k \cdot C_s \tag{5.1}$$

where: K_m = mass transport coefficient, cm/s

C_0 = CO concentration in the gas phase, mol/cm^3

C_S = CO concentration on the catalyst surface, moli/cm^3

k = kinetic constant for the reaction on the surface, s^{-1}

a_v = specific geometrical surface : particle surface/particle volume, cm^{-1}

From the equation (A.1) is obtained:

$$C_s = \frac{C_0}{(1 + k / a_v K_m)} \tag{5.2}$$

The intra diffusion resistances are negligible if C_s is close to C_0, that means for the equation (A.2) if $k / K_m \cdot a_v << 1$.

The kinetic constant has been evaluated in condition of higher activity, at 155°C, assuming a power law kinetics for the CO oxidation, and a first order dependence in CO. For CO inlet concentration in N_2 equal to 5000 ppm, 0.5vol% O_2 and 50vol% H_2, a k value of 250 s^{-1} has been estimated.

The parameter a_v has been assumed equal to 400 cm^{-1} considering that for spherical particles it is equal to $6/d_p$ where d_p is the particle mesh size assumed of 150μm.

For estimating the mass transport coefficients the Satterfield and Sherwood correlation (1963) has been used:

$$K_m = \frac{j_D \cdot G}{\rho \cdot N_{Sc}^{-2/3}} \tag{5.3}$$

where:

$$j_D = 1.66 \cdot (Re_p^{-0.51}) \qquad \text{(Froment and Bishoff, 1968)} \tag{5.4}$$

$$N_{Sc} = \frac{\mu}{\rho \cdot D} \tag{5.5}$$

$$G = \frac{\rho \cdot Q}{S \cdot \varepsilon} \tag{5.6}$$

$$Re_p = \frac{d_p \cdot G}{\mu} \tag{5.7}$$

In the expressions previously used, S is the area of the annular section of the reactor used in laboratory for the reaction tests and it is equal to 0.67 cm^2, ε is the reactor vacuum degree and it is assumed equal to 0.37 (corresponding to the maximum package degree for spherical particles).
Taking into account the composition of the reacting mixture (50vol% H_2, 0.5 vol% CO, 0.5vol% O_2, in N_2) the density and the viscosity of a mixture composed by 50vol% of H_2 and 50vol% of N_2 has been used. At 150°C it has been calculated:

ρ = 0.428 kg/m^3 e μ = 0.02 cp (Perry, 1985).

The diffusivity of the carbon monoxide in N_2, *D*, expressed in $cm^2 \cdot s^{-1}$, has been estimated by using the formula: (Satterfield, Sherwood, 1963):

$$D_{CO-N_2} = 1.858 \cdot 10^{-3} \cdot T^{1.5} \cdot \frac{\left[\left(M_{CO} + M_{N_2}\right)/\left(M_{CO} \cdot M_{N_2}\right)\right]^{1/2}}{P \cdot \sigma^2_{CO-N_2} \cdot \Omega_D} \tag{5.8}$$

where T is the temperature (K), P the pressure (atm), M_{CO} and M_{N2} are respectively the molecular weight of CO ed nitrogen, Ω_D, the collision integral, that is an adimensional function of the temperature and of the intermolecular potential, which has been evaluated by the Leonard – Jones expression.
Thus from the (A.8) equation the diffusivity of CO in N_2 has been estimated 0.38 $cm^2 \cdot s^{-1}$.
By the use of the expression (A.3) it is obtained a value of K_m and the ratio $k/a \cdot K_m$ is thus estimated to be 0.007. This result suggests the absence of inter-diffusion limits to the kinetic of the process.
It has been verified the absence of inter-diffusion limits to the reaction kinetic by performing experiments at a constant contact time but changing contemporary the gas flow rate and the amount of catalyst loaded.

Indeed, considering a first order reaction, if the kinetic is the controlling mechanism, the dependence of the CO conversion from the contact time is expressed by the correlation (1), in which, it is evident that the CO conversion depends on the temperature, by the kinetic constant, and on the contact time.

$$X_{CO} = 1 - \exp(-k_c \tau) \qquad k_c = f(T) \qquad (5.9)$$

On the contrary if the controlling mechanism is the mass transport in the gas phase, the equation (2) is valid, in which the CO conversion depends not only on the contact time, but also explicitly on the flow rate by the mass transport coefficient.

$$X_{CO} = 1 - \exp(-k_m \tau) \qquad k_m = f(v, d_p, ...) \qquad (5.10)$$

The experiments in figure 5.1 shows that by changing the flow rate and the amount of catalyst loaded, at a constant contact time, the CO conversion curve towards the temperature does not change, meaning that no inter-diffusion limits occur to limit the kinetic of the process.

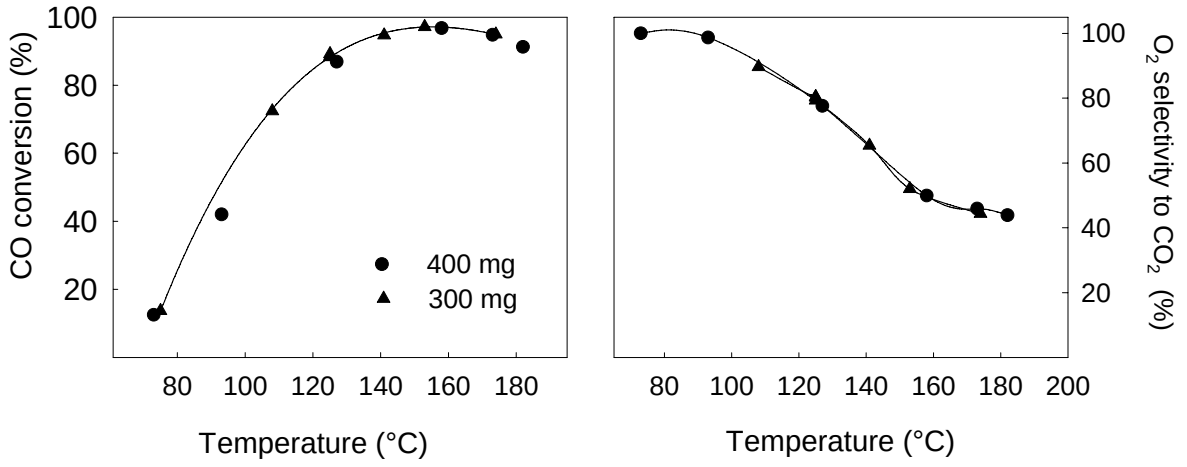

Figure 5.1: Reaction tests performed on 4.2 CuO/CeO_2 sample by changing the flow rate and grams of catalyst loaded at a constant contact time. (•) 48 Nl/h and 400mg; (▲) 36Nl/h and 300 mg. Reaction conditions: 0.5 vol% CO; 0.5 vol% O_2; 50 vol% H_2; in N_2. W/F= 0.03 g·s/cm^3.

For excluding intra-diffusion limits inside the pores, to the kinetic of the reaction, it has been verified that the efficiency factor of the catalyst η, which appear in the expression of the effective reaction rate is close to one:

$$r_{eff} = k \cdot C_S \cdot \eta \tag{5.11}$$

Thus considering spherical particles, the following expression may be considered:

$$\Phi_S = \frac{d_p}{2} \cdot \sqrt{\frac{k}{D_{eff}}} \tag{5.12}$$

where Φ_S is the Thiele modulus, D_{eff} ($cm^2 \cdot s^{-1}$) is the effective diffusivity of CO in N_2 and is equal to $D \cdot \varepsilon / \tau$, τ being the tortuosity into the pores.

If the Thiele modul is known, the efficiency may be obtained as:

$$\eta = \frac{3}{\Phi_S} \cdot \left(\frac{1}{\tanh(\Phi_S)} - \frac{1}{\Phi_S} \right) \tag{5.13}$$

In table 3.1 the results obtained by considering a particle mesh size of 300 or 150 have been reported.

Table3.1: Estimation of the efficiency factor by the thiele modulus and by the Prater criteria:

d_p (μm)	$k / k_m \cdot a_v$	Φs	η	r ($mol \cdot s^{-1} \cdot cm^{-3}$)	Φ
150	$7.6 \cdot 10^{-3}$	0.63	0.975	$3.5 \cdot 10^{-5}$	0.39
300	$2.2 \cdot 10^{-2}$	1.26	0.908	$3.4 \cdot 10^{-5}$	1.58

The estimated values for the Thiele number are close to one thus suggesting the occurrence of a mixed regime.

Alternatively the criteria suggested by Satterfield e Sherwood may be used. In this case a parameter **Φ** is defined as:

$$\mathbf{\Phi} = \frac{d_p^2 \cdot r}{4 \cdot D_{eff} \cdot C_S} \tag{5.14}$$

if **Φ**< 0.3, thus the diffusion inside the pores is not the limiting step.

In the formula (A.12) *r* is the effective reaction rate per unit volume of catalyst. :

Appling the (A.12) $\Phi \sim 0.3$ is obtained, confirming the occurrence of a mixed regime

Similarly for verifying the absence of intra-diffusion limits, activity tests have been performed on a fixed catalyst, at a fixed contact time, just changing the particle mesh size.

If the controlling mechanism is the kinetics, at a constant temperature, the reaction rates obtained on catalysts with different particle mesh size must be the same. Indeed, in both the cases the efficiency is equal to one, and thus is obtained (3).

$$\frac{r_1}{r_2} = \frac{k_{c1} C_{CO}\, \eta_1}{k_{c2} C_{CO} \eta_2} = \frac{\eta_1}{\eta_2} = 1 \qquad (5.15)$$

On the contrary if the controlling mechanism is the diffusion inside the pores thus the ratio between the two rates may be written as (4).

$$\frac{r_1}{r_2} = \frac{k_{c1} C_{CO}\, \eta_1}{k_{c2} C_{CO} \eta_2} = \frac{\eta_1}{\eta_2} \neq 1 \qquad (5.16)$$

So that the two rates will be different.

In figure 5.3 it has been demostrated that internal diffusional limits are present for a particle size higher than 300μm. Thus the reaction tests have been performed using a medium particle size between 125-220μm.

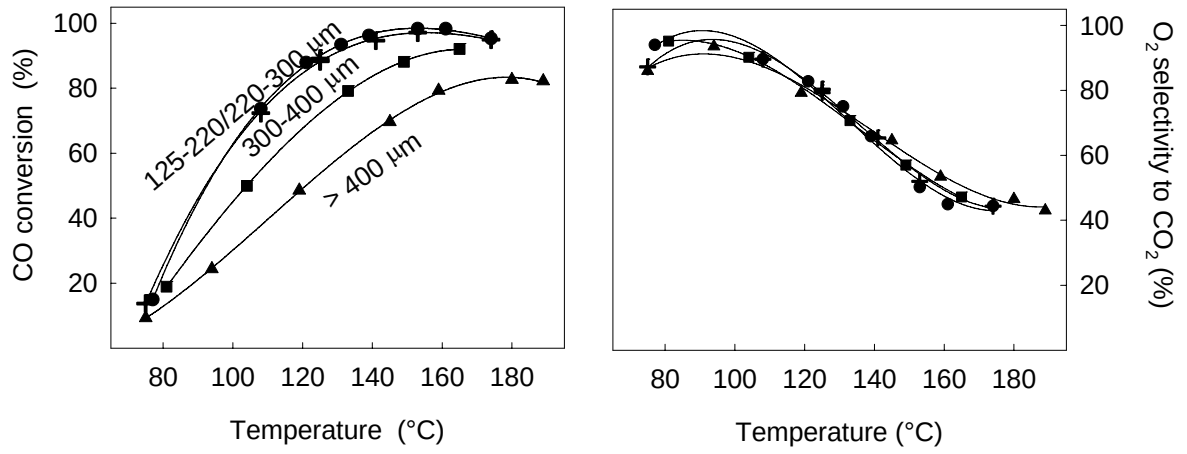

Figure 5.2: Reaction tests performed on 4.2 CuO/CeO_2 sample by the mesh size at a constant contact time. (●) 125-220 μm; (+) 220-300 μm; (■) 300-400 μm(▲) >400 μm. Reaction conditions: 0.5 vol% CO; 0.5 vol% O_2; 50 vol% H_2; in N_2. W/F= 0.03 g·s/cm^3.

5.2 Experimental characterisation of the reaction kinetics

The kinetics of CO preferential oxidation in the presence of large amounts of H_2 has been experimentally characterized by carrying out reaction tests under different and variable experimental conditions. More specifically, the effect of temperature, contact time, inlet concentrations of reactants (CO and O_2) products (CO_2 and H_2O) has been investigated. The sample used for these tests is the 4 CuO/CeO_2 with a particle mesh size 125-200μm. Catalyst has been stabilized for 40h under reaction conditions and for 62h in a stream of 1vol% CO at 100°C.

5.2.1 The effect of the temperature on the reaction kinetics

Figure 5.3 reports the results of the reaction tests carried out over 4 CuO/CeO_2 catalyst sample for the preferential oxidation of CO in a mixture containing 0.5vol% CO, 0.5vol% O_2, 50 vol% H_2 in N_2 at a contact time of 0.02 $g \cdot s/cm^3$ and variable temperature.

As previously discussed in the chapter III, the catalyst exhibits high activity and high selectivity towards CO oxidation. 100% selectivity to CO_2 is shown till 100°C, in correspondence to a conversion of CO equal to 30%; this high value of selectivity was detected by measuring a stechiometric O_2 consumption for the conversion of sole carbon monoxide. At higher temperatures (T>100°C), the oxidation of hydrogen starts to take place too, giving a higher O_2 conversion; the CO conversion carries on increasing with increased temperature but only up to 150°C, where a maximum is observed. Indeed, at higher temperature carbon monoxide conversion starts to decrease (while the consumption of O_2 is quite complete).

In chapter 4, it has been evidenced the presence of a maximum for CO conversion with temperature which can be related to the different dependence on temperature of the kinetics of the two reactions of hydrogen and CO oxidation (different activation energy), or to the occurrence of limits imposed on the CO conversion by the reverse water gas shift reaction.

On the basis of such considerations it is possible to identify in the CO conversion, three different zones. In the first zone, from room temperature up to about 90°C, only the CO oxidation reaction occurs. The second zone proceeds between 90 and 150°C and is characterised by the fact that both reactions take place with selectivity to the CO oxidation lower than 100%, but still quite high for potential applications. Finally, in the third zone, above 150°C, the hydrogen oxidation strongly prevails, limiting the CO conversion.

The effect of different variables on the kinetic of CO oxidation must be hence studied on the left hand side of CO conversion maximum. Thus, two temperatures have been chosen as characteristic

for investigating the effect of the experimental conditions adopted: 92°C, the highest temperature at which the oxidation of hydrogen does not take place or proceeds very slowly, and 132°C a temperature at which both reactions significantly occur, even though the selectivity to CO_2 remains quite high (~80%).

The effect of some parameters such as the addition of CO_2 or H_2O addition to the reaction mixture, that shifts the CO conversion curve towards higher temperatures, have been studied in correspondence of higher temperature (116-132-200°C).

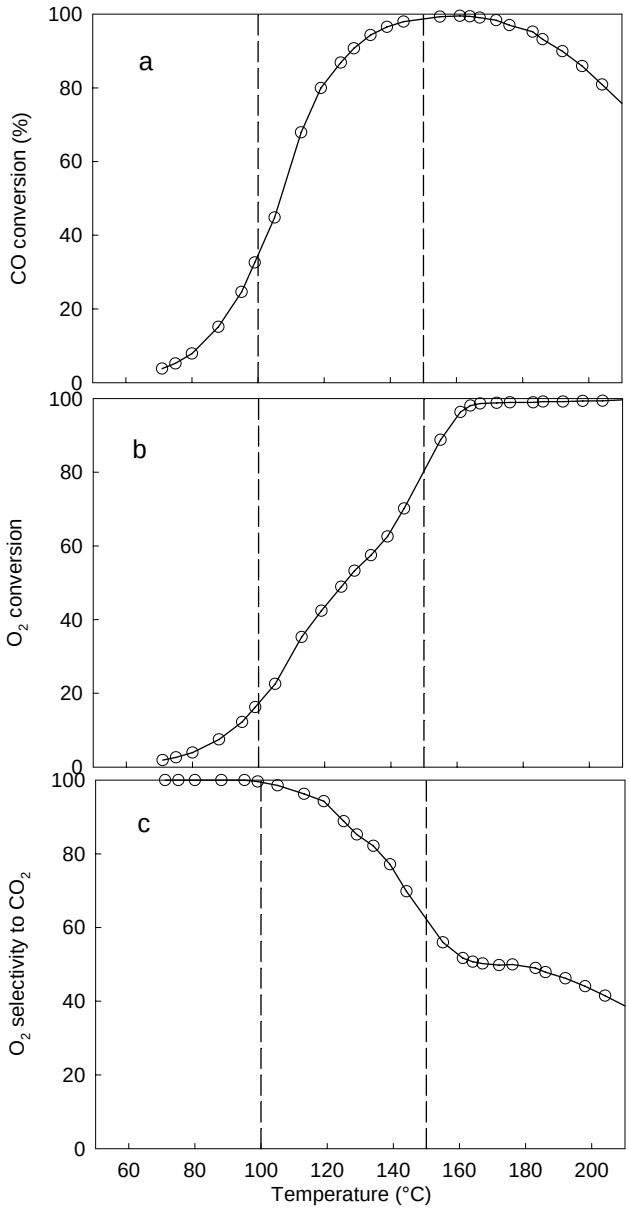

Figure 5.3: CO (a) and O_2 (b) conversions and O_2 selectivity to CO_2 (c) as functions of the reactor temperature in the absence of CO_2 and H_2O. Reaction conditions: 0.5vol% CO, 0.5vol% O_2, 50 vol% H_2 in N_2. W/F= 0.023 g·s/cm^3.

5.2.2 Effect of the WGS equilibrium on the CO conversion

As already underlined in previous sections, the conversion of CO does not increase monotonically with the temperature in the CO PROX tests on CuO/CeO_2.

The presence of a maximum for CO conversion with temperature is frequently observed in the CO PROX tests (Oh and Sinkevitch, 1993; Kahlich, 1997; Iragashi, 1997; Choi, 2004). Its origin could be related to two possible causes:

i) from one side the process could be intrinsically more selective at low temperature towards the CO oxidation because of the lower activation energy of this reaction in comparison to the oxidation of hydrogen. In this hypothesis by increasing the temperature the kinetics of the undesired reaction increases faster thus decreasing the overall selectivity of the process;

ii) on the other side a thermodynamic limit may interfere on the CO conversion if the catalyst is active towards the reverse water gas shift reaction.

Indeed, for noble metal based catalysts, up to a certain variable temperature, the reverse WGS proceeds in a significant amount, so that CO is produced from CO_2 and thus justifying the presence of a maximum in the CO conversion.

$$CO_2 + H_2 \leftrightarrow CO + H_2O \qquad (5.17)$$

In order to understand whether the reverse WGS reaction is catalyzed by the catalyst in the temperature range of interest (50-170°C), experiments are performed feeding only hydrogen (50vol%) and CO_2 to the reactor and measuring the amounts of CO eventually produced. Figure 5.4 shows the results of two different series of such tests.

On one hand, it has been tested the activity of catalyst under conditions as close as possible to those of PROX experiments, but in the presence of CO and O_2: 1% CO_2 and 50% H_2 (diluted by nitrogen). On the other hand, it has been verified the eventual production of CO, also under more favourable conditions for the reverse WGS reaction, with larger concentration of CO_2 employed (20%).

In figure 5.4 it has been also plotted the limit values of CO concentration expected by thermodynamics. Results of such experiments show that the time-scale of the reverse water gas shift reaction is probably much larger than that of the oxidation of CO, since under the same contact time involved in the CO PROX tests the conversion of CO_2 to CO is negligible, although the thermodynamic limit is not very strict under the operating conditions of interest. Actually, the conversion of CO_2 becomes measurable only at temperatures higher than 200°C, i.e. outside the

range of interest for the process of CO removal in H_2 streams to fuel cells. This means that the catalyst is not prevented in principle to promote the complete oxidation of CO to CO_2, up to reduce its concentration to few ppm and that the volcano-shaped curve of CO conversion as function of temperature can be completely explained by the different dependence of the kinetics of the two reaction in competition on the temperature.

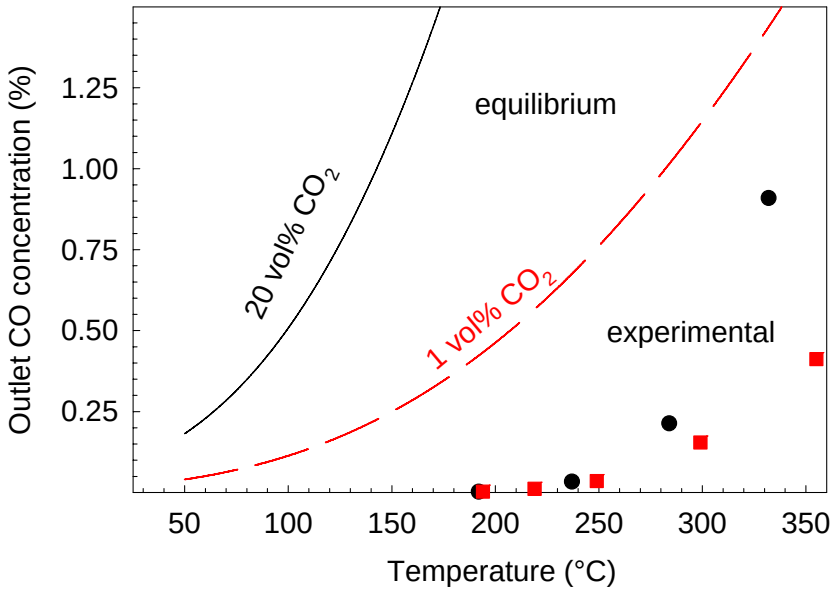

Figure 5.4: Study of the rWGS reaction on 5wt% CuO/CeO_2 sample. (line) theoretical calculation; (dotted) experimental data. Reaction conditions: τ = 0.03 g*s/cm^3; $[H_2]$ = 50 vol%; $[CO_2]$ = 1-20 vol%

5.2.2 Effect of contact time on the reaction kinetics

In figure 5.5 the effect of contact time on the CO oxidation kinetics has been studied at constant CO inlet concentration (0.5vol%), λ (= 2) and H_2 inlet concentration 50 vol%. The contact time has been varied, changing the flow rate on a catalyst bed containing 300mg of catalyst.

In such experiments, it is possible to measure the selectivity of the process while changing the CO/H_2 average ratio in the reactor without varying the temperature.

The results reported in figure 5.5 show that at low temperature, where the selectivity is still 100% (namely, H_2 is not converted at all), the conversion of CO increases with increasing the contact time, leaving at a constant level the selectivity of the process (namely, H_2 remains unconverted also when the H_2/CO becomes much larger). Moreover, a similar behaviour is also observed at 132°C, where selectivity is lower (about 80%) and conversion much higher (closer to 100%): in such conditions, selectivity still remains constant with increasing contact time, while the conversion of CO increases.

In these latter experimental conditions (relatively high temperature, and very high CO conversion) similar results were obtained by Ratnasamy et al. (2004) who confirmed that the selectivity is constant with changing the contact time.

If all this is true, the selectivity of the process should basically depend on the reaction temperature and very poorly on the CO/H_2 ratio in the reacting mixture, unless a very large difference exists between the kinetic laws of the two competitive reactions. For example, in the case of Pt catalyst for CO PROX such a consideration does not apply, since the selectivity towards the preferential oxidation of CO rather than of H_2 lies in the strong adsorption of carbon monoxide on the catalyst which in the range of optimal temperatures of the process largely cover the catalyst surface and prevents hydrogen to reach the active centers (Kahlich, 1997; Schubert, 1999). Thus, on Pt catalysts the selectivity is strongly dependent on CO/H_2 ratio and decreases when the concentration of CO becomes too low.

Anyway, to decrease the CO concentration in the gas mixture to the PEMFC tolerance limit (~10ppm) sacrificing as little fuel as possible (H_2) is the main requirement for the CO-PROX step in the fuel processor. The main goal of copper/ceria catalyst in CO-PROX reaction compared to gold and platinum based ones seems to be the highest oxygen selectivity, also at high CO conversion and the possibility to achieve deep abatement level by only increasing the contact time, since the selectivity only depends on the temperature.

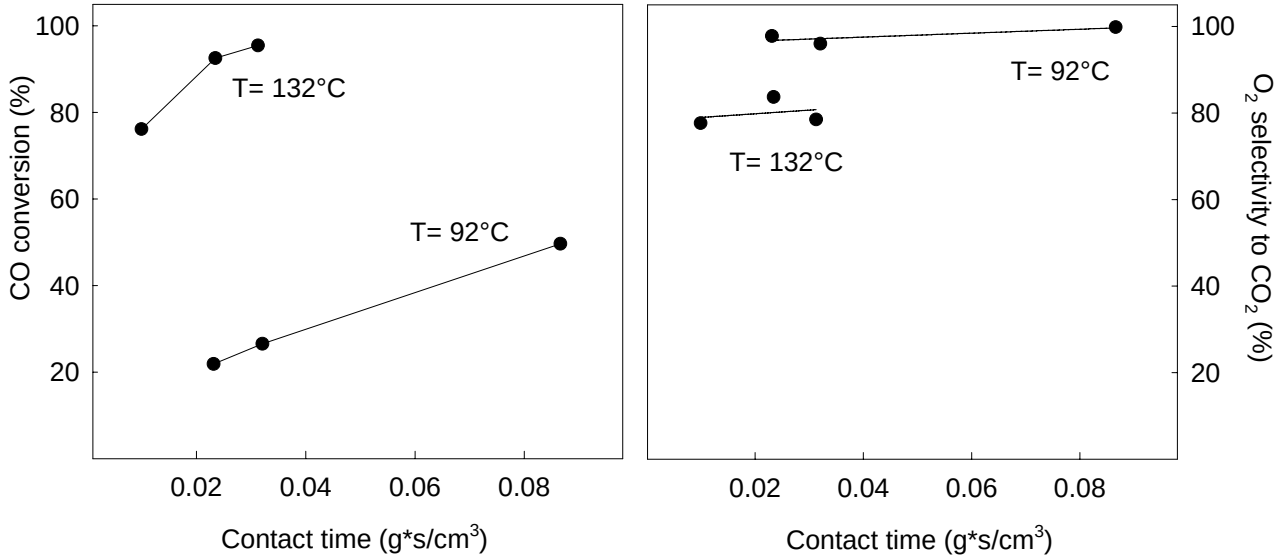

Figure 5.5: CO conversion and selectivity to CO_2 as functions of the contact time at 92°C - 132°C. Reaction conditions: 0.5vol% CO, 0.5 vol% O_2, 50 vol% H_2 in N_2.

5.2.3 The effect of the oxygen partial pressure (λ) on the reaction kinetics

The study of the dependence of the CO-PROX reaction kinetics on the oxygen partial pressure has been performed using a reacting mixture containing variable oxygen concentrations and 0.5 vol% CO, 50vol% H_2 in N_2, at two different contact times 0.009 and 0.032 g·s/cm^3 and temperatures of 92°C and 132°C. Figure 5.6 shows the behaviour of the CO conversion and selectivity to CO_2 as a function of the ratio λ between the actual O_2 concentration and the stechiometric one ($\lambda = \frac{2 \cdot P_{O2}}{P_{CO}}$).

At 92°C the CO conversion does not change significantly with λ, suggesting that, in these conditions, the kinetics of CO oxidation does not depend significantly from the oxygen partial pressure for oxygen concentration higher than the stoichiometric value (λ=1).

The selectivity to CO_2 slightly decreases suggesting a very weak positive effect on the hydrogen oxidation by the increased oxygen partial pressure even at so low temperature.

At 132°C the oxygen partial pressure has a more relevant effect when is increased up to the stoichiometric value. Neverthless increasing the oxygen concentration up to a value corresponding to doubled the stoichiometric one for the complete oxidation of CO (λ=2), the CO oxidation kinetics does not depend any more on λ. On the other hand the selectivity decreases when increasing λ, due to increased hydrogen conversion probably due to a not negligible effect of O_2 on the hydrogen oxidation kinetics.

Moreover, at 132°C, decreasing the contact time from 0.032 to 0.009 g·s/cm^3 the CO conversion is obviously significantly lower and hence, the effect of the oxygen partial pressure is magnified.

The selectivity to CO_2 presents exactly the same value obtained for the higher contact time, suggesting an exclusively dependence of the selectivity from the temperature, as revealed in figure5.6.

The independence of the CO oxidation reaction from the oxygen partial pressure has been previously reported by Liu et. al (1996).

Recently Hocevar et al. (2003) found that in CO-PROX conditions and on CuO/CeO_2 catalysts the oxygen concentration does not affect significantly the CO oxidation rate if a concentration higher than two times the stechiometic value is involved. In particular the oxidation of CO is completely unaffected by the oxygen concentration. Increasing the hydrogen content in the mixture, the CO conversion slightly depends on the oxygen content when this is increased from from λ=1 to λ=2.5. Those results are in good agreement with our observations.

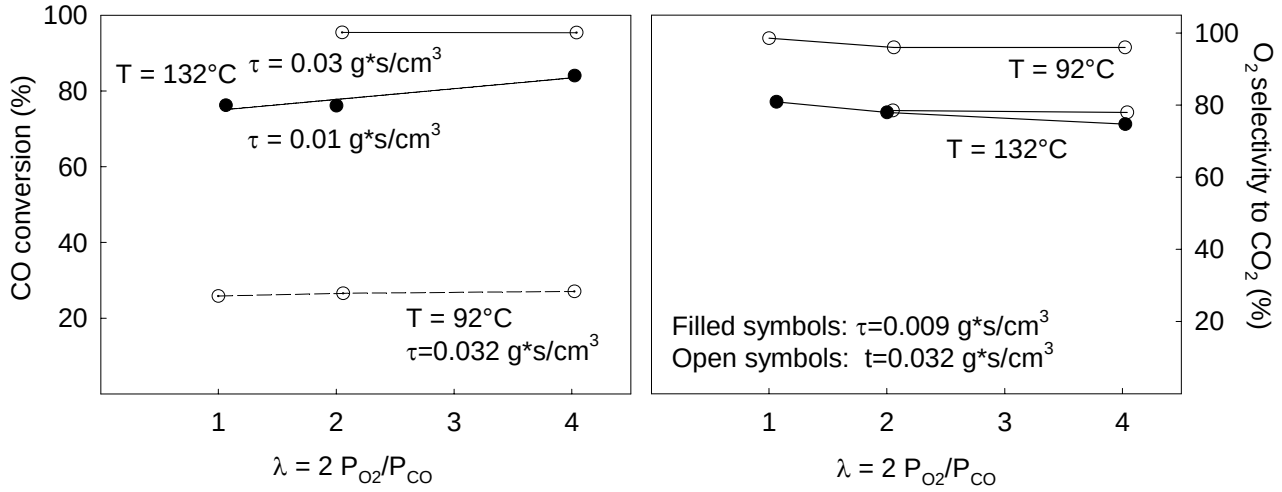

Figure 5.6: CO conversion and O_2 selectivity to CO_2 as functions of the inlet oxygen concentration expressed in term of λ (=2 P_{O2}/P_{CO}) at 92°C and 132°C.. Reaction conditions: 0.5vol% CO, 50 vol% H_2 in N_2. W/F= 0.09 g·s/cm^3 (filled symbols)-0.032 g·s/cm^3 (open symbols).

5.2.5 The effect of CO inlet concentration on the reaction kinetics

The effect of CO inlet concentration on the reaction kinetics has been investigated keeping constant either the O_2/CO ratio (fig. 5.7), or the oxygen partial pressure (fig.5.8).

The reaction conditions used for the study of the CO inlet concentration at a constant O_2/Cu ratio are: 50vol% H_2 in N_2, and contact time 0.009 and 0.032 g·s/cm^3.

At low temperature (92°C), increasing the CO inlet concentration the CO conversion decreases significantly. On the contrary at high temperature (132°C), the CO conversion increases with the CO inlet concentration. This effect is more evident when the contact time is decreased to 0.009 g·s/cm^3, because the conversion level attained is significantly lower.

If the CO conversion decreases with CO inlet concentration at a constant λ, thus the overall reaction order, that is the sum of the CO and oxygen reaction orders, must be lower than 1. On the contrary if increasing the CO inlet concentration, the CO conversion increases, the overall reaction order must be higher than 1.

The selectivity to CO_2 increases increasing the CO inlet concentration.

At 92°C this result is explainable considering that, at this temperature and for this contact time (0.032 g·s/cm^3) the H_2 oxidation reaction proceeds even if with very low H_2 conversions. Independently from the CO inlet concentration, about 55 ppm of H_2 have been estimated to react at 92°C. This result is in agreement with the observation discussed in chapter 3 by which the H_2 oxidation kinetic is independent by the presence of CO at low temperature. The small amount of oxygen involved in the reaction with hydrogen, has a bigger influence on the CO selectivity when few ppm of CO and O_2 (λ is constant) are fed, while decreasing this effect at higher value of the CO inlet concentration.

At 132°C with increasing the CO inlet concentration the selectivity increases. Indeed, the CO oxidation rate is more than linearly promoted by the presence of CO while weakly depends on the inlet oxygen partial pressure (see preceding paragraph). The hydrogen oxidation kinetics, is promoted by the increase of the oxygen partial pressure being independent from the CO inlet partial pressure.

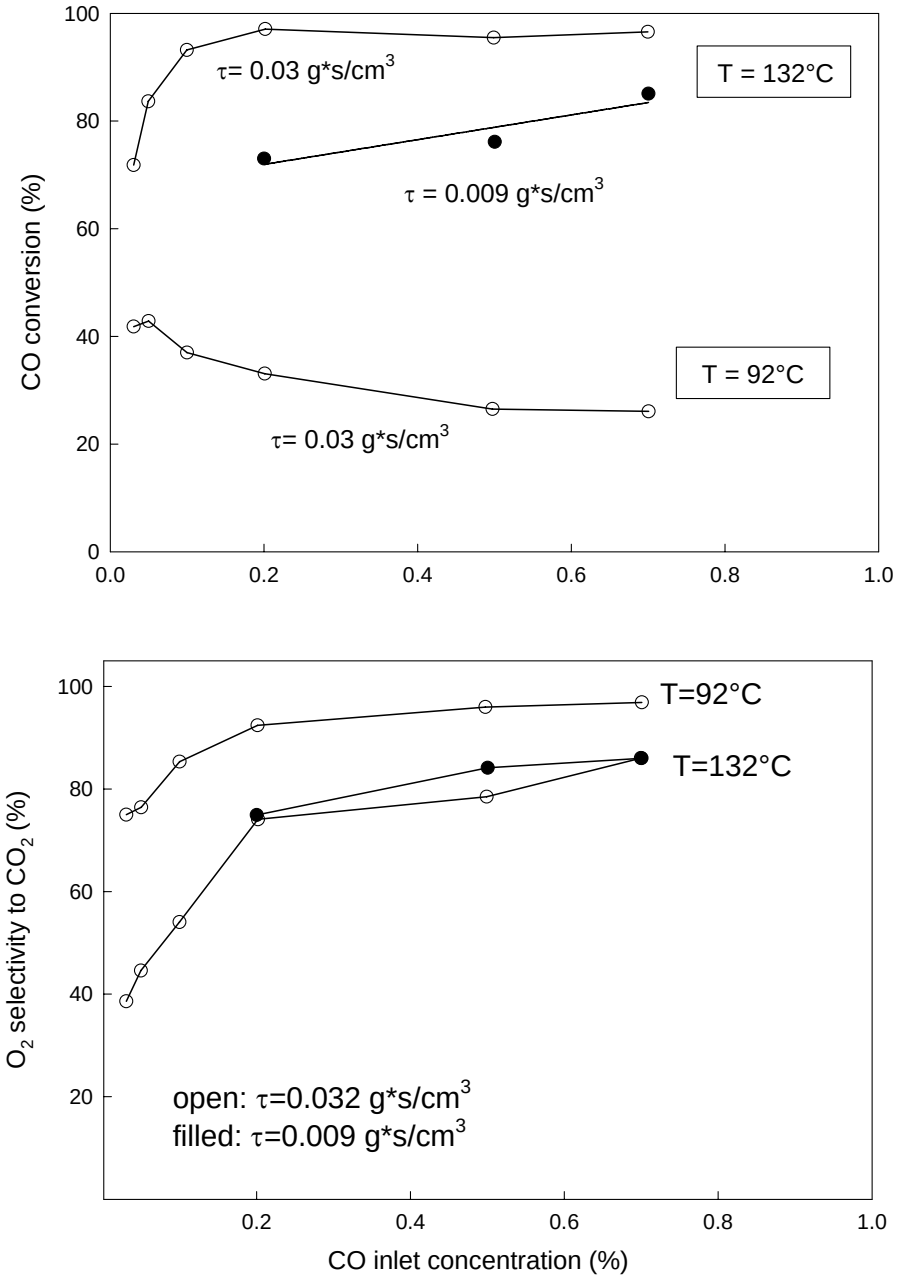

Figure 5.7: CO conversion and O_2 selectivity to CO_2 as functions of the inlet carbon monoxide concentration at 92°C and 132°C.. Reaction conditions: λ=2, 50 vol% H_2 in N_2. W/F= 0.09 g·s/cm^3 (filled symbols)-0.032 g·s/cm^3 (open symbols).

The effect of the CO inlet concentration has been studied also keeping constant the oxygen partial pressure feeding to the system a mixture constituted also by: 0.5vol% CO, 50vol% H_2, in N_2 at a contact time 0.009 g·s/cm^3.

Fig. 5.8 reports the results of such experiments. As expected, the effect of the CO inlet concentration on the CO conversion and selectivity are similar to those observed keeping constant

λ, because of the weak effect on the kinetics observed for the O_2 partial pressure. Indeed in the previous paragraph it has been demonstrated that the oxygen partial pressure does not have an effect on the CO oxidation kinetics unless a stoichiometric concentration is used (λ = 1) and in particular if λ≥2 the oxygen concentration does not have any effect.

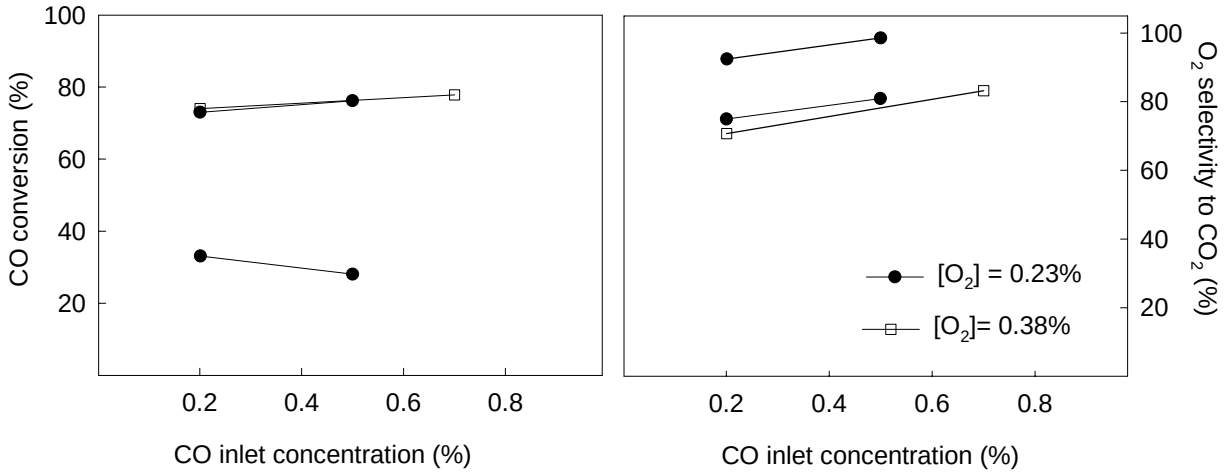

Figure 5.8: CO conversion and O_2 selectivity to CO_2 as functions of the inlet carbon monoxide concentration, keeping constant P_{O2} and at 92°C and 132°C.. Reaction conditions: P_{O2}= 0.23-0.38 vol%, 50 vol% H_2 in N_2. W/F= 0.09-0.032 g·s/cm^3.

The dependence of the CO conversion from the CO inlet concentration observed at 92°C is in agreement with previous literature studies on CuO/CeO_2 catalysts. Liu et al.(1996) observed for the CO oxidation reaction that the reaction order in P_{CO} seems to decrease from one to zero increasing P_{CO} at a constant P_{O2}.

Moreover those results are confirmed by the study of Hocevar et al. (2004) performed in CO-PROX conditions but only up to 92°C, a temperature so low that the H_2 oxidation reaction does not take place.

Nor any of the literature study analyzes the CO oxidation reaction dependence from the CO inlet concentration, in real CO-PROX conditions and in a temperature range in which both CO and H_2 oxidation reactions take place.

5.2.6 The effect of H_2 inlet concentration on the reaction kinetics

Figure 5.9 shows the effect of the hydrogen concentration in the reaction mixture on the CO conversion and selectivity to CO_2.

The CO conversion is completely unaffected by the hydrogen partial pressure except at 200°C, because at such a high temperature, increasing the hydrogen concentration dramatically decreases the selectivity.

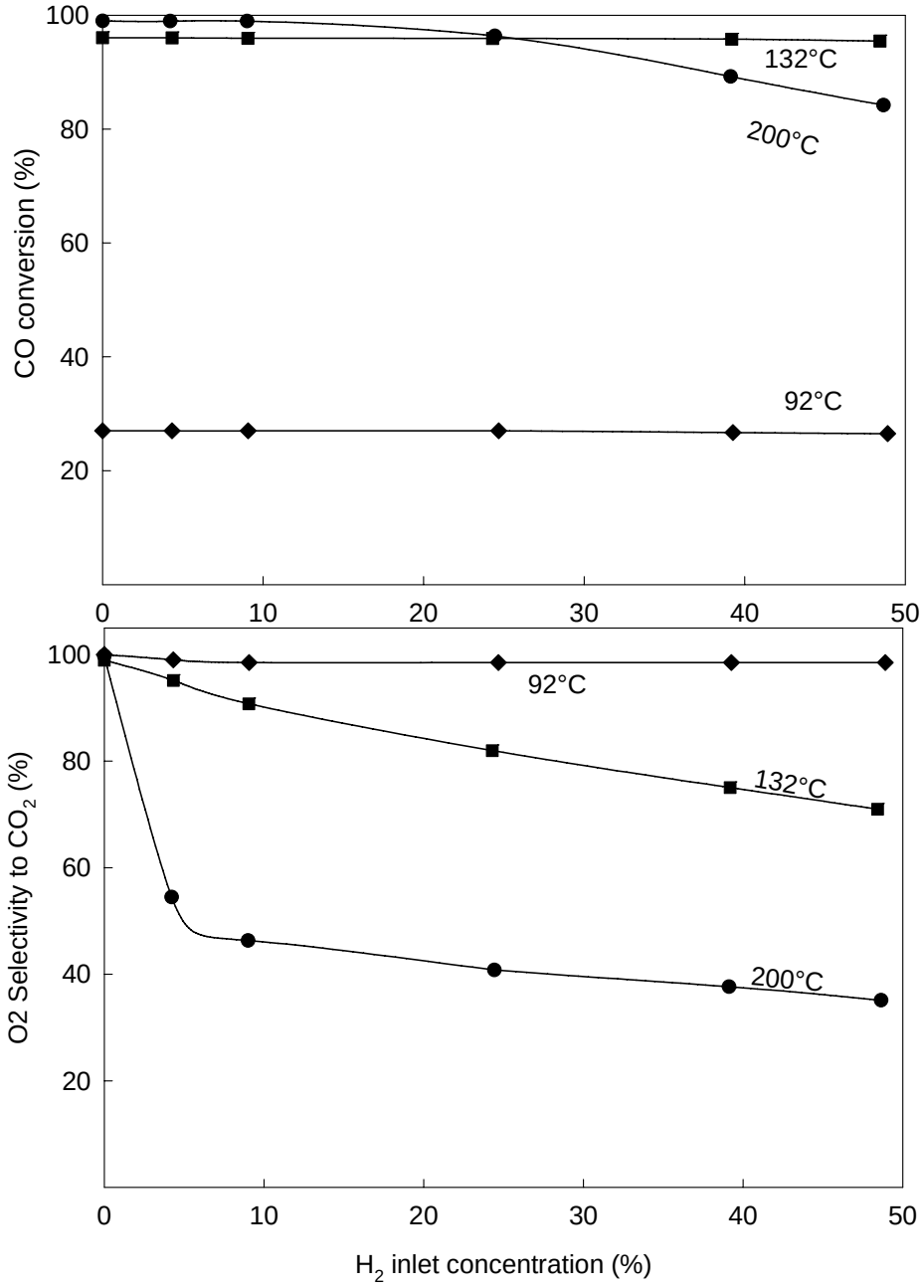

Figure 5.9: CO conversion and O_2 selectivity to CO_2 as a function of the inlet Hydrogen concentration in the absence of CO_2 and H_2O at 92°C - 132°C – 200°C. Reaction conditions: 0.5vol% CO, 0.5 vol% O_2 in N_2. W/F= 0.032 g·s/cm^3.

At temperature so high as 200°C, the oxygen concentration is close to zero, thus the dramatic increase in the H_2 oxidation reaction rate, embezzles the oxygen from reaction environment thus limiting the CO conversion.

This result is in agreement with the observation of Hocevar et al. (2003) that found that on CuO/CeO_2 catalysts the CO conversion is literally independent from the hydrogen partial pressure in all the temperature range investigated ($T \leq 150°C$) as long as there is enough oxygen fed to the reactor ($\lambda > 2.5$).

5.2.7 The effect of the presence of CO_2 and H_2O in the reaction mixture

The effect of the presence of H_2O and CO_2 in the feed on the activity and the selectivity of the process in the presence of excess hydrogen, was also examined, since those species are present in significant amounts in the reformed gases and are also the reaction products.

Initially the effect of the addition of CO_2 and H_2O has been studied separately using a mixture containing: 50vol% H_2, 0.5vol% CO, 0.5vol% O_2 in N_2 and at a contact time of 0.032 g·s/cm^3. At a constant temperature (92-116-132-200°C) the CO_2 concentration or alternatively the H_2O concentration have been varied. The CO_2 inlet concentration has been veried between 0 and 20vol%, while H_2O concentration has been varied between 0 and 10vol%. The H_2O has been added to the reaction mixture by saturation of the reaction stream. To obtain high H_2O partial pressure the saturator has been placed in a thermostatic bath.

Successively the effect of the contemporary addition of CO_2 and H_2O has been studied. In this second case, in the reaction stream with similar composition of the previous case (50vol% H_2, 0.5vol% CO, 0.5vol% O_2 in N_2) and with a constant H_2O concentration, the CO_2 concentration has been varied between 0 and 20 vol%. The latter experiment has been repeated in correspondence of two different H_2O partial pressures (0.5-1.5vol%), obtained changing the saturation temperature for the reaction mixture.

The effect of the presence of CO_2 in the reaction gas mixture on the conversion and selectivity is shown in figure 5.10.

The presence of CO_2 in the reactant feed has a negative effect on the performance of the samples, lowering their catalytic activity. This effect is more pronounced at low temperature, as suggested by the shape of the CO conversion curves as a function of the CO_2 conversions. At 200°C the CO oxidation conversion is unaffected by the presence of CO_2.

The presence of carbon dioxide shows to be not very relevant in changing the intrinsic selectivity of the process, so meaning that both reactions, the oxidations of CO and H_2, are depressed by the presence of CO_2, and in a similar way.

The negative effect of the CO_2 addition on the CO oxidation kinetics is probably due to competitive adsorption of CO and CO_2 on the catalyst surface.

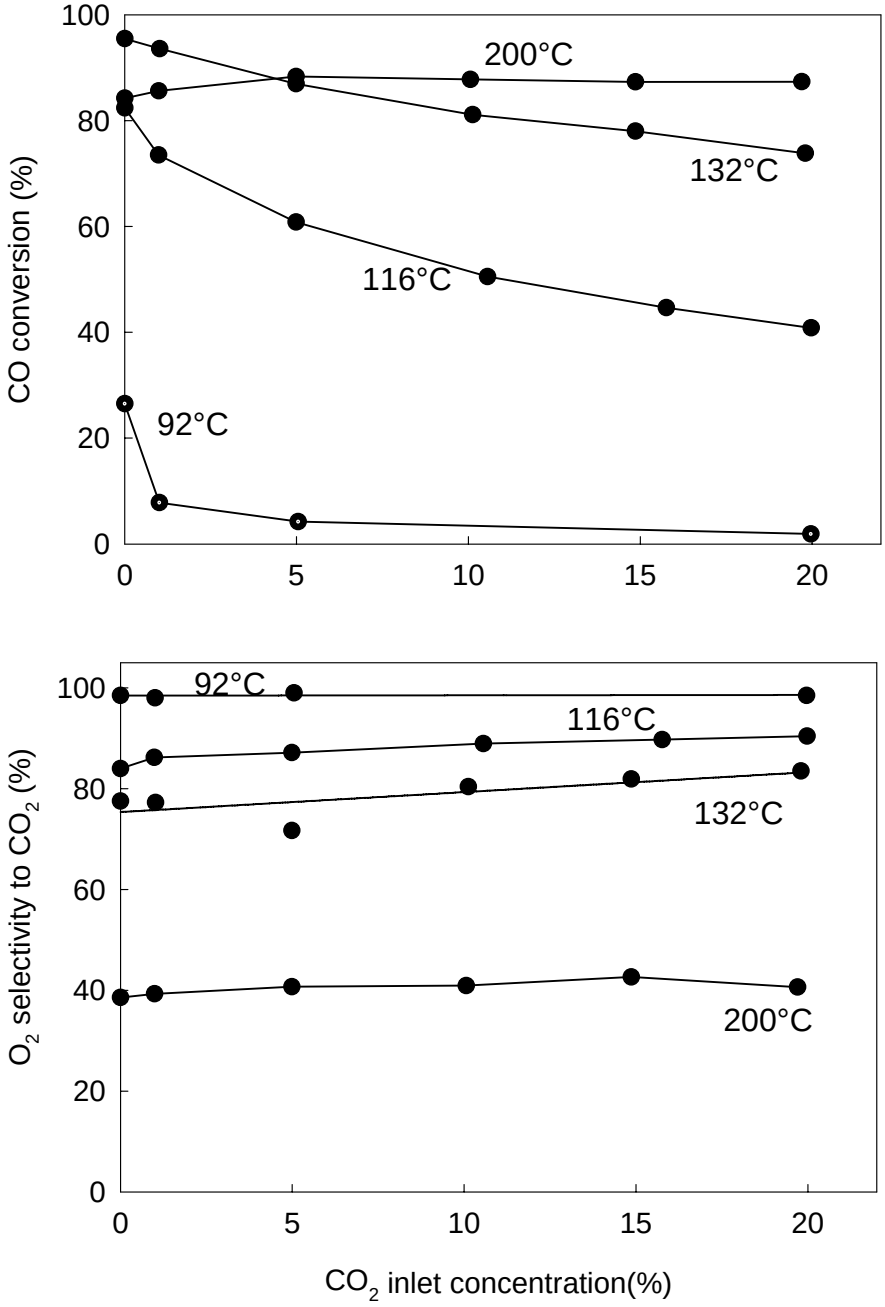

Figure 5.10: CO conversion and O_2 selectivity to CO_2 as a function of the CO_2 inlet concentration in the absence of H_2O at 92°C – 116 - 132°C – 200°C. Reaction conditions: 0.5vol% CO, 0.5 vol% O_2 , 50 vol% H_2, in N_2. W/F= 0.032 g·s/cm^3.

Water content is one of the most critical factors in the PROX reaction and is very important for proper operation of the fuel cell stack. Contradictory viewpoints still exist as to whether acts

positively for CO oxidation or not. Actually the presence of water has different effect depending on the nature of the catalysts.

Many research groups have reported that water enhances the CO oxidation reaction for a certain range of temperatures on platinum catalysts (Schubert, 1997; Malansilp, 2002; Wang, 2002; Choi, 2004). Three different explanations have been suggested for the water enhancement on those catalysts: (1) the promotion of the reverse water gas shift reaction, (2) the role of the adsorbed group, or (3) the change of Pt metal state. The first explanation is the most plausible

On the other hand Korotkikh and Farrauto reported that the addition of small amount of water (3vol%) decreases the CO conversion on gold catalysts. Grisel and Nieuwenhuys (2001) and Avgouropoulos et al. (2002) also reported that H_2O had a detrimental effect on the CO oxidation activity of Au based catalysts and on CuO/CeO_2 catalysts.

The influence of the presence of H_2O in the feed on our catalyst is summarized in figure 5.11.

At a constant temperature (116°C-132°C-200°C) the H_2O concentration has been varied between 0 and 20 vol%. The presence of water vapour provokes a significant decrease on the activity of the catalysts. Increasing the temperature this effect becomes less evident, so that at 200°C the CO conversion is unaffected by the presence of H_2O.

The selectivity to CO_2 is weakly but positively affected by the water vapour partial pressure for H_2O concentration lower than 2 vol%. For H_2O inlet concentration higher than 5vol% the selectivity remains unchanged.

It is assumed that when water is present in the reactant feed, the catalytic activity degrades due to the blocking of the active sites. It is possible that for low H_2O partial pressure, the presence of H_2O affects more negatively the H_2 oxidation reaction thus increasing the selectivity. When the H_2O inlet concentration exceeds 5 vol% both CO and H_2 oxidation reaction are similarly affected by the presence of H_2O.

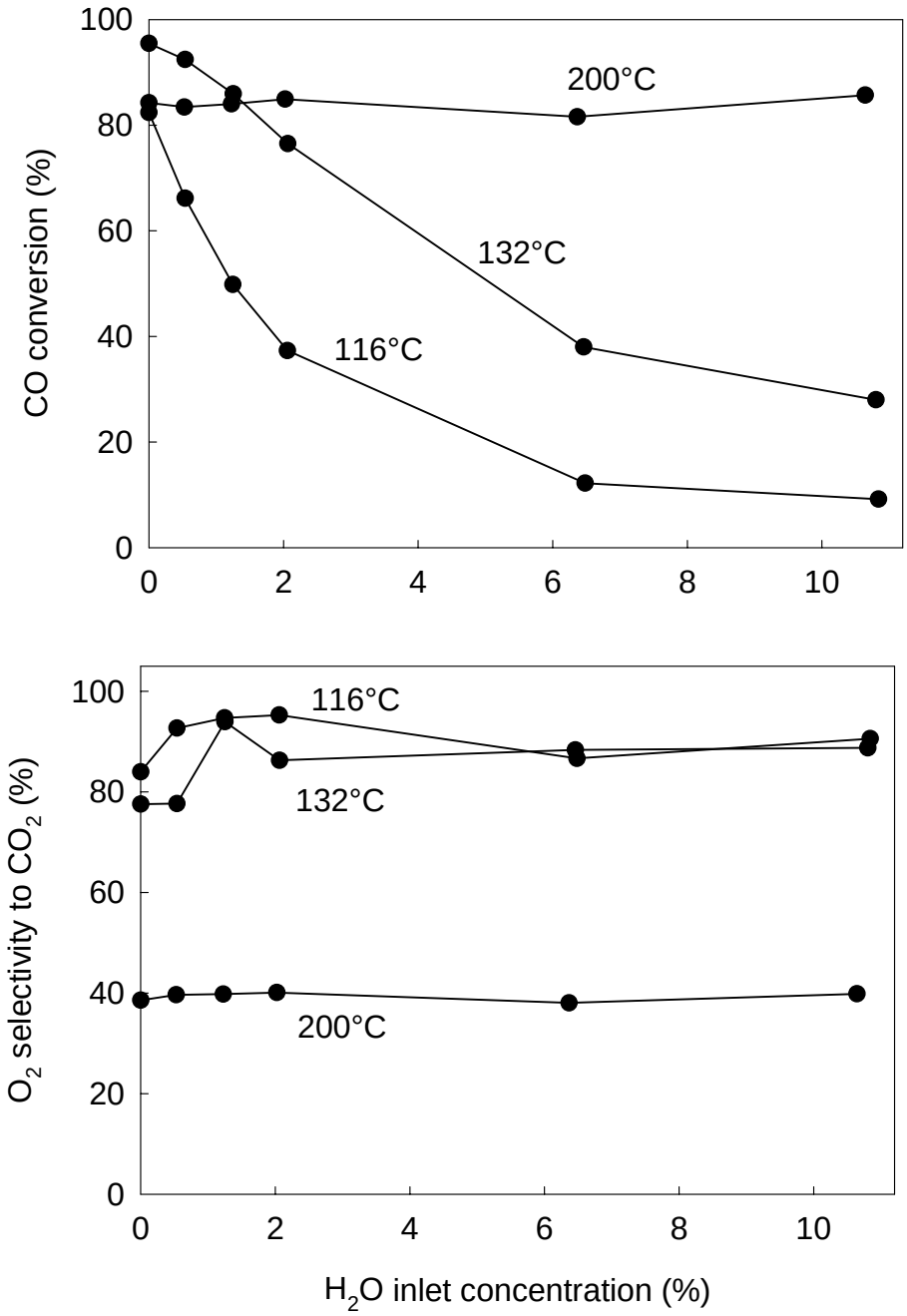

Figure 5.11: CO conversion and O_2 selectivity to CO_2 as a function of the H_2O inlet concentration in the absence of CO_2 at 116°C- 132°C – 200°C. Reaction conditions: 0.5vol% CO, 0.5 vol% O_2 , 50 vol% H_2, in N_2. W/F= 0.032 g·s/cm^3.

The experiments in which the contemporary addition of both CO_2 and H_2O has been studied are reported in figure 5.12 and 5.13 using a mixture containing respectively 0.5vol% or 1.5vol% of H_2O.

The negative effect of the CO_2 and H_2O addition are summed in those reaction tests, further lowering the CO conversion with respect to the lonely addition of CO_2 or H_2O. The negative effect of the CO_2 addition is more evident increasing the H_2O partial pressure. Indeed, at a fixed H_2O partial pressure, increasing the CO_2 inlet concentration the CO conversion decreases, while comparing a reaction test in which the CO_2 concentration is the same, increasing the H_2O partial pressure the CO conversion decreases.

The selectivity to CO_2 does not change significantly with addition of both CO_2 and H_2O.

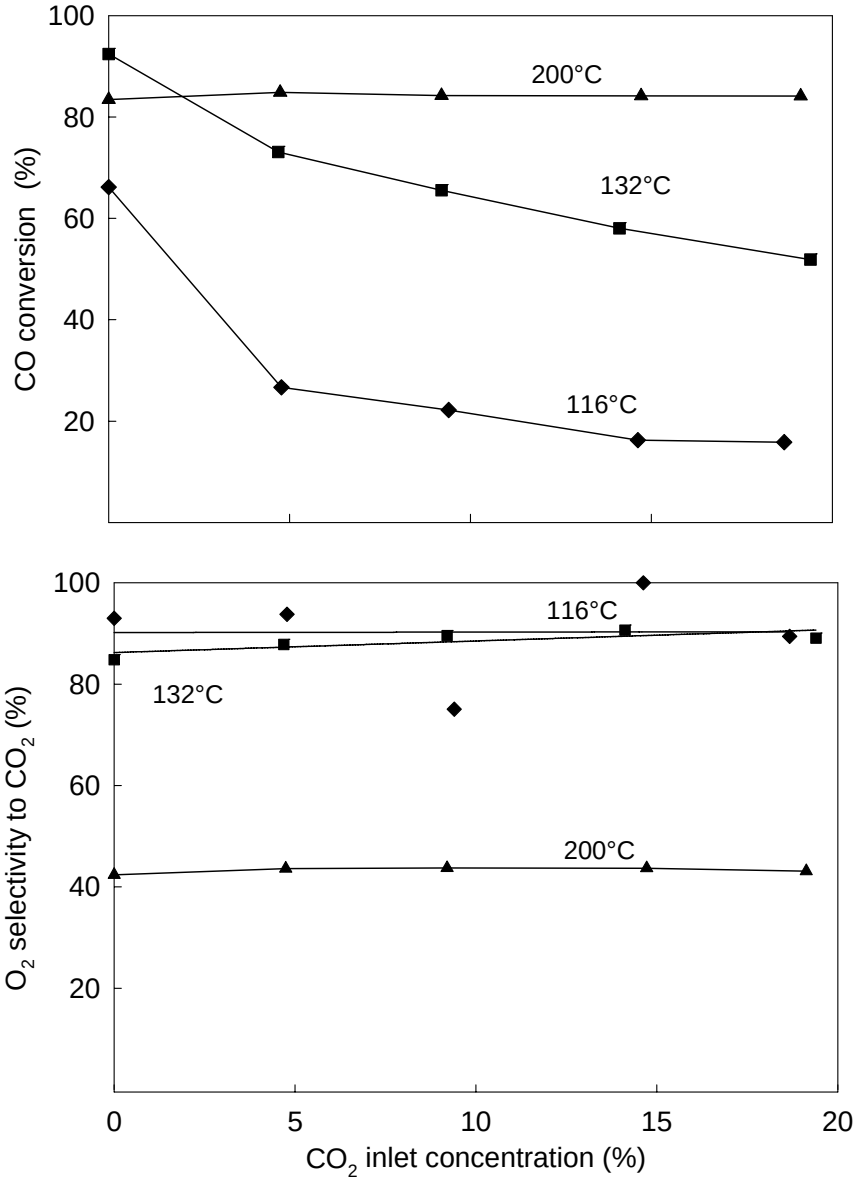

Figure 5.12: CO conversion and O_2 selectivity to CO_2 as a function of the CO_2 inlet concentration in the presence of H_2O at 116°C- 132°C – 200°C. Reaction conditions: 0.5vol% CO, 0.5 vol% O_2 , 50 vol% H_2, 0.5vol% H_2O in N_2. W/F= 0.032 g·s/cm^3.

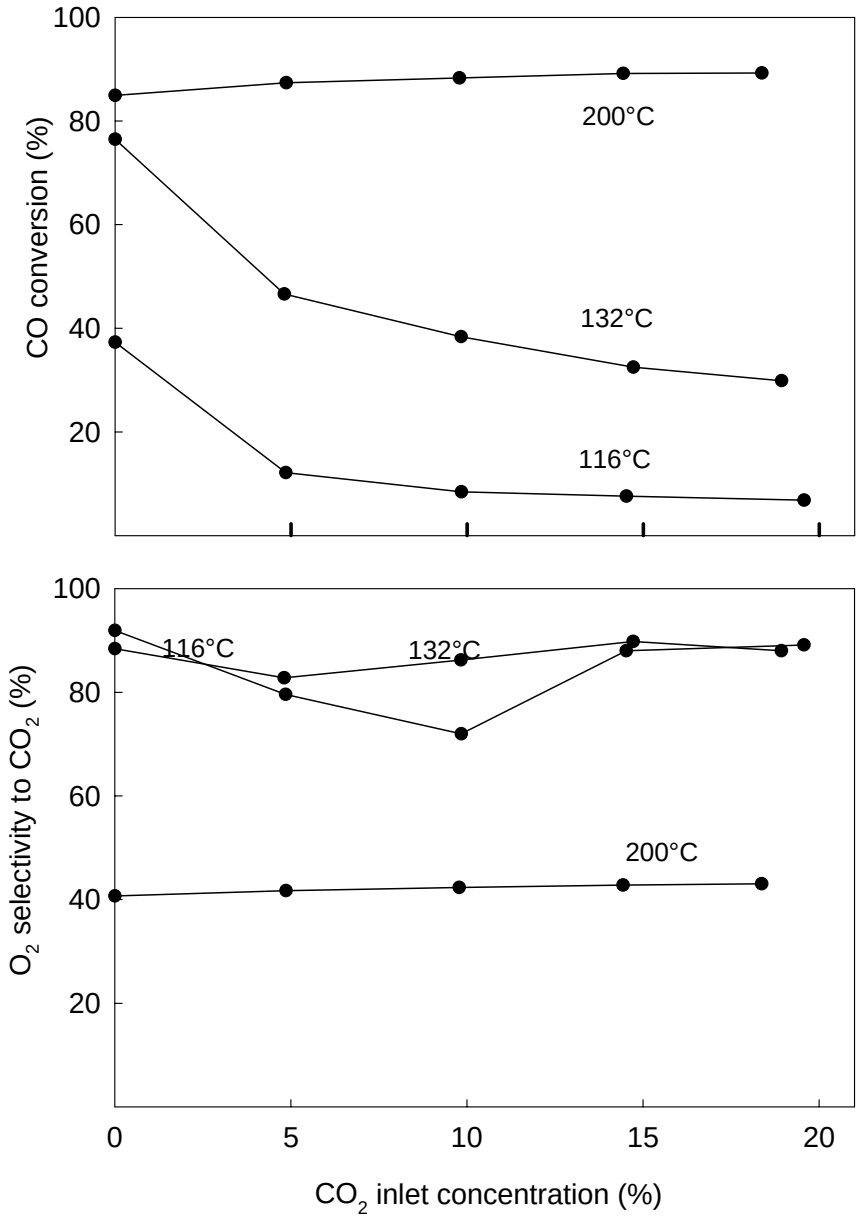

Figure 5.13: CO conversion and O_2 selectivity to CO_2 as a function of the CO_2 inlet concentration in the presence of H_2O at 116°C- 132°C – 200°C. Reaction conditions: 0.5vol% CO, 0.5 vol% O_2 , 50 vol% H_2, 1.5 vol% H_2O in N_2. W/F= 0.032 g·s/cm^3.

5.2.7 The effect of temperature in the presence of CO_2 and H_2O

In figure 5.14 reaction tests performed at different contact times, in absence and in presence of CO_2 and H_2O are reported, in term of CO and O_2 conversion, and selectivity to CO_2 as a function of the temperature.

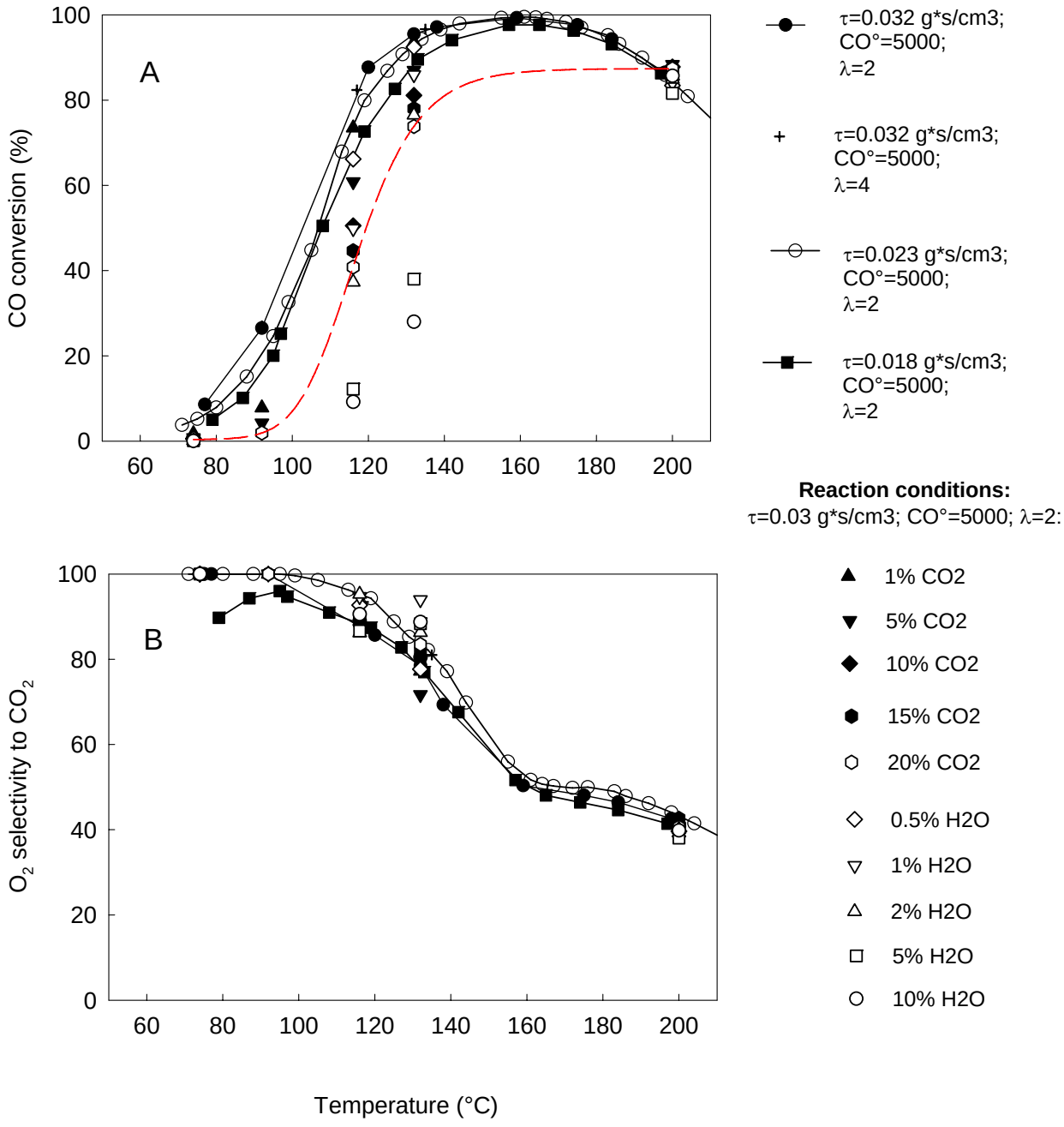

Figure 5.14: CO conversion (A) and O_2 selectivity to CO_2 (B) as a function of the temperature both in absence than in the presence of CO_2 and H_2O. Red, dotted curve refers to the extrapolation of the CO conversion trend versus temperature for a mixture containing: 0.5vol% CO; 0.5vol%O_2; 50vol% H_2 and 20vol% CO_2.

As discussed in the previous paragraph, the presence of CO_2 and H_2O has a negative effect on the CO oxidation kinetics. In figure 5.14 the CO conversion as a function of the temperature is reported. The presence of CO_2 and/or H_2O shifts the CO conversion curve to higher temperature (dotted curve) as expected by the previous studies. Nevertheless despite of this dramatic effect of CO_2 and H_2O addition on the catalyst activity, the selectivity seems not to be influenced by the presence of reformate specie, being a unique function of the temperature as showed in figure 5.14B.

5.3 Modelling the kinetics

In the kinetic study several kinetic models were tested in order to investigate the competitive role of CO and H_2 oxidation over the catalyst, in the presence and absence of reformate species.

5.3.1 Model equations

The catalytic reactor is an isothermal fixed bed reactor and can be modelled as a plug flow reactor at constant pressure, as discussed in the experimental section.
In the kinetic model of CO-PROX reactor the main reactions, which occur in competition, are:

(5.18) $$CO + \frac{1}{2}O_2 \rightarrow CO_2$$

(5.19) $$H_2 + \frac{1}{2}O_2 \rightarrow H_2O$$

In addition to these two reactions, the reverse water gas shift reaction (rWGS) could be considered too. Pt based catalysts showed to be active towards the rWGS reaction in the same temperature range, in which are active for CO-PROX (100-300°C) (Choi, 2004).

(5.20) $$H_2O + CO \leftrightarrow CO_2 + H_2 \qquad \Delta H^{\circ}_{298} = -41.1\frac{kJ}{mol}$$

Nevertheless, it has been demonstrated (pag. 78) that in the temperature range of interest (from room temperature to 200°C), the rWGS reaction is not catalysed by CuO/CeO_2 in all conditions investigated. Thus, for describing our system only the reaction (1) and (2) need to be considered.

5.3.2 Kinetic models

In the hypothesis of neglecting the mole variation, the mass balance equations on CO and O_2 read:

(5.21) $$\frac{dX_{CO}}{d\tau} = -\frac{r_{CO}}{C^{\circ}_{CO}}$$

(5.22) $$\frac{dX_{O2}}{d\tau} = -\frac{r_{O2}}{C^{\circ}_{O2}}$$

where

(5.23) $$r_{O2} = \frac{1}{2} \cdot \left(r_{CO} + r_{H2}\right)$$

5.3.2.1 Power law kinetics

A first approach to the kinetic study was conducted through a simplified power law model, which represented a useful tool to derive the dependence of the reaction rate on the CO, O_2 and H_2 concentration under the conditions of interest.

The following empirical expression has been used for the rate of CO oxidation:

(5.24) $$r_{CO} = k_{CO} \cdot P_{CO}^{\alpha} \cdot P_{O2}^{\beta}$$

where P_{CO} and P_{O2} are the CO and oxygen partial pressures, α and β the apparent reaction orders for CO and oxygen, while k_{CO} is the kinetic constant for the CO oxidation reaction.

The hydrogen reaction (2) in a hydrogen rich environment can be modelled using an empirical rate expression:

(5.25) $$r_{H2} = k_{H2} \cdot P_{O2}^{\gamma}$$

in which the kinetic constant k_{H2} embeds the hydrogen partial pressure dependence, and γ is the apparent reaction order towards O_2.

The kinetic constants in each rate expression are assumed to have Arrhenius-like dependence on temperature:

(5.26) $$k_{CO} = k_{CO}^{0} e^{-(E_{CO}/R \cdot T)}$$

(5.27) $$k_{H2} = k_{H2}^{0} e^{-(E_{H2}/R \cdot T)}$$

where k_{CO}^{0} and k_{H2}^{0}, and E_a^{CO} and $E_a^{H_2}$ are the pre-exponential factors and the activation energies of CO and H_2 oxidation reactions respectively.

5.3.2.2 Mechanistic rate expressions

The power law rate expression does not reflect the actual reaction mechanism occurring in the CO-PROX reaction, and its validity is limited to the range of fitting of the experimental data.
Hence, other rate expressions were tested for modelling the system, starting from mathematical considerations based on the dependence of the reaction rates on the main parameters.
The rate expressions tested may be divided in two classes:

a) Rate expressions with a quadratic dependence on the CO partial pressure in the kinetic term, and no dependence on the oxygen partial pressure.

5.28) $$r_{CO} \propto \frac{K \cdot k_c P_{CO}^2}{1 + \sum_i K_i \cdot P_i^n}$$

b) Rate expressions with linear dependence on the CO partial pressure and 1/2 dependence on the oxygen partial pressure.

5.29) $$r_{CO} \propto \frac{K \cdot k_c P_{CO} \cdot P_{O2}^{0.5}}{1 + \sum_i K_i \cdot P_i^n}$$

or:

5.30) $$r_{CO} \propto \frac{k_c P_{CO} \cdot P_{O2}^{0.5}}{\sum_i k_i \cdot P_i^n}$$

Since the above reported mathematical expressions represent the kinetic rate of actual reaction mechanism, such as Langmuir-Hinshelwood, Eley-Rideal or Mars-Van Krevelen, the constants embedded have physical meanings: K is the productoria of the adsorption constants, k_c the kinetic constant of CO surface reaction, P_i the partial pressure of the component i, K_i the adsorption

constant of the specie i, and k_i the kinetic constants. The kinetic constants are assumed to have an Arrhenius dependence on the temperature, while a Vant' Hoff dependence is assumed for the adsorption constant.

Hence, in the expressions (a) and (b) the terms at the denominator are adsorption terms, which take into account the inhibition effect caused by the presence of species adsorbed on the active sites.

In particular, the rate expressions must to take into account the dependence of the kinetics on the CO_2 partial pressure, since CO_2 strongly adsorbs on the CuO/CeO_2 catalyst surface and reduces the reactivity of CO oxidation. In fact, CO_2 is always present in the reaction mixture both in the feed, produced in the fuel processor, and as product of the reaction of CO oxidation:

(5.31) $$P_{CO2} = P^0_{CO2} + P^0_{CO} \cdot X_{CO}$$

where P^0_{CO2} is the inlet CO_2 concentration, while P^0_{CO} and X_{CO} are respectively the inlet CO partial pressure and the CO conversion.

Due to the linear dependence of the CO_2 and CO partial pressures, for correctly predicting the CO apparent reaction order it is critical to consider the effect of CO_2 in the rate expression.

5.3.2.3 Parameter estimation

In the equations (4) and (5) the X_{CO} and X_{O2} are functions of temperature, pressure, contact time, and of the set of kinetic parameters (activation energies, pre-exponential factors, reaction orders, adsorption constants), indicated as $\vartheta°$:

(5.32) $$X^i_{CO} = \mathrm{f}(\mathrm{T}, \mathrm{P}, \tau, \vartheta°)$$

We tested the above described kinetic models by performing the parameter estimation.

At a fixed temperature, pressure, and for an assigned value of the parameters $\vartheta°$, equations (4-5) are solved and the conversion of CO and O_2 at the exit of the reactor are evaluated: $X^{Calc}_{i,CO}$ and $X^{calc}_{i,O2}$.

The calculated conversions are then compared with the experimental data, by defining two function Φ_{CO} and Φ_{O2} each defined as the square of the difference between predicted and observed conversions:

(5.33) $$\Phi_{CO} = \sum_{i=1}^{N} \left(X_{i,CO}^{\exp} - X_{i,CO}^{Calc} \right)^2$$

(5.34) $$\Phi_{O2} = \sum_{i=1}^{N} \left(X_{i,O2}^{\exp} - X_{i,O2}^{Calc} \right)^2$$

The target function which has to be minimised is Φ equal to the sum of the errors on the predicted CO and O_2 conversions:

(5.35) $$\Phi = \Phi_{CO} + \Phi_{O2}$$

The MatLab subroutine FMINS searches the minimum of the function Φ.

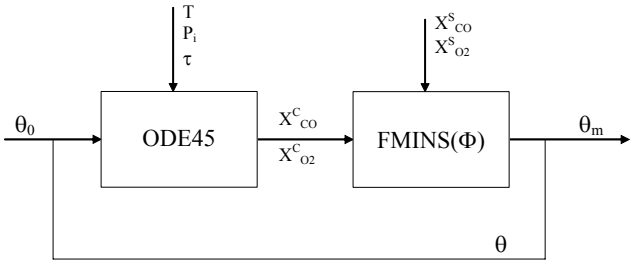

Figure 5.15:Flowsheet of the Matlab program.

In the program two MatLab subroutines are used: the ode45 for solving the differential equations, and the function FMINS for minimizing the errors.

The ode45 is based on an explicit Runge-Kutta (4,5) formula and it allows the solution of the partial differential equations (4-5).

The subroutine FMINS uses the "Nelder-Mead simplex search" algorithm. It is a direct search method which, by comparing the new error (Φ_n) with the preceding lower error (Φ_{n-i}), is able to drive the system towards the solution with the lowest error. It stops only when this error is lower than a fixed tolerance, that in our case is fixed at 10^{-10}. The problem of this subroutine is that it reaches the local minimum closer to the initial value, which is a relative minimum. In consequence, the solution of the problem is strictly dependent on the initial value assigned at the variables.

In fact, a critical point of this work was the choice of the initial values for the variables. Case by case, different criteria has been chosen for the assignment of the initial parameter.

The quality of the fitting is obtained by the estimation of three indexes easily calculable:

1. The value of the function Φ in correspondence of the minimum

2. The value of the standard deviation σ^2 defined as:

(5.36) $$\sigma^2 = \frac{\Phi}{n_{\exp} - n_{par}}$$

where $n_{\exp}$ is the number of experiments performed, and n_{par} the number of parameters presents in the kinetic model proposed. The standard deviation measures the quality of the fitting related to the number of experimental tests and parameters in the model; the higher σ^2, the higher is the quality of the fitting. An acceptable value for σ^2 is 10^{-2}-10^{-3}.

3 The value of the correlation coefficient defined as:

(5.37) $$R^2 = 1 - \frac{\Phi}{\sum_i X_{CO}^2 + \sum_i X_{O2}^2}$$

This coefficient gives the quality of the fitting only in relation to the experimental data. It is in the range between 0 and 1, and the closer is to 1, the higher is the estimation of the parameter of the model. An acceptable value for R^2 is R^2>0.9.

5.3.2 Results

5.3.2.1 Power law model

In the power law model, the reaction rates assume the following expressions:

(5.38) $$r_{CO} = k_{CO} \cdot P_{CO}^{\alpha} \cdot P_{O2}^{\beta}$$

(5.39) $$r_{H2} = k_{H2} \cdot P_{O2}^{\gamma}$$

(5.40) $$k_{CO} = k_{CO}^{\circ} e^{-(E_{CO}/R \cdot T)}$$

(5.41) $$k_{H2} = k_{H2}^{\circ} e^{-(E_{H2}/R \cdot T)}$$

The above rate expressions do not take into account the effect of CO_2 and H_2O on the reaction kinetics. Hence, only the catalytic tests performed in absence of reformate species have been considered in the data fitting (n_{exp}= 72).

By using data at different temperatures seven parameters were estimated: α, β, γ, k_{CO}^{0}, $k_{H_2}^{0}$, E_a^{CO} and $E_a^{H_2}$.

When using data at a constant temperature, the number of parameters decreases to five (α, β, γ, k_{CO}, k_{H_2}).

In this case, the initial values/first estimate of the activation energy and of the pre-exponential factor of the reaction of CO oxidation have been estimated by means of the regression of the experimental data at low CO conversion, for which a first order kinetic in CO and zero order in O_2 is arbitrarily assigned (E_{CO}^{a}= 21000 cal/mol; k_{CO}^{0}= 10^{12} mol·h^{-1}·gr^{-1}·atm^{-1}). The initial value of the H_2 activation energy is assumed higher than that of CO (E_{H2}^{a}= 30000 cal/mol), in accordance with the results of the reaction tests on CO and H_2 oxidation, carried out separately (Chapter 4). The initial values of the reaction order of the reactants are all assumed equal to 1 (α=β=γ=1).

By fitting the experimental data, the following empirical rate expressions were derived for CO and H_2 oxidation:

$$r_{CO} = k_{CO} \cdot P_{CO}^{1.02} \cdot P_{O2}^{10^{-4}}$$

$$k_{CO} = k_{CO}^{0} e^{-(E_{CO}/R \cdot T)} \qquad k_{CO}^{0} = 1.4 \cdot 10^{12} \frac{mol}{h \cdot g \cdot atm^{\alpha+\beta}} \quad E_{CO}^{a} = 19900 \frac{cal}{mol}$$

and:

$$r_{H2} = k_{H2} \cdot P_{O2}^{0.2}$$

$$k_{H2} = k_{H2}^{0} e^{-(E_{H2}/R \cdot T)} \qquad k_{H2}^{0} = 1.6 \cdot 10^{17} \frac{mol}{h \cdot g \cdot atm^{\alpha+\beta}} \qquad E_{H2}^{a} = 35000 \frac{cal}{mol}$$

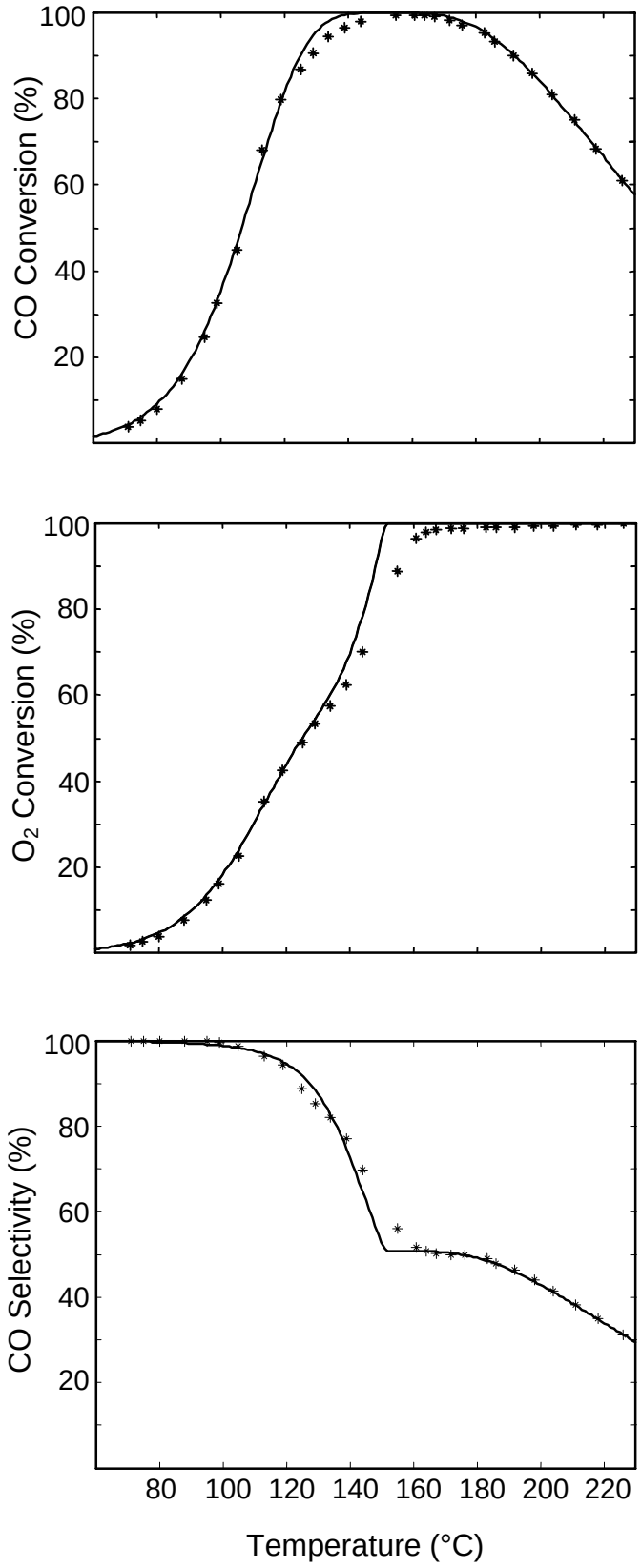

Figure 5.15: Numerical fitting (line) of the experimental data (symbols). Reaction conditions: 0.5vol% CO; 0.5vol% O_2; 50vol% H_2 in N_2. W/F= 0.03g*s/cm^3.

In Figure 5.15 CO and O_2 conversions are plotted versus temperature as obtained by the experimental data and data fitting. The quality of the fitting is quite accurate (R^2=0.995) as shown in figure 5.15, both for oxygen and CO conversion.

Numerical results suggested that the oxidation of CO exhibited a first order apparent dependence on CO partial pressure (α=1.02), and a very weak dependence on the oxygen partial pressure ($\beta=10^{-4}$). The weak dependence of CO oxidation kinetic on the oxygen partial pressure is in accordance with the experimental results showed (pag.82).

Also for H_2 oxidation, a weak dependence on the oxygen partial pressure has been estimated (γ=0.2), even though higher than that evaluated for CO oxidation kinetics.

Remarkably, the estimated activation energy for CO oxidation (20000 cal/mol) was lower than the activation energy for H_2 oxidation (36000 cal/mol), in accordance with the presence of a maximum in the CO conversion that was experimentally found, and that is generated by the competition of the two reactions whose kinetics are differently activated by the temperature.

This result confirms that on CuO/CeO_2 catalysts the WGS equilibrium plays an extremely limited role (if any), and is not relevant in explaining the presence of the maximum in the CO conversion, unlikely on Pt based catalysts.

Actually, the power law kinetics resulted a useful tool for qualitatively the presence of the maximum in the CO conversion and deriving an estimation of the apparent reaction orders. Nevertheless, such simplified kinetic law is unable to reproduce the inversion of the CO reaction order, experimentally observed in the isothermal study at varying the partial pressure of CO (pag. 90) nor of course can give useful knowledge on the reaction mechanism.

Hence, the CO conversion curve has been ideally considered composed by two different zones: the low temperature zone from room temperature up to 115°C and the high temperature one (T>115°C), and the power law rate has been separately applied in the two zones.

In the low temperature region, where the reaction of hydrogen oxidation is only weakly activated, it was demonstrated by the experiments that the apparent CO reaction order is lower than one. In the high temperature zone, where the H_2 oxidation kinetics is competitive with the CO oxidation, experiments showed that the CO apparent reaction order is higher than one.

By modelling each zone with its own power law kinetic equation, it was possible to fit the two branches of the CO conversion versus temperature zone. In particular, by fitting the experimental data at 92°C, the apparent CO and oxygen reaction orders were estimated, as reported in table 5.2, and were used as initial values for the fitting of the entire body of data obtained in the low temperature branch below 115°C.

Table 5.2: Parameters estimated by the isothermal study at 92°C

T (°C)	α	β	γ	k_{CO} (mol·h^{-1}·gr^{-1}·atm$^{-(\alpha+\beta)}$)	k_{H2} (mol·h^{-1}·gr^{-1}·atm$^{-(\alpha+\beta)}$)	R^2
92	0.7	0.04	0.5	0.4	$1.3\cdot10^{-5}$	0.986

The resulting empirical rate expressions in the **low temperature zone**, obtained through the data fitting, are reported below:

$$r_{CO} = k_{CO} \cdot P_{CO}^{0.7} \cdot P_{O2}^{0.07}$$

$$k_{CO} = k_{CO}^{\circ} e^{-(E_{CO}/R\cdot T)} \qquad k_{CO}^{\circ} = 1.3\cdot10^{12} \frac{mol}{h \cdot g \cdot atm^{\alpha+\beta}} \qquad E_{CO}^{a} = 20900 \frac{cal}{mol}$$

and

$$r_{H2} = k_{H2} \cdot P_{O2}^{0.1}$$

$$k_{H2} = k_{H2}^{\circ} e^{-(E_{H2}/R\cdot T)} \qquad k_{H2}^{\circ} = 1.1\cdot10^{17} \frac{mol}{h \cdot g \cdot atm^{\alpha+\beta}} \qquad E_{H2}^{a} = 36250 \frac{cal}{mol}$$

With analogous procedure, the isothermal study at 132°C led to the estimation of the initial values of CO and oxygen apparent reaction orders, to be used in the fitting of the experimental data in the **high temperature zone** (> 115°C):

Table 5.3: Parameters estimated by the isothermal study at 132°

T (°C)	α	β	γ	k_{CO} (mol·h^{-1}·gr^{-1}·atm$^{-(\alpha+\beta)}$)	k_{H2} (mol·h^{-1}·gr^{-1}·atm$^{-(\alpha+\beta)}$)	R^2
132	1.3	0.007	0.2	270	0.021	0.997

The fitting extended to all the data above 115°C gives the following values of the parameters:

$$r_{CO} = k_{CO} \cdot P_{CO}^{1.3} \cdot P_{O2}^{0.04}$$

$$k_{CO} = k_{CO}^{\circ} e^{-(E_{CO}/R\cdot T)} \qquad k_{CO}^{\circ} = 1.6\cdot10^{12} \frac{mol}{h \cdot g \cdot atm^{\alpha+\beta}} \qquad E_{CO}^{a} = 18300 \frac{cal}{mol}$$

and:

$$r_{H2} = k_{H2} \cdot P_{O2}^{0.2}$$

$$k_{H2} = k_{H2}^{\circ} e^{-(E_{H2}/R \cdot T)} \qquad k_{H2}^{\circ} = 1.5 \cdot 10^{17} \frac{mol}{h \cdot g \cdot atm^{\alpha+\beta}} \qquad E_{H2}^{a} = 35100 \frac{cal}{mol}$$

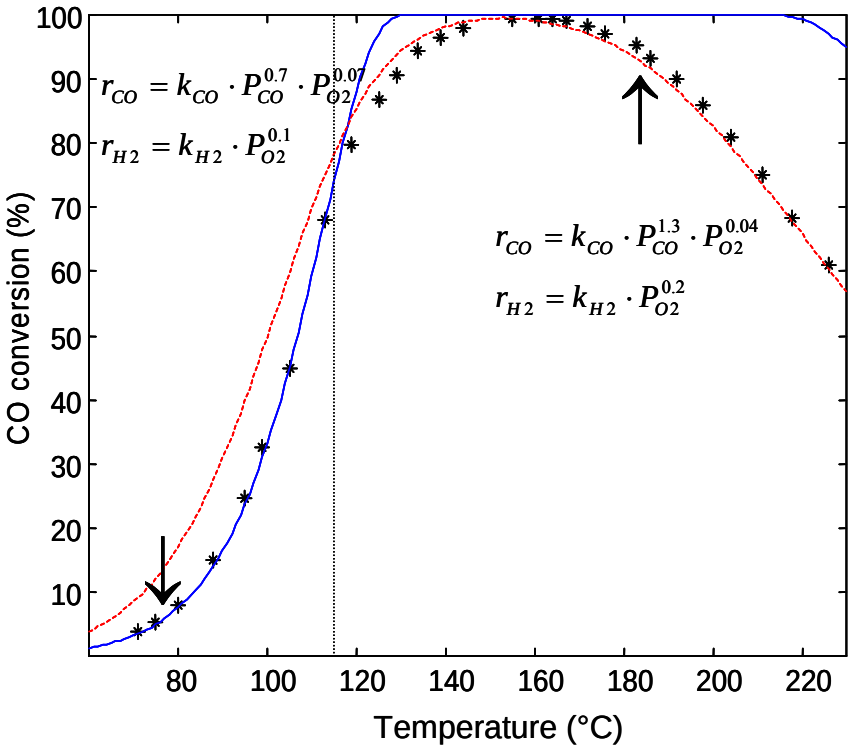

Figure 5.16: Data fitting (line) of the experimental data (dotted). Reaction conditions: 0.5vol% CO; 0.5vol% O_2; 50vol% H_2 in N_2. W/F= 0.03g*s/cm^3.

In the entire temperature range both oxidation reactions exhibited a very weak dependence on the oxygen partial pressure (respectively 0.007 and 0.2). The apparent CO reaction order was estimated at about 0.7 in the low temperature zone and 1.3 in the high temperature zone, coherently with the experimental observations above reported.

Interestingly, the experimental data at 92°C and 132°C could not have been fitted by imposing a common CO reaction order equal to 1. In fact, the regression procedure did not find any significant set of parameters for describing the system at low temperature, while a good fitting was obtained only for the isothermal data at 132°C, as shown by the results reported in figure 5.17 and in table 5.4.

Table 5.4: Parameters estimated by the isothermal study at 132°C

T (°C)	α	β	γ	k_{CO} (mol·h^{-1}·gr^{-1}·atm$^{-(\alpha+\beta)}$)	k_{H2} (mol·h^{-1}·gr^{-1}·atm$^{-(\alpha+\beta)}$)	R^2
132	1	0.2	0.17	76	0.017	0.994

At 132°C, the increasing trend of the CO conversion with increasing the CO partial pressure at a constant λ, is accurately reproduced by the model (fig. 5.17) even if in the rate expression an apparent reaction order in CO equal to 1 has been imposed. The increasing trend of the CO conversion is indeed due to a significant dependence of the kinetics on the oxygen partial pressure, whose apparent reaction order β has been estimated as 0.2. In particular the model predict for the two kinetics of CO and H_2 oxidation, a similar dependence on the oxygen partial pressure (β≈γ).

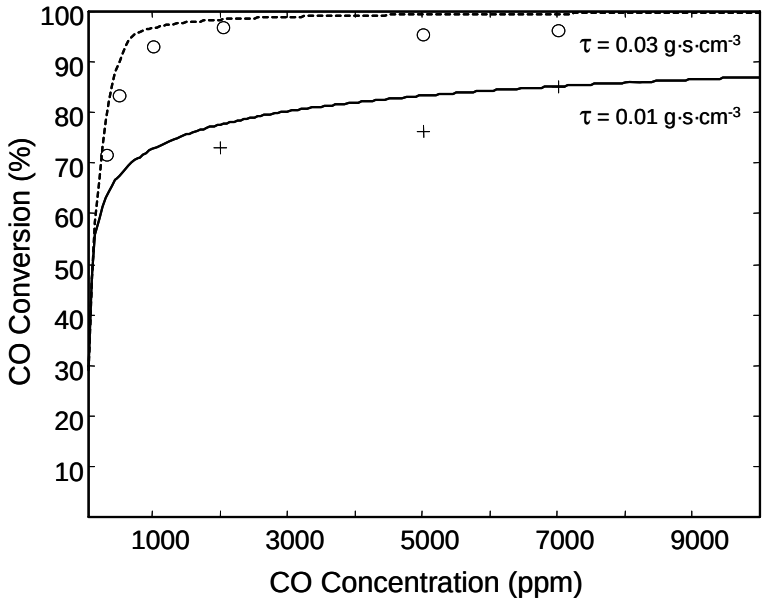

Figure 5.17: CO conversion as a function of the CO partial pressure at 132°C and two different contact time. Experimental data (symbols) and values predicted by the model (line). (o) 0.03 g·s/cm^3; (+) 0.01 g·s/cm^3.

5.3.2.2 Mechanistic rate expressions

The need for two distinct power law expressions for the description of the experimental results, in conjunction to the significant effect of adsorption of CO_2 on the catalyst surface, suggest that less simplified rate expression should be used.

Some empirical rate expression was tested to fit the experimental data obtained under isothermal conditions, at 92°C and 132°C.

In particular, in table 5.5 some rate expressions of type (a) are summarized and compared in terms of the fitting parameters numerically obtained in correspondence of each temperature (ϑ), and in terms of quality of the fitting (R^2).

The terms at the denominator represent adsorption terms, and accordingly the corresponding constants have a negative dependence on temperature, while for the term at the numerator the dependence on temperature is unknown, since k_1 represents the productoria of kinetic and adsorption constants.

Among the rate expressions of type (a) tested, the best fitting was obtained with the rate expression III, due to its unique capability of fitting the effect of the CO partial pressure on the kinetics both at 92°C and 132°C (the data at 92°C were fitted with $R^2 = 0.998$, while the data at 132°C with $R^2 = 0.996$).

The rate expression III can be representative of an Eley-Rideal mechanism, where two molecules of CO adsorb on a single adsorption site, and react with the oxygen in the gas phase and having as a limiting step the CO adsorption, as described below:

(a) $2\ CO + \square \rightarrow CO\text{-}\square\text{-}CO$

(b) $CO\text{-}\square\text{-}CO + O_2 \Leftrightarrow 2\ CO_2\square$

(c) $2\ CO_2\square \Leftrightarrow 2\ CO_2 + \square$

where $\square$ is the adsorption site and

Step (a): adsorption of CO

Step (b): reaction between adsorbed CO and molecular oxygen

Step (c): desorption of CO_2

Assuming that the reactions (b) and (c) are at equilibrium, the CO reaction rate may be written as:

(5.42) $$r_{CO} = \frac{k_c \cdot P_{CO}^2 \cdot a_v}{1 + K_{CO} \cdot P_{CO}^2 + K_{CO2} \cdot P_{CO2}}$$

where a_v is a constant representing the overall concentration of active sites.

Remarkably, this mechanism is quite unusual and not consistent for the CO oxidation reaction on transition metal oxide, and its lack of consistency is due not only to the expected presence of the adsorption of two CO molecules on a single site on the catalyst surface, but also to the participation of the oxygen in the gas phase to the reaction.

Table 5.5: Results of the mathematical model by assuming the following kinetic expressions. T is the isothermal temperature, θ the set of parameters estimated, R^2 the error of the estimation, while the quality of the fitting of effect of CO, CO_2 inlet partial pressure and of the contact time has been estimated (YES) accurately or not (NO).

Kinetic expression	T (°C)	ϑ	R^2	Effect		
				CO	**CO_2**	**τ**
$r_{co} = \frac{k_1 \cdot P_{CO}^2}{1 + k_3 \cdot P_{CO_2}}$	92	k_1=9.25 10^9 k_3=2.42 10^{10}	0.976	NO	YES	YES
	132	k_1=21551 k_3=41.6	0.997	NO	YES	NO
$r_{co} = \frac{k_1 \cdot P_{CO}^2}{1 + k_2 \cdot P_{CO} + k_3 \cdot P_{CO_2}}$	92	k_1=1.24 10^{16} k_2=4.22 10^{15} k_3=1.41 10^{16}	0.979	NO	YES	YES
	132	k_1=45647 k_2=1350.6 k_3=67.2	0.999	YES	YES	YES
$r_{co} = \frac{k_1 \cdot P_{CO}^2}{1 + k_2 \cdot P_{CO}^2 + k_3 \cdot P_{CO_2}}$	92	k_1=9.42 10^{15} k_2=7.95 10^{17} k_3=1.23 10^{16}	0.998	YES	YES	YES
	132	k_1=27390 k_2=176480 k_3=43.2	0.996	NO (for τ=0.01)	YES	YES
$r_{co} = \frac{k_1 \cdot P_{CO}^2}{1 + k_3 \cdot P^2_{CO_2}}$	92	k_1=11058 k_3=3.2 10^7	0.986	YES	NO	NO
	132	k_1=19530 k_3=179.8	0.996	NO	YES	NO
$r_{co} = \frac{k_1 \cdot P_{CO}^2}{1 + k_2 \cdot P_{CO} + k_3 \cdot P^2_{CO_2}}$	92	k_1=2.09 10^{16} k_2=7.86 10^{15} k_3=2.26 10^{19}	0.993	YES	NO	YES
	132	k_1=44572 k_2=1416.1 k_3=351.3	0.999	YES	YES	YES
$r_{co} = \frac{k_1 \cdot P_{CO}^2}{1 + k_2 \cdot P_{CO}^2 + k_3 \cdot P^2_{CO_2}}$	92	k_1=1.36 10^{15} k_2=1.57 10^{11} k_3=5.36 10^{18}	0.976	NO	NO	NO
	132	k_1=25731 k_2=1.77 10^5 k_3=210.8	0.998	NO (for τ=0.01)	YES	YES

In table 5.6 the results relative to rate expressions having a form (5.29) and (5.30) have been reported.

In the expressions VIII and IX the constant k_1 at the numerator is a productoria of kinetic and adsorption constants while all the term at the denominator presents adsorption terms.

The equations (a) and (b) differentiate for the presence of a quadratic dependence of the denominator.

In the equation X, k_1 and k_2 represent kinetic constants, while k_3 the adsorption constant for CO. With the latter expression the program is unable to fit the data at 132°C, while a good quality fitting is obtained both with the equations VIII and IX.

Both the equations VIII and IX tested at isothermal conditions at 92 and 132°C, were able to correctly predict the inversion in the CO reaction order, the effect of the oxygen partial pressure, the effect of the contact time and of CO_2 addition. Moreover, the model correctly predicts the dependence of the adsorption constants with the temperature.

Table 5.6: Results of the mathematical model by assuming the following kinetic expressions. T is the isothermal temperature, R^2 the error of the estimation.

Rate equation	**T (°C)**	R^2
VIII $r_{co} = \frac{k_1 \cdot P_{CO} \cdot P_{O2}^{0.5}}{\left(1 + k_2 \cdot P_{CO} + k_3 \cdot P_{O2}^{0.5} + k_4 P_{CO2}\right)}$	92	0.9949
	132	0.9983
IX $r_{co} = \frac{k_1 \cdot P_{CO} \cdot P_{O2}^{0.5}}{\left(1 + k_2 \cdot P_{CO} + k_3 \cdot P_{O2}^{0.5} + k_4 P_{CO2}\right)^2}$	92	0.9963
	132	0.998
X $r_{co} = \frac{k_1 \cdot P_{CO} \cdot P_{O2}^{0.5}}{\left(k_2 \cdot P_{CO} + k_3 \cdot P_{O2}^{0.5} + k_4 P_{CO2}\right)}$	92	0.9949
	132	_

The rate expressions VIII, IX, X can be reported respectively to:

1 an Eley Rydeal mechanism in which the limiting step is the reaction between adsorbed oxygen and gas phase CO (rate expression VIII);
2 a Langmuir-Hinshelwood mechanism in which the limiting step is the reaction between adsorbed CO and adsorbed O_2 (rate expression IX);
3 a Mars and van Krevelen mechanism (rate expression X)

In all the cases the O_2 reaction order of ½ suggests an adsorption with dissociation for the oxygen molecule.
The Eley-Rydeal mechanism may be represented in this case as:

(a) $\frac{1}{2}\ O_2 + \square \Leftrightarrow 2\ O\square$

(b) $CO + O\square \rightarrow CO\text{-}O\square$

(c) $CO\text{-}O\square \Leftrightarrow CO_2 + \square$

where □ is the oxygen adsorption site, O□ adsorbed oxygen, and CO-O□ adsorbed CO_2.
Step (a): O_2 adsorption with dissociation
Step (b): reaction between adsorbed O_2 and gas phase CO
Step (c): desorption of CO_2

Assuming that the the reaction step (b) is limiting, and assuming equilibrium on the adsorption sites, the resulting rate expression is:

(5.43) $$r_{CO} = \frac{k_c \cdot P_{CO} \cdot \sqrt{K_{O2} \cdot P_{O2}}}{1 + K_{CO} \cdot P_{CO} + \sqrt{K_{O2} \cdot P_{O2}} + K_{CO2} \cdot P_{CO2}}$$

where k_c is the kinetic constant, K_{CO} is the CO adsorption constant, K_{O2} is the O_2 adsorption constant, and K_{CO2} the CO_2 adsorption constant.
An LH mechanism may instead occur according to the following steps:

(a) $CO + \square \Leftrightarrow CO\square$

(b) $\frac{1}{2} O_2 + \square \Leftrightarrow 2\ O\square$

(c) $CO\square + O\square \rightarrow CO\square\text{-}O\square$

(d) $CO\square\text{-}O\square \Leftrightarrow CO_2 + 2\,\square$

where □ is an adsorption site, CO□ adsorbed CO, O□ adsorbed oxygen, and CO□-O□ adsorbed CO_2.

Step (a): the adsorption of

Step (b): adsorption with dissociation of the oxygen molecule

Step (c): reaction between adsorbed CO and adsorbed O_2

Step (d): CO_2 desorption and consequent liberation of two adsorption sites.

Assuming that the reaction step (c) is limiting, assuming equilibrium on the adsorption sites, the resulting rate expression is:

(5.44) $$r_{CO} = \frac{k_c \cdot P_{CO} \cdot \sqrt{K_{O2} \cdot P_{O2}}}{\left(1 + K_{CO} \cdot P_{CO} + \sqrt{K_{O2} \cdot P_{O2}} + K_{CO2} \cdot P_{CO2}\right)^2}$$

where $k_1^{'}$ is the kinetic constant, K_{CO} is the CO adsorption constant, K_{O2} is the O_2 adsorption constant, and K_{CO2} the CO_2 adsorption constant.

Finally, the Mars and van Krevelen kinetics may be represented similarly to an L-H mechanism. The only difference is that for the derivation of the rate expression is not necessary to impose equilibrium on the adsorption sites. Kinetics considerations brought to the following rate expression:

(5.45) $$r_{CO} = \frac{k_c \cdot P_{CO} \cdot \sqrt{K_{O2} \cdot P_{O2}}}{\left(0.5 \cdot K_{CO} \cdot P_{CO} + \sqrt{K_{O2} \cdot P_{O2}} + K_{CO2} \cdot P_{CO2}\right)}$$

Sedmak et al. (2004) obtained a good accuracy by fitting the data collected up to 90°C on CuO/CeO_2 sample with a Mars and van Krevelen kinetic equation in CO-PROX conditions. In accordance with those results our model reproduced the data with a good accuracy at 92°C while the Mars and Van Krevelen kinetic expression failed at higher temperature, when the hydrogen oxidation kinetics is well developed.

In figure 5.18 the data fitting and the predicted values of the kinetic and adsorption constants obtained with the equation VIII and IX are showed.

The fitting obtained with the equation VIII reproduce with a good accuracy the effect of the CO partial pressure at both 92°C and 132°C. The effect of the oxygen partial pressure (λ) is slightly overestimated at 92°C. The estimated value of R^2 at 92°C is 0.9949, while at 132°C is 0.9983.
Also the rate expression IX is able to fit the data relative to the CO partial pressure effect on both 92°C and 132°C. The effect of lambda at 92°C seems to be well fitted and the overall R^2 at this temperature is lower than in the previous case (0.9963). Nevertheless at 132°C the R^2 value is higher than that obtained with the equation VIII probably because of a worst fitting on the effect of CO_2.
A rough evaluation of the kinetic parameters (activation energies, pre-exponential factors, heat of adsorption) can be obtained from the predicted values of the constants in the rate expression at 92°C and 132°C, by assuming an Arrhenius dependence of the kinetic constant from the temperature, and a Vant'Hoff dependence for the adsorption constants (table 5.7).

Table 5.7: Parameters estimation by the data fitting at 92°C and 132°C.

Parameter	*VIII*	*IX*
k_0 ($mol \cdot h^{-1} \cdot gr^{-1} \cdot atm^{-(\alpha+\beta)}$	$6.4\ 10^{+10}$	$6.5\ 10^{+30}$
E_a (cal/mol)	17200	49000
ΔH^0_{CO} (cal/mol/K)	$-3 \cdot 10^{+5}$	$-3 \cdot 10^{+4}$
ΔS^0_{CO} (cal/mol/K)	-800	-90
ΔH^0_{O2} (cal/mol/K)	-10^{+5}	$-5 \cdot 10^{+3}$
ΔS^0_{O2} (cal/mol/K)	-300	-11
ΔH^0_{CO2} (cal/mol/K)	$-2.7 \cdot 10^{+5}$	$-3.5 \cdot 10^{+4}$
ΔS^0_{CO2} (cal/mol/K)	-660	-80

The rate expression VIII predicts a value of the heat of adsorption which is suspiciously high (of 10^{+5} order). On the contrary the rate expression IX calculate heat of adsorption with plausible order of magnitude (10^{+4}).

In conclusion, numerical results showed that different models are able to reproduce the given set of experimental data. However, the best fitting was obtained by the mechanism IX.

Kinetic expression (VIII)	T (°C)	ϑ	R^2
$r_{co} = \frac{k \cdot K_{O_2} \cdot P_{CO} \cdot P_{O_2}^{1/2}}{1 + K_{CO} \cdot P_{CO} + K_{O_2} \cdot P_{O_2}^{1/2} + K_{CO_2} \cdot P_{CO_2}}$	92	k = 3.4 $K_{co} = 9.8 \cdot 10^{16}$ $K_{o2} = 1.3 \cdot 10^{16}$ $K_{co2} = 8.5 \cdot 10^{17}$	0.9949
	132	k = 35.2 $K_{co} = 9.6 \cdot 10^{-4}$ $K_{o2} = 38.7$ $K_{co2} = 52.2$	0.9983

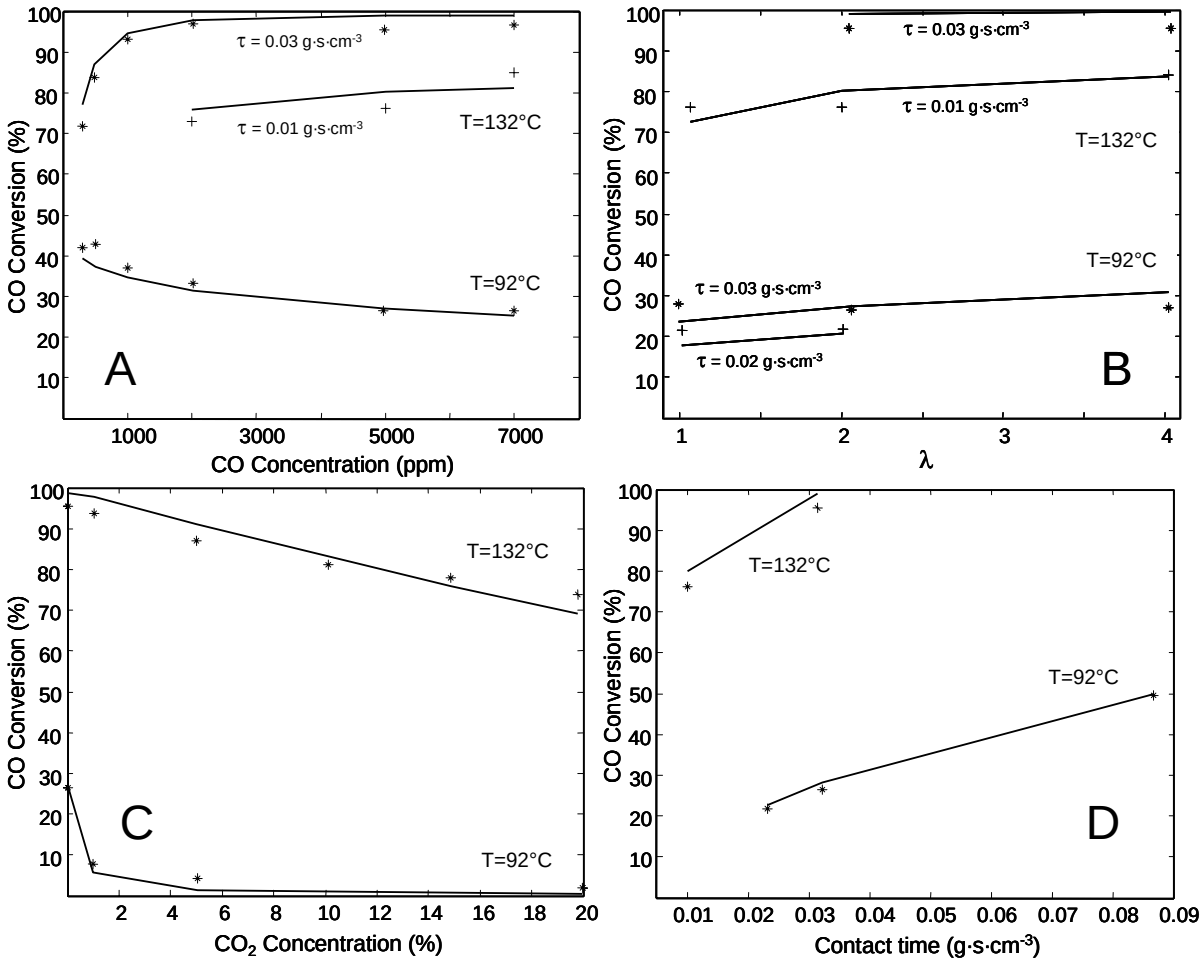

Figure 5.18:CO conversion as a function of the CO concentration (A), CO conversion as a function of λ (B) simulated with the kinetic expression VIII, (C), CO conversion as a function of the contact time (D) simulated with the kinetic expression VIII. (symbols) experimental data; (line) fitting.

Kinetic expression (IX)	T (°C)	ϑ	R^2
$r_{co} = \frac{k \cdot K_{CO} \cdot K_{O_2} \cdot P_{CO} \cdot P_{O_2}^{1/2}}{(1 + K_{CO} \cdot P_{CO} + K_{O_2} \cdot P_{O_2}^{1/2} + K_{CO_2} \cdot P_{CO_2})^2}$	92	k = 29.1 K_{co} = 0.39 K_{o2} = 33.7 K_{co2} = 975.5	0.9963
	132	k = 23040 K_{co} = $5 \cdot 10^{-3}$ K_{o2} = 7.7 K_{co2} = 7.6	0.998

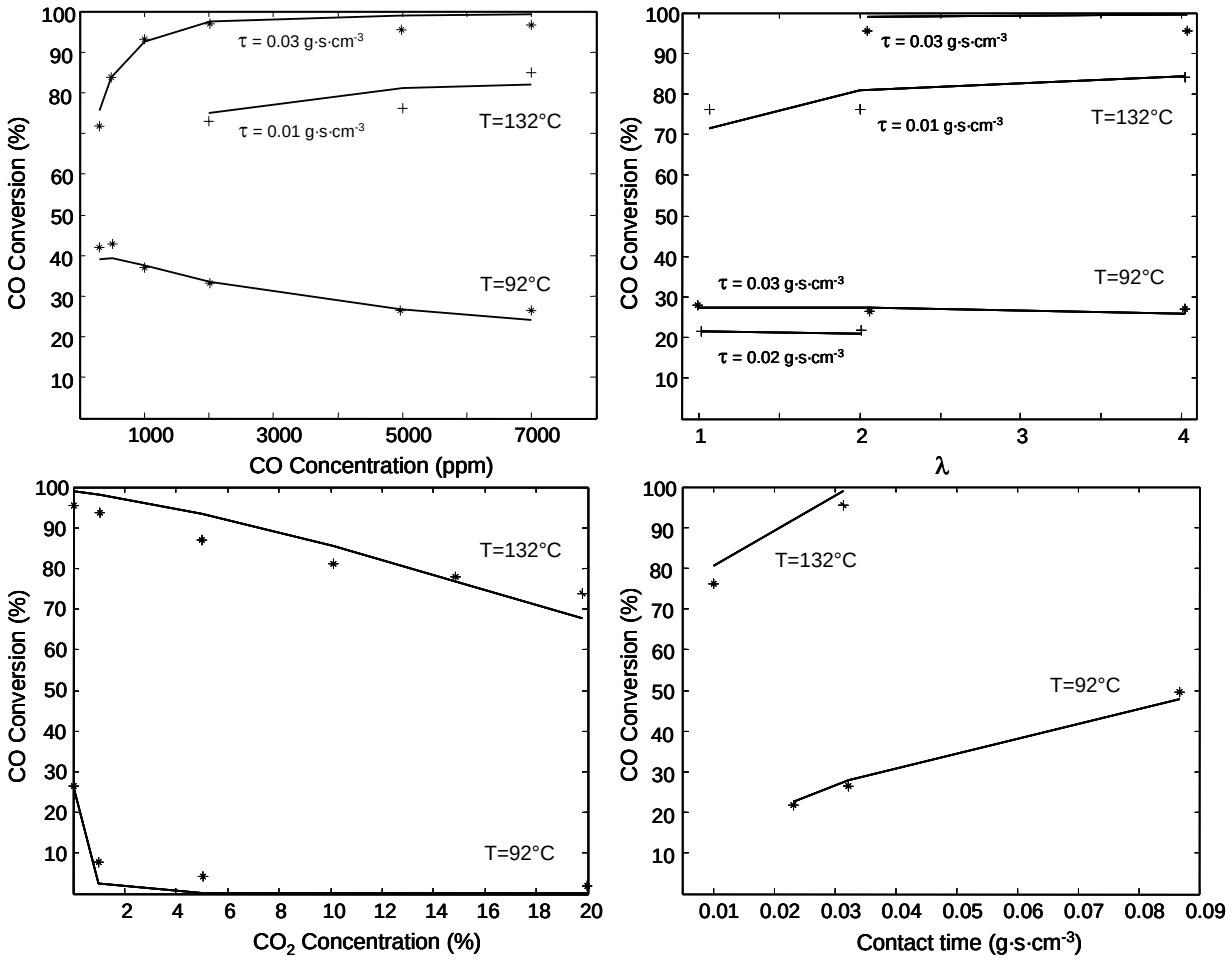

Figure 5.19: CO conversion as a function of the CO concentration (A), CO conversion as a function of λ (B), CO conversion as a function of the CO_2 partial pressure (C), CO conversion as a function of the contact time (D) simulated with the kinetic expression IX. (symbols) experimental data; (line) fitting.

5.3.3 Concluding remarks

The kinetic study was undertaken at two level of complexity. At the lower level, a power law kinetic rate was applied to fit the experimental data, while at higher level, more complex expression of the reaction rate were used, where also the adsorption terms were included.

The power law expression for the reaction rate resulted quite accurate for describing the dependence on temperature at fixed inlet conditions, giving a qualitative explanation to the experimentally measured maximum in CO conversion in terms of competition of the CO and H_2 oxidation reaction, excluding the effect of the reverse water gas reaction. Nevertheless, the power law model is not adequate to describe the effect of changing the partial pressures of the reactants and the addition of CO_2 to the feed.

Numerical results of more complex rate expressions, as derived from some classic kinetic models, such as the Eley-Rideal, the Langmuir-Hinshelwood and the Mars and van Krevelen mechanisms, showed that more than one model is able to fit the experimental data.

In particular, the best fittings were obtained in the hypothesis of adsorption of oxygen on the catalyst surface, and its subsequent reaction with CO, either in the gas phase (Eley-Rideal mechanism) or as adsorbed molecule (Langmuir-Hinshelwood mechanism). More plausible appears the LH model, where reasonable values of the adsorption energies are predicted.

More work has to be devoted to the development of the mathematical model on the basis of a more extensive body of experimental data and with the support of specific characterization techniques, in order to discern among different mechanism.

CHAPTER 6

Redox properties of CuO/CeO_2 catalysts

It has been already evidenced that cerium oxide when interacting with metal oxides shows a strong tendency in modifying its redox properties and those of the metal supported on its surface. Actually, ceria is able to work as an electronic and structural promoter in heterogeneous catalysis, due to the ability in stabilizing unsual metal particle structure, by means of electron transfer processes or chemical bonding -compound formation- between metal and support.

The greatest evidence of the presence of SMSI on ceria supported catalysts is the enhanced reducibility of the sample and/or of its chemisorption capability. This is also the reason why it is evident a decrease of the reduction temperature of both active phase and support in ceria-supported metal catalysts.

Such a promotion of reducibility has been also observed when the metal supported on ceria is copper, as Cu exhibits electronic properties very similar to those of many noble metals. For instance, Zimmer (2002) showed that in TPR of H_2 over CuO/CeO_2, both cerium and copper were reduced at temperatures lower than for pure oxides.

Moreover, redox properties surely play a relevant role in the catalysis of oxidation reactions, such as the conversion of CO to CO_2 or H_2 to H_2O. The existence of a correlation between the reducibility of CuO/CeO_2 and its activity in CO oxidation has been demonstrated by Tang (2004).

For these reasons the study of catalyst redox properties seems very interesting and will be faced in this section by illustrating the results of TPR/TPD/TPO tests together with chemisorption experiments of both CO and H_2. It is worth noting that such a study aims to characterise the catalysts by means of transient analyses using CO and H_2 as reducing agents, namely those molecules that are also the reactants (preferred or not) in the process under investigation. To this purpose two samples have been chosen as model catalysts, the first containing a copper loading corresponding to a monolayer concentration (~4 wt%), and the other one containing an excess CuO (9 wt%).

Copper oxidation state in the “as prepared” catalyst should be mainly +2, as also affirmed by some specific study (Martinez-Arias, 1997). However, the state of copper under reaction conditions is not known and much more questionable.

6.1 Hydrogen Temperature Programmed Reduction tests

Figure 6.1 shows the profile of H_2 consumption measured in a H_2-TPR test, carried out by heating the catalyst sample (4% wt. CuO) from room temperature up to 430°C, in a 2vol% H_2/N_2. Two different curves are reported in the same figure: curve *a* refers to the first test performed on the fresh catalyst, while the second one (curve *b*) is related to the same test carried out on the same sample for the second time, after deep reduction of catalyst at 430°C (four hours) and subsequent reoxidation and cooling.

In both experiments, no catalyst reduction is observed at room temperature, hydrogen consumption is only observed at higher temperatures. However, the overall consumption of H_2 during the whole experiment corresponds in both cases to more than the theoretical complete reduction of copper in the sample, under the hypothesis that Cu goes from the oxidation state +2 to zero. Indeed, such an ideal H_2/Cu ratio of complete copper reduction (with no other species reduced in the test) should be one, while the amount of hydrogen consumed in the TPR over the fresh sample corresponds to H_2/Cu = 1.44.

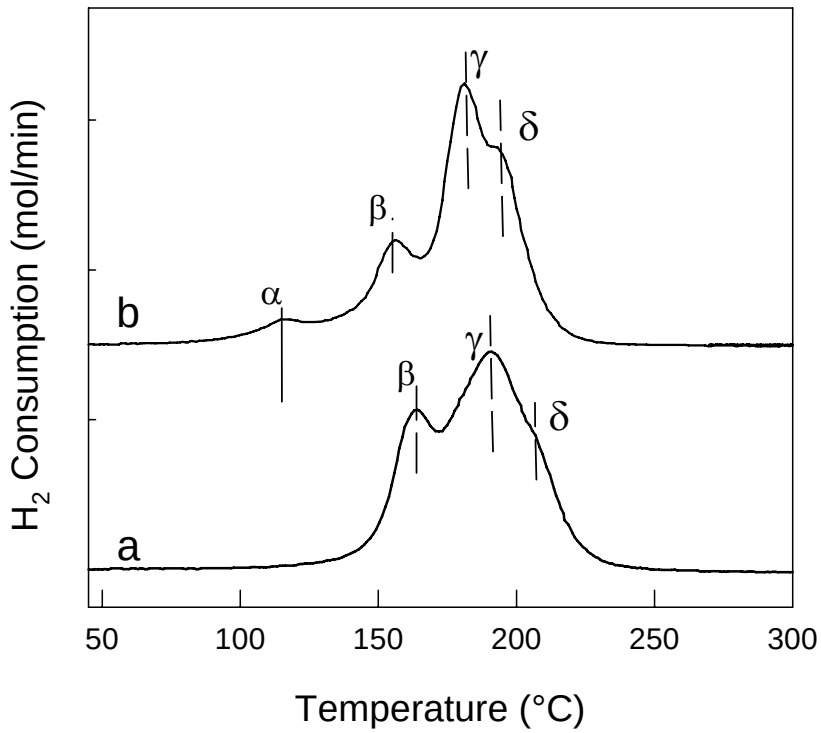

Figure 6.1: Hydrogen Temperature Programmed Reduction on 4wt% CuO/CeO_2. (a) fresh sample; (b) sample reduced at 430°C for 1h; and reoxidized at 430°C for 2h.

Even if it is known that pure ceria is not reduced by H_2 at temperatures lower than about 500°C, as already shown in Fig. 4.4, such a large H_2/Cu ratio suggests the participation of the support to reduction phenomena. Hence, what is happened is something very similar to that has been demonstrated for noble metals supported on ceria. Zimmer et al. in 2002 showed that also for CuO/CeO_2, both copper and cerium are activated by H_2 with a increase of ceria reducibility. Some of the TPR tests performed (and not reported here) have been prolonged above 500°C and demonstrated that the reduction peak typically observed at 500°C in the TPR over pure CeO_2, and generally attributed to the reduction of superficial cerium is no more present, indicating that the promotion effect on the reducibility concerns with the superficial ceria and not to the bulk (which remains reducible at temperatures above 800°C).

For our sample, the amount of ceria reduced in the TPR of 4 CuO/CeO_2 has been calculated, assuming that copper is completely reduced from Cu^{+2} to Cu° (and also reported in Table 6.1). This quantity is 265 μmole/g of ceria, corresponding to the reduction of about 9% of the whole cerium in the sample. This amount has been compared to that corresponding to the peak at 500°C in the TPR of pure ceria (Fig. 4.4), attributed to surface ceria, which is equal to 355 μmole/g (12% of cerium).

Table 6.1: H_2 TPR analysis results performed on CeO_2; 4wt% and 9wt% CuO/CeO_2 sample:

Catalyst	*Cu, μmoli/g*	*H_2, μmoli/g*	*H_2/Cu (*)*	*% $Ce^{+4} \rightarrow Ce^{+3}$*
CeO_2 (*)	_	355	_	12
4 CuO/CeO_2	532	773	1.44	9.5
4 CuO/CeO_2 (**)	532	790	1.47	9.5
9 CuO/CeO_2	1164	1280	1.1	4

(*) Amount relative to the peak at 450°C

(**) Second H_2 TPR

Since the two values are quite close, it is possible to hypothesise that ceria reduced at very low temperature in the presence of copper is surface ceria.

The lower amount evaluated in the TPR of CuO/CeO2 with respect to that of the peak at 500°C of pure ceria, can be related to copper deposition hindering the exposure of some surface ceria.

Anyway, on the 4 CuO/CeO_2 sample we measure a hydrogen consumption of 59 μmol/g in the high temperature region of our tests (around 400°C) that we have attributed to the reduction of a residual fraction of surface ceria probably not involved in the strong-metal-support interaction with the copper, and hence reduced under conditions similar to those to pure ceria. Such phenomenon also

explains the differences observed in the amount of cerium reduced in the Cu-Ce sample with respect of pure ceria. Finally, since we are interested in characterizing the amount of ceria involved in the strong-metal-support interaction with copper or – in other words – the amount of ceria reducible at relatively low temperature (so low to be considered significant under CO-PROX reaction conditions) we will not quantify the hydrogen consumption relevant to the surface ceria reduced at 400°C, in our tables.

Figure 6.1 also reports the TPR profile obtained on the same (fresh) sample after a pre-treatment of deep reduction (with H_2 for 4h at 430°C), and then of complete re-oxidation (at 430°C for 2h). In this way the sample results more "aged" and most of its properties more stable (re-dispersion of copper being the major reason of this). Actually, such an interest towards this second TPR tests is related to the observations that H_2 TPR on CuO/CeO_2 are reproducible after this first redox treatment. More specifically, TPR analysis have been repeated on different batchs. On samples prepared by wet impregnation, but with variable parameters in the preparation method (water excess, pressure and temperature during evaporation) a certain qualitative differences in the first TPR have been observed, but after the deep reduction and the subsequent complete reoxidation at 430°C a perfect agreement in the profiles among the different samples have been detected.

Actually, the reducing treatment seems to lose the memory of the material history, rearranging the copper in a more uniform and stable distribution. Similar observations were also reported by Martinez-Arias et al. (1999) which studied CuO/CeO_2 catalysts prepared via wet impregnation.

Moreover, in chapter 4 it has been shown that a redox cycle in CO or in hydrogen has a promoting effect on the catalytic performances. This effect could be associated to the copper redispersion here observed after the first TPR. In the literature it has been demonstrated the existence of a correlation between the copper dispersion and activity in CO oxidation (2004), but generally the copper dispersion is increased by changing preparation methods. Nevertheless our experimental results suggests that the other possibility to increase the copper dispersion is by carrying out a redox cycle, and thus it could be virtually possible to obtain by simple preparation methods a catalyst as active as those obtained by more complicated preparation tecniques, which generally involve the use of more poisoned or more expensive salt precursors.

Looking more into details the TPR profile, Fig. 6.1 shows for the fresh sample (curve a) three main reduction peaks at 160°C, 190°C and a shoulder at 205°C (defined as β, γ, and δ peaks respectively), while a small hydrogen consumption has been measured also at 400°C (59 μmol/g). Moreover a hydrogen production (4μmol/g), probably due to desorption of H_2, is observed at around 300°C. H_2 TPD tests performed on the sample demonstrated that no significant amounts of hydrogen adsorption is detectable at room temperature on our samples pre-oxidised before the test.

Nevertheless, Pintar et al. (2005) shows by means of TPD analysis on samples pre-reduced with H_2 at 400°C, and cooled down in H_2 down to -20°C, that hydrogen may adsorb on copper-ceria catalysts, and is desorbed in the TPD at about 200°C. According to Pintar et al. (2005), the H_2 desorption monitored during the TPR test should refer to some hydrogen adsorbed on reduced sites formed on the catalyst surface during the reduction and at a temperature higher than room temperature.

As it is possible to see in the profile of curve b of Fig 6.1, the TPR of the aged sample also shows the presence of 3 main reduction peaks at 120°C, 160°C, and 180°C in addition to a shoulder at 194°C (α, β, γ, and δ peaks respectively). In comparison with the fresh sample, the reduction temperature of the δ-peak is decreased and the peak width is smaller, suggesting a more uniform distribution of the associated species. Actually, before trying to make any interpretation on the nature of the different species giving rise to the different reduction peaks, it seems quite trivial to assess that the reduction temperature of copper is more and more decreased as higher is the degree of dispersion on the support and probably the interaction with ceria itself. Bulk CuO in the same TPR test is reduced at about 300°C, eventually present CuO segregated microclusters in the Cu-Ce sample could be probably reduced at lower temperature due to smaller size, but certainly higher than all the other form of copper existing in the catalyst.

Thus, the reducing high-temperature treatment induces a sites redistribution which makes more homogeneous the distribution of the δ species, and also generates the formation of the new more reducible species at very low temperature (120°C). It is worth to underline that as a consequence of this copper re-dispersion, confirmed also by XRD analysis, the H_2 consumption calculated after the stabilizing treatment is slightly higher than that of the fresh sample (H_2/Cu = 1.47).

By comparing the H_2 uptake across each peak in the two TPR profiles is interesting to note that there is a strong similarity between the γ e δ peaks while the β peak is higher for the fresh sample but in the aged one there is the appearance of the α peak too. Deconvolution of curves confirm such an impression and also reveals that the sum of H_2 micromols consumed in the α e β peaks in *curve b* corresponds almost exactly to H_2 micromols of the single β peak in *curve a* (Figure 6.1). This observation could suggest that the reducing treatment mainly re-disperd the copper species already very interacting with support, generating a more reducible specie (α) from the β specie.

However, the attribution of each reduction peak to different specific species is a quite complex matter because of the involvement of the surface ceria in the reduction phenomena. Nevertheless, the identification of the reduction peaks could help to identify the chemical species involved in the reaction of interest which proceeds at very low temperature, in a reducing mixture containing both CO and hydrogen, following a redox mechanism (see chapter 5).

When a quantitative analysis was not considered (Zheng, 1997; Kundakovic, 1998), the reduction peaks have been considered corresponding to the reduction of better and worse dispersed copper species, not taking into account of the participation of the ceria to the reduction phenomena. Those interpretations started from the hypothesis that all the copper is in the +2 oxidation state because the catalyst is generally prepared via incipient wetness impregnation and subsequently calcined at 400°C. However, as pointed out above, such an interpretation seems not completely convincing, since from a quantitative analysis it seems sure that also a fraction of the ceria is reduced in the TPR experiment. Nevertheless also in more recent works, where a quantitative analysis of the TPR is performed the ceria reduction is not taken into account in the peak identification (Tang, 2004; Pintar, 2004).

Actually, characterization studies (Luo, 1997; Martinez-Arias, 1999-2004; Shan, 2003; Tang, 2004) and our TPR data analysis, suggest the presence in the sample of CuO aggregates, whose dispersion, for a fixed preparation method, depends on the copper content. For higher copper load, copper species have more chances to aggregate during the preparation procedure thus forming big CuO aggregates. Relatively larger copper oxide clusters are more difficult to be reduced. Moreover our calculations suggest that also ceria is reduced at temperature lower than 300°C. Ceria involved in this process has been already identified as surface ceria highly interacting with copper. For samples with a copper concentration close to the theoretical monolayer almost all surface ceria is in direct contact with copper, while only a small fraction of surface ceria keeps unchanged the redox properties of the. Moreover, isolated copper ions or ionic pairs Cu^{+2}-Cu^{+2}may enter in the ceria structure thus altering its redox properties, as suggested by the XPS and EPR characterization studies of Martinez-Arias et al. (1999).

With the purpose of identifying some of the reduction peaks, we have carried out a TPR test over a more Cu-concentrated sample: 9 CuO/CeO_2. In Figure 6.2 the TPR profile obtained for the sample containing 9wt% CuO after the stabilising pre-treatment (curve b) is compared with the H_2 TPR already analysed for the sample 4 CuO/CeO_2 under the same conditions.

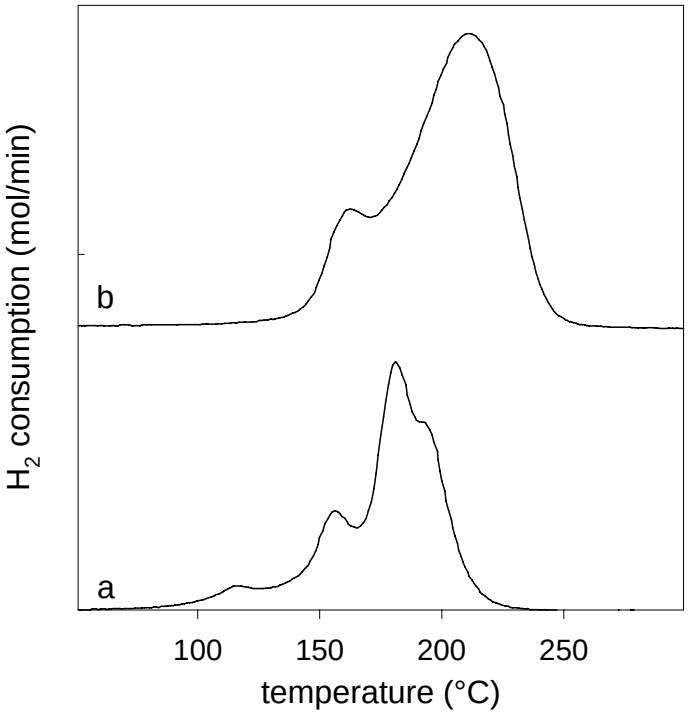

Figure 6.2: H_2 TPR analysis performed on (a) 4 CuO/CeO_2 ; (b) 9 CuO/CeO_2 sample.

For the 9 CuO/CeO_2, a H_2/Cu ratio of 1.1 has been measured, as is also reported in Tab. 6.1, suggesting a more limited participation of ceria to the overall reduction of catalyst (116 μmol/g, corresponding to about 4wt% of the total cerium). Moreover, the TPR profile of the 9wt% sample shows only two reduction peaks, respectively at 150°C and 210°C. In comparison with the 4 CuO/CeO_2, it is evident the disappearance of the α peak and the increased intensity of the δ peak which can be associated to the CuO clusters, whose formation (and segregation) appears as statistically more easily in correspondence of this high copper loading, and that are also detectable by XRD analysis.

These findings can be useful to definitely identify the δ peak and in addition, interesting information about the properties of the α peak starts to rise, taking into account the already observed (chapter four) and somewhat surprising lower activity in the CO oxidation (but also lower selectivity in the CO PROX process) of the catalyst containing 9%wt. of CuO with respect to the "optimal" sample, which contains less than half the amount of copper.

Another way we find useful to characterize the different peaks found in the TPR tests is to perform TPO analysis (Temperature Programmed Oxidation) coupled with (partial) oxidation treatments under different conditions followed by specific TPR tests. In the following, we will present the TPO analysis performed on both 4wt% and 9wt% CuO/CeO_2. Subsequently the other cited experiments will be introduced, explained and their results reported.

TPO tests, hence, aims to characterise the re-oxidation of catalysts previously reduced by H_2 (and, in the following, also by CO) by feeding a gas mixture with a very moderate oxidising power (to enhance as more as possible the analysis sensitivity and widen the time length of all phenomena). Specifically, the reducing pre-treatment was carried at 430°C (under H_2 flow), followed by a purging stadio at the same temperature and a cooling down to room temperature in nitrogen while the oxygen concentration in the feed of the test was set equal to 1000 ppm. Oxygen analyser allows us to measure the quantity of O_2 consumed in the different phases of the run, and to realize the instant of equilibration/stabilisation at room temperature, a certain period after the start of feeding the oxidising mixture. Starting from that moment, the sample was externally heated at 10°C/min, while oxygen consumption remains monitored.

Results of the TPO tests for the catalyst under investigation are reported in Fig. 6.3. The profile represents the consumption of oxygen as a function of the time.

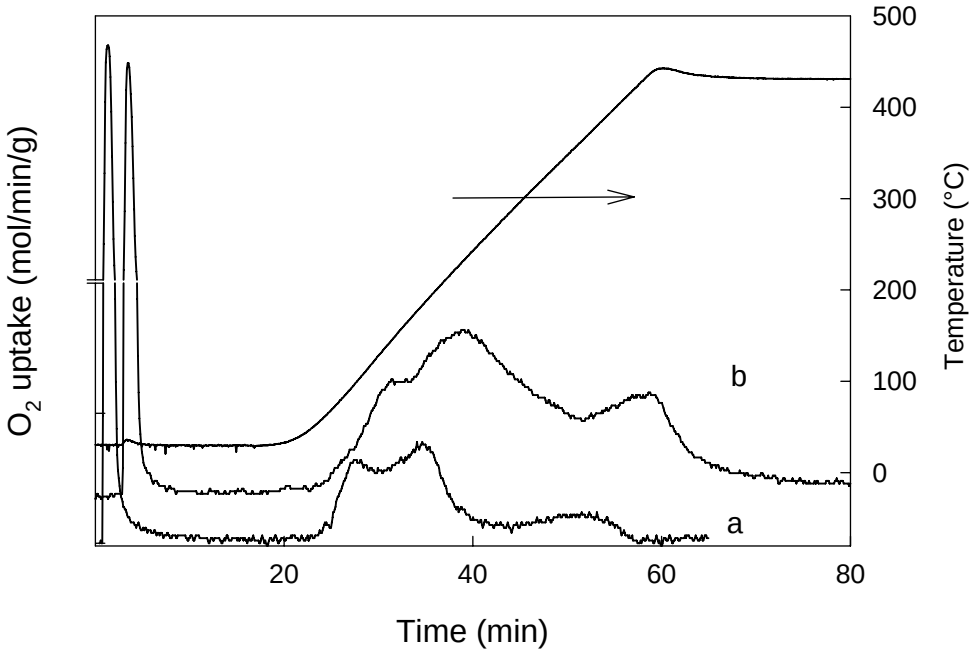

Figure 6.3: TPO analysis on 4 CuO/CeO_2 sample (curve a) and 9 CuO/CeO_2 (curve b).

For both samples, it has been measured a significant re-oxidation already under isothermal conditions at room temperature.

This phenomenon has been quantified and illustrated in Tab. 6.2: for 4 CuO/CeO_2, the oxygen uptake at RT corresponds to an O_2/Cu ratio equal to 0.36, while for 9 CuO/CeO_2, the oxygen uptake is relative lower, both with respect to the copper content ($O_2/Cu = 0.16$) and as absolute value (197 compared to 182 μmol/g). Actually, the absolute values of O_2 uptake seem very close between the

two different samples, suggesting also that increasing catalyst Cu content, the number of easily re-oxidisable sites at RT may not change.
Such a reoxidation process at RT occurred very rapidly giving rise to a sharp peak that last no more than 15 min, after which the sample clearly needed higher temperature to undergo further re-oxidation.

Table 6.2: TPO analysis results performed on CeO_2; 4wt% and 9wt% CuO/CeO_2 sample. Oxygen uptake and O_2/Cu evaluated at room temperature, and in the whole analysis.

CuO (wt%)	*H_2 TPR*	**Room Temperature**		**Whole run (up to 430°C)**	
	H_2/Cu	O_2 uptake (μmol/g)	O_2/Cu	O_2 uptake (μmol/g)	O_2/Cu
4	1.47	197	0.36	406	0.76
9	1.1	182	0.16	687	0.59

Thus, the further oxidation was observed during the subsequent TPO measurement. For the more active and less Cu-containing catalyst, the TPO consisted of two quite well-defined peaks at 100 and 200°C and a broader shoulder at 380°C (fig.4.4). This shoulder can be considered a part of the 200°C peak, originated as a consequence of a thermal overshoot.
The TPO profile on 9 CuO/CeO_2 appears a little different: an increase and further broadening of the second reduction peak (200°C) is observed. According to us, such finding could be immediately put into correlation with the reoxidation of XRD detectable CuO clusters. As we have also evidenced in the H_2 TPR of this sample, it is characterised by a larger amount of bulk CuO segregated that resulted the most difficult species to be reduced, and hence, in the TPO appear a the most difficult also to re-oxidise, in good consistency with the idea that redox properties of the transition metal can be strongly enhanced by the interaction with ceria. However, such general behaviour of TPO profile with three main peaks (at RT, 100 and 200°C) has been also reported by other authors (Zimmer, 2002; Pintar, 2005).
Looking at the quantitative analysis of the whole TPO test it is revealed a good agreement of the redox stoichiometry between the uptake of H_2 during TPR and of O_2 in the TPO for both samples. Tab. 6.2 shows that the value of the ratio H_2/Cu in the TPR are quite double the values of O_2/Cu in the TPO, so in line with the trivial stoichiometry:

$$Cu^{+2} + H_2 \rightarrow Cu° + 2\ H^{+} \qquad \text{(reduction stage)}$$

$$Cu° + ½\ O_2 \rightarrow Cu^{+2} + O^{-2} \qquad \text{(re-oxidation stage)}$$

From the TPO analysis, it seems not possible to recognize a stepwise oxidation from Cu^0 to Cu^{+1} and from Cu^{+1} to Cu^{+2}. Indeed, if we assume complete reduction and oxidation in the initial and final state of the TPO, we would expect a quantitative agreement between the copper reduced in the first two peak, with that reduced in the third, which is not observed.

In conclusion such experiments also confirm that the re-oxidation treatment we carried out at 430°C assures to be completely able to reoxidize the sample after an H_2 reduction. However, looking at Table 6.2, on the most active and interesting catalyst about 50% of the whole oxygen is recovered at RT yet, while other two reoxidation peaks are shown at 100°C and 200°C.

The chemical species re-oxidized at room temperature are very interesting for the catalysis of CO PROX because able to exhibit a fast kinetic of re-oxidation at temperatures lower than those of the reaction process. Moreover, the interest towards those species is increased by the observation that their number does not change with increasing the copper load from 4wt% to 9wt%. Indeed it has been showed in chapter 4 that those two samples exhibit a similar oxidation capacity (similar oxygen conversions) despite of the fact that the sample with 9wt% has more than the double of the copper load. This suggests that the number of species involved in the oxidation reactions must be the same in the two samples.

The catalyst sites re-oxidized at room temperature may be identified on the basis of the results of Martinez-Arias et al. (2004). which observe a complete ceria re-oxidation at room temperature, involving firstly ceria not affected by the presence of copper and subsequently ceria in contact with copper, followed by the partial re-oxidation of some well-dispersed copper species in intimate contact with ceria. Moreover, the re-oxidation which occurs in correspondence of the temperatures 100°C and 200°C is correlable exclusively to the re-oxidation of copper species. In particular, on the basis of the Martinez-Arias model the copper clusters should be the most difficultly re-oxidable species. This is in agreement with our experiments which shows that the reoxidation peak at 200°C can be attributable to the CuO clusters re-oxidation.

To further investigate such aspects, a TPR analysis has been performed on the sample reduced at 430°C and subsequently re-oxidized only at RT (Fig. 6.4). The TPR profile of the test carried out after partial re-oxidation of catalyst (only at RT) is reported in Fig. 6.4 (curve b), and put in comparison with the standard test carried out on the same sample after a fully re-oxidising pre-treatment.

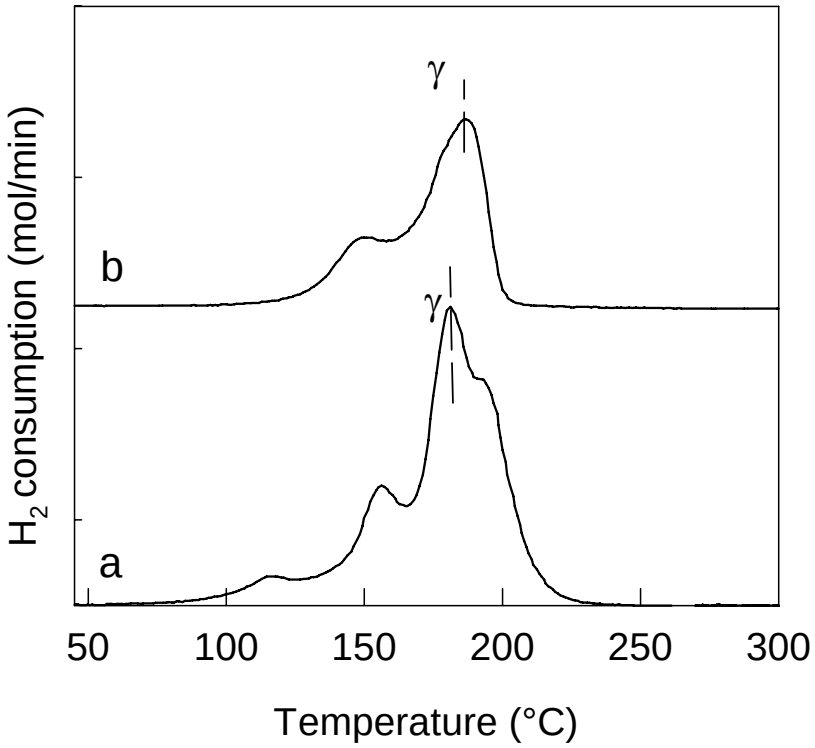

Figure 6.4: H_2 TPR on 4 CuO/CeO_2 after different re-oxidation treatments subsequent the standard pre-reduction at 430°C: (a) fully re-oxidised sample at 430°C for 2h; (b) partially re-oxidised sample at RT for 1h.

The first difference that appears between the two TPR is that the uptake of hydrogen is significantly lower after a partial re-oxidising treatment, as expected. A ratio $H_2/Cu = 0.74$ has been measured, namely about half value of the standard TPR test (1.47; Tab. 6.1). This value is in very good agreement with the value of O_2 uptake ($O_2/Cu = 0.36$) measured at RT (Tab. 6.2). Only two main reduction peaks are obtainend with maximum temperatures at 140°C and 180°C. The area of the reduction peak at 180°C corresponds to an H_2 consumption close to that of the γ peak in the (a) TPR, which hence seems unchanged.

Following the hypotheses enunciated above, the peak γ can be thus identified as that corresponding to the reduction of ceria involved in the strong-metal-support interactions, a species that is completely re-oxidised at RT, while the β peak may refer to the corresponding copper entities in intimate contact with ceria too.

A similar test has been performed on the sample with 9wt% copper load too. Performing a H_2 TPR on the sample partially re-oxidised ($O_2/Cu=0.16$) for 1h at RT after the complete reduction at 430°C, a reduction profile similar to that of the 4 CuO/CeO_2 is obtained. A quantitative analysis confirms data previously evidenced by the TPO analysis, i.e. the amount of the specie able to be

reoxidised at RT (H_2/Cu = 0.32 → 373μmol/g) is the same in both 4 (396 μmol/g) and 9wt% CuO samples.

In conclusion a tentatively peak attribution can be done. According to the redox model proposed by Tang et al. (2004), we believe that the reduction starts from the easier reducible species which could be identified with highly dispersed copper microclusters and/or copper entities in the ceria structure (α+β peaks). The reduction extends later to the ceria at the border line regions which has been identified in the γ peak. Indeed it has been shown that this specie (γ) is very easily reoxidable (complete reoxidation at RT) as expected also by Martinez-Arias redox model. After the reduction of the Cu/Ce at the borderline regions the bulk CuO starts to be reduced. Comparing TPR analysis of two samples with different copper loads (4 vs 9 wt%) the reduction of the bulk CuO is attributed to the high temperature peak (δ). The reduction of the remaining surface ceria takes place at 400°C.

It has been shown that the ceria at the borderline regions present a constant concentration changing copper load from 4 to 9 wt%, probably because also in the less Cu-rich catalyst the monolayer coverage has been reached, as already hypothesised in the preparation of catalysts.

6.2 Carbon Monoxide Temperature Programmed Reduction tests

The redox properties of copper/ceria catalysts have been investigated by employing also CO as reducing agent in the TPR tests. The interest towards such a study is not only connected to the more complete characterization of catalyst reducibility due to the different reducing power and general chemical properties of carbon monoxide with respect to hydrogen, but also in the fact that CO and H_2 are the two molecules in competition in the CO-PROX reaction.

Anyway, in this section the results of CO TPR tests will be presented after the discussion of the results of TPD experiments (Temperature Programmed Desorption) of both CO and CO_2, because when using CO as reducing agent a significant CO uptake has been detected already at RT. Such a phenomenon has been hence more deeply investigated in order to clarify the nature of the interaction of CO with catalyst already at very low temperatures, before trying to interpret the whole CO TPR experiment.

TPD tests were carried out on samples pre-stabilized (reduced at 430°C for 4h and subsequently re-oxidized at 430°C for 2h), and then saturated under atmosphere at controlled CO or CO_2 concentration, respectively 0.5 vol.% for CO (half an hour) and 1 vol.% for CO_2 (one hour); subsequently nitrogen was fluxed for half an hour to purge the sample (the desorbed species were monitored), before start running the temperature ramp. The desorption of carbon-containing species was conducted by means of the on-line analyser: after the adsorption of CO, both CO and CO_2 are subsequently found among desorbed gases with heating the sample; on the contrary in the CO_2 TPD, only carbon dioxide itself is desorbed during the temperature ramp.

Fig. 6.5 reports the results of the CO TPD. In the saturation/adsorption phase pre-TPD, it has been estimated a CO uptake of about 195µmol/g which corresponds to a CO/Cu ratio of 0.36. Washing the sample at room temperature in N_2, the amount of carbon monoxide released by the catalyst sample corresponded to a CO/Cu =0.06 (i.e. most of CO remains adsorbed at room temperature). Thus, the effective quantity of carbon-containing compounds remained on catalyst surface at room temperature in a somewhat state is corresponding to a CO/Cu ratio equal to 0.3 (Tab. 6.4).

Table 6.4: Summary of the CO TPD results performed on 4 CuO/CeO_2

Net CO uptake (µmol/g)*	*163*
CO/Cu	0.3
CO production (µmol/g)	*49*
CO/Cu	0.09
CO_2 production (µmol/g)	*109*
CO_2/Cu	0.2
C bal (%)	2.9

* intended as the total uptake at room temperature scrubbed from the aliquot released in the N_2 washing treatment.

Further increasing the temperature, the catalyst releases both CO and CO_2 suggesting the occurrence of a reaction between CO and some oxygen species and consequently of a reduction of catalyst. Generally, it is possible to hypothesise the presence of two kind of CO adsorption sites, one more reducible that give rise to CO_2, and another one responsible of the CO adsorption at RT. It is worth to note that both CO (CO/Cu= 0.09) and CO_2 (CO_2/Cu= 0.2) are desorbed at about 100°C, although while the CO peak is symmetric the CO_2 peak is much broader and carbon dioxide is completely desorbed only at about 400°C.

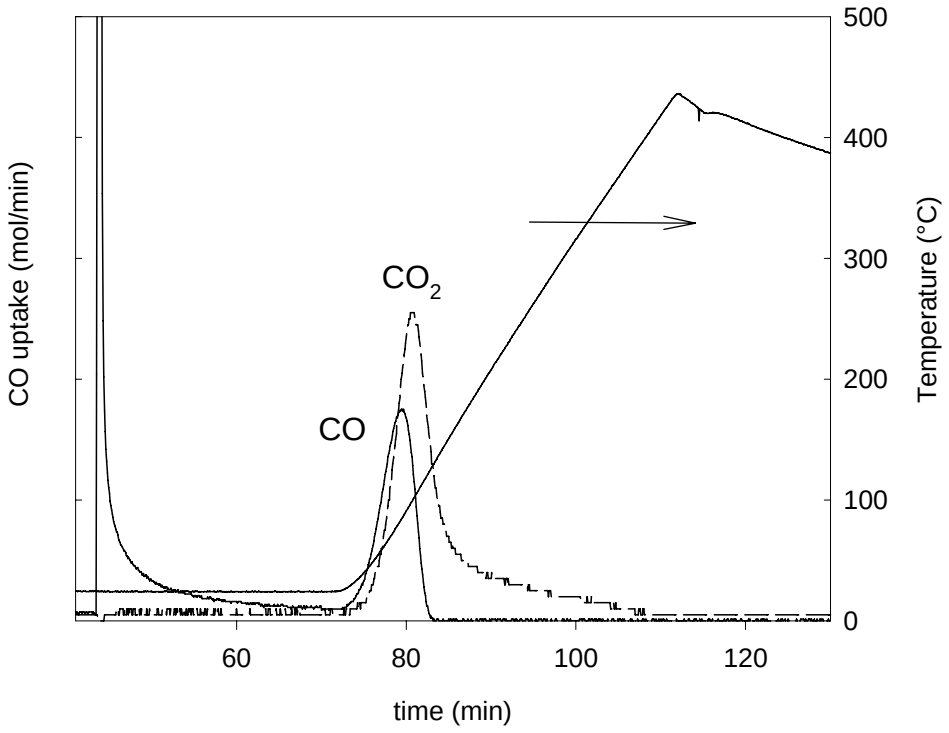

Figure 6.5: CO TPD on 4 CuO/CeO_2 pre-stabilized and saturated with a mixture of 0.5vol% CO (diluted in nitrogen) for 30 min at RT. Heating rate: 10°C/min

In a separate TPD test of CO_2 reported in figure 6..6, we found that the desorption temperature for carbon dioxide is 100°C and the amount of CO_2 adsorbed at room temperature corresponds to a CO_2/Cu ratio of 0.074, i.e. Moreover, the shape of the CO_2 desorption curve in the CO TPD is different from that of the CO_2 TPD in the high temperature region (fig.6.6). The broadness of CO_2 desorption peak in the CO TPD could suggest the presence of two different sites which are reduced by CO. The first one is responsible of the CO_2 desorption at 100°C similarly to the CO_2 TPD and is probably reduced by CO already at room temperature, while the second site is responsible of the broad shape of the CO_2 profile, that means that it forms and/or desorbs carbon dioxide at higher temperature. Actually, the presence of adsorbed CO_2 already at RT in a sample treated with CO was

also reported by Martinez- Arias (1999). The authors observes by means EPR and XPS analysis that the Cu^{+2} reducibility with CO at low temperature decreases with its aggregation degree, that means that the first copper species involved in the reduction with CO at room temperature are in the order those with higher degree of coordinative unsaturation. Moreover, no CO_2 evolution was observed at room temperature indicating that the generated CO_2 remains chemisorbed on the sample, probably forming carbonate species adsorbed on the ceria support.

In conclusion, it seems possible to distinguish three species responsible of the adsorption of CO at room temperature. Only one is responsible of a proper adsorption of CO at RT, other two are instead reduced by CO, one already at room temperature storing CO_2 as reduction product, the other one needing higher temperature to be reduced by CO and contemporarily to desorb the product carbon dioxide. In other words, by contacting with CO the oxidised catalyst even at relatively very low temperature (RT) a partial reduction of catalyst results unavoidable.

The catalytic species reduced by CO at room temperature are of great interest because, if easily re-oxidable can be involved in the CO preferential oxidation reaction at low temperature. Therefore, in the following a study finalized to characterize those species is reported with a particular attention to their selectivity to oxidize CO more than H_2 and their re-oxidation ability.

CO TPD tests were hence performed also on samples with different reduction degree. The attempt in controlling the oxidation state of catalyst should in our hypothesis allow us to verify the further reduction of catalyst sites due to the adsorption of carbon monoxide.

Such condition of controlled reduction degree was obtained by treating the catalyst with H_2 under defined temperatures. Before running the CO TPD, the sample is fluxed in a H_2 stream at different temperatures for ½ h. The sample is purged with N_2 at the reduction temperature for half an hour and subsequently cooled down in N_2 before starting the CO TPD analysis. A variable catalyst reduction degree is obtained by changing the temperature of the treatment with H_2: such reduction degree is calculated by measuring the amount of hydrogen consumed at the reduction temperature, and subtracting the fraction of H_2 subsequently released during the purging stage (all these quantities are well measured by the on-line analyser). The conditions adopted, the catalyst reduction degree realised and the results in terms of quantity adsorbed and desorbed in the TPD tests are reported in Tab. 6.4, while the profiles of CO and CO_2 desorbed during time are reported in Fig.6.6.

The results of the different TPD tests show that CO desorption peak does not change too much until the reduction degree is $H_2/Cu < 1$ and is very similar to the case of TPD of CO over the pre-oxidised catalyst. Surprisingly, the peak of CO_2 desorbed seems quite unaffected when $H_2/Cu = 0.9$, so suggesting that the catalyst, even if partially pre-reduced could be still reduced by CO (to form CO_2) at room temperature. In particular, the values reported in Tab. 6.5 show that the amount of

catalyst sites reduced by CO is not changed (CO_2/Cu = 0.22 vs 0.2), even if a large pre-reduction with H_2 has been performed on the sample.

The CO desorption peak completely disappears with increasing the reduction degree from 0.9 to 1.1, while the peak of CO_2 desorbed in the TPD decreases in a more gradual way. However, the amount of desorbed CO_2 is not exactly calculated because not all the CO_2 comes out at 430°C as it is evident by the carbon balance, reported in Tab. 6.5. Actually CO_2 could react with some hydroxo specie adsorbed on the catalyst surface forming methanol, or could form carbonates which decomposes at temperature higher than 430°C. Fig. 6.6 clearly shows that increasing the reduction degree the main peak of CO_2 desorption decreases but minor peaks at higher temperatures seem even to enlarge, while CO_2 concentration does not reach the baseline also at high temperature.

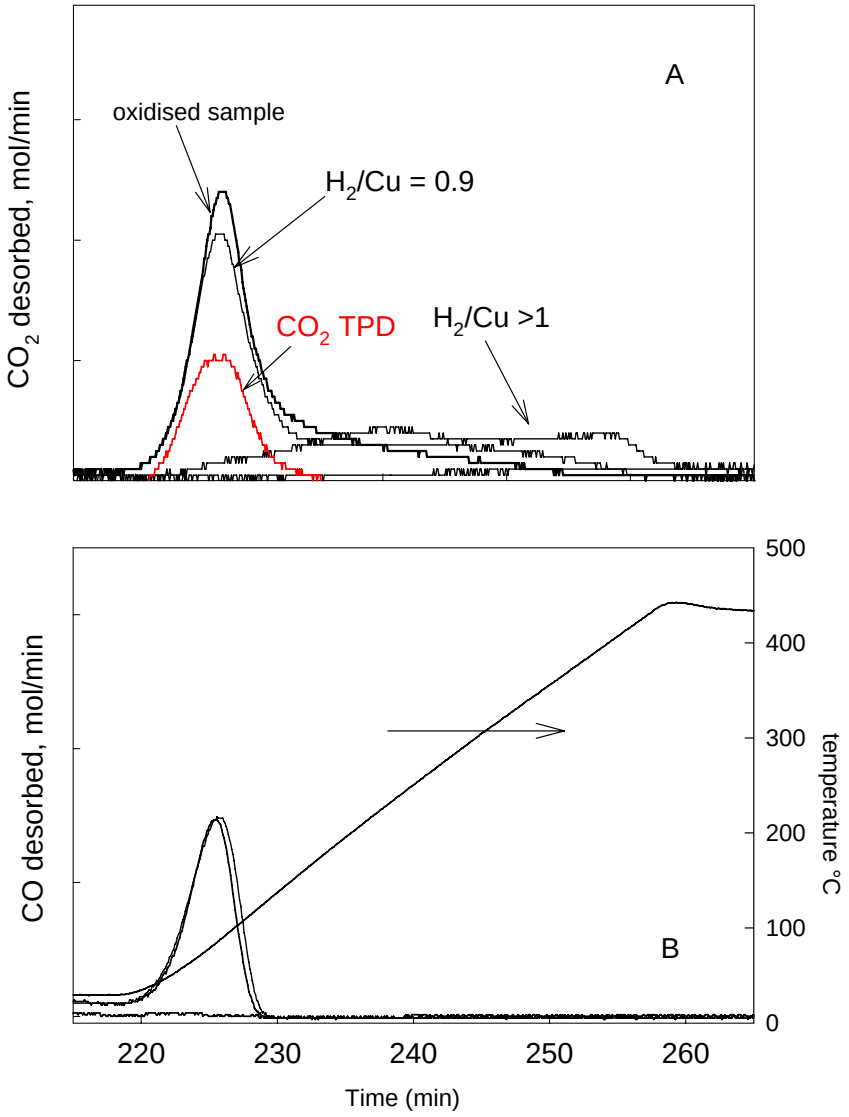

Figure 6.6: CO_2 (A) and CO (B) desorbed in the CO TPD(black) performed on 4 CuO/CeO_2 with different degree of pre-reduction or during the CO_2 TPD (red)

For a completely reduced sample, the CO uptake measured at room temperature corresponded to a CO/Cu ratio of 0.19 and is almost completely desorbed as CO_2 notwithstanding the maximum degree of reduction already reached, at least under the reducing effect of H_2. In fact, the formation of CO_2 on the strongly reduced catalyst could be associated to the reduction of some other species, presumably on the ceria surface, not previously reduced by the hydrogen because of the different reducing power between CO and H_2.

Table 6.5: CO uptake on 4 CuO/CeO_2 with different reduction degrees obtained reducing in H_2 at a fixed temperature for ½ h and subsequently purging in N_2 at the same temperature.

Reduction Temperature (°C)	*H_2/Cu pre-CO TPD*	*CO uptake, CO/Cu*	*CO desorption, CO/Cu*	*CO_2 production, CO_2/Cu*	*C bal (%)*
(oxidised sample)	0	0.30	0.090	0.20	2.8
100	0.9	0.33	0.09	0.22	6
110	1.1	0.25	0.001	0.12	61
430	1.49	0.19	0.007	0.16	12
430 + Reox RT	0.79 *(O_2/Cu = 0.35)*	0.18	0.020	0.18	4.6

In conclusion it has been demonstrated that the species which are reduced by CO at room temperature are also very selective towards CO oxidation more than H_2 being stable in a reducing atmosphere up to a certain catalyst reduction level. This observation increases out interest towards those species as possibly involved in CO-PROX reaction.

In order to study their re-oxidation ability a CO TPD has been performed on a sample completely reduced at 430°C and reoxidized only at RT for 1h (the results are those summarised in the last row of Tab. 6.4). Under similar conditions (see Tab. 6.2), we have evaluated that oxygen at room temperature is able to re-oxidise about half sites of the catalyst. The uptake is corresponding to a O_2/Cu ratio equal to 0.35 and should be compared to the H_2/Cu ratio equal to 1.49 during to deep reduction at 430°C. Under such conditions, the CO TPD once again is somewhat similar to the TPD of the pre-oxidised sample. Fig. 6.7 reports both the desorption of CO and of CO_2 during the experiment.

Specifically, the overall amount of CO uptake at RT on the partially reoxidized sample (CO/Cu=0.18) is lower than that consumed for completely reoxidized sample (CO/Cu=0.3). Nevertheless, only a small amount of CO (CO/Cu=0.02) is detected in the gas phase heating the sample, while the rest of carbon is desorbed as CO_2, whose total amount (CO_2/Cu = 0.18) is close to

the value measured on the completely oxidized sample. Nevertheless the shape of CO_2 desorbed in the TPD is quite different from the case of the pre-oxidized sample and more similar to the the TPD of all other partially pre-reduced catalyst, with a broad peak at high temperature. Figure 6.7 shows that the main peak at about 100°C has lower intensity, while at higher temperature the signal is very broad and the baseline is reached only at the highest temperature of the experiment, as already observed for the partially pre-reduced sample.

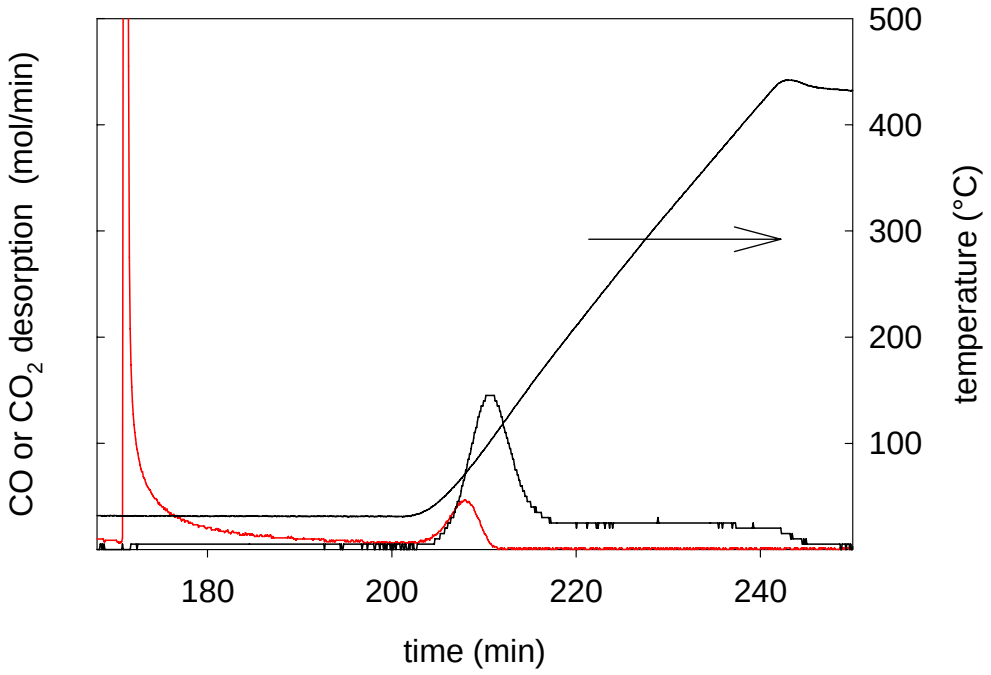

Figure 6.7: CO_2 and CO desorbed in the CO TPD performed on 4 CuO/CeO_2 prereduced at 430°C and partially reoxidated at RT for 1h.

A general conclusion from such experiments is that CO preferentially adsorbs on a catalyst completely oxidised, but the largest part of CO fed to the catalyst at room temperature reduces the catalyst with the consequent production of CO_2. Such a phenomenon is visible whatever the oxidation state of catalyst, even with the catalyst deeply reduced in H_2 at 430°C. However, reducing the catalyst in H_2 up to a catalyst degree corresponding to a ratio H_2/Cu= 1.1 does not significantly change the number of CO adsorption sites at room temperature. A further reduction of the sample leads to lowering the number of those sites.

Finally, since the CO_2 peak is almost completely restored after a reoxidation at RT, it is possible to assume that most of the species that are reduced and re-oxidised in a easier way (at the lowest temperature) are also those reduced by CO at room temperature. Instead, the CuO clusters, not

completely re-oxidized at RT, are probably responsible for the adsorption of the fraction of CO evolved at higher temperature.

The reduction of a fraction of catalyst as a consequence of CO adsorption and CO_2 evolution has been verified with a TPO test (Temperature Programmed Oxidation) performed just after the CO TPD. Figure 6.8 shows the profile of O_2 concentration during time (and increasing temperature). The largest part of O_2 uptake occurs at RT and is not reported in the Figure 6.8 (O_2/Cu=0.07), while a smaller quantity of catalyst sites is reoxidized between 100 and 200°C (O_2/Cu=0.03).

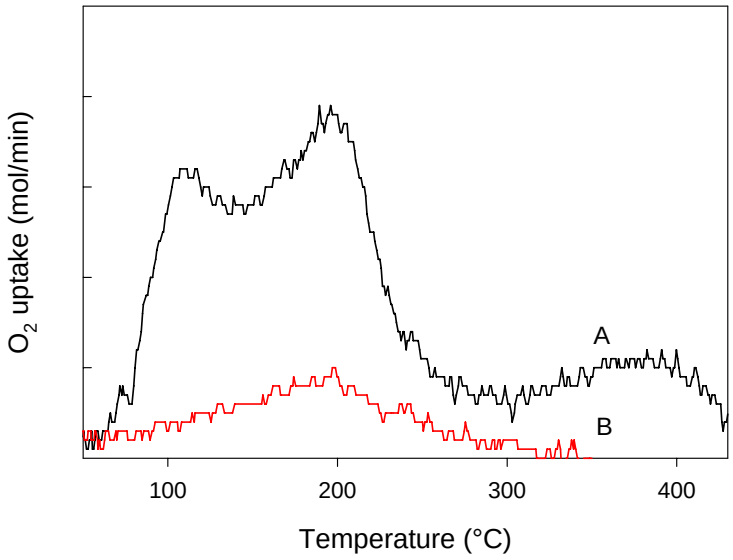

Figure 6.8: TPO of 4 CuO/CeO_2, after H_2 TPR (A); CO TPD (B).

In conclusion CO adsorption on a CuO/CeO_2 catalyst with different reduction degree has shown that at room temperature CO is preferentially adsorbed on a catalyst completely oxidised. From the comparison with literature results, it seems possible to associate those specie with copper with high unsaturation degree and ceria. Moreover the fact that those species are easily reoxidated yet at room temperature, let us to identify those adsorption sites with the borderline regions between small copper cluster and the support. Indeed those species are easily reoxidable, and the related atoms present an high degree of coordinative unsaturation.

Moreover it is worth underlining that the number of sites which are reduced already at room temperature does not change with reducing the catalyst in hydrogen up to a H_2/Cu ratio equal to 1 and increasing the copper load on the support from 4 to 9wt%. Indeed a CO TPD has been also carried out on a sample with a copper load of 9wt%. In table 6.6, the CO uptake at room temperature is compared with 4 CuO/CeO_2.

Table 6.6: CO TPD results performed on 4 wt% and 9 wt% CuO/CeO_2

CuO wt%	*CO uptake (µmol/g)*	*CO/Cu*	*CO production (µmol/g)*	*CO/Cu*	*CO_2 production (µmol/g)*	*CO_2/Cu*	*C bal (%)*
4	163	0.3	49	0.09	109	0.2	2.9
9	167	0.14	38	0.032	130	0.11	0.71

Both the CO and CO_2 uptake does not change significantly increasing the copper load to 9wt% (163 vs 167 µmol/g), thus the corresponding CO/Cu ratio decreases (0.3 vs 0.14), so evidencing a surprising invariance of the amount of the sites responsible for the reduction in the presence of CO at low temperature. A similar result is also reported by Luo et al. (1997) which moreover observe an equal activity of the two samples for the CO oxidation reaction.

In conclusion, it has been identified a chemical specie which is reduced by CO and re-oxidated already at room temperature and that is in somehow resistant to the reduction by H_2. Moreover the number of those species is the same in two samples similarly active towards CO oxidation. At this stage it is clear that this chemical species is not only involved in the CO oxidation reaction at low temperature, being easily reducible and re-oxidizable, but it is also a selective specie towards CO more than H_2, thus it is of crucial importance in CO-PROX.

CO TPR tests have been carried out in a similar way in comparison with H_2 TPR. Figure 6.9 reports the profile of CO uptake and CO_2 desorption measured in a CO-TPR test, carried out by heating the catalyst sample (4 wt.% CuO) from room temperature up to 430°C, in a mixture of CO (1vol%) and N_2. Such CO-TPR test demonstrated to be enough repeatable both qualitatively and quantitatively by carrying out the same tests four times on an given sample, prepared in different batchs.

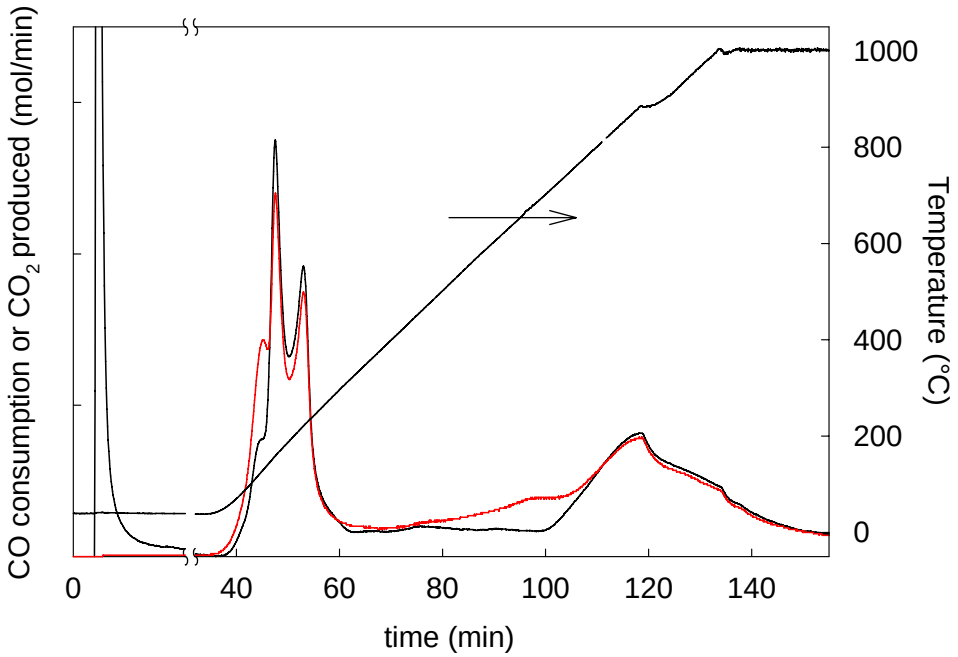

Figure 6.9: CO (black) and CO_2 (red) profiles detected during a CO TPR performed on 4 CuO/CeO_2 sample between RT to 430°C.

As demonstrated by investigating the adsorption of CO and carrying out TPD tests, when using CO as reducing agent a CO uptake should be expected already at RT. The numerical results are reported in table 6.7. Under the conditions examined, such a consumption of CO in isothermal environment is quantified to a CO/Cu ratio of about 0.36, of which the largest fraction has reacted with catalyst to reduce some surface species and produce CO_2 that remains adsorbed.

Table 6.7: CO TPR analysis results performed on CeO_2; 4wt% sample. CO uptake and O_2/Cu evaluated at room temperature, and in the whole analysis.

CuO (wt%)	T_f *(°C)*	**Room Temperature**		**Whole run (up to 430°C)**				
		CO uptake (µmol/g)	CO/Cu	CO uptake (µmol/g)	CO/Cu	CO_2 produced (µmol/g)	CO_2/Cu	C bal (%)
4	430	195	0.36	1005	1.87	836	1.56	16
4	1100	195	0.36	1963	3.65	1936	3.6	1.4

In the range of temperature of interest, namely those comparable to the H_2 TPR tests (i.e. from RT to about 400°C), also for CO TPR the overall consumption of the reductant during the whole experiment corresponds to more than the theoretical complete reduction of copper in the sample. Indeed, such an ideal CO/Cu ratio of complete copper reduction should be one, while the amount of CO consumed in the TPR corresponds to CO/Cu = 1.87.

The TPR profiles show that with increasing the temperature three main peaks of CO consumption, at 125, 160 and 216°C and a shoulder at about 100°C have been shown (fig.6.9). The CO_2 production follows the trend of the CO uptake, but its first peak is higher than that corresponding to CO probably due to the release of carbon dioxide produced in the CO uptake at RT (to which no peak of CO_2 production corresponds, as seen in the CO TPD tests).

Martinez-Arias et al. (1999) performing a CO TPR on a sample with 1wt% CuO impregnated on CeO_2 estimated a CO consumption of 42µmol/g at RT which corresponds to a CO/Cu ratio of about 0.27 namely very similar to ours. Two reduction peaks at 180 and 280°C were also detected. Only at 200°C, CO_2 has been detected at the outlet. The results of Martinez-Arias et al. (1999) are

quantitatively in agreement with ours, the qualitative differences being attributable to the different nature of copper species in a Cu-poorer catalyst.

In the whole CO TPR performed up to 1100°C a very good carbon balance (error = 1.4%) was obtained. Actually, between 400°C and 700°C there are two more peaks, one of CO uptake and the other of CO_2 production, with the latter that exceeds the first one. A possible explanation is that a fraction of the carbon dioxide produced at lower tempereature due to the catalyst reduction with CO forms some carbonate that remains adsorbed on ceria, and decompose in the higher temperature range, as also shown by Li et al. (1989). Carbonates formation on ceria after a reducing treatment in CO has been also detected by Martinez-Arias et al. (1999) by means IR analysis.

A TPO test was performed after the CO TPR, whose results are reported in figure 6.10. The oxygen uptake measured in the test stays in a O_2/Cu ratio of 0.88. This amount is in a good agreement with the redox stoichiometry which can be hypothesised on the basis of catalyst reduction in the CO TPR (CO/Cu = 1.87), namely the amount of O_2 consumed in the TPO is about half the CO consumed during the TPR. This means that the value of CO uptake measured in the TPR and confirmed by the parallel production of CO_2 should be all associated to the reduction of catalyst. Actually, such a value is even greater than the value of H_2/Cu measured in the TPR of hydrogen, thus suggesting that the number of catalyst sites reducible by CO and the reducing power of carbon monoxide are even higher than that of H_2.

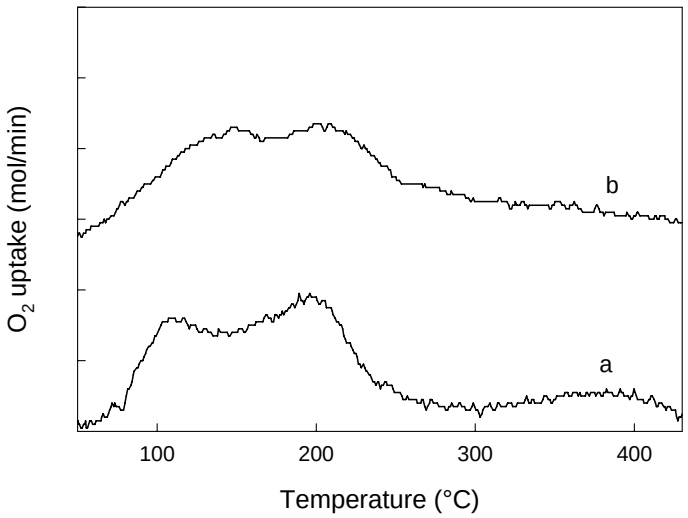

Figure 6.10: TPO analysis performed on 4 CuO/CeO_2 sample, after: H_2 TPR (a); a CO TPR (b).

By performing a comparison with a similar TPO test carried out after a TPR of hydrogen, the two main reoxidation peaks appear less pronounced, suggesting a re-dispersion of copper that brings probably to a more uniform distribution of the copper particles.

The overall O_2 uptake is higher than that calculated after a H_2 treatment because CO is a powerful reducing agent for this catalyst in the temperature range explored. At RT in particular the O_2 uptake after a CO treatment correspond to a O_2/Cu ratio of 0.41, while after a H_2 treatment was 0.36. This means that CO not only reduces more species than H_2, but also succeeds in reducing those species that seem in some way catalytically more active because more easily re-oxidisable.In order to evaluate the effect of a CO treatment at high temperature, a H_2 TPR has been performed on a sample that underwent the CO TPR and was subsequently re-oxidised at 430°C for 2h under O_2 flow. The overall H_2 uptake does not change (H_2/Cu = 1.46), but as can be seen in Fig. 6.11, the TPR profile qualitatively shows an increase of the low temperature peak (α) balanced by the decrease of the high temperature one, suggesting a further re-dispersion of the copper species as a consequence of a more reductant treatment. Such a re-dispersion of copper can be justify also the broader peaks detected in the TPO after CO TPR.

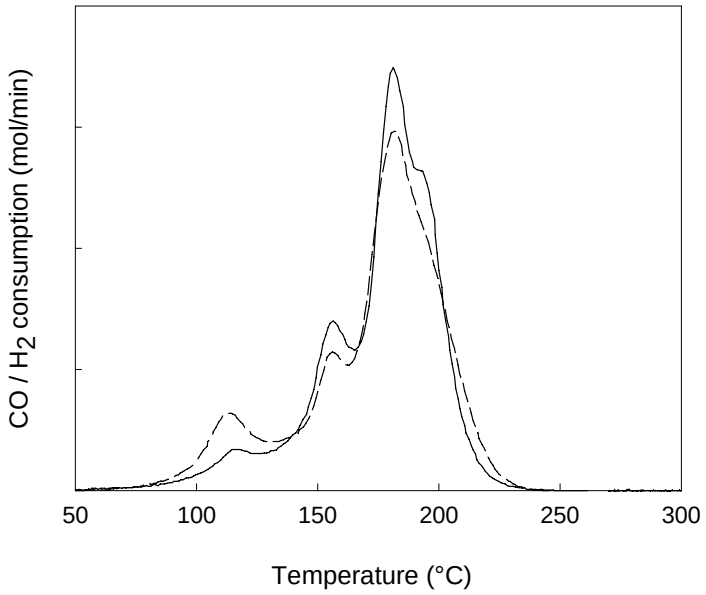

Figure 6.11: H_2 TPR performed on 4 CuO/CeO_2 sample pre-treated in H_2 (continue) or in CO (dotted) before the standard re-oxidation treatment.

Activity tests showed in chapter 4, demonstrated that a redox cycle in CO may increase the catalyst activity and this may be related to a copper particles redistribution.

Finally, a direct comparison between the CO and H_2 profile in their respective TPR tests has been proposed in Fig. 6.12. If we put on the same graph both TPR of CO and H_2, interesting consideration may be made. The CO TPR presents a CO uptake at RT that is absent when H_2 is used so meaning that at very low temperatures the reducing power of carbon monoxide is significantly higher than that of hydrogen. Surprisingly there is a perfect correspondence in the reduction temperatures of the α and β peaks, while in the region in which the main H_2 consumption occurs (180-210°C), only one peak, shifted to higher temperature, is present for CO.

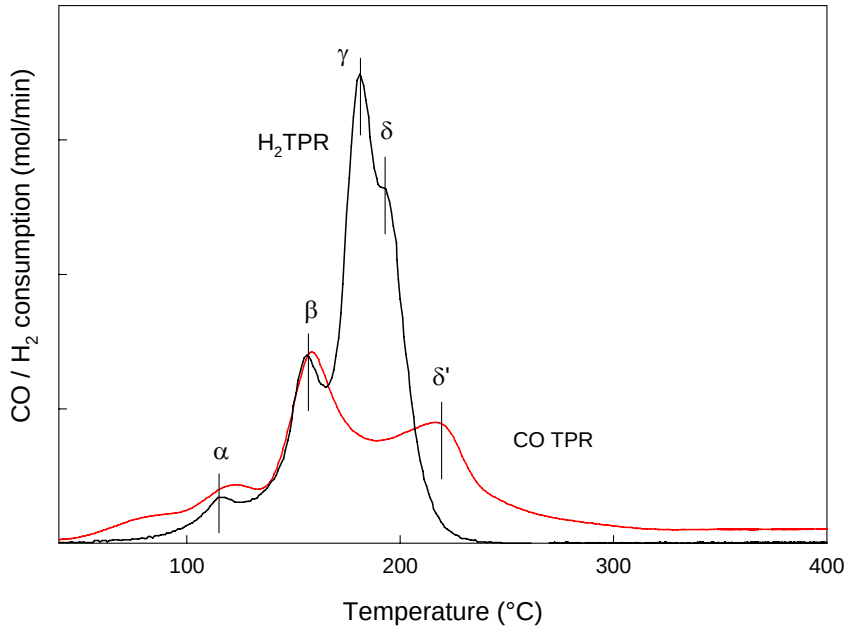

Figure 6.12: CO (red) and H_2 (black) profiles in their respective TPR tests on 4 CuO/CeO_2

The integral profiles in time of CO and H_2 consumptions are compared in figure 6.13. From RT up to 180°C the CO consumption is higher than the H_2 one, and also the overall CO consumption is higher than the H_2 one, indicating that, in the whole temperature range (RT-430°C), CO is able to reduce more sites than H_2 and at lower average temperatures. Another way to see the same phenomenon is that the tendency of catalyst of oxidising these reducing agents by means of superficial oxygen species is much stronger towards the conversion of CO to CO_2, at least in the range of temperatures from ambient to about 100-120°C. Such a phenomenon has of course direct and clear consequences on the catalytic properties of CuO/CeO_2 system in the CO PROX process. Neverthless, when the H_2 oxidation reaction starts (T>100°C) the H_2 reduction rate (shape of the fig.4.17 plot) is higher than that of CO.

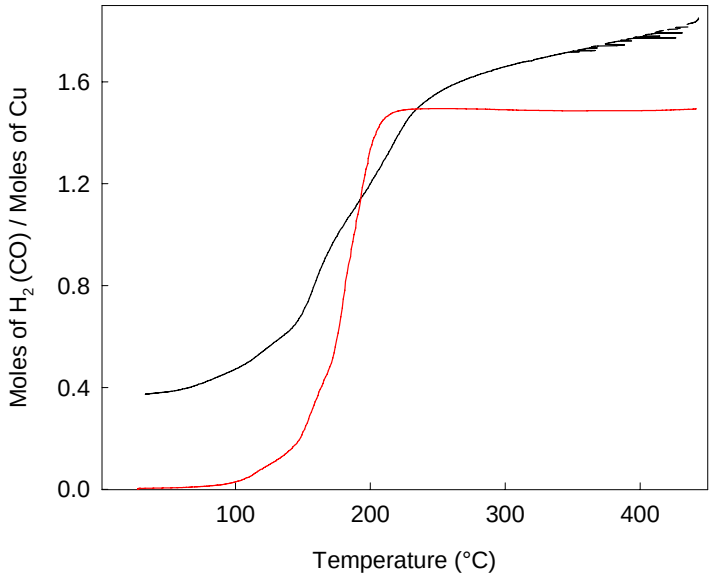

Figure 6.13: CO (black) and H_2(red) integral consumption during TPR tests as functions of temperature.

In order to characterize the specie responsible for the CO adsorption at RT a H_2 TPR has been performed on a sample previously saturated with CO at RT.

The CO consumption calculated after a CO saturation at RT corresponds, as expected, to a CO/Cu = 0.3. Thus the catalyst has been purged in N_2 for ½ h, and then the standard mixture of H_2 in N_2 used for H_2 TPR has been fluxed. During the sample heating CO and CO_2 desorption have been detected corresponding respectively to CO/Cu= 0.09 and CO_2/Cu= 0.2 so meaning that the mass balance on carbon-containing species is satisfied with good approximation (3%). The H_2 uptake in the subsequent TPR results lower than in the conventional H_2-TPR carried out over pre-oxidised samples (H_2/Cu = 1.31 instead of 1.47). It is worth to note that the catalyst reduction degree calculated by summing the CO_2 produced in the treatments with CO and subsequent washing in N_2 and the H_2 consumption (Red/Cu=1.51) is about equal or slightly higher than that obtained by standard TPR analysis (H_2/Cu= 1.47The sites which are reduced only by CO and not by H_2 below 430°C, are probably related to ceria position far from interface with copper oxide and also to bulk ceria as suggested by data analysis (the ceria micromols which participate to the reduction up to 430°C are higher than the number of ceria atoms at the surface).

The deconvolution of the H_2 TPR profile obtained after having treated the catalyst at room temperature with CO is reported in figure 6.14, where a clear decrease of the intensity of the β and γ peak is visible.

This result suggests that the species which are reduced in the presence of CO at RT are reduced in the presence of H_2 in the temperature range between 150 and 180°C.

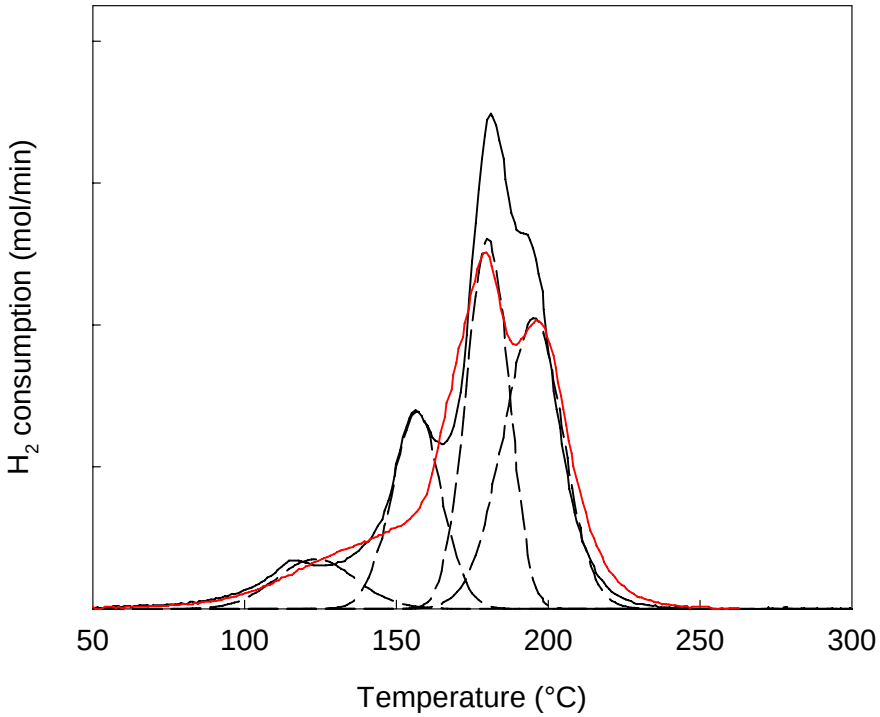

Figure 6.14: H2 consumption versus temperature: whole H_2 TPR profile (black curve) and its deconvolution (dotted curve). TPR on a sample saturated with CO (red).

Peaks identification in the CO TPR can be made on the assumptions already done in previous sections. At this stage it seems clear similarities and differences with the results of H_2 TPR. Moreover, repeating what done in the attempt to attribute the peaks in the H_2 TPR with defined species on the catalyst surface, CO TPR tests were done on a sample completely reduced in H_2 at 430°C and subsequently re-oxidised only at RT. In this way we know that bulk inactive CuO cluster should have been in the reduced state at the beginning of the TPR. Moreover, with the same aim to attribute peaks, a standard CO TPR was also carried out over a sample with higher copper load (9wt% CuO/CeO_2). Results are reported respectively in Fig. 6.15 and 6.16.

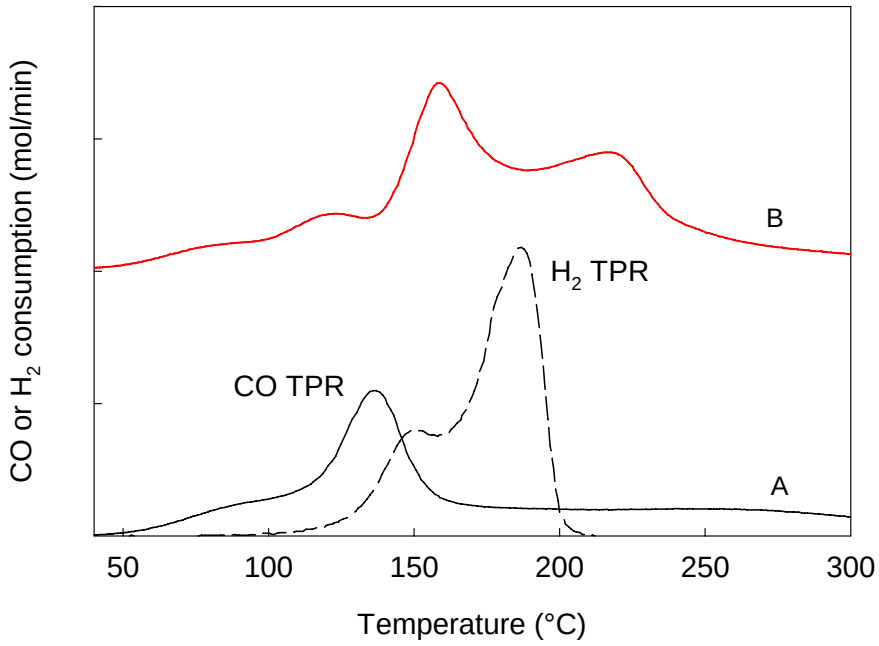

Figure 6.15: CO and H_2 TPR (A) performed on 4 CuO/CeO_2 reduced in H_2 at 430°C and re-oxidised at RT for 1h. Standard CO TPR (B)

The comparison between H_2 and CO TPR performed on a sample completely reduced and re-oxidized at RT has been presented in fig. 6.15. The CO TPR is characterized by a main peak at 135°C and by a broad peak extending from room temperature up to T > 300°C.

It is possible to associate the wide temperature peak to the reduction of ceria, while the peak at 135°C can be correlated to the reduction of some copper related species which are re-oxidized at RT (probably Cu^{+1} detected by Martinez-Arias (1999) on sample pretreated in CO at RT).

The amount of CO consumed during the such a TPR carried out after a partial re-oxidation of the catalyst (CO/Cu= 1.1) gives rise to an amount of sites that have been reduced that is higher than that expected on the basis of the oxygen uptake during the reoxidation at RT (O_2/Cu=0.36). This discrepancy is once again explainable taking into account the different reducing power between CO and H_2 already evidenced. It seems clear that the sample deeply reduced by hydrogen can be reduced further by CO which attacks some species not previously reduced in the H_2 treatment.

A CO TPR has been performed also on a sample containing 9wt% CuO (Fig. 6.16) and results are showed in table 6.8.

Table 6.8: CO TPR analysis results performed on 4wt% and 9wt% CuO/CeO_2 sample. CO uptake and CO/Cu evaluated at room temperature, and in the whole analysis.

CuO (wt%)	T_f	**Room Temperature**		**Whole run (up to 430°C)**				
		CO uptake (μmol/g)	CO/Cu	CO uptake (μmol/g)	CO/Cu	CO_2 uptake (μmol/g)	CO_2/Cu	C bal (%)
4	430	195	0.36	1005	1.87	836	1.56	16
9	430	193	0.17	1532	1.3	1356	1.16	12

It is worth to note that the CO consumption at RT does not change when increasing the copper load from 4 to 9wt%, as seen in the CO TPD tests.

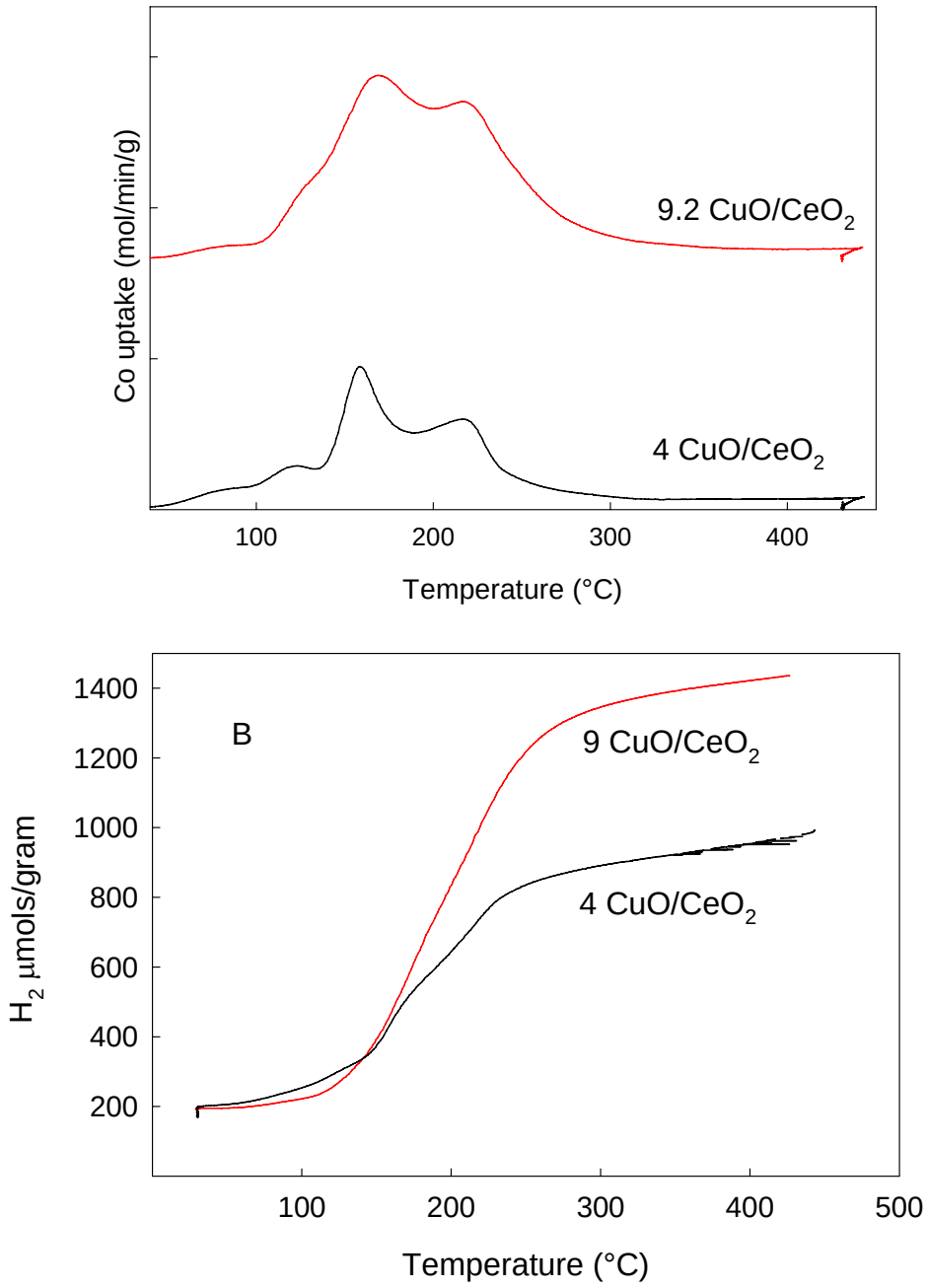

Figure 6.16: (A) CO TPR performed on 4 CuO/CeO_2 (black); 9 CuO/CeO_2 (red); (B) Micromoles of hydrogen consumed per gram of catalyst during the H_2 TPR reported in section A.

From the integral profiles showed in figure 6.16B, increasing the temperature the CO consumption is slightly higher in the catalyst with 4wt% CuO copper load, while from 140°C the CO consumption is higher for the 9wt% sample. In particular a huge increase of the high temperature peak is observed which thus can be related to the reduction of big CuO clusters also detectable by XRD analysis. The latter attribution is supported by a CO TPR performed on bulk CuO (not shown) which showed a lower CO/Cu ratio when using CO as reducing agent (CO/Cu= 0.7) in comparison

to H_2 (H_2/Cu=1) indicating that for this specie or H_2 is a more powerful reducing agent, or CO presents diffusion limitations. In summary, also in the presence of CO with increasing the copper content it increases the overall reducibility of the sample but it slightly shifts to higher temperatures.
In conclusion, it has been shown that the catalyst CuO/CeO_2 is reduced in the presence of CO also at room temperature. At this temperature only a small amount of CO_2 is detected, while it comes out raising up the temperature at about 100°C probably because of carbonate formation.
Increasing the catalyst reduction degree, the amount of CO_2 formed at room temperature decreases, thus suggesting that the catalytic sites which are reduced in the presence of CO already at room temperature are completely oxidated species. Accordingly to the literature (Martinez-Arias et al. 1999) those species have been identified in Cu^{+2} with high degree of coordinative unsaturation and ceria. Considering the easy reoxidation of those sites, we suggest the identification of those sites with copper-ceria at the borderline regions.
By means of TPR analysis it has been demonstrated that CO is a stronger reductant for CuO/CeO_2 catalyst in the low temperature region in comparison to H_2. Indeed, the CO TPR shows 4 main peaks, the first of those at room temperature. By comparing the H_2 and CO consumption profiles seems possible to suggest that the selective species towards CO between RT and 100°C, are reduced between 150 and 180°C in the presence of H_2. Moreover, a H_2 TPR performed on a sample after a CO TPD analysis showed a reduction in the intensity of the β and/or γ peaks, supporting the idea that the species reduced by CO oxidation at room temperature, are on the contrary reduced by H_2 at a temperature higher than 150°C. This species could be identified in the species γ of the H_2 TPR profile, already previously assigned to copper-ceria at the borderline regions.
The different profile of the CO and H_2 TPR found in our analysis could be explained by assuming a different reduction mechanism in a stream containing CO rather than H_2. It could be assumed that in the presence of CO the reduction process involves first the reduction of the copper-ceria at the borderline regions (corresponding to the γ specie in the H_2 TPR profile), followed by the reduction of the CuO microclusters corresponding to α and β species. Successively the reduction of bulk CuO it is assumed to take place (δ specie). Indeed, also in the CO TPR, the high temperature peak is tentatively attributable to the CuO bulk reduction.
In the presence of CO we may not exclude a stepwise reduction involving first the reduction to Cu^{+1} and subsequently a further reduction to Cu^0 as suggested from literature results (Martinez-Arias, 1999-2004).
On the contrary in the presence of H_2 the reduction takes place from the CuO microcristals (α and β species), which activate the reduction of the borderline regions (γ specie), and then extends to bulk CuO (δ specie).

The reduction mechanisms proposed, explain the observed invariance of the number of sites reduced by CO at room temperature on a catalyst pre-reduced in H_2 up to a H_2/Cu ratio close to 1. Indeed, in a hydrogen stream the reduction of those species does not take place by first but only up to a certain catalyst reduction.

The results obtained by the investigation of the redox properties of CuO/CeO_2 samples clarify many aspects of the CO preferential oxidation reaction. From this point of view the analysis of the redox properties performed up to this stage showed that CO is a stronger reducing agent for CuO/CeO_2 catalyst in the whole temperature range explored, thus explaining the good performances exhibited by this system in CO-PROX. Moreover, the activity of this catalyst at low temperature seems linked to the presence of species very easily reducible by CO, even at room temperature, easily reoxidable, but resistant towards hydrogen reduction. Those species have been assumed to be ceria highly interacting with copper generally defined as copper/ceria borderline regions. Increasing the copper content higher than 5wt% the concentration of these species does not change thus justifying the absence of an increased activity with increasing the copper load up to this limit.

Moreover the redox study showed that CuO big cluster are reduced by H_2 at a temperature lower than by CO, thus under reaction conditions those species could be selective towards hydrogen oxidation. Furthermore these species are reoxidated only at high temperature (≈200°C), thus their involvement in the reaction may be considered only at relatively high temperature (T>150°C).

6.3 H_2 TPR analysis on samples with different copper loads - Strong metal support interaction

The effect of the interaction of ceria with copper oxide is not independent on the amount of active phase loaded in the catalyst, and also the occurrence of a strong metal support interaction between CuO and CeO_2, with the consequent increase of reducibility of both cerium and copper, is strongly function of the content of copper on ceria (Zimmer, 2002; Shan, 2003; Tang, 2003). In order to investigate this aspect, H_2 TPR tests have been performed on samples with different copper loads.

In figure 6.16 the results are reported in term of hydrogen uptake per unit mass of catalyst, H_2/Cu ratio and percentage of ceria reduced in the experiment, calculated considering that each copper atom is completely reduced from the oxidation state +2 to zero.

Increasing the percentage of copper on the support, the uptake of hydrogen increases but less than linearly; in fact, the H_2/Cu ratio decreases. Assuming that copper is completely reduced from Cu^{+2} to Cu°, this means that increasing the copper percentage results in a decrease of the fraction of ceria reduced due to the promotion effect of the strong metal-support interaction so to occur at much lower temperature than on pure ceria.

A similar observation has been made by Shan et al. (2003) which analyzed catalysts prepared by citric acid complexation method, in order to induce the formation of a solid solution. Over those catalysts, they observed a decrease of the H_2/Cu ratio with increasing the copper load, at around H_2 consumption values very close to ours. Such a

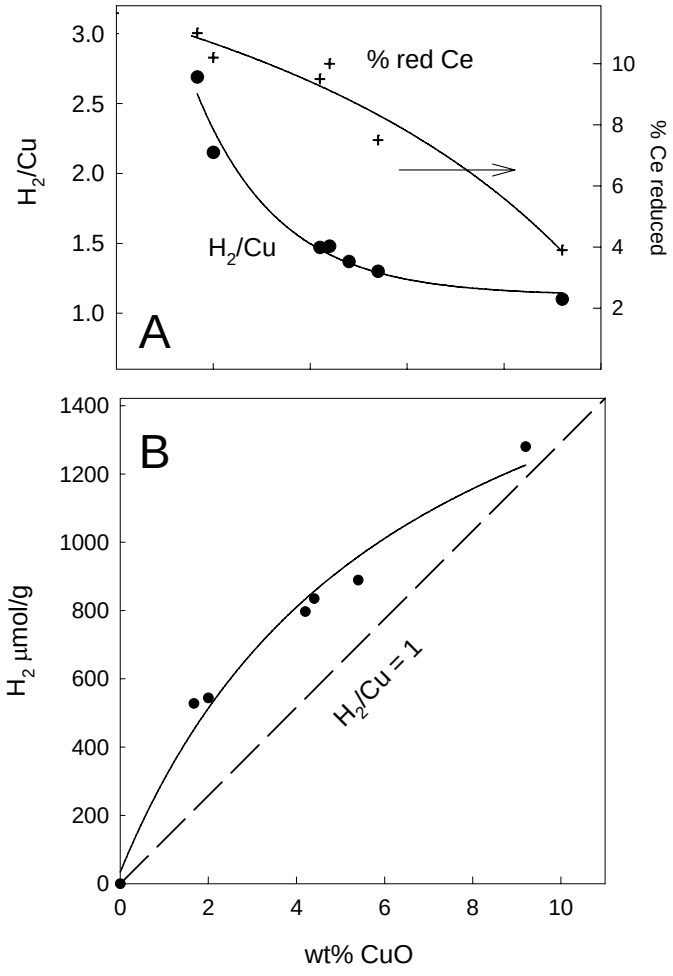

Figure 6.16: TPR of CuO/CeO_2 catalysts at variable Cu content: (A) H_2/Cu ratio, percentage of ceria reduced; (B) H_2 uptake per unit mass of catalyst in comparison with the theoretical stoichiometric consumption for complete reduction of the copper.

behaviour was explained by the authors considering that for low copper concentrations the Cu^{+2} ions may enter in the ceria fluorite structure inducing the formation of a defective oxygen sub-lattice, thus increasing the reducibility of ceria. Increasing the copper load, small CuO clusters are formed, and cover part of the oxygen vacancies that led to the decrease of the adsorbed oxygen, and the Cu^{+2} in the solid solutions were not reduced completely. A further increase of the copper load generates bulk CuO, which may present diffusion limitation to complete reduction, thus further decreasing the H_2/Cu ratio.

For our samples, prepared by wet impregnation, a technique which does not favour the formation of solid solutions among CuO and CeO_2, the interaction between copper and ceria may be considered limited to the surface. Thus, low copper concentration may induce an increased reducibility of ceria, because of the formation of strong-metal-support-interactions which we can consider limited to the borderline regions between CuO micro-crystals and the surface of ceria. Foger et al. (1987) assumed that there are a limited number of anchoring sites which may generate such an interaction. When copper loading exceeds the concentration of these sites, CuO clusters are formed. Thus, the global amount of hydrogen uptake continues to increase, but linearly, with the copper concentration, thus decreasing the H_2/Cu ratio (figure 6.16B). A further increase of the copper loading may reduce the surface area, covering the copper-ceria active sites, thus decreasing the overall reducibility of the sample, also under the stoichiometric value (H_2/Cu = 1) if diffusion limitations take place.

According to our hypothesis, the participation of ceria to the reduction process should have a maximum with the percentage of copper if a maximum temperature is fixed (300°C) in the TPR analysis. Indeed a minimum copper content is expected to activate the ceria in the low temperature region by increasing the concentration of the copper in the anchoring sites which should generate the strong-metal support interaction.

This is observable in the experiments reported by Tang et al. (2004) referred to samples prepared via co-precipitation method. Increasing the copper loading the reduction of ceria gradually shifts to lower temperature. In the sample containing 5wt% Cu the reduction starts at about 100°C. Above a certain value (wt% Cu > 20%) the reduction of the sample shifts again to higher temperature.

In conclusion it has been demonstrated that the addition of copper on ceria, via impregnation method, is able to induce strong-metal support interactions between the active phase and support, which induce the reduction of the ceria at very low temperature (H_2/Cu>1).

This promoting effect has been attributed to the presence of copper particles in some anchoring sites present on the ceria surface, that is possible to identify with oxygen vacancies. The copper promoting effect has been demonstrated to decrease when the copper load exceeds the

concentration of the anchoring sites on the ceria surface, giving rise to CuO microclusters and then to bulk CuO.

6.4 CO and H_2 Chemisorption measurements

H_2 and, separately, CO chemisorption measurements have been carried out at constant temperature on a completely oxidised sample, stabilized with the standard procedure.

The adsorption tests for H_2 shows that hydrogen is not consumed at room temperature neither at temperatures lower than 70°C, as expected by the results of TPR tests. Nevertheless for temperature higher than 90°C, a H_2 consumption is detected. In figure 6.17, the H_2 concentration profile during an experiment of hydrogen chemisorption performed at 110°C is shown. More in details, it is reported the value of the concentration of hydrogen measured at the reactor outlet during time on stream after the having fed to the reactor a reacting mixture containing H_2 (2% vol.).

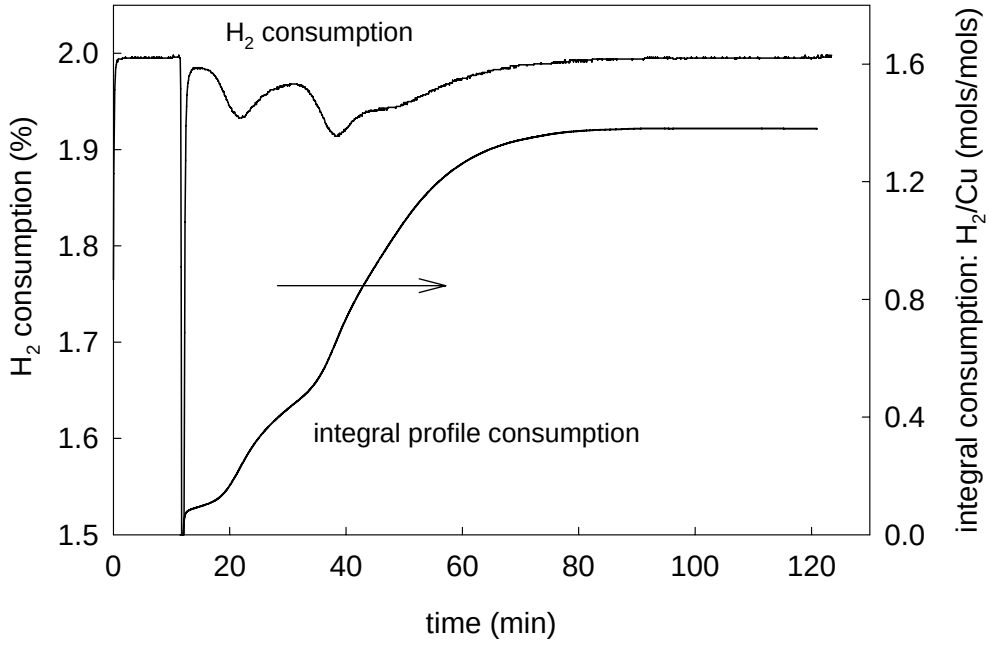

Figure 6.17: Isothermal hydrogen uptake and integral consumption on 4 CuO/CeO_2 sample as functions of time. T = 110°C. H_2 concentration in the feed: 2% vol.

The first sharp peak is the hydrogen uptake for filling the empty volume of the reactor (holdup). Nevertheless the amount of H_2 needed for filling the reactor and the connection tubes (theoretically estimated and experimentally evaluated with a blank tests) are less than that corresponding to the sharp peak shown by this analysis, suggesting the occurrence of an immediate reduction of the sample when H_2 is introduced. Such a phenomenon is even clearer by looking at the integral H_2 consumption reported in figure 6.17. Actually, at the very beginning of the experiment, the hydrogen uptake of the catalyst corresponds to a H_2/Cu ratio equal to 0.09. For a couple of minutes, the integral consumption profile seems to reach a plateau but after few minutes a new peak of H_2

consumption is clearly observable. This phenomenon is repeated one more time, so that at the end of the experiment, the global hydrogen uptake is composed of three main peaks, one at the very start of the run, the other two respectively after about 10 and 25 minutes: moreover, a broad shoulder is observed after about 40 min that seems to disappear only after half a hour more.

The overall hydrogen uptake at the end of the experiment is reported in Tab. 6.9, where are also reported the values of the amount of hydrogen desorbed in a N_2 TPD conducted up to 430°C. For the experiment of H_2 chemisorption at 110°C, the amount of hydrogen desorbed in the TPD was 103 μmol/g of H_2 (H_2/Cu=0.19) with a major peak at about 170°C.

Tab. 6.9: H_2 chemisorption measuraments on 4 CuO/CeO_2

Temperature (°C)	*H_2 uptake (μmol/g)*	*H_2/Cu*	*H_2/Cu desorbed in subsequent TPD*
70	19	0.03	
100	722	1.33	0.09
110	756	1.39	0.19

From these data, it is possible to calculate the hydrogen consumed for catalyst reduction by subtracting from the overall hydrogen uptake at 110°C, the amount of H_2 desorbed in the subsequent TPD. Hence, an effective catalyst reduction corresponding to a H_2/Cu ratio of 1.1 is obtained in the isothermal experiment at 110°C.

The H_2 consumption peaks observed in figure 6.17 as a function of the time may be associated to a catalyst reduction and to a hydrogen adsorption probably on reduced sites, since no H_2 adsorption has been observed on completely oxidized catalyst at room temperature.

Actually, only a small fraction of H_2 consumed at 110°C adsorbs on the catalyst while the great part must be associated to a catalyst reduction. For these reasons the H_2 consumption peaks observed as a function of the time may not be completely explained by adsorption-desorption mechanisms, but may be related to some induction phenomena occurring during the catalyst reduction.

Two possible mechanisms have been though to explain this singular behaviour. The easiest explanation is that the initial reduction of the catalyst involves the copper which change its oxidation state from $Cu^{+2} \rightarrow Cu^{+1}$. When all the copper is in the oxidation state +1 both H_2 adsorption, and a further catalyst reduction may occur. Indeed the initial reduction to Cu^{+1} could lowers the activation energy for the further reduction to Cu^0. Moreover the final H_2/Cu ratio higher than one (1.1), suggests that another species is involved in the reduction at 110°C. The reduction of ceria already at so low temperature is quite difficult to be predicted by the previous explanation.

Another hypothesis to explain the induction phenomena observed at 110°C is that the reduction happened by a chain-mechanism involving first the most dispersed copper particles. The reduction of those species lowers the activation energy for the reduction of the species at the border line

regions. In our opinion the reduction extends from the copper microclusters to the ceria at the border line followed by the initial reduction of the bigger copper clusters, in agreement with the observations of the TPR analysis. Probably at 110°C only a small part of the CuO big clusters are reduced, this explaining the gap between the H_2/Cu ratio calculated in this isothermal reduction (H_2/Cu=1.1) and the overall hydrogen consumption measured by an H_2 TPR (H_2/Cu=1.47) that is carried out up to 430°C.

A similar isothermal study has been made when using CO as reducing agent.

It has been previously discussed the results of a CO TPD analysis performed on 4 CuO/CeO_2 sample, which showed that catalyst is partially reduced by CO already at room temperature.

At 70°C after 1h in flux of CO, a CO consumption corresponding to CO/Cu ratio 0.85, has been calculated. In figure 6.18 the chemisorption of CO is reported for a temperature of 100°C.

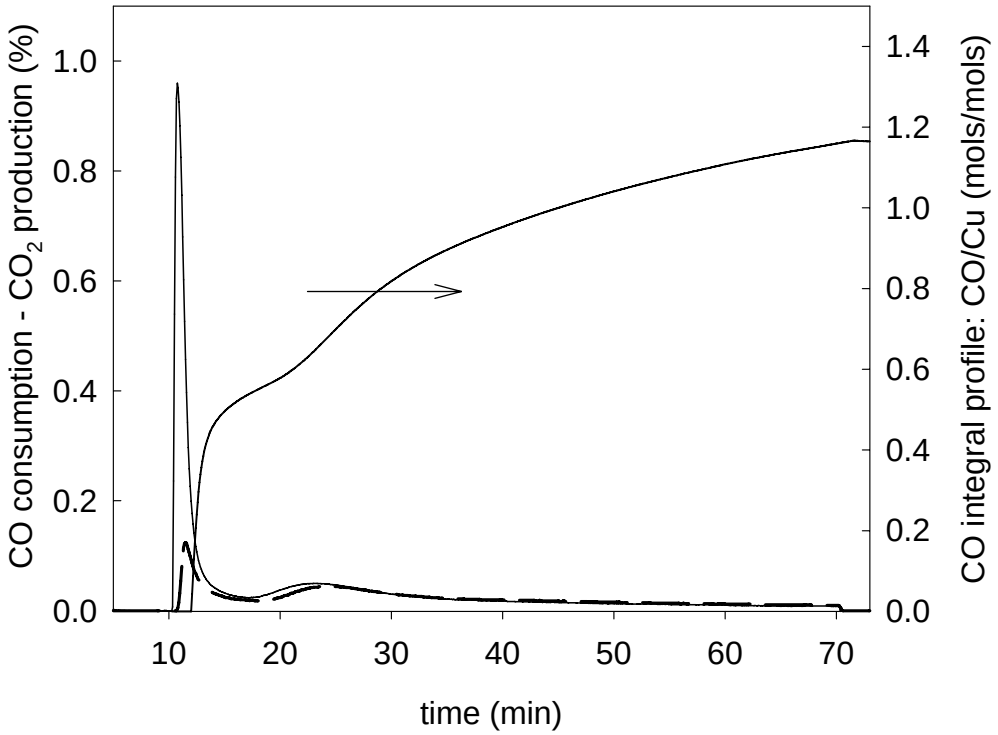

Figure 6.18: Isothermal CO consumption (continue) and CO_2 production (dotted), integral CO consumption as functions of the time at 100°C on 4 CuO/CeO_2.

It is interesting to underline that the heat of adsorption of CO is significantly higher that that of H_2, as it clearly appears from the temperature increase (4°C) detected after the CO admission (not shown), while no thermal effect where detected after the H_2 admission.

A huge CO consumption corresponding to a CO/Cu ratio of 0.5 occurs in the first 5 minutes from the CO injection (fig.6.18). Correspondingly a CO_2 production is detected even if in amount lower

than the CO consumption (CO_2/Cu = 0.1). After 10 minutes another small CO consumption peak is observed, simultaneously to a CO_2 peak production. After 1h in the CO stream the CO/Cu ratio corresponds to 1.28. Washing the sample in N_2 at 100°C and heating the catalyst sample up to 430°C produces the desorption of only CO_2. The amount of CO_2 detected satisfies the carbon balance with a good approximation.

The CO consumption peak appearing after at 15 minutes, because associated to a contemporary CO_2 production peak, must be related to an induction phenomena occurring during the reduction, similarly to what is observed in the presence of H_2. In the case of CO, an initial consumption corresponding to CO/Cu= 0.5 could explain the induction by a stepwise reduction of the catalyst from Cu^{+2} to Cu^{+1} and subsequently from Cu^{+1} to Cu^0. Nevertheless this explanation fails when considering that the final CO/Cu ratio measured is greater than that corresponding to the reduction of the all copper. Moreover it is well known by the literature (Martinez-Arias, 1997-1999-2000; Trovarelli 2000), and it has been widely confirmed by our experiments the involvement of the ceria in the reduction phenomena in the presence of CO for temperature well lower than 100°C. Indeed our results strongly suggest the participation of the support already in the reduction occurring at room temperature. Those considerations may suggest that the reduction starts from the borderline regions involving both copper and ceria accordingly to what is observed by the CO TPD (pag.145). Thus the reduction may proceeds involving first the CuO microclusters which may then induces the reduction of bigger CuO clusters.

Martinez-Arias observed an increase of the Cu^0 carbonyls by treating the catalyst in CO at a temperature higher than room temperature. Increasing the reduction temperature below to 200°C only a very small amount of carbonyls are formed, despite of the fact that even if weakly than on Cu^{+1}, carbon monoxide adsorbs on Cu^0. This behaviour has been explained by the presence of electronic interactions between small metallic copper particles and reduced ceria. The driving force for this metal-support interaction could be the achievement of a relatively strong reduction of the ceria surface by treatment at temperature higher than 100°C. Thus electron transfer from Ce^{+3} towards the Cu particles could then produce a Cu-CO interaction even weaker than on neutral Cu^0.

In our experiments we do not observe any CO desorption from a catalyst previously saturated in CO at 100°C. The possible explanation is that if Cu^{+1} is formed, CO adsorbed is quickly converted into CO_2 because of the high temperature. Moreover the fact that on metallic copper the CO adsorption is not observed is in agreement with our previous analysis on CO TPD performed on a catalyst completely reduced.

In conclusion, induction phenomena in the redox process of the CuO/CeO_2 catalyst both in the presence of CO and H_2 has been observed. The CO oxidation takes place from room temperature,

while the reduction of the catalyst in the presence of H_2 require a certain light-off temperature of about 100°C.

In both cases at least two steps in the reduction have been observed which may not be completely explained by a stepwise reduction from Cu^{+2} to Cu^{+1} and from Cu^{+1} to Cu^{0} because of the involvement of ceria in the overall consumption of the reducing agent. Nevertheless those analyses confirms the TPR/TPD/TPO results which identified CO as a more powerful reducing agent for CuO/CeO_2 catalysts in comparison with H_2. Indeed at a constant temperature the final catalyst reduction degree is higher in the presence of CO than with H_2.

A similar chemisorption study has been done using as a probe molecule O_2 on a sample completely reduced at 430°C.

Up to 100°C no induction phenomena in the re-oxidation process has been detected. Indeed the oxygen consumption shows only a sharp peak which extinguishes completely after 15 minutes and corresponding to a O_2/Cu ratio of 0.78. This value is exactly what expected by the TPO experiments, for a reoxidation up to 100°C.

6.5 CO and H_2 contemporary addition: TPR and chemisorption measuraments

A mixture of CO and H_2 was fluxed at 100°C on the sample 4 CuO/CeO_2. The CO and H_2 consumptions have been reported in figure 6.19A while in figure 6.19B the CO and H_2 integral consumptions are plotted.

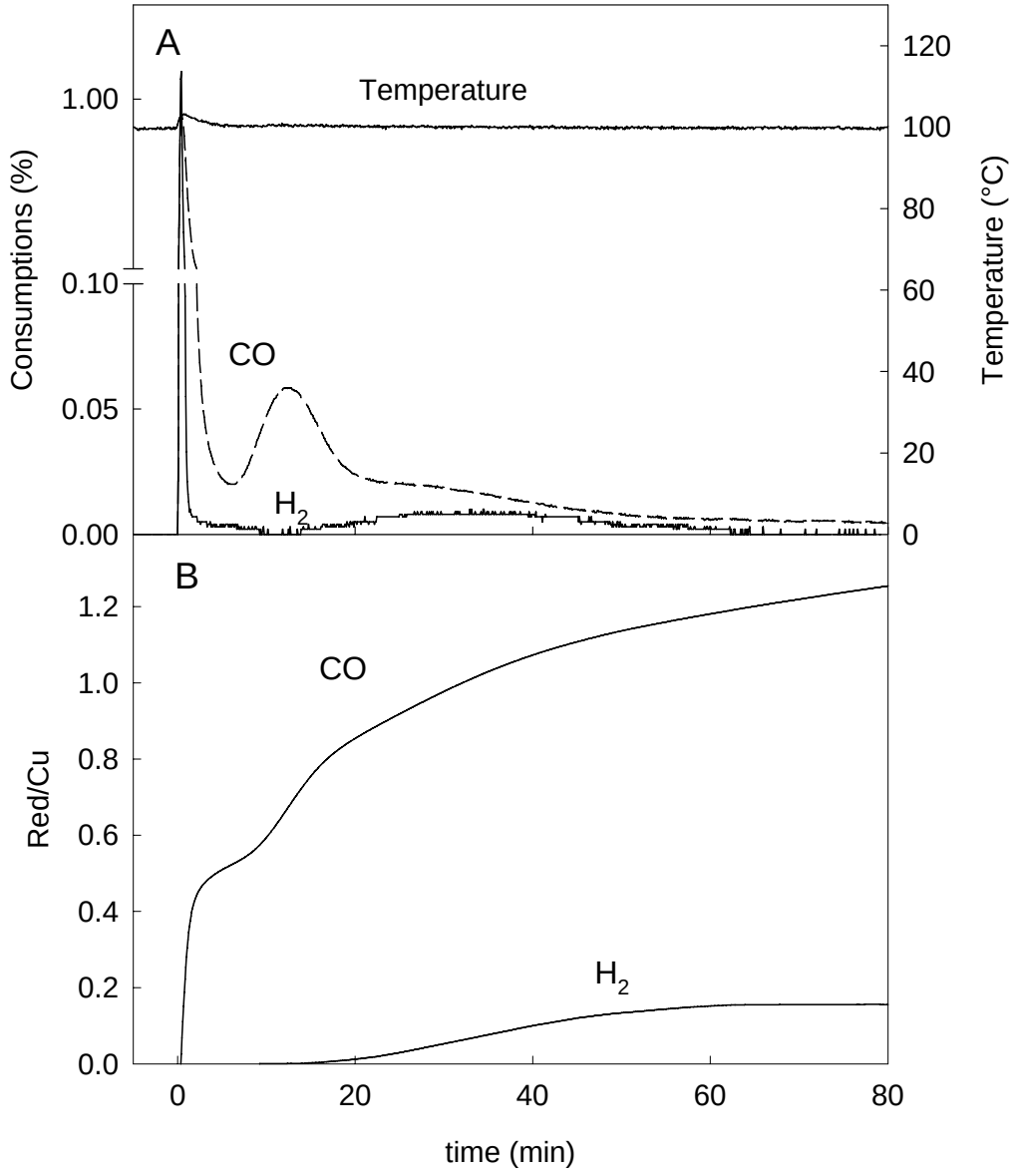

Figure 6.19: (A) CO and H_2 consumptions as a function of the time; (B) CO and H_2 integral consumption as a function of the time on 4wt% CuO/CeO_2 at 100°C. Mixture composition: 1vol% CO; 2vol% H_2; N_2 balance; τ=0.07 g*s/cm^3.

Similarly to the CO chemisorption experiments a huge CO consumption when switching the reducing mixture to the reactor has been detected. After the admission the CO profile presents a peak at about 15 minutes, which roughly extinguishes after 20minutes in correspondence of a CO/Cu ratio equal to 0.85. Roughly in correspondence of the end of the main CO peak, hydrogen uptake starts. After 100min, the overall CO/Cu ratio is 1.22 while the H_2/Cu is 0.15.

After this isothermal reduction experiment, N_2 has been fluxed on the sample and a TPD has been performed, heating the sample at 10°C/min. During this step not only CO_2 but also H_2 have been detected among desorbed gases (figure 6.20). The amount of H_2 which desorbs between 100°C and 430°C closely corresponds to the amount consumed at 100°C (H_2/Cu=0.149).

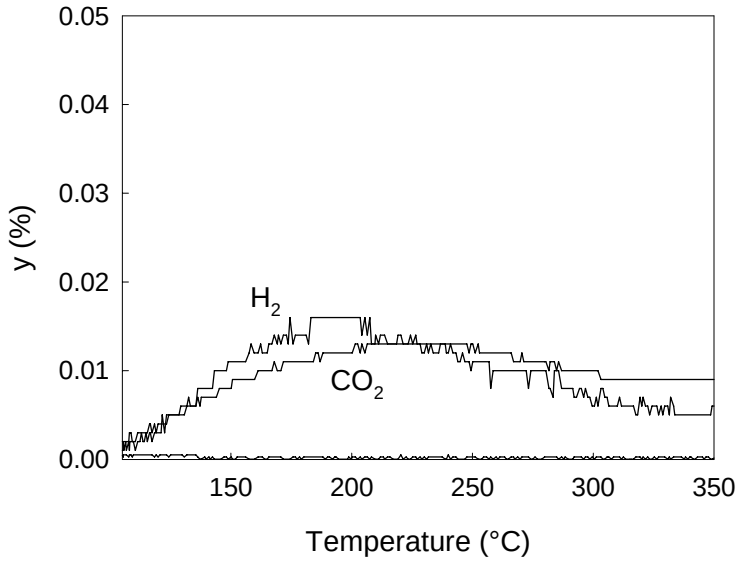

Figure 6.20: CO_2 and H_2 profiles detected during N_2 TPD performed after the CO and H_2 chemisorption at 100°C.

From this analysis it appears that at 100°C, in the contemporary presence of CO and H_2, the catalyst is reduced only by CO while H_2 adsorbs on the reduced catalyst.

A temperature programmed reduction test has been performed on the same sample contemporarily feeding CO and H_2 (fig. 6.21). Results are quite surprisingly, since the presence of H_2 does not significantly influence the CO uptake profile up to 150°C, when a H_2 consumption has been detected too. As a consequence the CO high temperature reduction peak disappears (δ peak) in the presence of H_2. For temperature higher than 190°C H_2 production has been detected, as evident from the negative H_2 consumption in the figure 6.21a. Actually, by calculating the overall H_2 uptake, a negative number is obtained meaning that at a certain point H_2 is produced in amount greater than that previously consumed.

Following the integral consumption profiles (fig.6.21b), up to a CO/Cu ratio of 0.8, no H_2 consumption is detected. When the H_2 consumption starts the CO profile consumption in the presence of H_2 is lower than in absence. Up to 200°C, H_2 starts to be produced thus the H_2 profile presents a maximum. After 70 minutes the H_2 integral profile becomes negative.

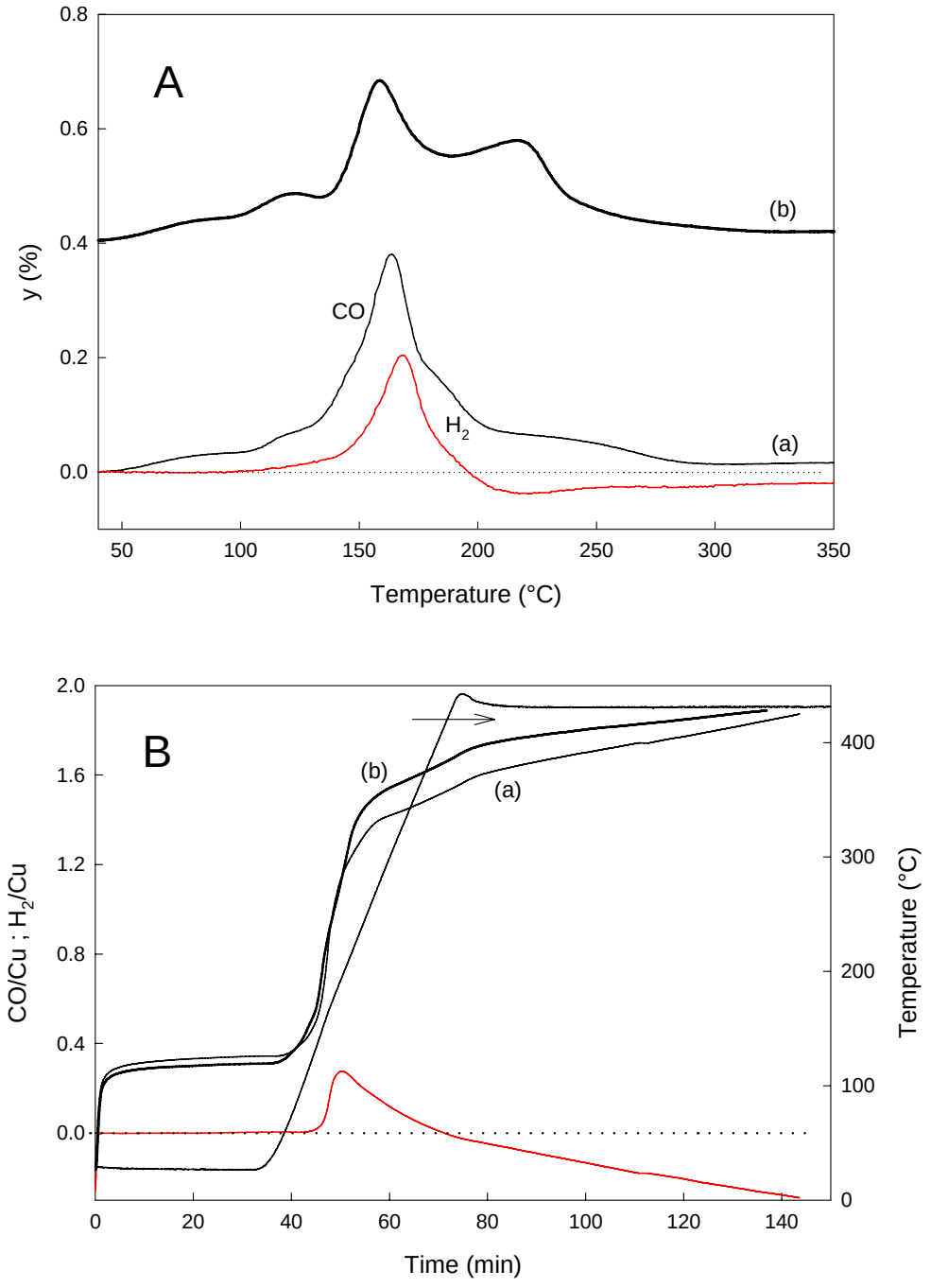

Figure 6.21:A: (a) CO (black) and H_2 (red) TPR analysis on 4 CuO/CeO_2 feeding CO and H_2 at the same time. (b) Standard CO TPR on 4 CuO/CeO_2. B: CO and hydrogen integral consumption referred to experiments (a) and (b).

If the amount of H_2 produced was equal to the amount consumed, the H_2 production could be simply related to a H_2 desorption due to a competitive adsorption with CO at higher temperature. Nevertheless the excess H_2 produced may be justified by the occurrence of the WGS reaction up to 200°C between CO fed to the reactor and the H_2O formed by the hydrogen oxidation at the expense of catalyst reduction. The latter hypothesis, or at least a combination of the two possibilities, seems to be the most plausible explanation to justify the calculated final negative H_2 uptake.

The most important information coming from this experiment is that, increasing the temperature in the contemporary presence of CO and H_2, the CO consumption profile remains unchanged up to 200°C. At this temperature, the reduction peak previously denoted as δ peak disappears, suggesting that this specie is more selective towards H_2. The δ peak was tentatively assigned to CuO big clusters, for which it was demonstrated that H_2 is a better reducing agent than CO.

In conclusion the isothermal and the transient analysis performed contemporary adding CO and H_2 confirmed that CO is a stronger reducing agent for the catalyst studied. The CO oxidation is unaffected by the presence of H_2 up to a temperature of 100°C, thus up to that temperature H_2 works as a diluent. The transient analysis revealed that the Cu species selective towards H_2 adsorption more than towards CO are those giving rise to the CO high temperature reduction peak (δ specie) tentatively assigned to CuO big clusters reduction, and confirmed the H_2 adsorption on reduced sites.

6.6 Transient analysis

The highly reductive nature of the CO-PROX mixture opens the debate about the oxidation state of catalyst under reaction conditions. This question is strictly related to the identification of the species responsible for the high selectivity to oxidize CO in an environment containing a hydrogen concentration of one order of magnitude higher than that of CO.

The catalyst is prepared by starting from copper in the oxidised state Cu^{+2}, but of course, all the investigations on the redox properties of the catalyst, the fact that the reaction mixture is strongly reducing and the evidence that the oxidation state of catalyst sites easily changes in the presence of CO and H_2 leave opened the question about the state of catalyst under reaction conditions and consequently the active and selective sites for the process.

In order to study such an aspect, we tried to follow the transformations occurring on the catalyst surface in the presence of an atmosphere representative of the reaction conditions. Specifically, we followed the transient period before the achievement of a steady-state condition by continuously monitoring the gas composition at the outlet of the reactor, after having fed a mixture composed by: 1000ppm CO; 2000ppm O_2; 2vol% H_2 diluted in N_2. The choice of such a mixture characterised by more diluted CO and H_2 concentrations than generally employed in the kinetic tests, is due to the attempt to limit the thermal effects connected to the proceeding of reaction and the necessity to slow down the transient phenomena.

Transient analysis experiments have been made after a general stabilization of the system: a quick N_2 purging flux at reaction temperature has been fed to the reactor, and subsequently the chosen pre-treatment is carried out. Finally, once steady-state is established and the transient analysis is finished, a H_2 TPR has been performed to evaluate the catalyst oxidation state under reaction conditions.

This study was performed on the 4 CuO/CeO_2 catalyst at different reaction temperatures. The temperature values chosen are those insuring a CO PROX selectivity equal (70°C) or lower (144-204°C) than 100% under the reaction consitions used.

In figure 6.22 the experiment previously described, conducted on a fresh sample at a temperature of 72°C, has been reported. It is visible that when the reaction mixture is switched to the reactor a sharp peak corresponding to reactor holdup of reactants is shown. In this phase an eventual consumption of any reactant due to adsorption or reaction is also already possible, as seen in chemisorption tests. Later on, the reactants concentrations reach a steady state condition. The amount of CO and oxygen consumed in the first 2 min is higher than that calculated for the holdup (table 6.10), indicating that something is reacting. Indeed CO_2 formation is contemporarily

measured too, although the production of carbon dioxide in the first 2 minutes is not sufficient for the carbon balance. Adsorption of carbon dioxide rather than carbon monoxide may explain this behaviour, as evidenced by studying CO TPR and CO TPD tests.

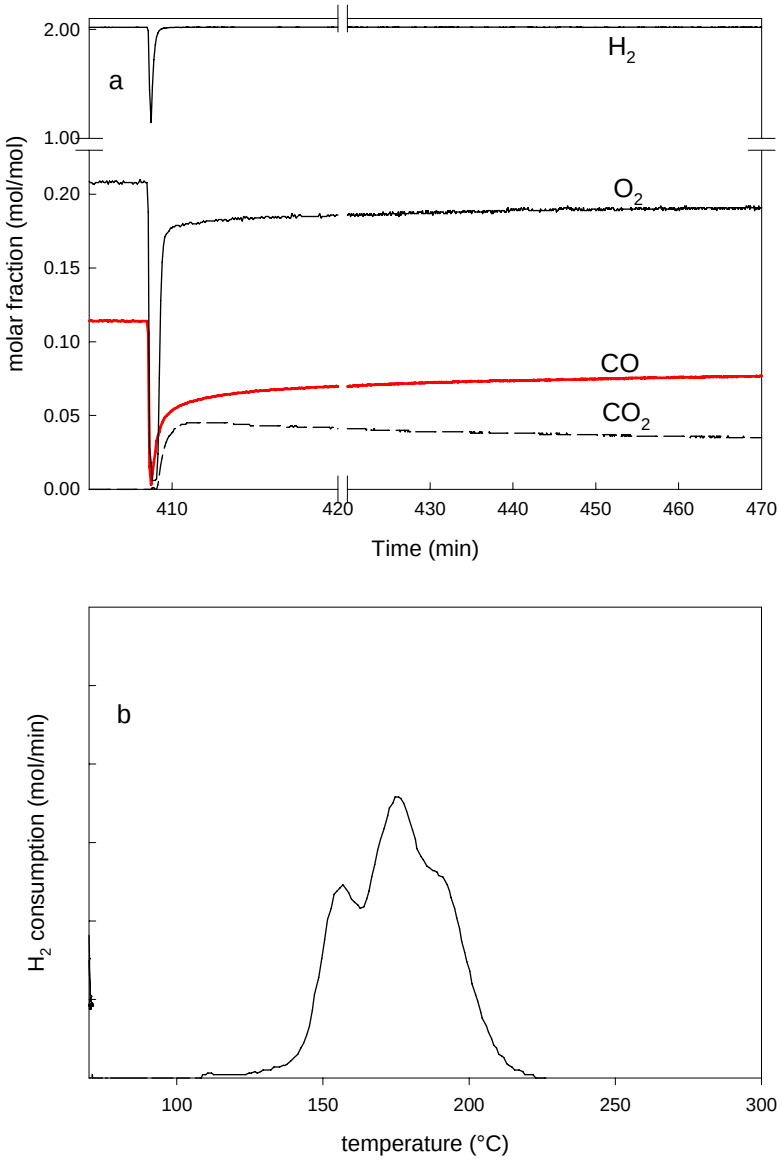

Figure 6.22: Transient analysis at 72°C over 4 CuO/CeO_2: a) evolution of outlet gas composition; b) subsequent TPR of H_2. Catalyst pre-oxidised and washed with N_2 at the reaction temperature. Reaction mixture: 1000ppm CO; 2000ppm O_2; 2vol% H_2 diluted in N_2.

The oxygen consumed in the first two minutes corresponds to that necessary to oxidize CO. The H_2 concentration comes back to the inlet value just after the holdup consumption, the amount of H_2 uptake corresponds precisely to the holdup revealing that no hydrogen has reacted and confirms that at this temperature CO PROX selectivity is about 100%.

The H_2 TPR performed after the stabilisation of the steady-state gives rise to an H_2/Cu ratio of 1.49 that is an indirect measurement of the reduction degree of the catalyst under reaction conditions.

This value is exactly the same obtained over the standard TPR test carried out over the pre-oxidised catalyst (see Tab. 6.1) and hence would reveal that under reaction conditions and 70°C, the catalyst is in the full oxidized state. It is interesting to note that, despite of the different experimental conditions (contact time) the TPR profile is similar to that performed on a fresh, completely oxidized sample (see previous paragraphs).
The same results are obtained on the sample stabilized in a reducing atmosphere and subsequently reoxidized. In this case a CO conversion of 1% higher is obtained (Tab. 6.10).

Table 6.10: Transient experiment performed on reduced (R) or oxidised (O) 4 CuO/CeO_2 catalyst. Steady state results and H_2/Cu ratio obtained in the subsequent H_2TPR.

Temperature (°C)	*Oxidation state*	*CO conversion (%)*	*H_2 conversion (%)*	*Selectivity (%)*	*H_2/Cu TPR*
72	Fresh	33.2	0	100	1.49
72	O	34	0	100	1.47
70	O	27	0	100	
70	R	17	0	100	0.85
104	O	69	0	100	1.47
144	O	90	0.18	96.5	1.52
144	R	88	0.29	94.6	1.10
204	O	98	3.35	56.9	1.18
204	R	98	3.54	54.6	1.00

In figure 6.23 the transient experiment at 70°C performed on a sample completely reduced in H_2 at 430°C for 1h is reported. When the reaction mixture is introduced in the reactor, the concentrations of the reacting species follows different trends. The oxygen presents a huge peak, after which the concentration goes to a steady state. The CO shows initially a sharp peak whose area corresponds to that necessary to fill the reactor, and subsequently a new CO consumption peak reaching a steady state condition after about 7min from the start of the experiment. The CO_2 production starts in correspondence of the second peak of CO consumption.
The TPR analysis performed after the test gives a H_2/Cu ratio of 0.85, indicating that the catalyst under the reaction conditions has been only partially reoxidized. Indeed the amount of O_2 consumed in the first 2min of the reaction is much higher than that necessary to produce CO_2. The excess oxygen consumed in the first minutes corresponds to 282μmol/g, while 227 μmol/g have been calculated for a catalyst reoxidation corresponding to a H_2/Cu equal to 0.85. The gap in the measured oxygen concentrations could be explained by the low sensitivity of the paramagnetic detector used for the O_2 analysis.

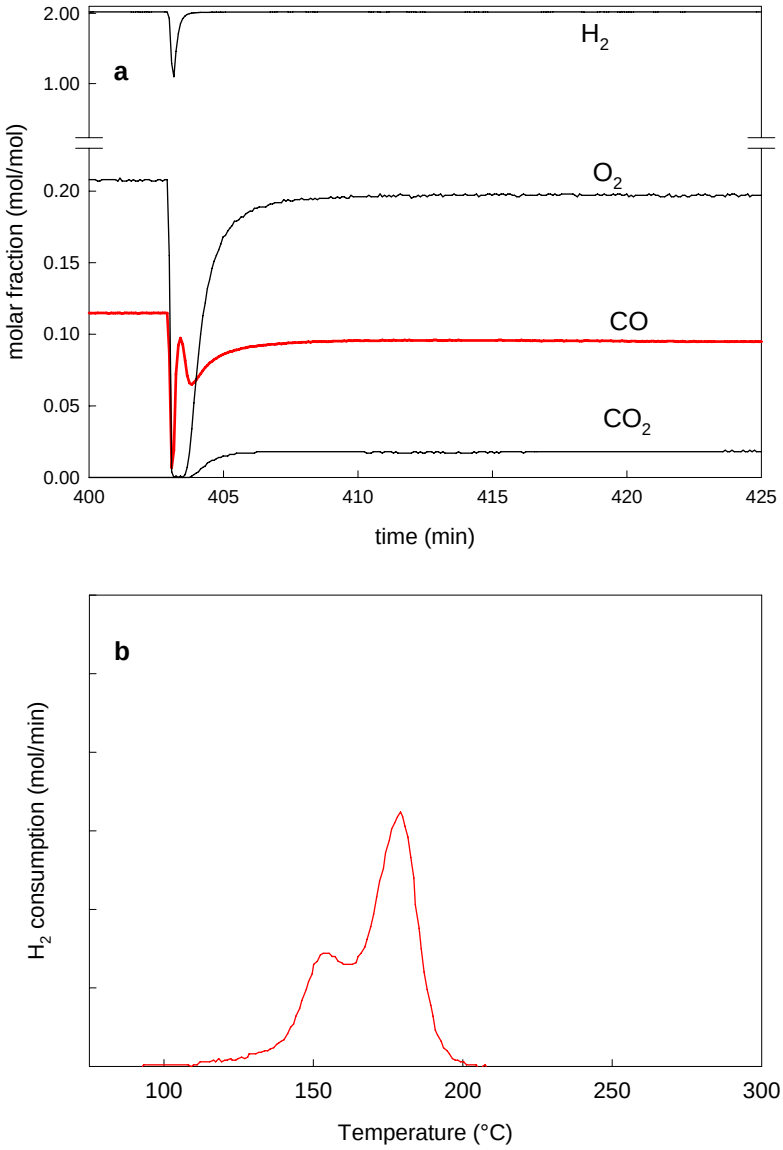

Figure 6.23: Transient analysis at 72°C over 4 CuO/CeO_2: a) evolution of outlet gas composition; b) subsequent TPR of H_2. Catalyst pre-treated in H_2 at 430°C, cooled down in N_2 to reaction temperature. Reaction mixture: 1000ppm CO; 1000ppm O_2; 2vol% H_2 diluted in N_2.

Comparing the TPR profile with those obtained in our previous studies it seems possible to qualitatively and quantitatively associate this TPR with that obtained for a sample completely reduced and reoxidized at room temperature. In that case a $H_2/Cu = 0.75$ has been calculated. Here the entity of the reoxidiation is a little higher because of the different temperature at which the reoxidation takes place (70°C vs RT).

At the steady state the CO conversion on a prereduced catalyst is lower than on the oxidised one (17 vs 27%).

The CO profile and the quantitative analysis seems to suggest that in this temperature region, in which the selectivity is 100%, the catalyst is active only in an oxidized state. Indeed, despite of the previous experiment in which CO adsorbed instantaneously on the catalyst producing CO_2, here the CO adsorption and the subsequent CO_2 production seems to be slowed down by the necessity of a previous partial reoxidation of the sample. Moreover, a partial reoxidation of the sample does not give back the same CO conversion, calculated on a completely oxidated sample.

Table 6.10 shows that at 144°C the CO conversion is 90% and the O_2 selectivity is 96.5% on the oxidised sample. The subsequent H_2 TPR reveals that also at that temperature the catalyst is in a completely oxidated state (H_2/Cu = 1.52).

At the same temperature, the prereduced sample shows a little smaller CO conversion (88%) in agreement with the results obtained at 70°C. Moreover, at 144°C the H_2 conversion is higher on the prereduced sample than on the oxidated one (0.3 vs 0.2), thus the O_2 selectivity is smaller (96.5 vs 94.5). Following the hydrogen profile in the first minutes after the reaction mixture injection it is possible to see that, the H_2 concentration takes more time to reach a steady state than in the case of the oxidised sample. In figure 6.24 this transient study is reported in term of absolute amount of H_2 consumed after the injection. The shape of the curve referred to the prereduced sample is lower than that of the oxidised one and at the steady state more micromols of H_2 are consumed on the prereduced sample.

This result seems to suggest that more H_2 is converted when the catalyst is reduced.

The H_2/Cu ratio estimated by the TPR performed after the reaction at 144°C, indicates that the prereduced sample is not yet completely reoxidized after the reaction (H_2/Cu= 1.1).

At 204°C a completely equal CO conversion (98%) and H_2 conversion a bit higher in the case of reduced sample (3.54 vs 3.35%) have been measured. A similar H_2/Cu ratio have been estimated by the TPR (H_2/Cu=1.2 vs 1.0). On both samples the H_2/Cu ratio is lower than that corresponding to the total oxidated sample (H_2/Cu= 1.47), thus suggesting that in this temperature range the catalyst is partially reduced under reaction conditions.

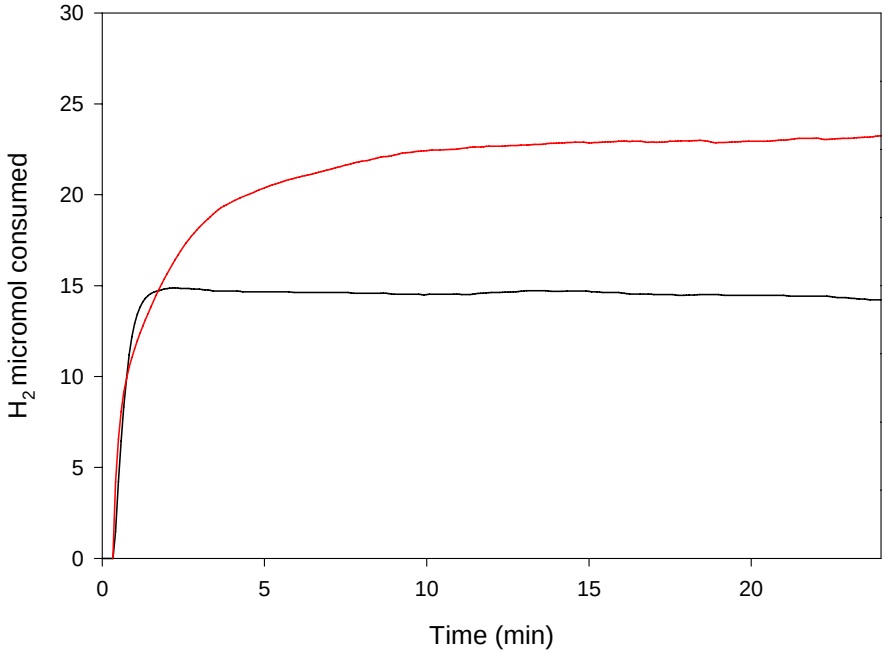

Figure 6.24: H_2 evolution as a function of time after the injection on a oxidized sample (black) or reduced one (red). Transient experiment performed on pre-reduced 4 CuO/CeO_2 at 70°C.

In summary, the transient analysis suggests that under reaction conditions, in the regions of 100% selectivity, the copper is in the fully oxidated state even if the atmosphere is highly reducing. This result is suggested by the H_2/Cu ratio calculated on the oxidised sample after the reaction. Moreover, the oxidation state +2 is kept up to a temperature ≤ 150°C.

When the catalyst is partially reduced a lower CO conversion and lower O_2 selectivity are calculated. Thus the CO oxidation reaction is favoured when all the catalyst is in the oxidation state +2, while a different oxidation state favours the H_2 conversion.

Summarizing, the transient experiment added crucial informations on the comprehension of the CO-PROX reaction: 1) the copper species active towards CO oxidation must be in oxidated state, 2) the catalyst keeps a completely oxidated state up to 150°C despite of the reducing character of the reacting mixture, 3) stabilization of reduced species on the catalyst favours hydrogen oxidation kinetics.

CO TPD experiments performed on samples with different reduction levels, suggested that CO preferentially adsorbs on a completely oxidized catalyst thus anticipating and confirming the results of the transient experiments.

Moreover the fact that the catalyst maintains its completely oxidated state up to 150°C is a surprising result but it is easily explainable on the basis of the knowledge acquired in the redox study which showed that hydrogen works as a diluent up to a temperature of at least 100°C. From

this observation results that the reacting mixture has an oxidant character and not a reducing one as expected, because only CO acts as a reducing agent, while O_2 has a concentration at least the double of the stoichiometric one for the CO oxidation reaction. Moreover the redox study showed that the species more active towards the CO oxidation are also easily re-oxidized at very low temperature, thus confirming that the re-oxidation rate is enough high to keep the completely oxidized state of the catalyst even for temperature as high as 150°C.

Nevertheless at higher temperatures the re-oxidation rate competes with the hydrogen oxidation rate, which probably occurs on reduced sites as suggested by the redox study which demonstrate that H_2 does not adsorb on a completely oxidized sample, while adsorbs on a partially reduced one. Moreover at temperatures higher than 150°C, the redox study suggests that CuO big clusters participate to the reduction preferentially interacting with H_2 thus decreasing the overall selectivity of the process.

7 Concluding Remarks

Copper/ceria and copper/ceria-zirconia catalysts have been studied for the reaction of CO preferential oxidation in a gas containing large quantities of hydrogen. These systems were selected on the basis of a bibliographic research during the first year of the PhD, as alternative to the much more expensive noble metals and also as more promising systems.

The first part of this work has been devoted to the determination of the optimal catalyst composition as concerns both the choice of the support and the best copper loading. Comparison between ceria and ceria-zirconia supports suggested that the enhanced oxygen mobility induced by zirconium substitution into ceria lattice does not lead to increased activity but to a worse selectivity related to the stronger activation of H_2 oxidation.

Catalysts supported on ceria have a higher intrinsic tendency to oxidize CO rather than hydrogen, in comparison to ceria-zirconia systems due to the reduced overlapping of the temperature range required for H_2 and CO oxidation and have been deeper studied in the second part of the thesis.

From the analysis of catalysts with different CuO coverage an optimal copper loading between 3.5 and 4.5 wt% CuO, corresponding to the theroretical monolayer, has been found for copper/ceria catalysts, since formation of CuO aggregates for higher copper content depressing both activity and selectivity. Moreover calcinations temperature should never exceeds 600°C in order to avoid a relevant reduction of surface area due to catalyst sintering.

In term of activity the catalyst is comparable to commercially available Pt based systems which works at higher temperature, but CuO/CeO_2 catalyst performances are much higher in term of selectivity, considering that Pt based catalyst shows a constant selectivity, between 40-25%, in all the range of temperature explored, whilst CuO/CeO_2 provides 100% in the temperature range 50-110°C corresponding to 50% CO conversion and 60-80% in the range around 100% CO conversion (110-160°C).

The reaction kinetics has been investigated on a catalyst sample whose composition corresponds to the best formulation. The first efforts were devoted to the investigation of the origin of a maximum of CO conversion with temperature which limits the conversion of CO that can be achieved. The different activation energy of the reactions of CO and H_2 oxidation explains the presence of a maximum. At low temperature, only CO oxidation is activated, because the energetic barrier to the oxidation of H_2 is too high, while at higher temperature the process selectivity tends to decrease due to the activation of H_2 molecule. **T**wo power law rate equations for the two oxidation reactions have been use to model the process kinetics in a first approximation. The estimated values of the activation energy for the two reactions in competition, lower for the CO oxidation reaction and

higher for the H_2 oxidation allow the correct prediction of the presence of a maximum of CO conversion as a function of the temperature. The occurrence of H_2 oxidation, competing with CO oxidation, leads to oxygen consumption thus limiting the CO conversion. On the other hand the occurrence of reverse WGS reaction, that has been generally proposed to explain the presence of the maximum, has been experimentally excluded up to 250°C.

In agreement with such findings, it has been evidenced that the CO conversion is a unique function of the reaction temperature and does not depend on CO/H_2 ratio for a wide range of concentration. Actually, because the selectivity of the process can be considered depending on the lower activation energy of the oxidation of CO, the CO/H_2 ratio plays a very secondary role and, remarkably, CO conversion can be enhanced by increasing the contact time without significantly affecting the selectivity. This means that at higher contact time ($0.09 g \cdot s/cm^3$) and relatively low temperatures (132°C), very high abatement levels of CO (only 25 ppm residual) can be achieved in correspondence of a very high selectivity (80%), with a consequent increasing interest in the use of CuO/CeO_2 catalyst as an effective catalyst for CO-PROX.

Requirements of potential catalysts for CO-PROX include not only the high selectivity and activity towards the CO oxidation reaction but also a good tolerance to reformate species such as CO_2 and H_2O eventually present in the gas to be treated. Experimental tests in the presence of reformate species showed a decrease of the activity of copper-ceria catalysts in the low temperature region, and a substantial invariability of performances at higher temperatures. In particular, the CO conversion curve shifts to higher temperatures but is still in the range of interest for the CO-PROX process (80-200°C). On the other side, the selectivity is unaffected by the presence of reformate species, remaining a unique function of the temperature. Thus the performances of the catalyst can still remain high by working at both higher temperatures and contact time.

The negative effect of H_2O addition on the catalyst activity may be easily explained by a pore blocking effect while the effect of CO_2 addition required a more detailed characterization study, but is certainly due to the strong adsorption of carbon dioxide on catalyst sites.

Oxygen partial pressure shows a negligible effect on the reaction kinetics and process selectivity, at least in the range of value of interest for CO PROX (O_2 stoichiometrically in excess with respect to CO oxidation). The slight dependence of the selectivity on the oxygen concentration suggested that both CO and H_2 oxidation kinetics are weakly affected by O_2 partial pressure. This result was confirmed by the power law kinetic model which predicted a zero dependence for the CO oxidation and an apparent reaction order 0.2 for the H_2 oxidation. Thus the catalytic system maintains its high selectivity constant under more oxidant conditions too, because the kinetics of both oxidations show

a very weak dependence on the oxygen concentration. This result suggests that on these systems the re-oxidation rate does not represent the limiting step for any of the two reactions in competition.

The dependence of CO oxidation kinetics on the concentration of carbon monoxide showed a surprising inversion in the CO apparent reaction order, depending on the temperature range of interest. The apparent reaction order is lower than one (namely 0.7) at low temperature (in the region in which a 100% selectivity towards CO oxidation is found) and significantly higher than unity (about 1.3) at higher temperatures.

Mechanistic rate expressions have been tested under isothermal conditions for modelling the effect of CO, O_2, CO_2 and contact time. In these expressions the negative effect of the CO_2 addition has been considered by introducing a term that expresses the competitive adsorption of carbon dioxide on the active sites.

The rate expressions which are able to correctly predict the experimental effects reported are all characterised by fractional expressions with constant exponent for all species (one for CO and 0.5 for O_2) and involve the reaction between adsorbed oxygen and adsorbed CO (LH mechanism) or gaseous CO (Eley-Rideal).

The redox properties of CuO/CeO_2 catalysts have been studied in order to better clarify the reaction mechanism and identify the active species responsible for the high activity and selectivity.

The results of reduction studies carried out with the use of H_2 as probe molecule, suggested a significant partecipation of the surface ceria to the overall reduction of the sample even in the very low temperature region, where it is known that pure ceria is not reducible. The increased reducibility of both copper oxide and ceria in the supported CuO/CeO_2 catalyst is an effect of the presence of “strong metal support interactions”, occurring between ceria and the metal-phase and well documented for noble metals but still unclear when the active phase is a transition metal. The reduction of the ceria at low temperature can be activated even by a limited number of copper atoms (CuO< 1.6wt%) while excess copper forms CuO clusters, which do not contribute to increase the ceria reducibility.

An increase of activity observed after a first cycle of a redox treatment has been associated to the increased dispersion of copper which may also improve the degree of interaction between metal and support. Generally an high degree of interaction between the two phases has been reached by preparation methods like co-precipitation or sol-gel which favour the interaction between the two precursors during the preparation steps. Nevertheless our experimental results suggest that the other possibility to increase the copper dispersion is by a redox cycle, and thus it could be virtually possible to obtain by simple preparation methods a catalyst so active as those obtained by more

complex procedure, which generally involve the use of more poisoned or more expensive salt precursors.

The study of the redox properties in the presence of a single reducing agent let to recognize a different sequence in the reduction steps occurring on the catalyst depending on the reducing agent used: CO or H_2. In the presence of H_2, the catalyst reduction takes place for temperatures higher than 100°C and starts from well dispersed CuO microcrystals, extending later to surface ceria interacting with copper and then to bulk CuO.

On the contrary, in the presence of CO the reduction starts already at room temperature and directly from the borderline regions of the CuO micro-crystals, while subsequently the reduction proceeds involving the reduction of the CuO micro-crystals and surface ceria. The catalytic sites which are reduced by CO at room temperature, are also re-oxidized by a treatment in air at the same temperature. On the contrary, it has been demonstrated that such catalytic species are resistant towards the reduction with H_2 up to about 150°C. These active centers have been identified as copper-ceria at the borderline regions and due to their redox properties are clearly involved in the CO oxidation at low temperature and are also very selective towards the reduction in CO more than H_2. In particular, the presence of these species may explain the 100% selectivity showed by the catalyst for temperature lower than 100°C.

Reduction by CO prevails also when CO and H_2 are contemporary present, the latter giving rise to a small adsorption only when the catalyst is enough reduced, however, at higher temperature the reduced CuO clusters preferentially reacts with H_2 rather than with CO. Thus in the contemporary presence of CO and H_2, the latter works as a diluent up to a temperature of at least 120°C, while CuO clusters have been identified as the only species selective for the reduction in H_2 more than CO.

These observations are in good agreement with the results of kinetic analysis showing that the CuO/CeO_2 selectivity is a unique function of the temperature and also explaining the lower selectivity of catalysts with a CuO loading exceeding the monolayer coverage, which generates larger concentration of CuO aggregates.

Transient reaction experiments have been performed with the purpose of coupling the observation of the kinetic study with the knowledge acquired in the investigation on the redox properties.

Such experiments showed that the oxidised catalyst exhibits always higher and faster performances than the reduced one. The reduced catalyst becomes active towards the CO oxidation only after an initial transient corresponding to the partial reoxidation of the sample (larger O_2 consumption than CO oxidation stoichiometry is observed before stready-state). Therefore, it can be concluded that the active specie towards CO oxidation at low temperature is Cu^{2+}, or more in detail, assuming that

the reaction takes place at the border line regions, Cu^{2+}-O^{2-}-Ce^{4+}. The easy reoxidation revealed for this species is in agreement with the completely oxidated state detected after reaction at low temperature and suggests that the catalyst is easily reoxidated by O_2 from gas phase according to a Langmuir-Hinshelwood or Eley-Rideal mechanism. It has been demonstrated that the active site for the CO oxidation are easily re-oxidized already at room temperature thus explaining the observed independence of the kinetics on the oxygen concentration.

Increasing the temperature the hydrogen oxidation reaction starts, promoted by the partial reduction of the sample which induces H_2 adsorption. Thus, it can be assumed that at high temperature the hydrogen oxidation occurs on pre-reduced sites. At high temperature this reaction proceeds faster than the reoxidation of copper sites thus stabilizing reduced sites and decreasing the selectivity of the process.

At high temperature, bulk CuO is active towards oxidation reactions too. Such specie catalyses H_2 oxidation, thus further decreasing the overall selectivity of the process.

In conclusion, in this thesis the catalytic behaviour of the different copper species present on a CuO/CeO_2 monolayer catalyst has been deeply described through a comparative study of redox and catalytic properties of the sample. Active species have been determined defining their role in the selectivity of the process. From the knowledge acquired it could be possible to optimize the catalyst performances by increasing the concentration of the species identified as the more active and selective towards CO oxidation, which are interacting copper-ceria species, in a completely oxidized form. Moreover, it could be avoided the formation of CuO clusters which, on the contrary, are selective towards H_2 oxidation. These goals could be achieved by using a copper concentration close to the monolayer and by using preparation methods in which the degree of interaction between the support and the metal may be controlled and maximized.

The observation that the selectivity of the catalyst is a unique function of the temperature for a wide range of concentration of the reactant, suggests the best operative conditions in which a CO-PROX reactor may work, which are, low temperature and relatively high contact time.

In order to propose the use of CuO/CeO_2 catalysts for practical applications, preparation of these samples in structured forms is required to avoid pressure drops deriving from the different flow rate regimes occurring in an automobile. Therefore, the possibility to depose CuO/CeO_2 catalyst onto a monolite should be considered in the near future paying attention to the stability of the material and to the preservation of catalyst properties in this new form. If these properties are only slightly affected, the high contact time which may be reached in a monolite structure will let to operate at low temperature, thus reaching high conversion with a low sacrifice of H_2, and thus increasing the

overall efficiency of the fuel processor in comparison to those systems which use Pt based catalysts for the CO-PROX unit.

References

1. Akiyama H., Moise C., Yamanaka T., Jacobi K., Matsushima T., (1997) Selective modification of reaction sites for carbon monoxide oxidation on a platinum (113) surface, Chemical Physics Letters 272, 219-224
2. Amphlett J.C., Mann R.F., Peppley B.A:, (1996), On board hydrogen purification for steam reformation/PEM fuel cell vehicle power plants. International Journal of Hydrogen Energy, 21 (8), 673-678
3. Armor J.N., (1999) The multiple roles for catalysis in the production of H_2, Applied Catalysis A: General 176, 159-176
4. Avgouropoulos G., Ioannides T., Matralis H., Batista J., Hocevar S., (2001) CuO-CeO_2 mixed oxide catalysts for the selective oxidation of carbon monoxide in excess hydrogen, Catalysis Letters, 73, 33-40
5. Avgouropoulos G., Ioannides T., Papadopoilou Ch., Batista J., Hocevar S., Matralis H.K., (2002) A comparative study of Pt/γ-Al_2O_3, Au/α-Fe_2O_3 and CuO/CeO_2 catalysts for the selective oxidation od carbon monoxide in excess hydrogen, Catalysis Today 75, 157-167
6. Avgouropoulos G., Ioannides T., (2003) , Selective CO oxidation over CuO-CeO_2 catalysts prepared via urea-nitrate combustion method, Applied Catalysis, A, vol. 244, no.1, p. 155-167
7. Bera P., Aruna S.T., Patil K.C., Hegde M.S., (1999), Studies on Cu/CeO_2: A New NO Reduction Catalyst, Journal of Catalysis, 186, 36
8. Bernal S., Calvino J.J., Caqui M.A., Gatica J.M., Larese C., Perez Omil J.A., Pintado J.M., (1999) Some recent results on metal/support interaction effects in NM/CeO2 (NM:noble metal) catalysts, Catalysis Today 50, 175-206.
9. Bethke G.K., Kung H.H., (2000) Selective CO oxidation in a hydrogen-rich stream over Au/□-Al_2O_3 catalysts,, Applied Catalysis A: General 194-195, 43-53
10. Bielanski A., HAber J., (1991) Oxygen in catalysis, Dekker, New York

11. Boaro M., Vicario M., de Leitenburg C., Dolcetti G., Trovarelli A., (2000) The Dynamics of Oxygen storage in ceria-zirconia model catalysts measured by CO oxidation under stationary and cycling feedstream compositions, Journal of Catalysis, 193, 338-347

12. Boaro M., Trovarelli A., Hwang J.H., Mason T.O., (2002) Electrical and oxygen storage/release properties of nanocrystalline ceria-zirconia solid solutions, solid State Ionics 147, 85-95

13. Boaro M., Vicario M., de Leitenburg C., Dolcetti G., Trovarelli A., (2003) The use of temperature-programmed and dymanic/transient methods in catalysis: Characterization of ceria-based, model three-way catalysts, Catalysis Today 77, 407-417

14. Bryesse M., Guenin M., Claudel B., Latreille H. and Veron J., (1972) Catalysis of carbon monoxide oxidation by cerium dioxide. Correlations between catalytic activity and electrical conductivity, Journal of Catalysis 27 (2), 275

15. Choi Y., Stenger H.G., (2004), Kinetics, simulation and insights for CO selective oxidation in fuel cell application, Journal of Power source 129, 246-254.

16. Claudel B.M., and Brau G.G., (1969), Catalytic properties of nonstoichiometric uranium-thorium mixed oxides in carbon monoxide oxidation, Journal of Catalysis 14, 322

17. Dudfield C.D., Chen R., Adcock P.L, (2000a) Evaluation and modelling of a CO selective oxidation reactor for solid polymer fuel cell automotive applications, Journal of power Sources 85, 237-244

18. Dudfield C.D., Chen R., Adcock P.L., (2000b) A compact CO selective oxidation reactor for solid polymer fuel cell powered vehicle application, Journal of power Sources 86, 214-222

19. Fernandez-Garcia M., Rebollo E.G., Guerrero Ruiz A., Conesa J.C., Conesa J.C., and Soria J., (1997), Influence of ceria on the dispersion and reduction/oxidation behaviour of alumina-supported copper catalysts, Journal of catalysis 172, 146-159.

20. Ford R.R., (1970) Carbon Monoxide adsorption on the transition metals, Advanced in catalysis 21, 51-150.

21. Fuel cell Handbook (fifth Edition), (2000), http://www.fuelcells.org/fchandbook.pdf

22. Fuller, M. J.; Warwick, M. E., (1974) Catalytic oxidation of carbon monoxide on tin (IV) oxide-copper (II) oxide gels. Journal of Catalysis 34(3), 445-53.

23. Golodets G.I., (1983), Heterogeneous catalytic reactions involving molecular oxygen, Studies in surface science and catalysis 15, 878

24. Grisel R.J., Nieuwenhuys B.E., (2001) Selective oxidation of CO, over Supported Au catalysts, Journal of Catalysis, 199, 48-59.

25. Haruta M., Tsubota S., Kobayashi T., Kageyama H., Genet M., Delmon B., (1993), Low-temperature Oxidation of CO over Gold supported on TiO_2, α-Fe_2O_3, and Co_3O_4, Journal of Catalysis 144, 175-192

26. Hocevar S., Batista j., Levec J.,(1999)Wet oxidation of phenol on $Ce_{1-x}Cu_xO_{2-\delta}$ catalyst, J. Catalysis , vol. 184, p. 39-48.

27. Hocevar S., Krasovec U.O., Orel B., Arico A., Lim H., (2000) CWO of phenol on two differently prepared CuO-CeO_2 catalysts, Applied Catalysis B 28, 113-125.

28. Hori C.E., Permana H., Ng K.Y.S., Brenner A., More K., Rahmoeller K.M. Belton D., (1998) Thermal stability of oxygen storage properties in a mixed CeO_2-ZrO_2 system, Applied Catalysis: Environmental 16, 105-117

29. Hougen O.A., and Watson K.M., (1943), Solid catalysis and reaction rates, Industrial and engineering chemistry, 35/5, 529-541

30. Iragashi H., Uchida H., Suzuki M., Sasaki Y., Watambe M., (1997) Removal of carbon monoxide from hydrogen-rich fuels by selective oxidation over platinum catalyst supported on zeolite, Applied Catalysis A: General 159, 159-169

31. Janson J., Palmqvist A.E.C., Fridell E., Skoglundh M., Osterlund L., Thormahlen P., Langer V., (2000) On the catalytic activity of Co_3O_4 in Low-Temperature CO oxidation, Journal of catalysis 211, 387-397.

32. Jernigan G.G., and Somorjai, (1994), Carbon monoxide oxidation over three different oxidation states of copper: metallic copper, copper (I) oxide, and copper (II) oxide-A surface science and kinetic study, Journal of catalysis 147, 567-577.

33. Kahlich M.J., Gasteiger H.A. and Behm R., (1997) Kineticts of Selective CO Oxidation in H_2-Rich gas on Pt/Al_2O_3, Journal of catalysis 171, 93-105

34. Kahlich M.J., Gasteiger H.A. and Behm R, (1999) Kinetics of the Selective Low-Temperature Oxidation of CO in H_2-Rich Gas over Au/γ-Fe_2O_3, Journal of Catalysis 182, 430-440.

35. Kim D. H., LimM. S., (2002), Kinetics of selective CO oxidation in hydrogen-rich mixtures on Pt/alumina catalysts, Applied Catalysis A 224, 27-38.

36. Korotkikh O., Farrauto R., (2000) Selective catalytic oxidation of CO in H_2: fuel cell applications, Catalysis Today 62, 249-254

37. Kozlov A., Kim D.H., Yezerets A., Andersen P., Kung H., Kung M., (2002) Effect of preparation method and Redox treatment on the reducibility and structure of supported ceria-zirconia mixed oxide, Journal of catalysis 209 (2), 417-426.

38. Kundakovic L., Stephanopoulos M., (1998) Reduction characteristics of copper oxide in cerium and zirconium oxide systems, Applied Catalysis A; 171, 13-29

39. Kung M.C., Kung H.H., IR Studies of NH_3, (1985) Pyridine, CO, and NO Adsorbed on transition Metal Oxides, Catalysis Review, 27(3), 425-460.

40. Lamonier C., Ponchel A., D'Huysser A., et al.. (1999) Studies of cerium-metal-oxygen-hydrogen-system, Catalysis Today, 50, 247

41. Lee S.H., Han J., Lee K.Y., (2002) Development of 10-kWe preferential oxidation system for fuel cell vehicles, Journal of power sources 109, 394-402

42. Levenspiel O., (1999) Chemical Reaction Engineering, Wiley , New York

43. Lin H.K., Wang C.B., Chiu H.-C, Chien S.H., (2003) In situ FTIR study of cobalt oxides fort the oxidation of carbon monoxide, Catalysis Letters 86, 1-3.

44. Liu K., Korotkikh O., Farrauto R., (2002) Selective catalytic oxidation of CO in H_2: Structural study of Fe oxide-promoted Pt/alumina catalyst, Applied Catalysis A: General 226, 293-303

45. Liu W., Stephanopoulos M., (1995a) Total oxidation of carbon monoxide and methane over transition metal-fluorite oxide composite catalysts I, Journal of catalysis 153, 304-316

46. Liu W., Stephanopoulos M., (1995b) Total oxidation of carbon monoxide and methane over transition metal-fluorite oxide composite catalysts II, Journal of catalysis 153, 317-332

47. Liu W., Flytzani-Stephanopoulos, (1996), Transition metal-promoted oxidation catalysis by fluorite oxides: A study of CO oxidation over Cu-CeO_2, The Chemical Engineering Journal 64, 283-294

48. Luo M.F., Zhong Y.J., Yuan X.X., Zheng X. M., (1997), TPR, and TPD studies of CuO/CeO2 catalysts for low temperature CO oxidation, Applied Catalysis A: General 162, 121-131

49. Ma L., Luo M.F., Chen S., 2003, Redox behaviour and catalytic properties of $CuO/Ce_{0.8}Zr_{0.2}$ catalysts, 242, 151-159

50. Manasilp A., Gulari E., (2002) Selective CO oxidation over Pt/alumina catalysts for fuel cell applications, Applied Catalysis B: Environmental 37, 17-25

51. Marino F., Descorme C., Duprez D., (2004), Noble metal catalysts for the preferential oxidation of carbon monoxide in the presence of hydrogen (PROX), 54, 59-66

52. Martinez-Arias A., Gomez Rebollo E., Guerrero Ruiz A., Conesa J.C., andSoria J., (1997) Influence of ceria on thee dispersion and reduction/oxidation behaviour of alumina-supported copper catalysts, Journal of catalysis 172, 146-159.

53. Martinez-Arias A., Fernandez-Garcia M., Soria G. J., and Conesa J. C., (1999), Spectroscopic study of a Cu/CeO2 catalyst subjected to Redox treatments in carbon monoxide and oxygen, J. Catalysis, vol. 182, p. 367-377.

54. Martinez-Arias A., Fernandez-Garcia M., Galvez O., (2000), Comparative Study on Redox Properties and Catalytic Behaviour for CO oxidation of CuO/CeO_2 and $CuO/ZrCeO_4$ catalysts, Journal of Catalysis 195, 207-216

55. Martinez-Arias A., Fernandez-Garcia M., Hungria A.B., et al. (2003), Redox interplay at copper oxide-$(Ce, Zr)O_x$ interfaces: influence of the presence of NO on the catalytic activity for CO oxidation over $CuO/CeZrO_4$, Journal of Catalysis 214, 261-272.

56. Martinez-Arias A., Hungria A.B., Fernandez-Garcia M., Conesa J. C., and Munuera G., (2004), Interfacial Redox Processes under CO/O_2 in a nanoceria-supported copper oxide catalyst, Journal of Physical Chemistry B, , 108, 1783-17991

57. Nicholls D., (1990) Comprehensive Inorganic Chemistry, Pergamon Press, Oxford, cap. 41, 1053-1107,

58. Oh S.H. and Sinkevitch M.R., (1993) Carbon Monoxide Removal from Hydrogen-Rich Fuel Cell Feerstreams by Selective Catalytic Oxidation, Journal of Catalysis 142, 254-262

59. Omata K., Takada T., Kasahara S., Yamada M., (1996) Active site of substituted cobalt spinel oxide for selective oxidation of CO/H_2. Part II, Applied Catalysis A: General 146, 255-267

60. Perry H.R., Green D.W., (1985) Perry's Chemical Engineers Handbook, Seventh Edition, Mc Grow-Hill, Cap. 27

61. Pintar A., Batista J., Hocevar S., (2005), TPR, TPO, and TPD examinations of $Cu_{0.15}Ce_{0.85}O_{2-y}$ mixed oxides prepared by co-precipitation, by the sol-gel peroxide route, and by citric acid-assisted synthesis, Journal of Colloidal and Interface Science 285, 218-231

62. Qi Z., He C., Kaufman A., (2002) Effect of CO in the anode fuel cell on the performance of PEM fuel cell cathode, Journal of power sources, 111, 239-247

63. Ratnasamy P., Srinivas D., Satyanarayana C.V.V., Manikandan P., Senthil Kumaran R.S., Sachin M., Vasudev N. Shetti, (2004), Influence of thesupport on the preferential oxidation of CO in hydrogen-rich stream reformats over the CuO-CeO_2-ZrO_2 system, J. Catalysis 221, 455-465.

64. Rohland B., Plzak J., (1999), The PEMFC- integrated CO- a novel method of simplifying the fuel cell plant, Journal of Power Source, 84, 183-186

65. Rosso I., Galletti C., Saracco G., Garrone E., Specchia V., (2004) Developement of A zeolites-supported noble-metal catalysts for CO preferential oxidation: H_2 gas purification for fuel cell, Applied Catalysis B 48, 195-203,

66. Sanchez M.G., and Gazquez L.J., (1987), Oxygen Vacancy Model in Strong Metal-Support Interaction, Journal of catalysis, 104, 120-135

67. Satterfield C.N., Sherwood T.K., (1989) The role of diffusion in catalysis, Addison-Wesley Publishing Company, London

68. Schubert M., Gasteiger H., Behm J., (1997) Surface formates as side products in the selective CO Oxidation on Pt/α-Al_2O_3, Journal of catalysis 172, 256-258

69. Schubert M., Kahlich M.J., Gasteiger H., Behm J., (1999) Correlation between CO surface coverage and selectivity/kinetics for the preferential CO oxidation over Pt/α-Al_2O_3 and Au/γ-Fe_2O_3: an in situ Drifts study, Journal of Power Sources 84, 175-182

70. Schubert M.M., Hackenberg S., van Veen A., Muhler M., Plzak V., Behm R.J., (2001a) CO Oxidation over Supported Gold Catalysts-"Inert" and "Active" Support Materials and Their Role for the Oxygen Supply during reaction, Journal of Catalysis 197, 113-122

71. Schubert M.M., Plzak V., Garche J., Behm R.J, (2001b)Activity, selectivity, and long term stability of different metal oxide supported gold catalysts for the preferential CO oxidation in H_2-rich gas, Catalysis Letters 76, 143-150.

72. Sedmak G., Hocevar S., Levec J., (2003) Kinetics of selective CO oxidation in excess of H_2 over the nanostructured $Cu_{0.1}Ce_{0.9}O_{2-y}$ catalyst, Journal of catalysis 213, 135-150

73. Sedmak G., Hocevar S., Levec J. (2004), Transient kinetic model of CO oxidation over a nanostructured $Cu_{0.1}Ce_{0.9}O_{2-y}$ catalyst, Journal of catalysis, 222, 87-99.

74. Shan W., Shen W., Li C., (2003), Structural characteristics and Redox behaviours of $Ce_{1-x}Cu_xO_y$ solid solutions, Chemical materials 15, 4761-4767.

75. Simont, Garin F., Maire G., (1997) A comparative study of $LaCoO_3$, Co_3O_4 and $LaCoO_3$-Co_3O_4.I.Preparation, characterization and catalytic properties for the oxidation of CO, Applied Catalysis B:Environmental 11, 167-179

76. Snytnikov P.V., Sobyanin V.A., et al., (2003), Selective oxidation of carbon monoxide in excess hydrogen over Pt-, Ru- and Pd-supported catalysts, Applied catalysis A, 239, 149-156

77. Tanaka H., Shin-ichi I., Kameoka S., Tomishige K., Kunimori K., (2003), Catalytic performances of K-peromoted Rh/USY catalysts in preferential oxidation of CO in rich hydrogen, Applied Catalysis A, 250, 255-263

78. Tang X., Zhang B., Li Y., Xu Y., Xin Q., Shen W., (2004), Carbon monoxide oxidation over CuO/CeO2 catalysts, Catalysis Today 93-95, 191-198

79. Teng. Y., Sakurai H., Ueda A., Kobayashi T., (1999) Oxidative removal of CO contained in hydrogen by using metal oxide catalysts, International Journal of Hydrogen Energy 24, 355-358

80. Torres and Sanchez, (1997) Selective oxidation of CO in Hydrogen over Gold Supported on Manganese Oxides, Journal of Catalysis 168, 125-127

81. Trimm D.L., OnsanZ.I., (2001) On board fuel conversion for hydrogen-fuel-cell-driven vehicles, Catalysis Review, 43 (1&2), 31.84

82. Trovarelli A., (1996), Catalytic properties of ceria and CeO_2 –containing Materials, Catalysis Review Science Engineering 38, 439

83. Trovarelli A., Zamar F., Llorca J., de Lietenburg, Dolcetti G., Kisss J.T., (1997) Nanophase fluorite-structured CeO_2-ZrO_2 catalyst prepared by high-energy mechanical milling, Journal of catalysis 169, 490-502

84. Trovarelli A., (2002) Catalysis by Ceria and Related Materials, Catalytic Science Series-Vol2, Imperial college; London.

85. Wang J.B., Lin S.C., Huang T. J., (2002) Selective CO oxidation in rich Hydrogen over CuO/samaria-doped ceria, Applied Catalusis A: Gneral 232, 107-120

86. Westerterp K.R., van Swaaiy W.P.,and Beenackers A.A.C.M., (1993), Chemical Reactor Design and Operation, Wiley, New York

87. Worner A., Friedrich C., Tamme R., (2003) Development of a novel Ru-based catalyst system for the selective oxidation of CO in hydrogen rich gas mixtures, Applied Catalysis A: General, 1-14

88. Xia. G.G., Willis W.S., Wang J.Y., Suib S.L., (1999) Efficient stable catalysts for low temperature carbon monoxide oxidation, Journal of catalysis 185, 91-105

89. Yao H.C., and Yao Y.F.Y., (1984), Ceria in automotive exhaust catalysts, Journal of Catalysis 86, 254

90. Zimmer P., Tschope A., Birringer R., (2002), Temperature-Programmed reaction spectroscopy of ceria- and Cu/ceria-supported oxide catalyst, Journal of Catalysis, 205, 339-345